Midwest States Regional Pooled Fund Research Program
Fiscal Year 2012 (Year 22)
Research Project Number TPF-5(193)
NDOR Sponsoring Agency Code RPFP-12-CABLE1&2

DESIGN OF AN IMPROVED POST FOR USE IN A NON-PROPRIETARY HIGH-TENSION CABLE MEDIAN BARRIER

Submitted by

Robert W. Bielenberg, M.S.M.E., E.I.T.
Research Associate Engineer

Tyler L. Schmidt, B.S.C.E.
Graduate Research Assistant

Ronald K. Faller, Ph.D., P.E.
Research Associate Professor
MwRSF Director

Scott K. Rosenbaugh, M.S.C.E., E.I.T.,
Research Associate Engineer

Karla A. Lechtenberg, M.S.M.E., E.I.T.
Research Associate Engineer

John D. Reid, Ph.D.
Professor

Dean L. Sicking, Ph.D., P.E.
Emeritus Professor

MIDWEST ROADSIDE SAFETY FACILITY
Nebraska Transportation Center
University of Nebraska-Lincoln
130 Whittier Research Center
2200 Vine Street
Lincoln, Nebraska 68583-0853
(402) 472-0965

Submitted to

MIDWEST STATES REGIONAL POOLED FUND PROGRAM
Nebraska Department of Roads
1500 Nebraska Highway 2
Lincoln, Nebraska 68502

MwRSF Research Report No. TRP-03-286-15

May 7, 2015

TECHNICAL REPORT DOCUMENTATION PAGE

1. Report No. TRP-03-286-15	2.	3. Recipient's Accession No.	
4. Title and Subtitle Design of an Improved Post for Use in a Non-Proprietary High-Tension Cable Median Barrier		5. Report Date May 7, 2015 6.	
7. Author(s) Bielenberg, R.W., Schmidt, T.L., Faller, R.K., Rosenbaugh, S.K., Lechtenberg, K.A., Reid, J.D., and Sicking, D.L.		8. Performing Organization Report No. TRP-03-286-15	
9. Performing Organization Name and Address Midwest Roadside Safety Facility (MwRSF) Nebraska Transportation Center University of Nebraska-Lincoln 130 Whittier Research Center 2200 Vine Street Lincoln, Nebraska 68583-0853		10. Project/Task/Work Unit No. 11. Contract © or Grant (G) No. TPF-5(193) Supplement #44 & 45	
12. Sponsoring Organization Name and Address Midwest States Regional Pooled Fund Program Nebraska Department of Roads 1500 Nebraska Highway 2 Lincoln, Nebraska 68502		13. Type of Report and Period Covered Final Report: 2012-2015 14. Sponsoring Agency Code RPFP-12-CABLE1&2	
15. Supplementary Notes Prepared in cooperation with U.S. Department of Transportation, Federal Highway Administration.			

16. Abstract (Limit: 200 words)

The objective of this research study was to develop a revised post section for the non-proprietary high-tension cable median barrier that improved the safety and function of the post by lowering strong-axis forces. A total of twenty dynamic component tests were performed, along with one cable pull test – ten tests with the 7-gauge C-section post, eight with the 10-gauge C-Section posts, and three with the Midwest Weak Post (MWP). The tests were conducted with the posts installed in either a compacted, crushed limestone soil or a rigid sleeve in order to determine the force vs. deflection and energy vs. deflection characteristics of the various post configurations. Although the C-section posts were found to provide up to 58.7 percent and 70 percent reductions in strong-axis forces through 10 in. (254 mm) and 15 in. (381 mm) to that of the S3x5.7 (S76x8.5) posts, the C-section hinged at the location of the keyway when a keyway was punched in the posts and left a 15-in. (381-mm) stub sticking out of the ground. This behavior caused concerns for occupant compartment intrusions. Subsequently, the MWP was designed to bend over at the groundline while maintaining the desired strong- and weak-axis post forces. In dynamic tests, the MWP was found to provide up to 54.3 percent and 64 percent reductions in strong-axis forces through 10 in. (254 mm) and 15 in. (381 mm), as compared to the S3x5.7 (S76x8.5) posts. The weak-axis forces were found to be up to 14.3 percent and 6.7 percent greater than the S3x5.7 (S76x8.5) post through 10 in. (254 mm) and 15 in. (381 mm). These comparisons indicated that the MWP section had significantly reduced strong-axis capacity as compared to the S3x5.7 (S76x8.5) post while maintaining similar weak-axis capacity to the S3x5.7 (S76x8.5) post, as intended.

17. Document Analysis/Descriptors Highway Safety, Crash Test, Roadside Appurtenances, MASH, Cable Median Barrier, C-Section Posts, W3x5.7 Posts, Midwest Weak Post and Bogie Test		18. Availability Statement No restrictions. Document available from: National Technical Information Services, Springfield, Virginia 22161	
19. Security Class (this report) Unclassified	20. Security Class (this page) Unclassified	21. No. of Pages 225	22. Price

DISCLAIMER STATEMENT

This report was completed with funding from the Federal Highway Administration, U.S. Department of Transportation and the Midwest States Regional Pooled Fund Program. The contents of this report reflect the views and opinions of the authors who are responsible for the facts and the accuracy of the data presented herein. The contents do not necessarily reflect the official views or policies of the state highway departments participating in the Midwest States Regional Pooled Fund Program nor the Federal Highway Administration, U.S. Department of Transportation. This report does not constitute a standard, specification, regulation, product endorsement, or an endorsement of manufacturers.

UNCERTAINTY OF MEASUREMENT STATEMENT

The Midwest Roadside Safety Facility (MwRSF) has determined the uncertainty of measurements for several parameters involved in standard full-scale crash testing and non-standard testing of roadside safety features. Information regarding the uncertainty of measurements for critical parameters is available upon request by the sponsor and the Federal Highway Administration. Test nos. 4CMBC-1 through 4CMBC-16, CPK-1 and CPK-2, and CPZ-1 through CPZ-3 were non-certified component tests conducted for research and development purposes only.

The Independent Approving Authority (IAA) for the data contained herein was Dr. Cody Stolle, E.I.T., Research Assistant Professor.

ACKNOWLEDGEMENTS

The authors wish to acknowledge sources that made a contribution to this project: (1) the Midwest States Regional Pooled Fund Program funded by the Illinois Department of Transportation, Indiana Department of Transportation, Iowa Department of Transportation, Kansas Department of Transportation, Minnesota Department of Transportation, Missouri Department of Transportation, Nebraska Department of Roads, New Jersey Department of Transportation; Ohio Department of Transportation, South Dakota Department of Transportation, Wisconsin Department of Transportation, and Wyoming Department of Transportation for sponsoring this project; and (2) MwRSF personnel for installing the posts and conducting the component tests.

Acknowledgement is also given to the following individuals who made a contribution to the completion of this research project.

Midwest Roadside Safety Facility

J.C. Holloway, M.S.C.E., E.I.T., Test Site Manager
K.L. Krenk, B.S.M.A., Maintenance Mechanic (retired)
J.D. Schmidt, Ph.D., Research Assistant Professor
C.S. Stolle, Ph.D., Research Assistant Professor
A.T. Russell, B.S.B.A., Shop Manager
D.S. Charroin, Laboratory Mechanic
S.M. Tighe, Laboratory Mechanic
Undergraduate and Graduate Research Assistants

Illinois Department of Transportation

Priscilla A. Tobias, P.E., State Safety Engineer/Bureau Chief
Tim Sheehan, P.E., Safety Design Engineer
Paul L. Lorton, P.E., Safety Programs Unit Chief

Indiana Department of Transportation

Todd Shields, P.E., Maintenance Field Support Manager

Iowa Department of Transportation

Chris Poole, P.E., Roadside Safety Engineer
Brian Smith, P.E., Methods Engineer

Kansas Department of Transportation

Scott King, P.E., Road Design Bureau Leader
Kelly Cool, P.E., Road Design Leader
Thomas Rhoads, P.E., Engineering Associate III, Bureau of Road Design

Minnesota Department of Transportation

Michael Elle, P.E., Design Standards Engineer

Missouri Department of Transportation

Joseph G. Jones, P.E., Engineering Policy Administrator

Nebraska Department of Roads

Phil TenHulzen, P.E., Design Standards Engineer
Jim Knott, P.E., State Roadway Design Engineer
Jodi Gibson, Research Coordinator

New Jersey Department of Transportation

Dave Bizuga, P.E., Manager 2, Roadway Design Group 1

Ohio Department of Transportation

Maria E. Ruppe, P.E., Roadway Standards Engineer

South Dakota Department of Transportation

David Huft, P.E., Research Engineer
Bernie Clocksin, P.E., Lead Project Engineer

Wisconsin Department of Transportation

Jerry Zogg, P.E., Chief Roadway Standards Engineer
Erik Emerson, P.E., Standards Development Engineer
Rodney Taylor, P.E., Roadway Design Standards Unit Supervisor

Wyoming Department of Transportation

William Wilson, P.E., Architectural and Highway Standards Engineer

Federal Highway Administration

John Perry, P.E., Nebraska Division Office
Danny Briggs, Nebraska Division Office

TABLE OF CONTENTS

LIST OF FIGURES

LIST OF TABLES

1 INTRODUCTION

1.1 Background

In recent years, the Midwest Roadside Safety Facility (MwRSF) was tasked by the Midwest States Regional Pooled Fund to develop a non-proprietary high-tension cable median barrier. The design of the non-proprietary high-tension cable median barrier system had progressed through a series of crash tests that identified flaws in the system related to vehicle capture during testing in a v-ditch and deformations of the occupant compartment during sedan testing on level terrain [1-3]. These concerns led the researchers to revisit performance of the basic design elements of the barrier system.

Three design problems stood out that needed to be addressed to improve the system and meet the new TL-3 test requirements for cable median barrier found in the *Manual for Assessing Safety Hardware* (MASH). First, full-scale testing had shown that the current design of the cable median barrier had difficultly capturing vehicles when the barrier was placed down the slope. Full-scale test no. 4CMB-5 showed that impacting the system at a post and while airborne tended to pull down the top cable and compromise vehicle capture [2]. Second, full-scale test no. 4CMBLT-1 indicated that the current cable barrier system design could cause A-pillar crush in small cars and sedans, as shown in Figure 1 [3]. Review of the full-scale test results suggested that two factors contributing to the A-pillar crush were the lateral, or strong-axis, strength of the post and the release forces of the cable to post attachment. Finally, review of the behavior of the cable-to-post attachments in the current design found that the current attachment behavior was not optimized. The attachments appeared to be too strong vertically to release cables safely and effectively. With respect to the strong-axis release loads, it was observed that the strong-axis release forces were not sufficient to yield and displace the posts in the system to effectively

absorb energy. This behavior was believed to be critical to maximize energy dissipation and control deflections.

Figure 1. A-pillar Damage. Test No. 4CMBLT-1

Based on this analysis, the researchers began an effort to redesign several of the system components, including the cable-to-post attachments and the support posts. Redesign of the cable-to-post attachments was detailed in a previous report [4]. This report will detail the redesign of the cable barrier post itself.

The posts used in the non-proprietary high-tension cable median barrier serve to support the cables at the appropriate height and dissipate a portion of the kinetic energy of the impact vehicle through rotation and deformation at impact. The weak- and strong-axis capacities of

these posts and their interaction with the barrier cables and the vehicle have a significant effect on the performance of the barrier system. The current non-proprietary high-tension cable median barrier employed S3x5.7 (S76x8.5) steel posts, but it was believed that the post design could be optimized to improve barrier performance. The primary goal of the new post sections was to lower the lateral, or strong-axis, strength of the post. It was believed that a post with lower strong-axis capacity would result in lower forces imparted to the A-pillar and reduced A-pillar damage. Lowering the lateral capacity of the post would also allow for yielding and deflection of the post at lower loads, which was hoped to improve energy absorption as compared to the current post design. In addition, data analysis of current cable median barriers also suggested that cable median barriers with lower strong-axis post strengths have reduced tendencies for vehicle rollover [5].

1.2 Objective

The objective of this research study was to develop a revised post section for the non-proprietary high-tension cable median barrier that improved the safety and function of the post by lowering strong-axis forces.

1.3 Scope

Redesign of the non-proprietary high-tension cable median barrier post was accomplished through design, computer simulation, and component testing. The research effort began with an analysis of potential post sections, folded plate sections, and available sheet metal materials for use in the post design. Next, finite element computer simulation was used to evaluate the post sections prior to development of design prototypes. Finally, component testing of prototype post designs and additional computer simulations were conducted to select the optimum design.

2 DESIGN CRITERIA

The first step in the research effort to design an improved post for the non-proprietary high-tension cable median barrier was to determine the design criteria for the new post section with the goal of improving the performance of the barrier system. Several design criteria were identified for the post:

1. Lateral (strong-axis) capacity
    a. As noted previously, one of the main criteria for the new post design was to reduce the strong-axis capacity of the post section in order to limit the loading of the A-pillar by the cables and improve the energy dissipation of the system.
2. Longitudinal (weak-axis) capacity
    a. The longitudinal capacity of the new post section was desired to have equal or less strength than the current S3x5.7 (S76x8.5) post in order to reduce potential vehicle instabilities or snag concerns with vehicles impacting the posts during vehicle redirection.
3. Cable attachments
    a. The new post section needed to have a geometry that allowed for mounting of the cable-to-post attachments developed previously, including the tabbed bracket used for the lower three cables and the top cable attachment developed in the previous study [4], as shown in Figure 2.
4. Reduced cost
    a. It was desired to investigate the use of alternative shapes and post sections that could reduce the cost of the posts in the system.

With these criteria in mind, the researchers began the design and evaluation of potential post sections, as detailed in the subsequent chapter.

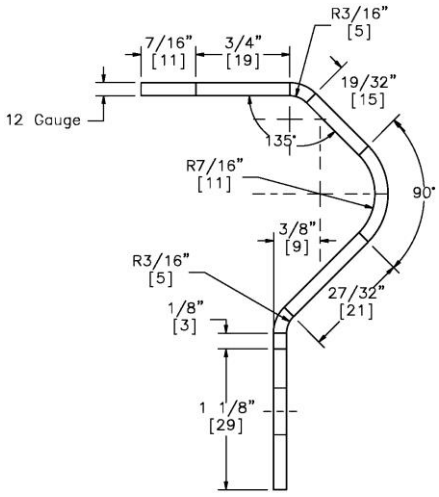

Tabbed Bracket Version 10

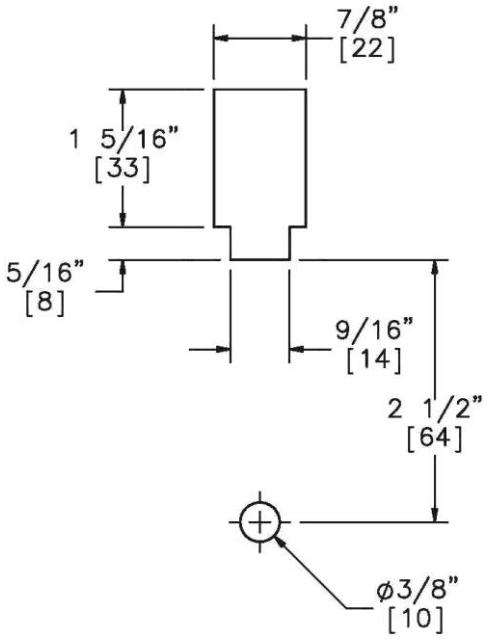

Keyway Version 8

Top Cable Attachment

Figure 2. Previously Developed Tabbed Bracket and Top Cable-to-Post Attachments

3 DESIGN OF ALTERNATIVE POST SECTIONS – ROUND 1

Development of the potential post sections for the non-proprietary high-tension cable median barrier involved reviewing available sections, investigation of non-standard sections fabricated from sheet metal, and finite element computer simulation of potential designs to suggest preferred designs for component testing.

3.1 Standard Structural Steel Sections

Currently available structural steel sections were reviewed for use as potential alternative sections. However, no existing structural steel shapes were identified that met the design criteria. Review of W and HP shape sections found that they were all heavier and had higher lateral and longitudinal capacities than the current S3x5.7 (S76x8.5) post. Similarly, S and M shapes could not be identified that reduced the lateral capacity of the post below the current section. C and MC sections were investigated, and a limited number of these sections were found with strengths in the desired ranges. However, the geometry of the C and MC sections were not conducive to mounting of cable-to-post attachments. L-angles and T shapes were disregarded due to their lack of symmetry. Thus, no existing structural steel sections were identified that could improve upon the S3x5.7 (S76x8.5) post.

3.2 Non-Standard/Fabricated Sections

The lack of existing steel sections that met the design criteria led the researchers to consider alternative post sections that could be fabricated from folded or rolled sheet steel. Fabrication of alternative sections from sheet steel posed several advantages. First, the geometry and section properties of the post could be tailored to meet the desired lateral and longitudinal capacities and facilitate the cable-to-post attachments. Second, the post sections could be fabricated from readily available sheet steel material using standard rolling and punching methods to create the post geometry and the keyways and notch in the posts. Third, the posts

could be designed to use less steel per linear foot than the S3x5.7 (S76x8.5) post. Thus, it was anticipated that the fabricated post sections would cost considerably less than the current post design.

A wide range of sheet steel materials are available in terms of the steel grade and the thickness or gauge. Review of potential steel grades for the fabricated post section found that the available grades of sheet steel could range from low-strength carbon steels with a broad strength specification and degree of variability to very high-strength sheet steels. The researchers chose a hot-rolled ASTM A1011 HSLAS Grade 50 sheet steel for the post section that compromised between these extremes. Hot-rolled ASTM A1011 HSLAS Grade 50 sheet steel is a structural steel sheet metal grade that provided consistent yield and ultimate strength values similar to the ASTM A992 specification used in structural steel W and S sections. In addition, the steel had relatively good ductility in order to provide reliable energy absorption through post deformation. Review of the available sheet metal gauges in that steel specification found that the steel could be obtained as thick as 7 gauge. Thicker gauge sheet was desired to provide sufficient structure to prevent flange deformation under the loading of the cable-to-post attachments and to prevent damage or buckling of the post section if the post was driven when installed.

The researchers selected a C-shaped folded post design for the initial investigation of alternative post designs. A C-shaped post provided several benefits, in that it allowed easy attachment of the cable-to-post connections, the section could be easily tuned to meet the design criteria, and it would be easy to fabricate due to the limited number of bends. The researchers chose two prototype post sections to evaluate through component testing, as shown in Figure 3. The C-shaped post cross sections were designed to have the same depth as the existing S3x5.7 (S76x8.5) post. The width of the post was lowered to reduce the lateral or strong-axis capacity of the post section while still providing sufficient area for mounting of the cable-to-post attachment

hardware. Two gauge thicknesses, 7 gauge and 10 gauge, were selected for the prototype posts in order to evaluate the reduced post capacity in both the strong and weak axes. Both post sections significantly reduced the post strength and the weight per foot of the post.

In order to evaluate the post designs a series of component tests of the post were conducted in soil and in rigid sleeves. The results of these tests are detailed in subsequent chapters.

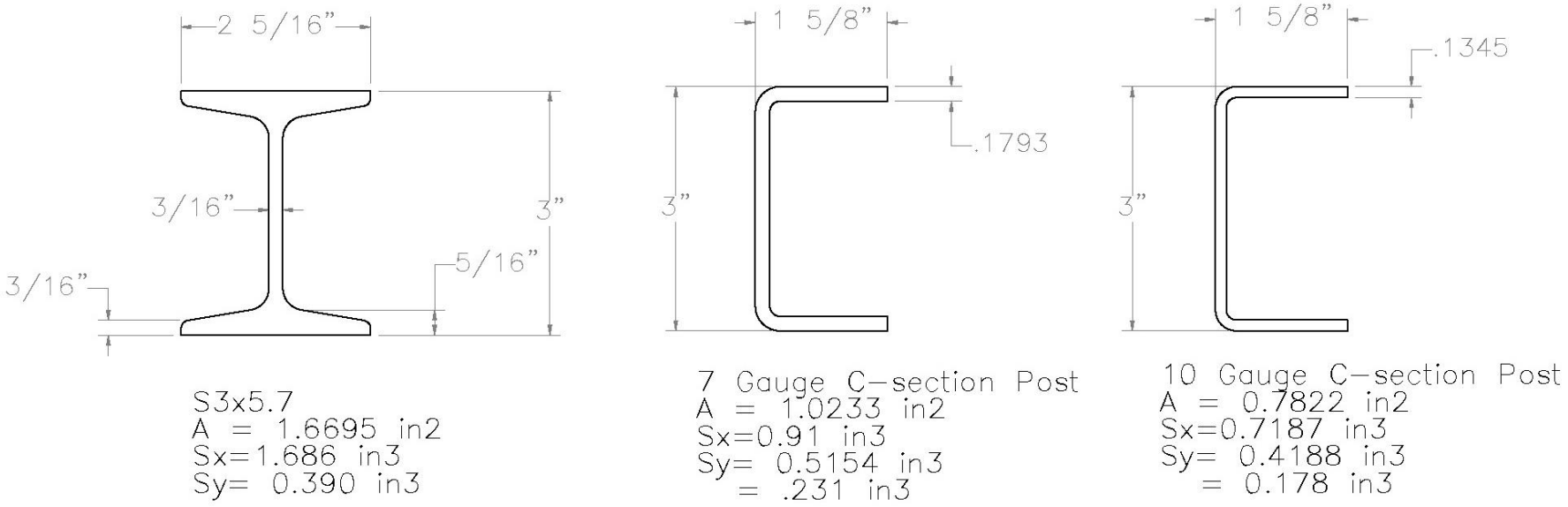

Figure 3. Comparison of Proposed C-Section Posts and S3x5.7 (S76x8.5) Post

Sx=Strong-axis section modulus

Sy=Weak-axis section modulus

4 TEST CONDITIONS

4.1 Test Facility

The testing facility is located at the Lincoln Air Park on the northwest side of the Lincoln Municipal Airport and is approximately 5 miles (8.0 km) northwest of the University of Nebraska-Lincoln city campus.

4.2 Equipment

Equipment and instrumentation utilized to collect and record data during the dynamic bogie tests included a bogie, onboard accelerometers, pressure tape switches, an optic speed trap, high-speed and standard-speed digital cameras, and a still camera.

4.2.1 Bogie

A rigid-frame bogie was used to impact the posts. A variable-height, detachable impact head was used in the testing. The bogie head was constructed of 8-in. (203-mm) diameter, ½-in. (13-mm) thick standard steel pipe, with ¾-in. (19-mm) neoprene belting wrapped around the pipe to prevent local damage to the post from the impact. The impact head was bolted to the bogie vehicle, creating a rigid frame with an impact height of 27 in. (686 mm). The bogie with the impact head is shown in Figure 4. The weight of the bogie with the addition of the mountable impact head and accelerometers were approximately 1,870 lb (848 kg).

A pickup truck with a reverse cable tow system was used to propel the bogie to a target impact speed of 20 mph (32 km/h). When the bogie approached the end of the guidance system, it was released from the tow cable, allowing it to be free-rolling when it impacted the post. A remote braking system was installed on the bogie, allowing it to be brought safely to rest after the test.

Figure 4. Rigid Frame Bogie and Guidance Track

4.2.2 Accelerometers

Three accelerometers were utilized to measure the acceleration in the lateral, longitudinal, and vertical directions. However, only the weak-axis accelerations were processed and reported. The accelerometers were mounted on the bogie vehicle near its center of gravity (c.g.).

The first accelerometer system, SLICE 6DX was a modular data acquisition system manufactured by Diversified Technical Systems, Inc. (DTS) of Seal Beach, California. The acceleration sensors were mounted inside the body of the custom-built SLICE 6DX event data recorder and recorded data at 10,000 Hz to the onboard microprocessor. The SLICE 6DX was configured with 7 GB of non-volatile flash memory, a range of ±500 g's, a sample rate of 10,000 Hz, and a 1,650 Hz (CFC 1000) anti-aliasing filter. The "SLICEWare" computer software program and a customized Microsoft Excel worksheet were used to analyze and plot the accelerometer data. The DTS-SLICE was used in test nos. CPK-1 and CPK-2, and CPZ-1 through CPZ-3.

The second accelerometer system was a two-arm piezoresistive accelerometer system manufactured by Endevco of San Juan Capistrano, California. Three accelerometers were used to measure each of the lateral, longitudinal, and vertical accelerations independently at a sample rate of 10,000 Hz. The accelerometers were configured and controlled using a system developed and manufactured by DTS. More specifically, data was collected using a DTS Sensor Input Module (SIM), Model TDAS3-SIM-16M. The SIM was configured with 16 MB SRAM and eight sensor input channels with 250 kB SRAM/channel. The SIM was mounted on a TDAS3-R4 module rack. The module rack was configured with isolated power/event/communications, 10BaseT Ethernet and RS232 communications, and an internal backup battery. Both the SIM and module rack were crashworthy. The "DTS TDAS Control" computer software program and a customized Microsoft Excel worksheet were used to analyze and plot the accelerometer data. The DTS was used in test nos. 4CMBC-1 through 4CMBC-16.

The third accelerometer, Model EDR-3, was a triaxial piezoresistive accelerometer system developed by Instrumental Sensor Technology (IST) of Okemos, Michigan. The EDR-3 was configured with 256 kB of RAM, a range of ±200 g's, a sample rate of 3,200 Hz, and a 1,120-Hz low-pass filter. The "DynaMax 1 (DM-1)" computer software program and a customized Microsoft Excel worksheet were used to analyze and plot the accelerometer data. The EDR-3 was used in all of the tests.

4.2.3 Pressure Tape Switches

Three pressure tape switches, spaced at approximately 3.3-ft (1.0-m) intervals and placed near the end of the bogie track, were used to determine the speed of the bogie before impact for test nos. 4CMBC-1 through 4CMBC-16. As the right-front tire of the bogie passed over each tape switch, a strobe light was fired, sending an electronic timing signal to the data acquisition system. The system recorded the signals and the time each occurred. The speed was then

calculated using the spacing between the sensors and the time between the signals. Strobe lights and high-speed digital video analysis are used only as a backup in the event that vehicle speeds cannot be determined from the electronic data.

4.2.4 Optic Speed Trap

The retroreflective optic speed trap was used to determine the speed of the bogie vehicle before impact in test nos. CPK-1 and CPK-2, and CPZ-1 through CPZ-3. Three retroreflective targets, spaced at approximately 4-in. (102-mm) intervals, were applied to the side of the bogie vehicle which broke the beam of light. When the emitted beam of light was returned to the Emitter/Receiver, a signal was sent to the Optic Control Box, which in turn sent a signal to the data computer as well as activated the External LED box. The computer recorded the signals and the time each occurred. The speed was then calculated using the spacing between the retroreflective targets and the time between the signals. LED lights and high-speed digital video analysis are only used as a backup in the event that vehicle speeds cannot be determined from the electronic data.

4.2.5 Digital Photography

One AOS VITcam high-speed digital video camera and two JVC digital video cameras were used to document each test. The AOS high-speed camera had a frame rate of 500 frames per second and the JVC digital video cameras had frame rates of 29.97 frames per second. The high-speed digital video camera and one digital video camera were placed laterally from the post, with a view perpendicular to the bogie's direction of travel. The second digital video camera was placed on the opposite side of the post with respect to the other two cameras. A Nikon D50 digital still camera was also used, to document pre- and post-test conditions for all tests.

4.3 End of Test Determination

When the impact head initially contacted the test article, the force exerted by the surrogate test vehicle was directly perpendicular. However, as the post rotated, the surrogate test vehicle's orientation and path moved farther from perpendicular. This introduced two sources of error: (1) the contact force between the impact head and the post has a vertical component and (2) the impact head slides upward along the test article. Therefore, only the initial portion of the accelerometer trace may be used since variations in the data become significant as the system rotates and the surrogate test vehicle overrides the system. For this reason, the end of the test needed to be defined.

Guidelines were established to define the end-of-test time using the high-speed digital video of the crash test. The first occurrence of either of the following events was used to determine the end of the test: (1) the test article fractures, or (2) the surrogate vehicle overrides/loses contact with the test article.

4.4 Data Processing

The electronic accelerometer data obtained in dynamic testing was filtered using the SAE Class 60 Butterworth filter conforming to the SAE J211/1 specifications [6]. The pertinent acceleration signal was extracted from the bulk of the data signals. The processed acceleration data was then multiplied by the mass of the bogie to get the impact force using Newton's Second Law. Next, the acceleration trace was integrated to find the change in velocity versus time. Initial velocity of the bogie, calculated from the pressure tape switch data, was then used to determine the bogie velocity, and the calculated velocity trace was integrated to find the bogie's displacement, which is also the deflection of the post. Combining the previous results, a force vs. deflection curve was plotted for each test. Finally, integration of the force vs. deflection curve provided the energy vs. deflection curve for each test.

5 DYNAMIC TESTING – C-SECTION POSTS

5.1 Scope

A series of dynamic component tests were conducted on two C-section alternative cable barrier post designs in order to compare their performance to the S3x5.7 (S76x8.5) steel post used in the previously tested version of the non-proprietary high-tension cable median barrier system. Sixteen dynamic component tests were conducted on folded sheet metal C-section posts with two different gauge thicknesses. All posts were fabricated from hot-rolled ASTM A1011 HSLAS Grade 50 sheet steel. The target impact speed was 20 mph (32 km/h) for all sixteen tests. There were eight tests conducted on the posts' strong axis and eight tests conducted on the posts' weak axis. From the sixteen tests, eight tests were conducted in soil and eight tests were conducted in a sleeve. The dynamic component test matrix is show in Table 1. The test setup and bent C-section post set-up are shown in Figures 5 through 7. Material specifications, mill certificates, and certificates of conformity for the post materials used in all sixteen tests are shown in Appendix A.

A compacted, coarse, crushed limestone material, as recommended by MASH [7], was utilized for test nos. 4CMBC-1 through 4CMBC-8. Soil specifications are shown in Appendix B. MASH adheres to the general philosophy that testing longitudinal barriers in stiff soil results in higher impact and barrier loads; increased occupant risk values; and increased propensity for rail rupture, pocketing, and snag. MASH has established a minimum post-soil resistance force standard to ensure systems are installed in strong, stiff soil. Therefore, test nos. 4CMBC-1 through 4CMBC-8 utilized heavily compacted soil. Test nos. 4CMBC-9 through 4CMBC-16 were conducted in a steel sleeve placed in concrete.

Table 1. Dynamic Post Testing Matrix, Test Nos. 4CMBC-1 through 4CMBC-16

Test No.	Post Type	Gauge	Impact Axis	Foundation Type	Post Length in. (mm)	Embedment Depth in. (mm)	Target Impact Velocity mph (km/h)
4CMBC-1	Bent C-Section	10	Strong	Soil	90 (2,286)	42 (1,067)	20 (32)
4CMBC-2	Bent C-Section	10	Strong	Soil	90 (2,286)	42 (1,067)	20 (32)
4CMBC-3	Bent C-Section	10	Weak	Soil	90 (2,286)	42 (1,067)	20 (32)
4CMBC-4	Bent C-Section	10	Weak	Soil	90 (2,286)	42 (1,067)	20 (32)
4CMBC-5	Bent C-Section	7	Strong	Soil	90 (2,286)	42 (1,067)	20 (32)
4CMBC-6	Bent C-Section	7	Strong	Soil	90 (2,286)	42 (1,067)	20 (32)
4CMBC-7	Bent C-Section	7	Weak	Soil	90 (2,286)	42 (1,067)	20 (32)
4CMBC-8	Bent C-Section	7	Weak	Soil	90 (2,286)	42 (1,067)	20 (32)
4CMBC-9	Bent C-Section	10	Strong	Sleeve	90 (2,286)	42 (1,067)	20 (32)
4CMBC-10	Bent C-Section	10	Strong	Sleeve	90 (2,286)	42 (1,067)	20 (32)
4CMBC-11	Bent C-Section	7	Strong	Sleeve	90 (2,286)	42 (1,067)	20 (32)
4CMBC-12	Bent C-Section	7	Strong	Sleeve	90 (2,286)	42 (1,067)	20 (32)
4CMBC-13	Bent C-Section	10	Weak	Sleeve	90 (2,286)	42 (1,067)	20 (32)
4CMBC-14	Bent C-Section	10	Weak	Sleeve	90 (2,286)	42 (1,067)	20 (32)
4CMBC-15	Bent C-Section	7	Weak	Sleeve	90 (2,286)	42 (1,067)	20 (32)
4CMBC-16	Bent C-Section	7	Weak	Sleeve	90 (2,286)	42 (1,067)	20 (32)

Test Quantity	Post Type	Bogie No.	Embedment Depth in. [mm]	Load Height in. [mm]	Impact Speed mph [km/h]	Impact Axis
2	10–Gauge C–Section Post	3	42 [1067]	27 [686]	20 [32.2]	Strong
2	10–Gauge C–Section Post	3	42 [1067]	27 [686]	20 [32.2]	Weak
2	7–Gauge C–Section Post	3	42 [1067]	27 [686]	20 [32.2]	Strong
2	7–Gauge C–Section Post	3	42 [1067]	27 [686]	20 [32.2]	Weak

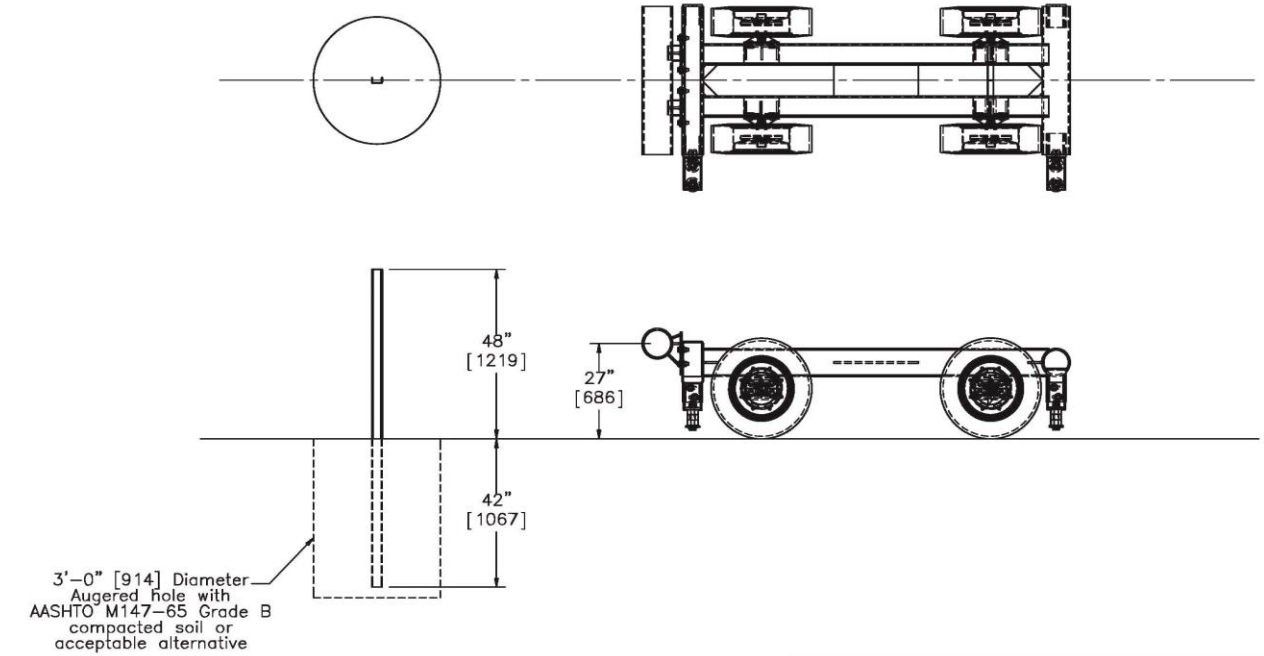

Note: (1) Drawing shows strong–axis test setup only. For weak axis, the post shall be rotated 90 degrees to its closed face.

MwRSF	Cable Median Barrier Bent C–Section	SHEET: 1 of 3
		DATE: 11/4/2014
Midwest Roadside Safety Facility	C–Section Soil Test	DRAWN BY: CWP/SDB
	DWG. NAME. 4CMBC–1_R4 / SCALE: 1:40 UNITS: in.[mm]	REV. BY: RWB/RKF

Figure 5. Test Setup, Test Nos. 4CMBC-1 through 4CMBC-8

Test Quantity	Post Type	Bogie No.	Embedment Depth in. [mm]	Load Height in. [mm]	Impact Speed mph [km/h]	Impact Axis
2	10–Gauge C–Section Post	3	42 [1067]	27 [686]	20 [32.2]	Strong
2	10–Gauge C–Section Post	3	42 [1067]	27 [686]	20 [32.2]	Weak
2	7–Gauge C–Section Post	3	42 [1067]	27 [686]	20 [32.2]	Strong
2	7–Gauge C–Section Post	3	42 [1067]	27 [686]	20 [32.2]	Weak

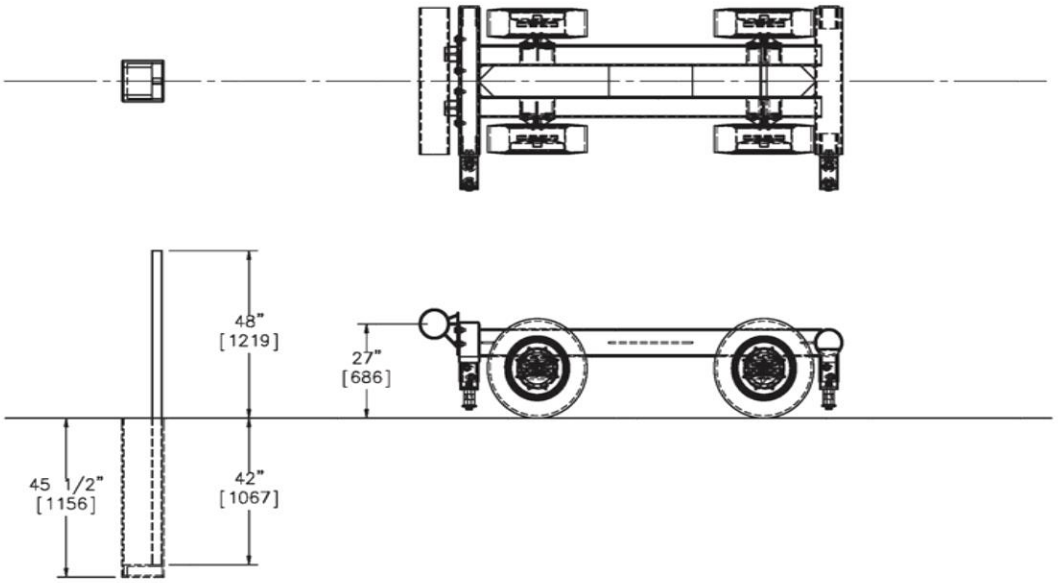

Note: (1) Drawing shows strong–axis test setup only. For weak axis, the post shall be rotated 90 degrees to its closed face.

(2) A 3–in. (76–mm) spacer is placed at the bottom of the rigid sleeve to raise the post to the correct height.

(3) Shim material to fit. Posts must be placed in holes with wood and steel shims and made tight (i.e., no gaps).

Midwest Roadside Safety Facility

Cable Median Barrier
Bent C–Section

C–Section Rigid Sleeve Test

SHEET: 2 of 3
DATE: 11/4/2014
DRAWN BY: CWP/SDB
REV. BY: RWB/RKF
DWG. NAME: 4CMBC–1_R4
SCALE: 1:40
UNITS: in.[mm]

Figure 6. Test Setup, Test Nos. 4CMBC-9 through 4CMBC-16

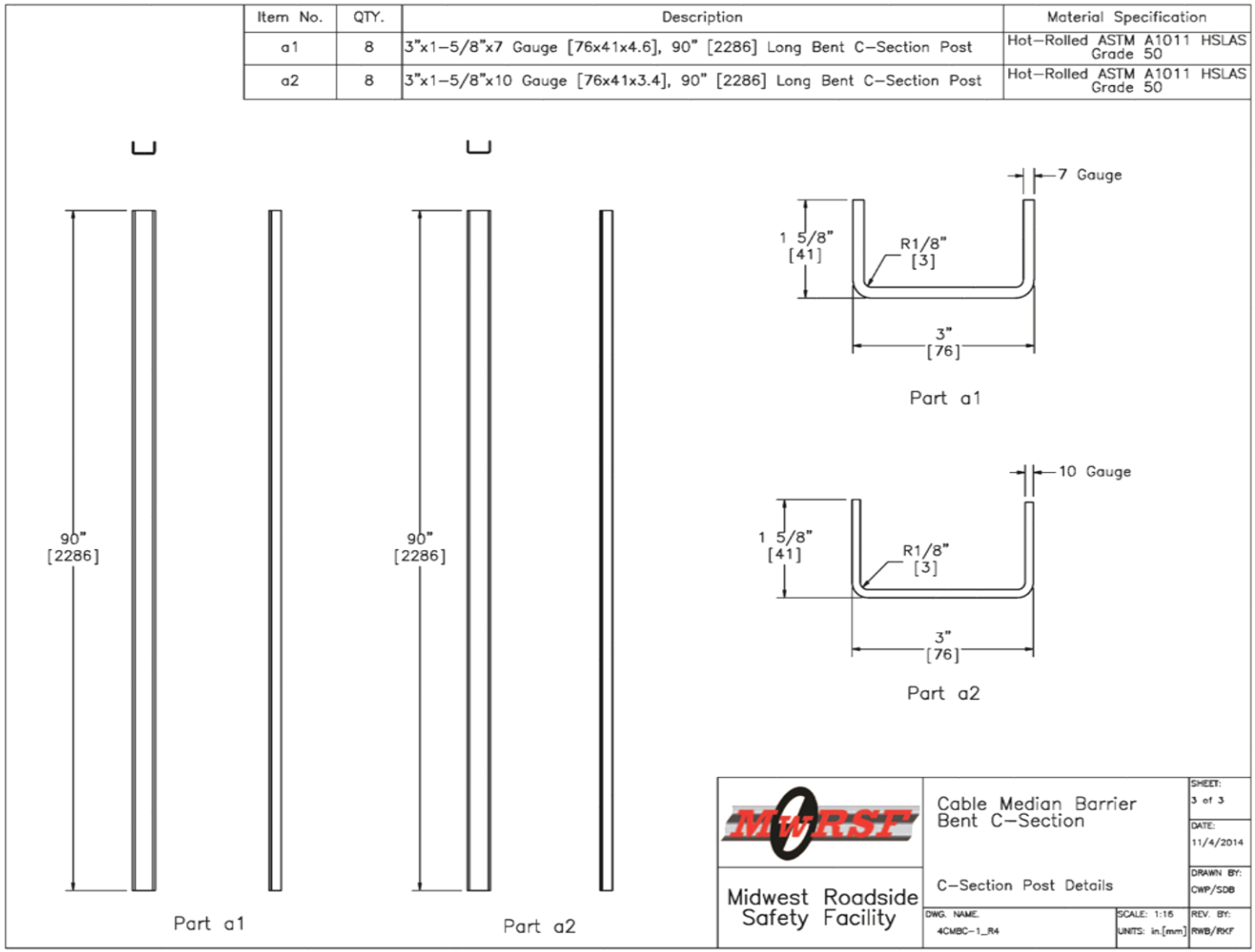

Figure 7. C-Section Post Details, Test Nos. 4CMBC-1 through 4CMBC-16

5.2 Dynamic Testing Results

The information desired from the bogie tests was the relationship between the applied force and deflection of the post at the impact location. This data was then used to find the total energy (the area under the force vs. deflection curve) dissipated during each test. The energy curve was used to compute the average force at a specific deflection using the following formula:

$$\bar{F} = \frac{Energy}{Deflection}$$

Although the acceleration data was applied to the impact location, the data came from the c.g. of the bogie. Error was added to the data since the bogie was not perfectly rigid and sustained vibrations. The bogie may have also rotated during impact, causing differences in accelerations between the bogie center of mass and the bogie impact head. While these issues may affect the data, the data was still valid. Filtering procedures were applied to the data to smooth out vibrations, and the rotations of the bogie during the tests were minor. One useful aspect of using accelerometer data was that it included influences of the post inertia on the reaction force. This was important as the mass of the post would affect barrier performance as well as test results.

Results of each test are discussed in the following sections. The accelerometer data for each test was processed to obtain acceleration, velocity, and deflection curves, as well as force vs. deflection and energy vs. deflection curves. The values described herein were calculated from either the DTS-SLICE or DTS data curves. Individual results for all accelerometers used during each test are provided in Appendix C.

5.2.1 Test No. 4CMBC-1

During test no. 4CMBC-1, the bogie impacted the 10-gauge C-section steel post embedded in soil at a speed of 20.2 mph (32.5 km/h). As a result of the strong-axis impact, the

post bent backward, twisted, and buckled approximately 6 in. (152 mm) above the groundline. The bogie overrode the post at a maximum deflection of 14.4 in. (366 mm).

Force vs. deflection and energy vs. deflection curves created from the DTS accelerometer data are shown in Figure 8. The forces fluctuated below 0.8 kips (3.6 kN) over the first few inches of deflection. The forces then escalated to a peak force of 1.8 kips (8.0 kN) at 8.8 in. (224 mm) of deflection, with slight fluctuation. The post provided an average resistive force of 1.0 kips (4.4 kN) through 10 in. (254 mm) of deflection and 0.9 kips (4.0 kN) through 15 in. (381 mm) of deflection. The average resistive force was calculated through 15 in. (381 mm) for comparison even though the maximum deflection was 14.4 in. (366 mm). The energy absorbed by the post was 10.2 kip-in. (1.2 kJ) through 10 in. (254 mm) of deflection and 13.6 kip-in. (1.5 kJ) through 15 in. (381 mm) of deflection. Pre-test and post-test photographs are shown in Figure 9. Time-sequential photographs are shown in Figure 10.

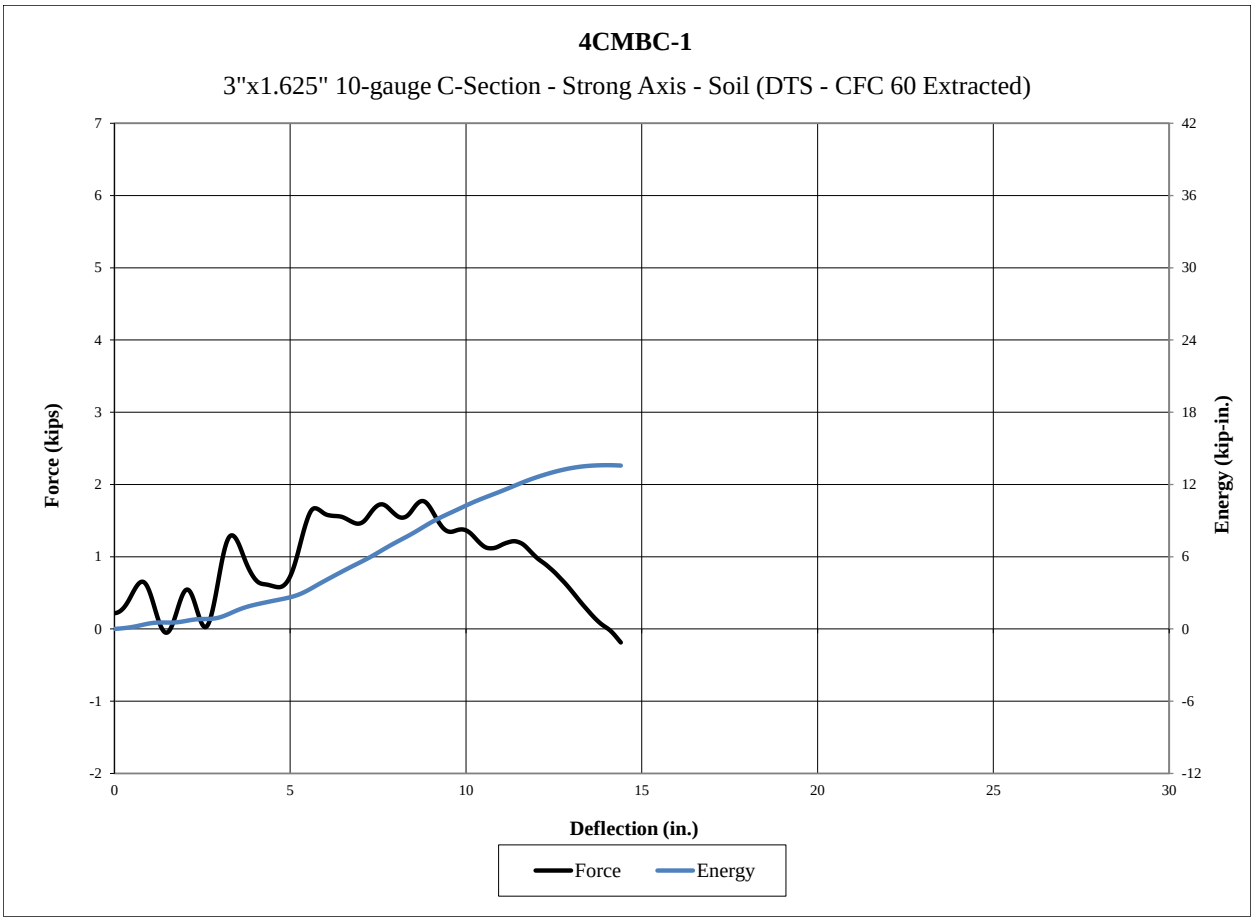

Figure 8. Force vs. Deflection and Energy vs. Deflection, Test No. 4CMBC-1

Pre-Test Post-Test

Figure 9. Pre-Test and Post-Test Photographs, Test No. 4CMBC-1


0.000 sec

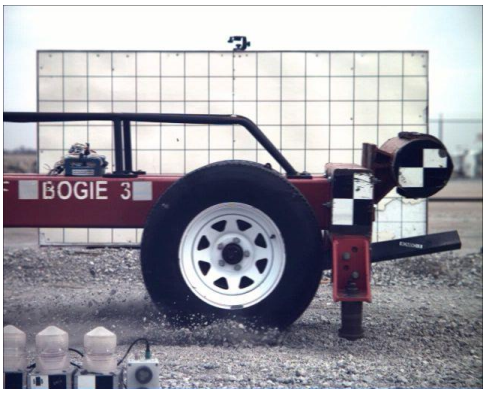

0.120 sec


0.030 sec

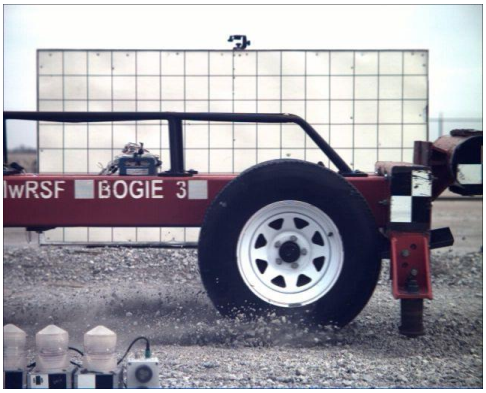

0.150 sec

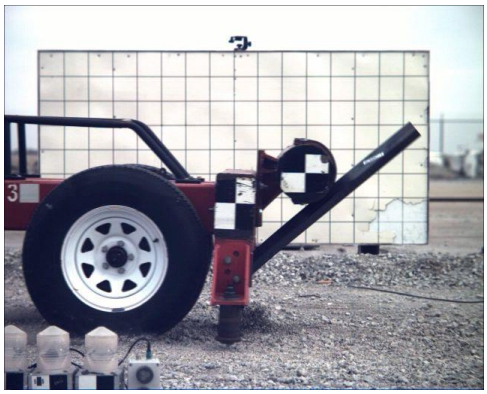
0.060 sec

0.180 sec

0.090 sec

0.210 sec

Figure 10. Sequential Photographs, Test No. 4CMBC-1

5.2.2 Test No. 4CMBC-2

During test no. 4CMBC-2, the bogie impacted the 10-gauge C-section steel post embedded in soil at a speed of 20.4 mph (32.8 km/h). As a result of the strong-axis impact, the post bent backward, twisted, and buckled approximately 6 in. (152 mm) above the groundline. The bogie overrode the post at a maximum deflection of 19.1 in. (485 mm).

Force vs. deflection and energy vs. deflection curves created from the DTS accelerometer data are shown in Figure 11. The forces quickly rose to a peak force of 4.4 kips (19.6 kN) at 1.5 in. (38 mm) of deflection. The post provided an average resistive force of 1.8 kips (8.0 kN) through 10 in. (254 mm) of deflection and 1.4 kips (6.2 kN) through 15 in. (381 mm) of deflection. The energy absorbed by the post was 17.9 kip-in. (2.0 kJ) through 10 in. (254 mm) of deflection and 21.0 kip-in. (2.4 kJ) through 15 in. (381 mm) of deflection. Pre-test and post-test photographs are shown in Figure 12. Time-sequential photographs are shown in Figure 13.

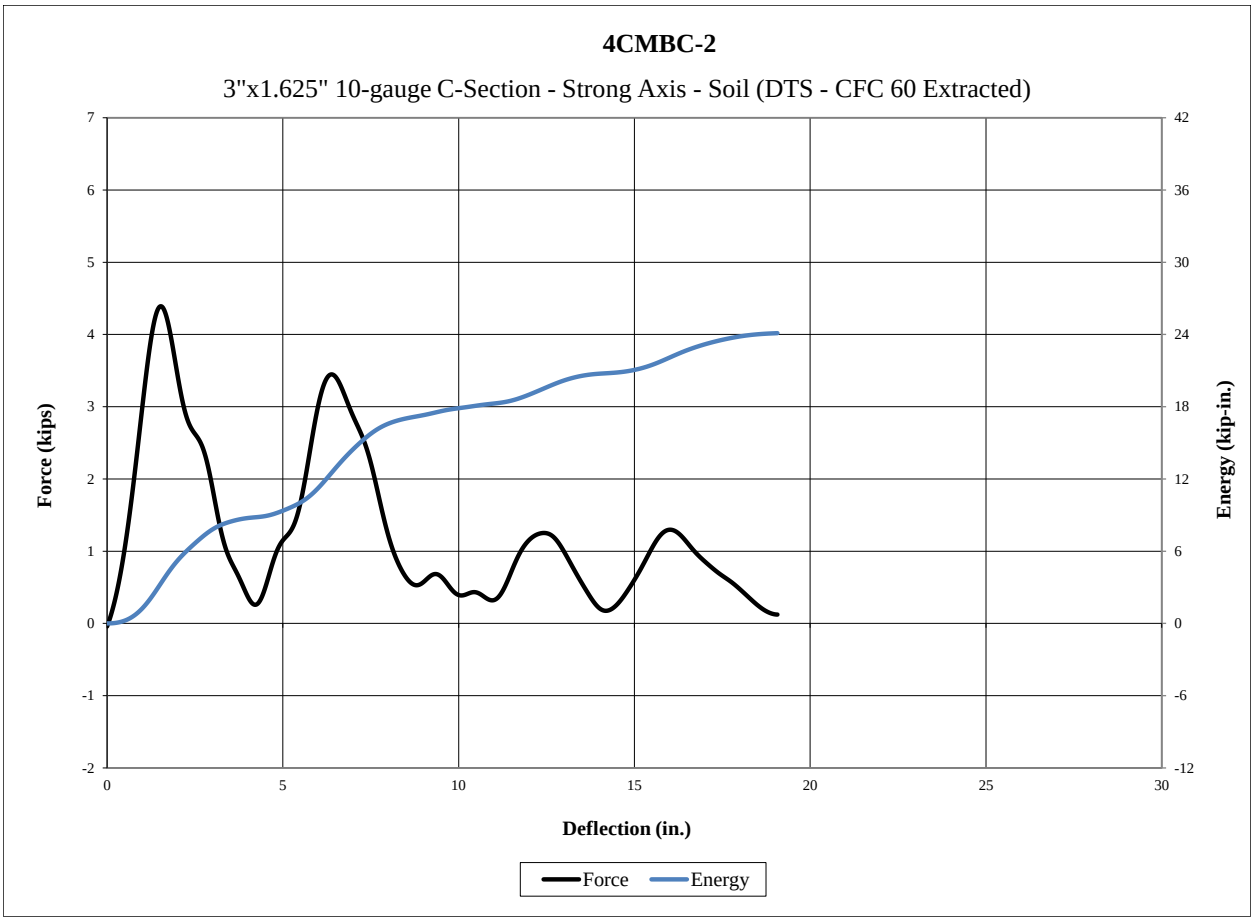

Figure 11. Force vs. Deflection and Energy vs. Deflection, Test No. 4CMBC-2

Pre-Test Post-Test

Figure 12. Pre-Test and Post-Test Photographs, Test No. 4CMBC-2


0.000 sec

0.120 sec


0.030 sec

0.150 sec

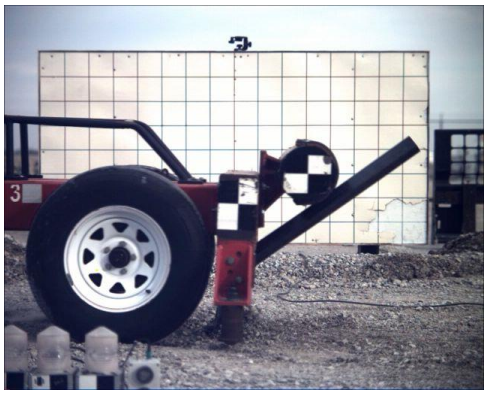
0.060 sec

0.180 sec

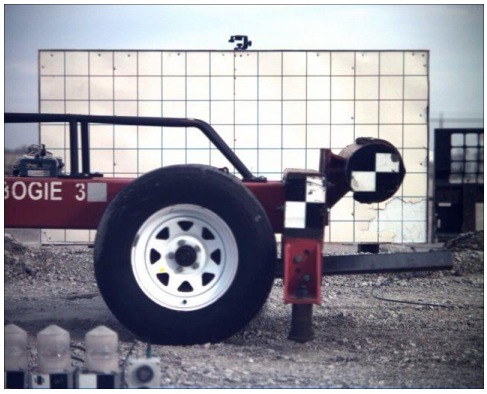

0.090 sec

0.210 sec

Figure 13. Sequential Photographs, Test No. 4CMBC-2

5.2.3 Test No. 4CMBC-3

During test no. 4CMBC-3, the bogie impacted the 10-gauge C-section steel post embedded in soil at a speed of 20.2 mph (32.5 km/h). As a result of the weak-axis impact, the post bent backward, and yielded approximately 2 in. (51 mm) below the groundline. The bogie overrode the post at a maximum deflection of 24.7 in. (627 mm).

Force vs. deflection and energy vs. deflection curves created from the DTS accelerometer data are shown in Figure 14. The forces quickly rose to a peak force of 3.7 kips (16.5 kN) at 2.0 in. (51 mm) of deflection. The post provided an average resistive force of 1.0 kips (4.4 kN) through 10 in. (254 mm) of deflection and 0.9 kips (4.0 kN) through 15 in. (381 mm) of deflection. The energy absorbed by the post was 10.5 kip-in. (1.2 kJ) through 10 in. (254 mm) of deflection and 13.6 kip-in. (1.5 kJ) through 15 in. (381 mm) of deflection. Pre-test and post-test photographs are shown in Figure 15. Time-sequential photographs are shown in Figure 16.

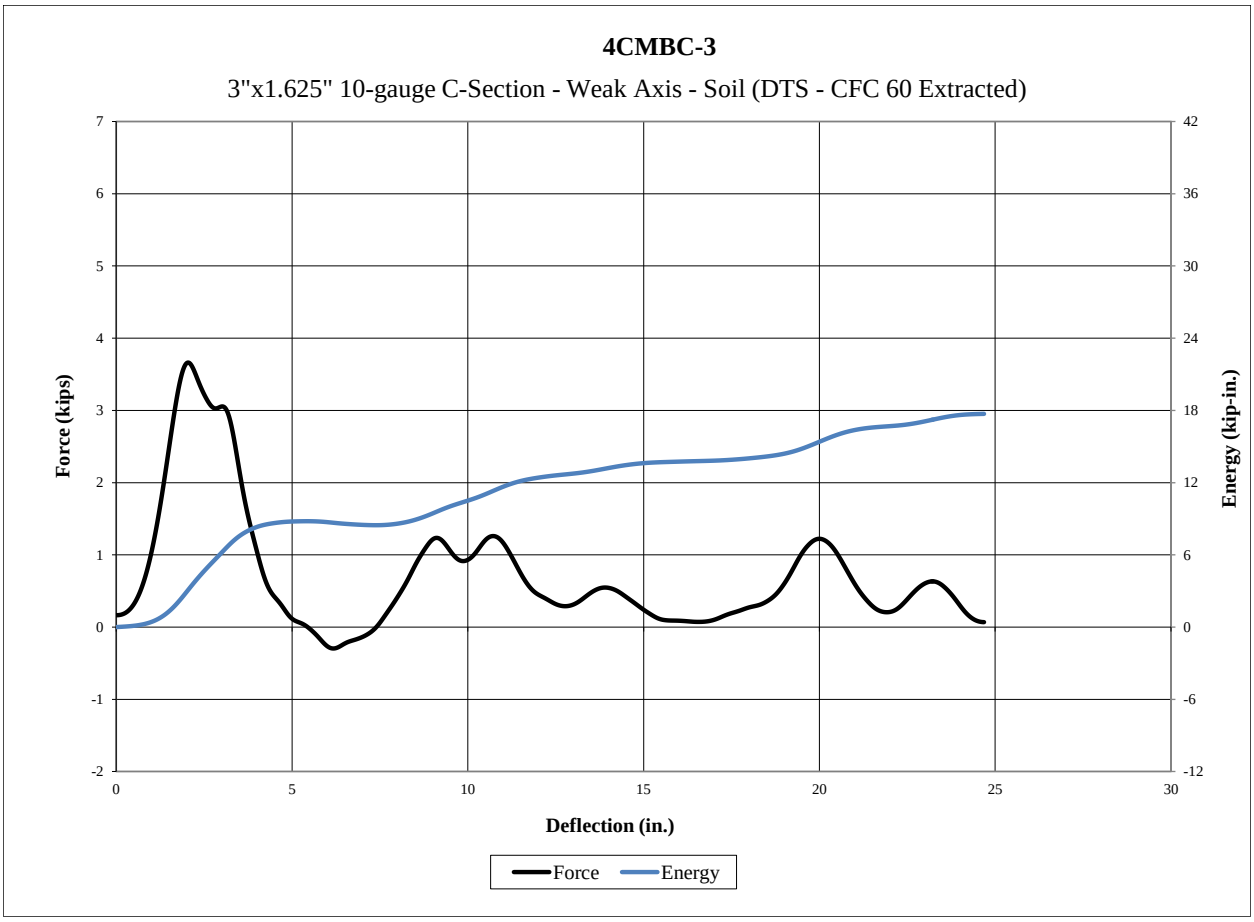

Figure 14. Force vs. Deflection and Energy vs. Deflection, Test No. 4CMBC-3

Pre-Test Post-Test

Figure 15. Pre-Test and Post-Test Photographs, Test No. 4CMBC-3


0.000 sec

0.120 sec


0.030 sec

0.150 sec

0.060 sec

0.180 sec

0.090 sec

0.210 sec

Figure 16. Sequential Photographs, Test No. 4CMBC-3

5.2.4 Test No. 4CMBC-4

During test no. 4CMBC-4, the bogie impacted the 10-gauge C-section steel post embedded in soil at a speed of 21.1 mph (34.0 km/h). As a result of the weak-axis impact, the post bent backward and yielded approximately 2 in. (51 mm) below the groundline. The bogie overrode the post at a maximum deflection of 22.1 in. (561 mm).

Force vs. deflection and energy vs. deflection curves created from the DTS accelerometer data are shown in Figure 17. The forces quickly rose to a peak force of 3.7 kips (16.5 kN) at 2.3 in. (58 mm) of deflection. The post provided an average resistive force of 0.9 kips (4.0 kN) through both 10 in. (254 mm) and 15 in. (381 mm) of deflection. The energy absorbed by the post was 8.6 kip-in. (1.0 kJ) through 10 in. (254 mm) of deflection and 13.5 kip-in. (1.5 kJ) through 15 in. (381 mm) of deflection. Pre-test and post-test photographs are shown in Figure 18. Time-sequential photographs are shown in Figure 19.

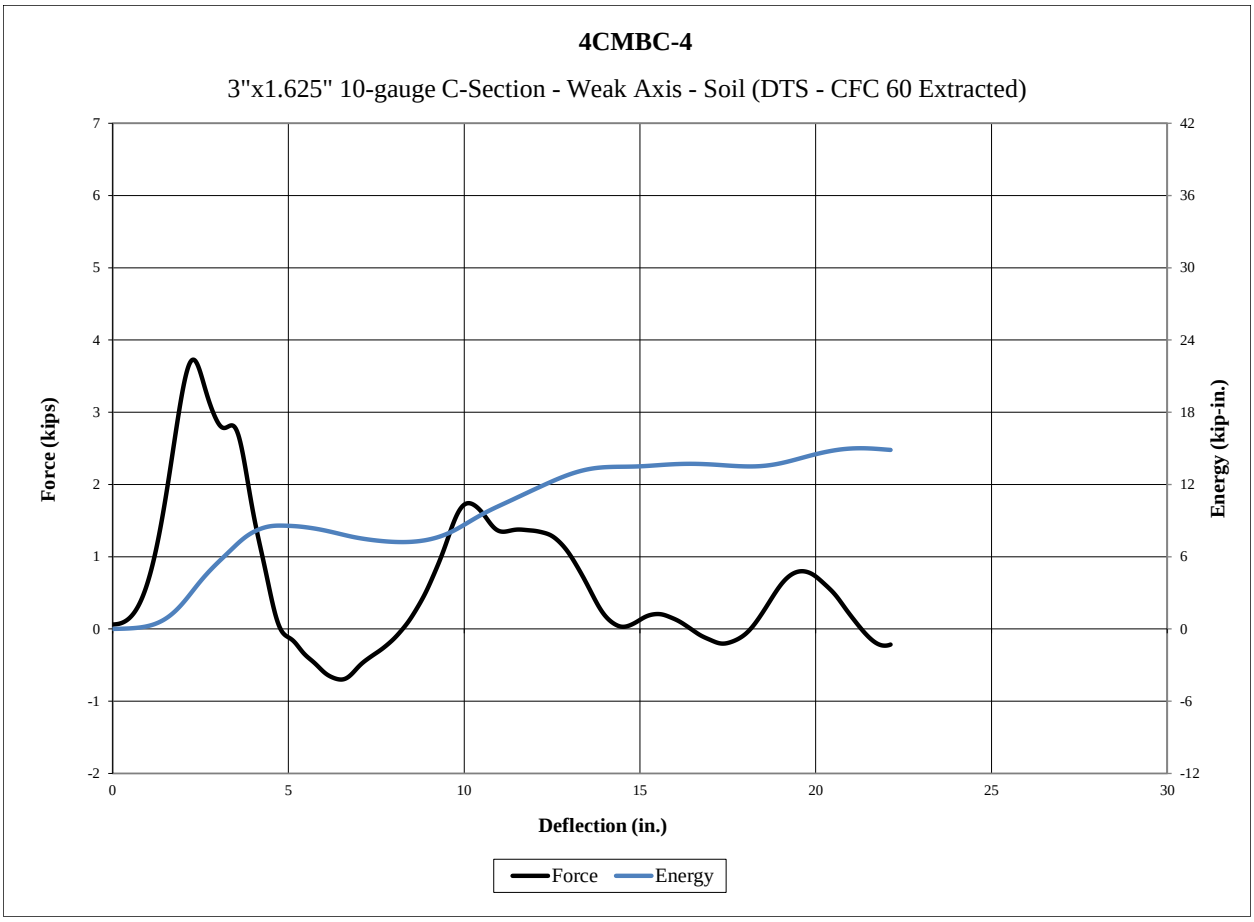

Figure 17. Force vs. Deflection and Energy vs. Deflection, Test No. 4CMBC-4

Pre-Test Post-Test

Figure 18. Pre-Test and Post-Test Photographs, Test No. 4CMBC-4


0.000 sec

0.120 sec


0.030 sec

0.150 sec

0.060 sec

0.180 sec

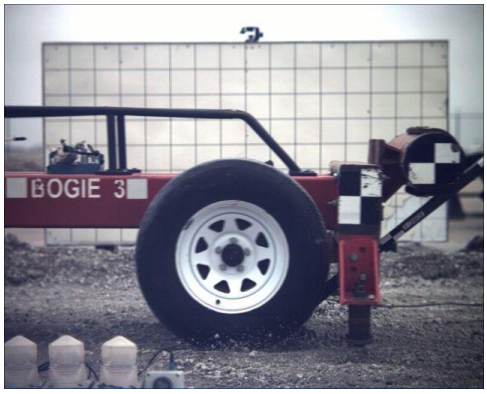

0.090 sec

0.210 sec

Figure 19. Sequential Photographs, Test No. 4CMBC-4

5.2.5 Test No. 4CMBC-5

During test no. 4CMBC-5, the bogie impacted the 7-gauge C-section steel post embedded in soil at a speed of 19.4 mph (31.2 km/h). As a result of the strong-axis impact, the post bent backward, twisted, and buckled approximately 6 in. (152 mm) above the groundline. The bogie overrode the post at a maximum deflection of 18.7 in. (475 mm).

Force vs. deflection and energy vs. deflection curves created from the DTS accelerometer data are shown in Figure 20. The forces quickly rose to a peak force of 5.4 kips (24.0 kN) at 2.1 in. (53 mm) of deflection. The post provided an average resistive force of 2.1 kips (9.3 kN) through 10 in. (254 mm) of deflection and 1.8 kips (8.0 kN) through 15 in. (381 mm) of deflection. The energy absorbed by the post was 20.6 kip-in. (2.3 kJ) through 10 in. (254 mm) of deflection and 27.7 kip-in. (3.1 kJ) through 15 in. (381 mm) of deflection. Pre-test and post-test photographs are shown in Figure 21. Time-sequential photographs are shown in Figure 22.

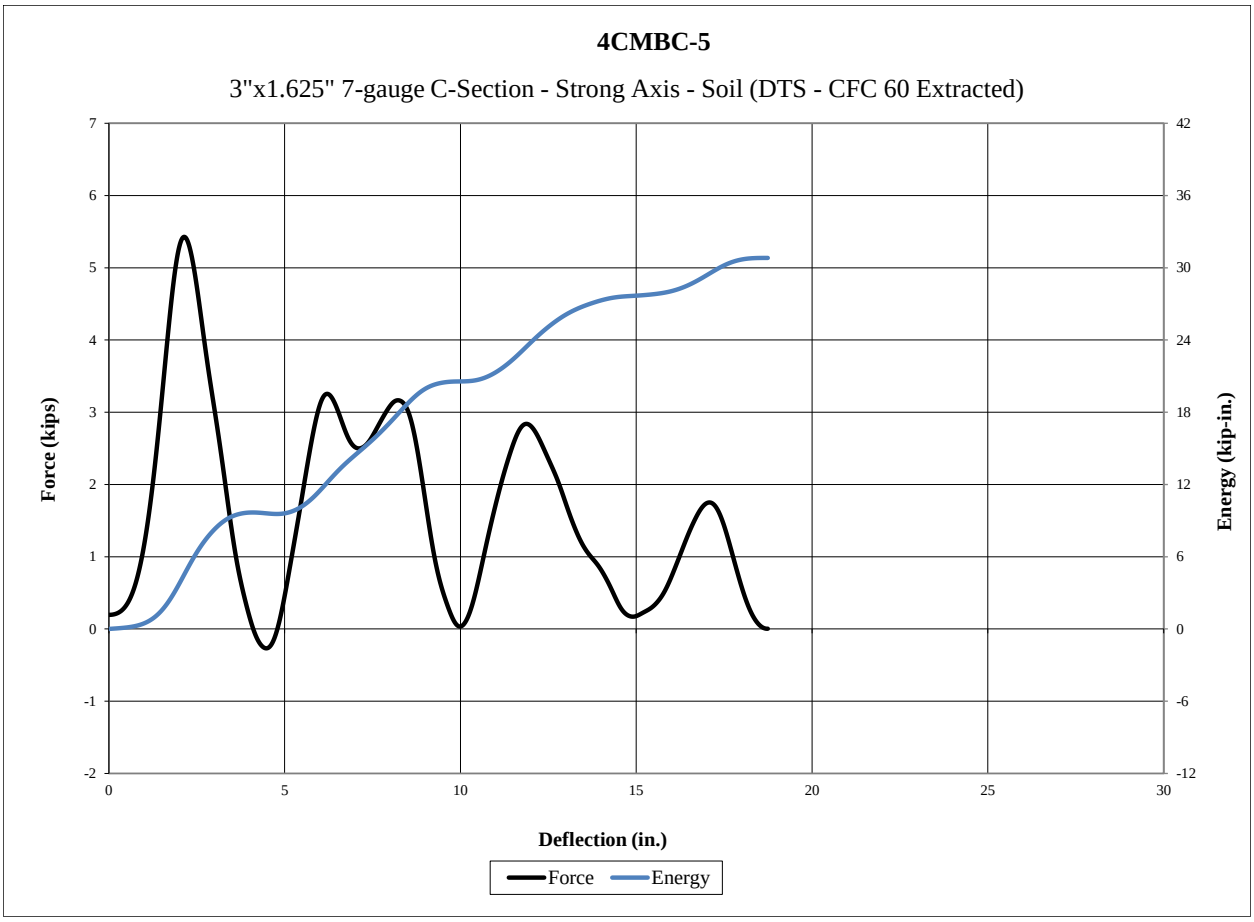

Figure 20. Force vs. Deflection and Energy vs. Deflection, Test No. 4CMBC-5

Pre-Test Post-Test

Figure 21. Pre-Test and Post-Test Photographs, Test No. 4CMBC-5


0.000 sec

0.120 sec


0.030 sec

0.150 sec


0.060 sec

0.180 sec

0.090 sec

0.210 sec

Figure 22. Sequential Photographs, Test No. 4CMBC-5

5.2.6 Test No. 4CMBC-6

During test no. 4CMBC-6, the bogie impacted the 7-gauge C-Section steel post embedded in soil at a speed of 20.4 mph (32.8 km/h). As a result of the strong-axis impact, the post bent backward, twisted, and buckled approximately 6 in. (152 mm) above the groundline. The bogie overrode the post at a maximum deflection of 19.3 in. (490 mm).

Force vs. deflection and energy vs. deflection curves created from the DTS accelerometer data are shown in Figure 23. The forces quickly rose to a peak force of 5.9 kips (26.2 kN) at 2.2 in. (56 mm) of deflection. There was a secondary force peak of 4.8 kips (21.4 kN) at 7.7 in. (196 mm) of deflection. The post provided an average resistive force of 2.4 kips (10.7 kN) through 10 in. (254 mm) of deflection and 1.9 kips (8.5 kN) through 15 in. (381 mm) of deflection. The energy absorbed by the post was 24.3 kip-in. (2.7 kJ) through 10 in. (254 mm) of deflection and 28.1 kip-in. (3.2 kJ) through 15 in. (381 mm) of deflection. Pre-test and post-test photographs are shown in Figure 24. Time-sequential photographs are shown in Figure 25.

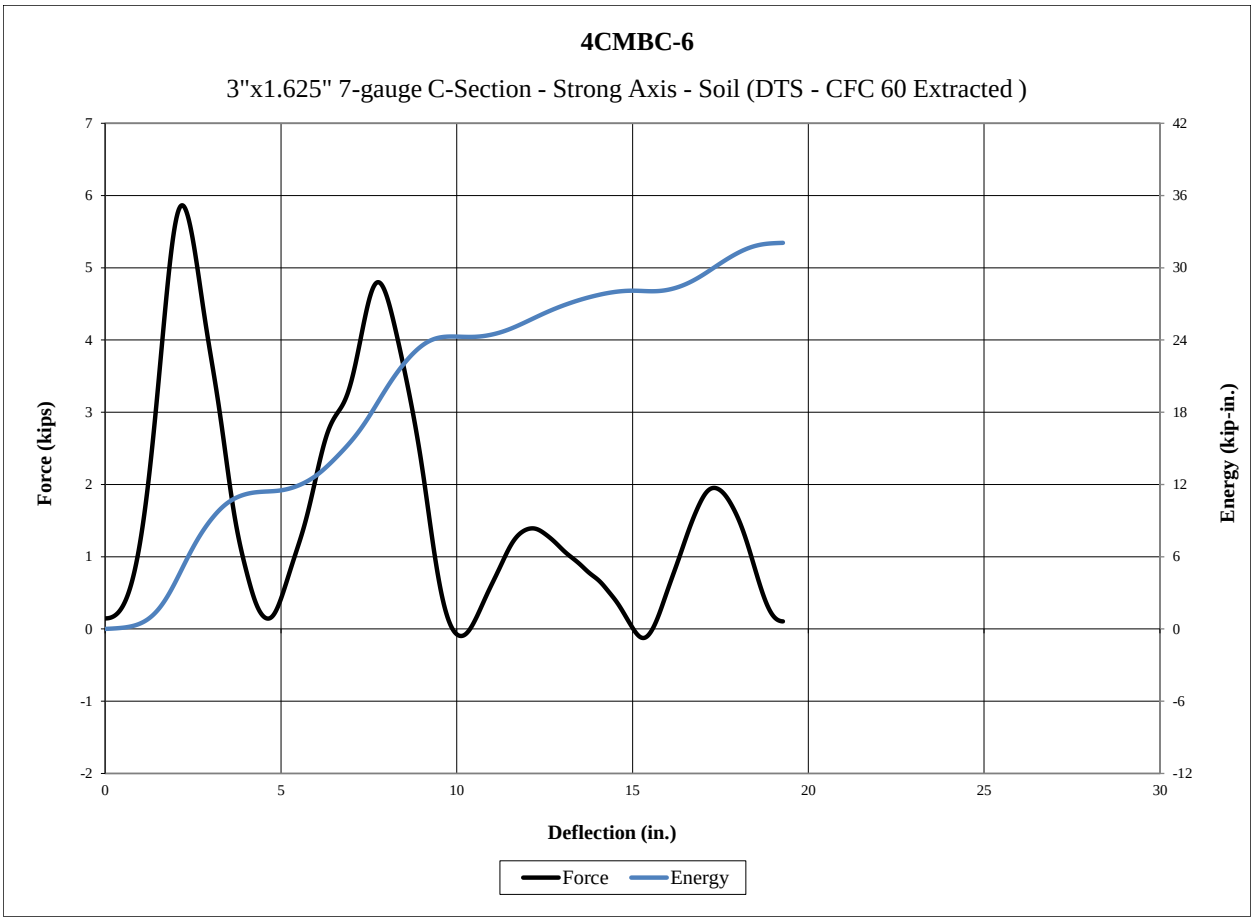

Figure 23. Force vs. Deflection and Energy vs. Deflection, Test No. 4CMBC-6

Pre-Test Post-Test

Figure 24. Pre-Test and Post-Test Photographs, Test No. 4CMBC-6


0.000 sec

0.120 sec


0.030 sec

0.150 sec

0.060 sec

0.180 sec

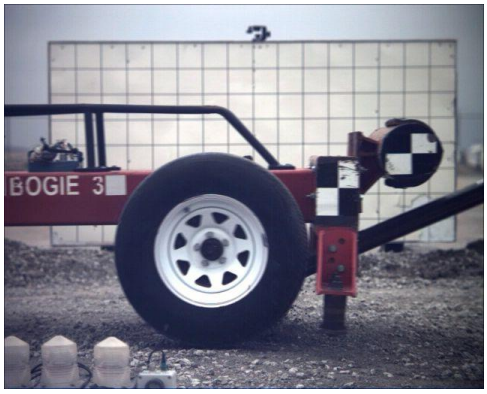

0.090 sec

0.210 sec

Figure 25. Sequential Photographs, Test No. 4CMBC-6

5.2.7 Test No. 4CMBC-7

During test no. 4CMBC-7, the bogie impacted the 7-gauge C-Section steel post embedded in soil at a speed of 21.9 mph (35.2 km/h). As a result of the weak-axis impact, the post bent backward, twisted, and yielded near the groundline. The bogie overrode the post at a maximum deflection of 24.0 in. (610 mm).

Force vs. deflection and energy vs. deflection curves created from the DTS accelerometer data are shown in Figure 26. The forces quickly rose to a peak force of 4.7 kips (20.9 kN) at 1.8 in. (46 mm) of deflection. The post provided an average resistive force of 1.5 kips (6.7 kN) through 10 in. (254 mm) of deflection and 1.4 kips (6.2 kN) through 15 in. (381 mm) of deflection. The energy absorbed by the post was 15.2 kip-in. (1.7 kJ) through 10 in. (254 mm) of deflection and 21.0 kip-in. (2.4 kJ) through 15 in. (381 mm) of deflection. Pre-test and post-test photographs are shown in Figure 27. Time-sequential photographs are shown in Figure 28.

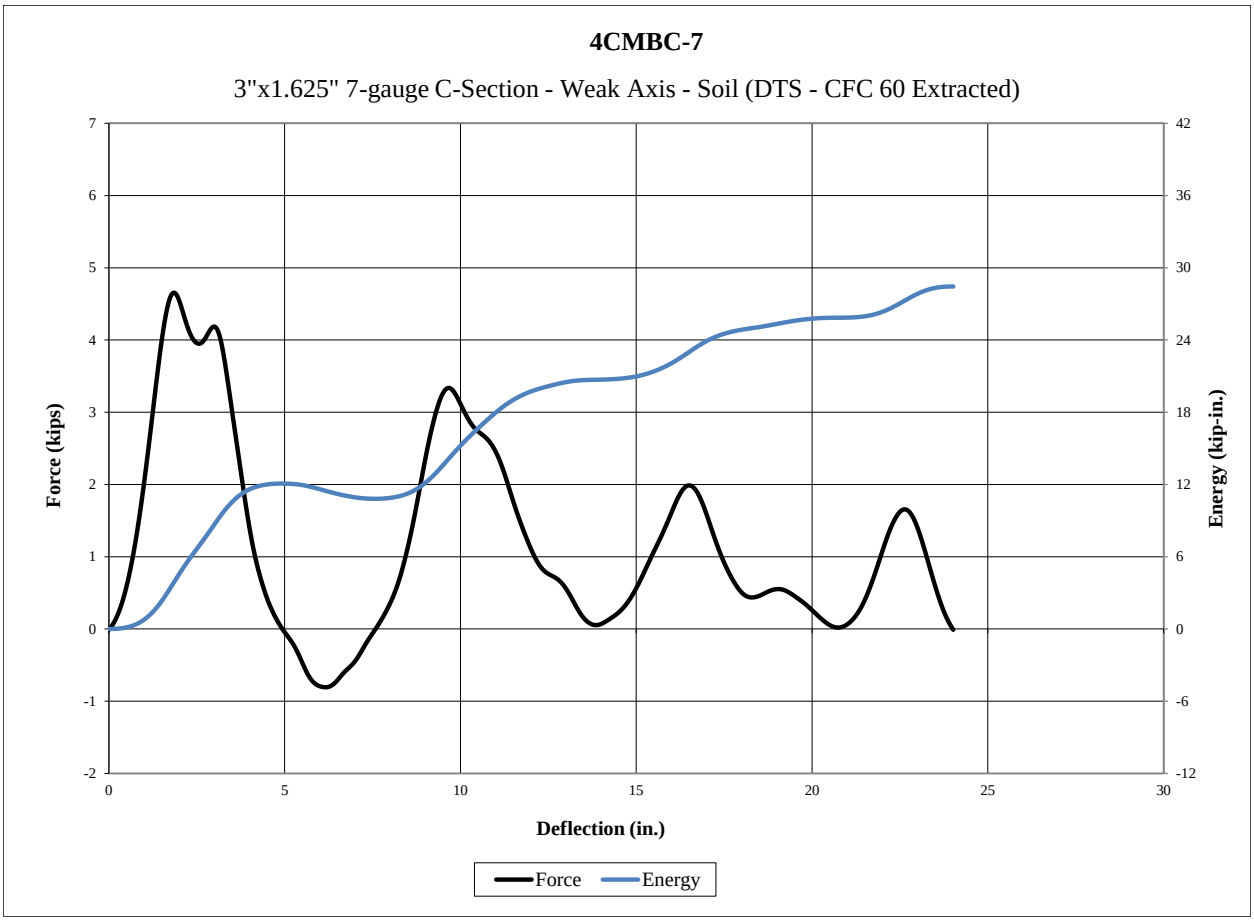

Figure 26. Force vs. Deflection and Energy vs. Deflection, Test No. 4CMBC-7

Post-Test

Post-Test

Figure 27. Pre-Test and Post-Test Photographs, Test No. 4CMBC-7

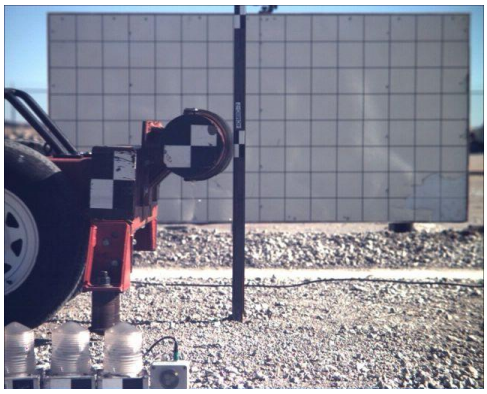
0.000 sec

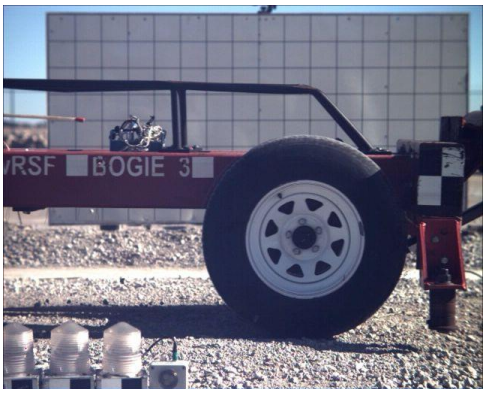

0.120 sec

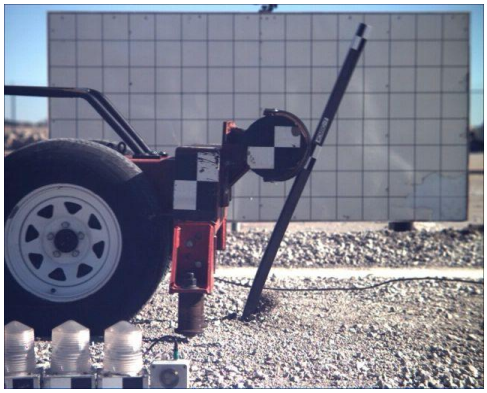
0.030 sec

0.150 sec

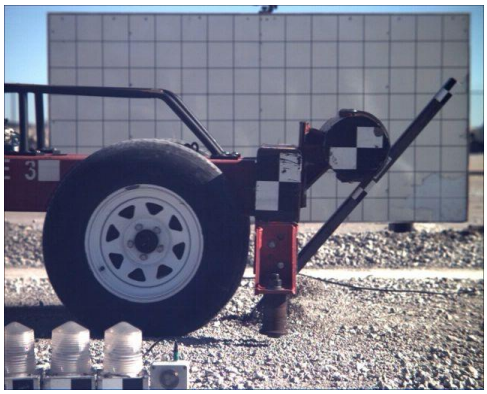
0.060 sec

0.180 sec

0.090 sec

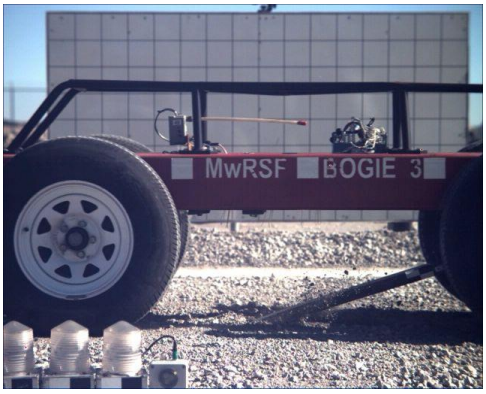

0.210 sec

Figure 28. Sequential Photographs, Test No. 4CMBC-7

5.2.8 Test No. 4CMBC-8

During test no. 4CMBC-8, the bogie impacted the 7-gauge C-Section steel post embedded in soil at a speed of 21.0 mph (33.8 km/h). As a result of the weak-axis impact, the post bent backward, twisted, and yielded near the groundline. The bogie overrode the post at a maximum deflection of 26.7 in. (678 mm).

Force vs. deflection and energy vs. deflection curves created from the DTS accelerometer data are shown in Figure 29. The forces quickly rose to a peak force of 4.2 kips (18.7 kN) at 1.7 in. (43 mm) of deflection. The post provided an average resistive force of 1.3 kips (5.8 kN) through 10 in. (254 mm) of deflection and 1.1 kips (4.9 kN) through 15 in. (381 mm) of deflection. The energy absorbed by the post was 12.6 kip-in. (1.4 kJ) through 10 in. (254 mm) of deflection and 17.2 kip-in. (1.9 kJ) through 15 in. (381 mm) of deflection. Pre-test and post-test photographs are shown in Figure 30. Due to technical difficulties, time-sequential photographs could not be collected.

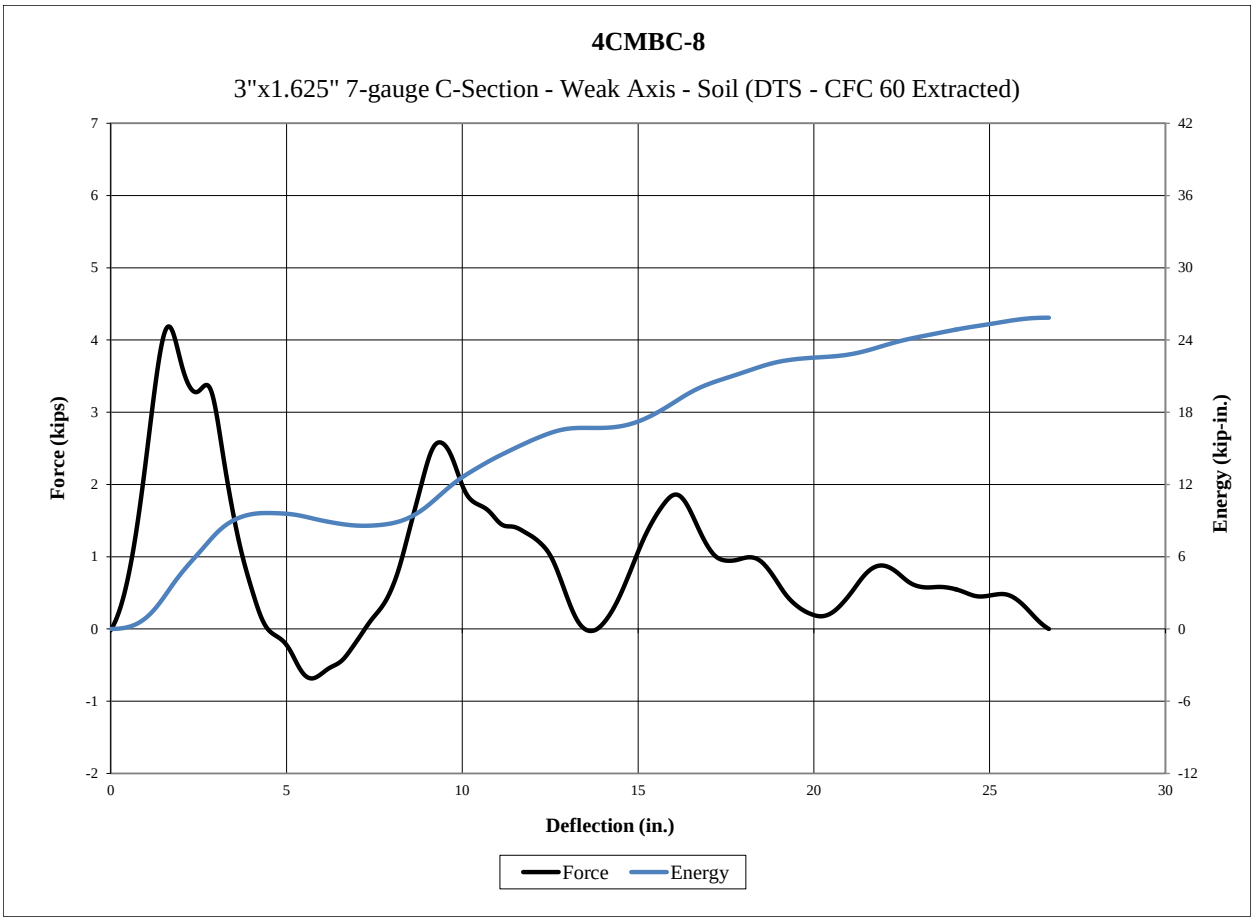

Figure 29. Force vs. Deflection and Energy vs. Deflection, Test No. 4CMBC-8

Pre-Test Post-Test

Figure 30. Pre-Test and Post-Test Photographs, Test No. 4CMBC-8

5.2.9 Test No. 4CMBC-9

During test no. 4CMBC-9, the bogie impacted the 10-gauge C-Section steel post in a rigid sleeve at a speed of 21.1 mph (34.0 km/h). As a result of the strong-axis impact, the post bent backward, twisted, and yielded approximately 13 in. (330 mm) above the groundline. The bogie overrode the post at a maximum deflection of 18.2 in. (462 mm).

Force vs. deflection and energy vs. deflection curves created from the DTS accelerometer data are shown in Figure 31. The forces quickly rose to a peak force of 4.5 kips (20.0 kN) at 2.3 in. (58 mm) of deflection. The post provided an average resistive force of 1.9 kips (8.5 kN) through 10 in. (254 mm) of deflection and 1.5 kips (6.7 kN) through 15 in. (381 mm) of deflection. The energy absorbed by the post was 19.0 kip-in. (2.1 kJ) through 10 in. (254 mm) of deflection and 21.8 kip-in. (2.5 kJ) through 15 in. (381 mm) of deflection. Pre-test and post-test photographs are shown in Figure 32. Time-sequential photographs are shown in Figure 33.

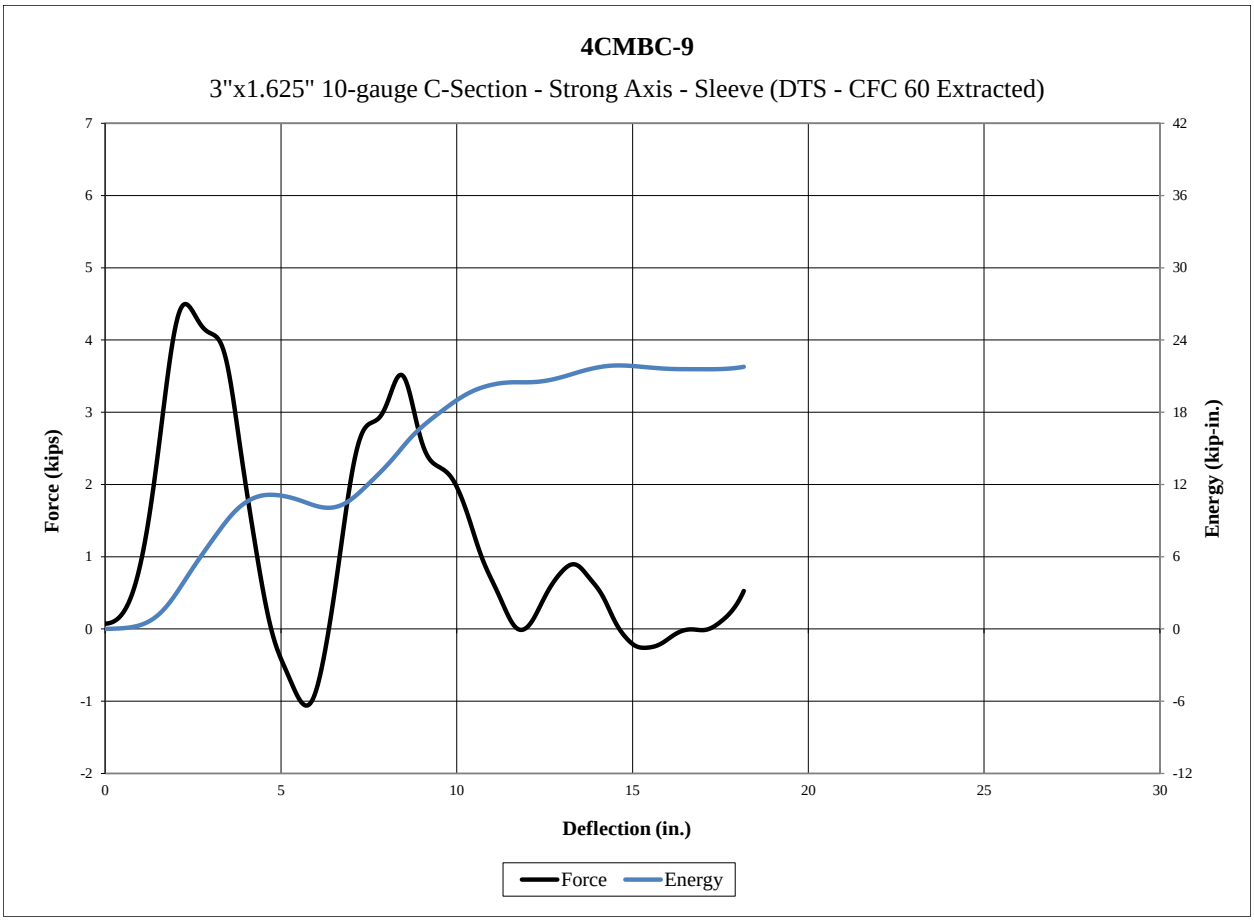

Figure 31. Force vs. Deflection and Energy vs. Deflection, Test No. 4CMBC-9

Pre-Test Post-Test

Figure 32. Pre-Test and Post-Test Photographs, Test No. 4CMBC-9

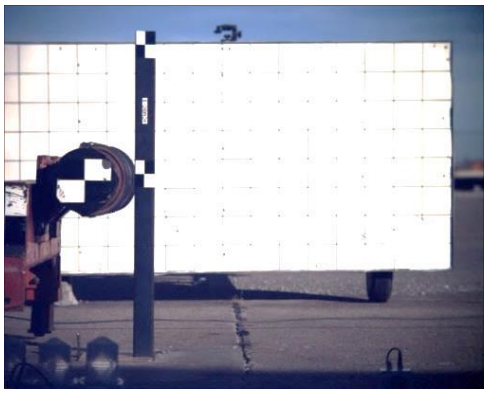
0.000 sec

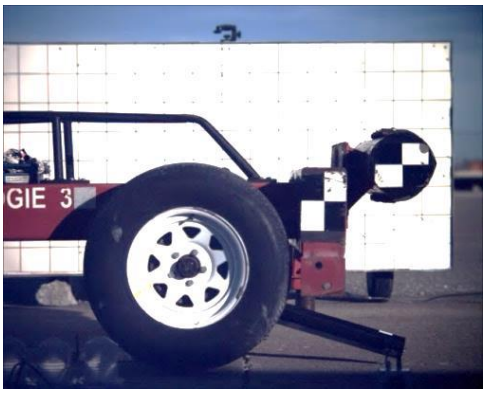

0.120 sec

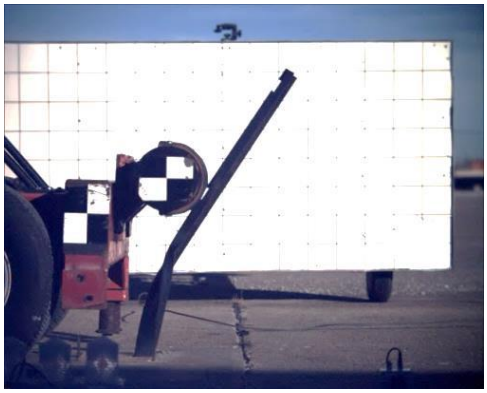
0.030 sec

0.150 sec


0.060 sec

0.180 sec

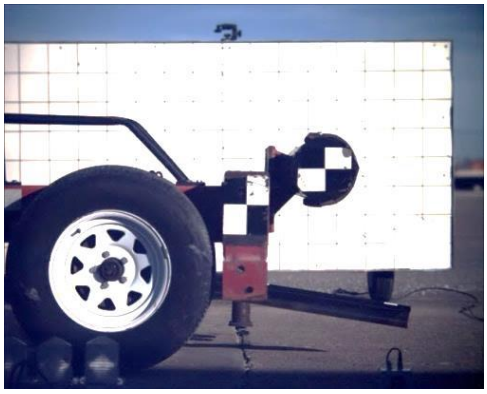
0.090 sec

0.210 sec

Figure 33. Sequential Photographs, Test No. 4CMBC-9

5.2.10 Test No. 4CMBC-10

During test no. 4CMBC-10, the bogie impacted the 10-gauge C-Section steel post in a rigid sleeve at a speed of 20.0 mph (32.2 km/h). As a result of the strong-axis impact, the post bent backward, twisted, and buckled approximately 13 in. (330 mm) above the groundline. The bogie overrode the post at a maximum deflection of 18.5 in. (470 mm).

Force vs. deflection and energy vs. deflection curves created from the DTS accelerometer data are shown in Figure 34. The forces quickly rose to a peak force of 4.3 kips (19.1 kN) at 1.8 in. (46 mm) of deflection. The post provided an average resistive force of 1.8 kips (8.0 kN) through 10 in. (254 mm) of deflection and 1.3 kips (5.8 kN) through 15 in. (381 mm) of deflection. The energy absorbed by the post was 18.4 kip-in. (2.1 kJ) through 10 in. (254 mm) of deflection and 20.2 kip-in. (2.3 kJ) through 15 in. (381 mm) of deflection. Pre-test and post-test photographs are shown in Figure 35. Time-sequential photographs are shown in Figure 36.

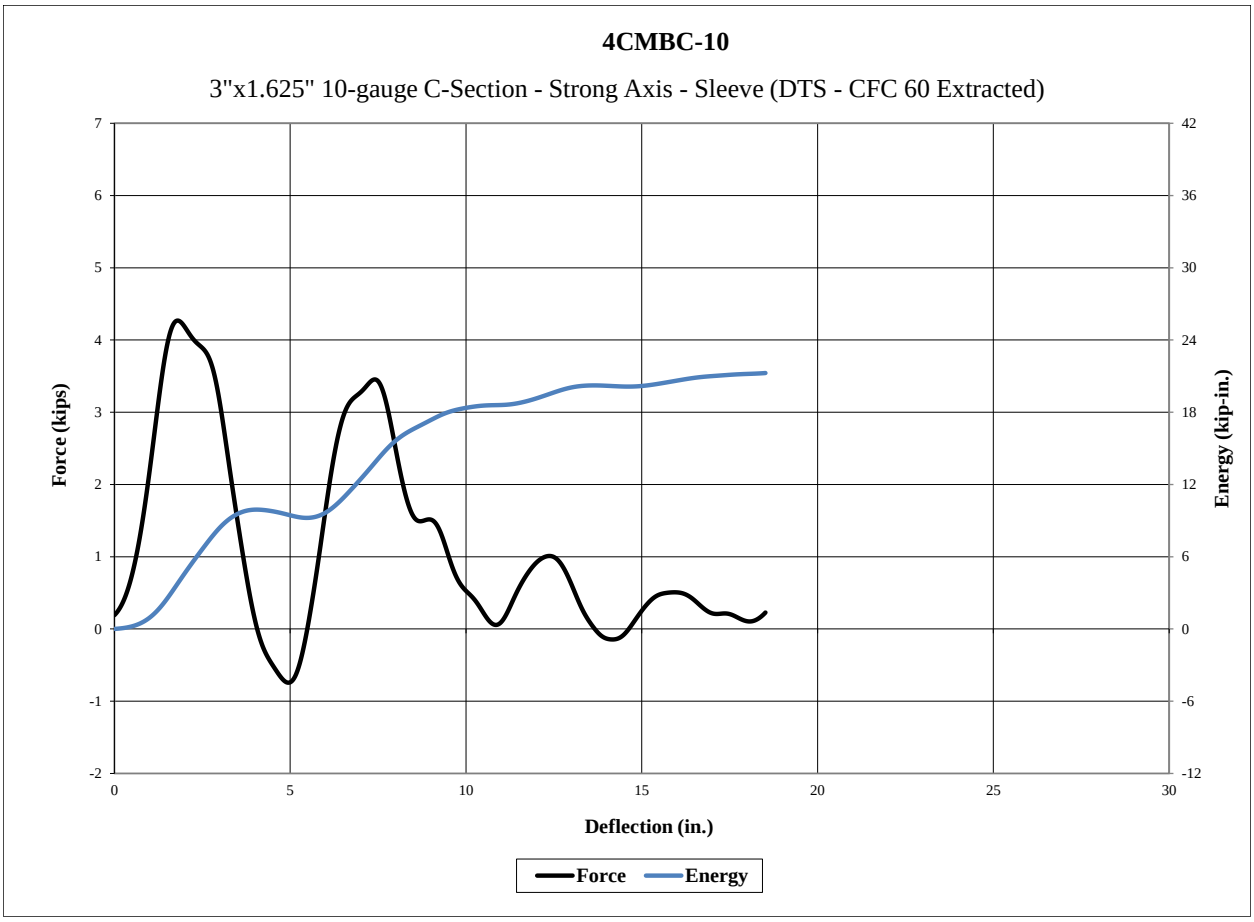

Figure 34. Force vs. Deflection and Energy vs. Deflection, Test No. 4CMBC-10

Pre-Test Post-Test

Figure 35. Pre-Test and Post-Test Photographs, Test No. 4CMBC-10

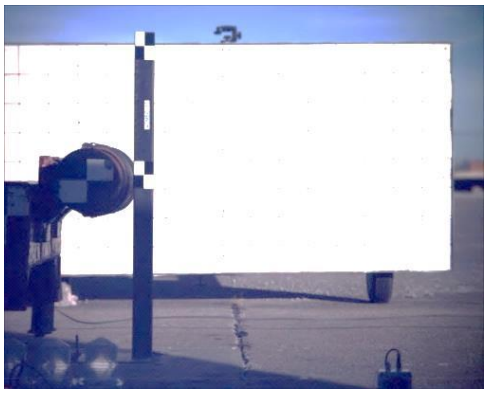
0.000 sec


0.120 sec

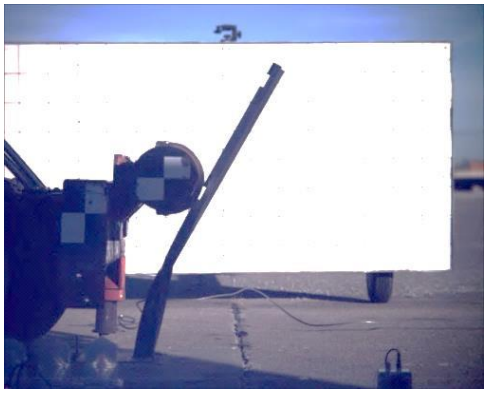
0.030 sec

0.150 sec

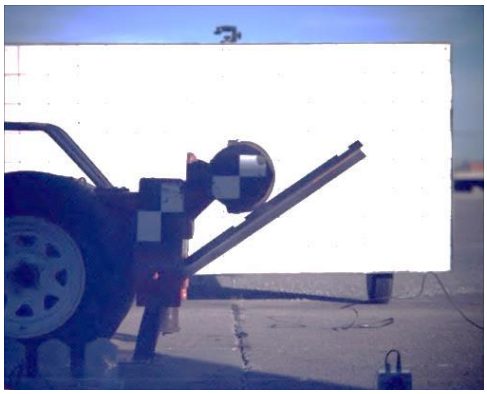
0.060 sec

0.180 sec

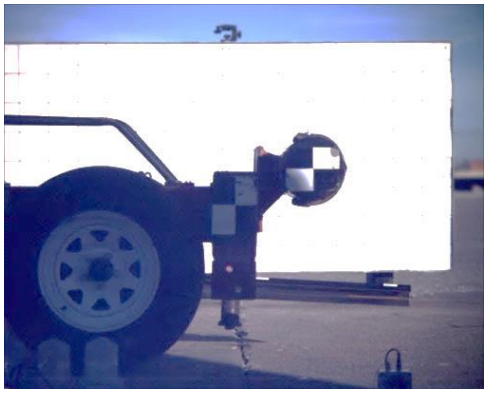
0.090 sec

0.210 sec

Figure 36. Sequential Photographs, Test No. 4CMBC-10

5.2.11 Test No. 4CMBC-11

During test no. 4CMBC-11, the bogie impacted the 7-gauge C-Section steel post in a rigid sleeve at a speed of 20.5 mph (33.0 km/h). As a result of the strong-axis impact, the post bent backward, twisted, and buckled approximately 11 in. (279 mm) above the groundline. The bogie overrode the post at a maximum deflection of 19.5 in. (495 mm).

Force vs. deflection and energy vs. deflection curves created from the DTS accelerometer data are shown in Figure 37. The forces quickly rose to a peak force of 5.5 kips (24.5 kN) at 1.9 in. (48 mm) of deflection. The post provided an average resistive force of 2.5 kips (11.1 kN) through 10 in. (254 mm) of deflection and 1.9 kips (8.5 kN) through 15 in. (381 mm) of deflection. The energy absorbed by the post was 24.8 kip-in. (2.8 kJ) through 10 in. (254 mm) of deflection and 29.1 kip-in. (3.3 kJ) through 15 in. (381 mm) of deflection. Pre-test and post-test photographs are shown in Figure 38. Time-sequential photographs are shown in Figure 39.

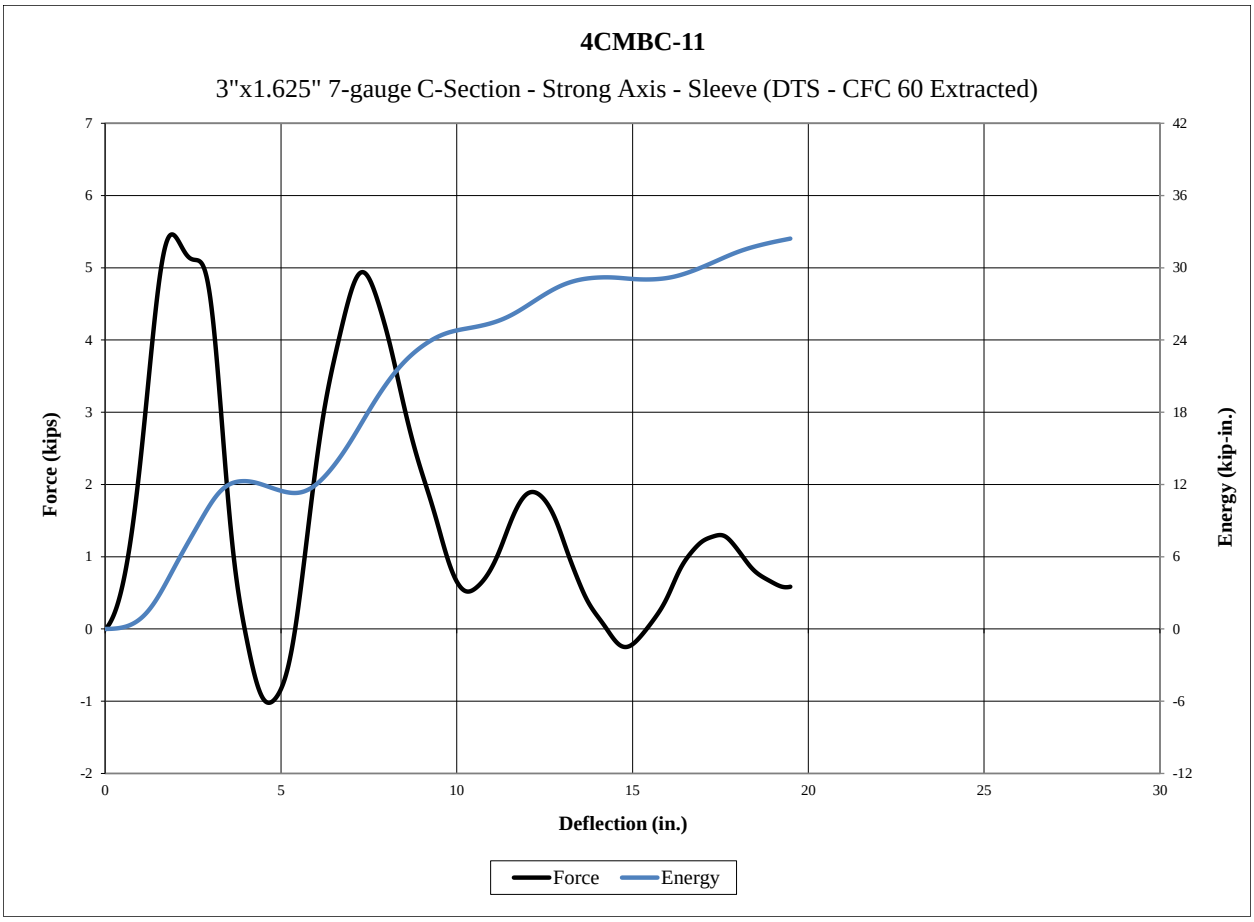

Figure 37. Force vs. Deflection and Energy vs. Deflection, Test No. 4CMBC-11

Pre-Test Post-Test

Figure 38. Pre-Test and Post-Test Photographs, Test No. 4CMBC-11

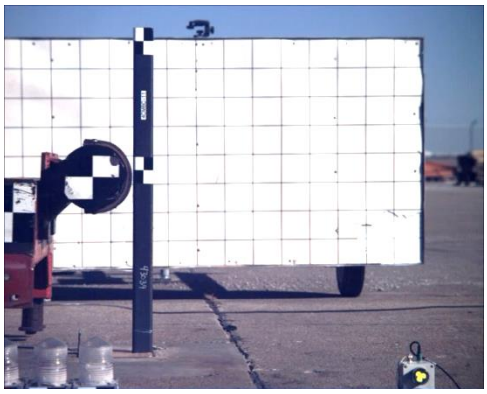
0.000 sec

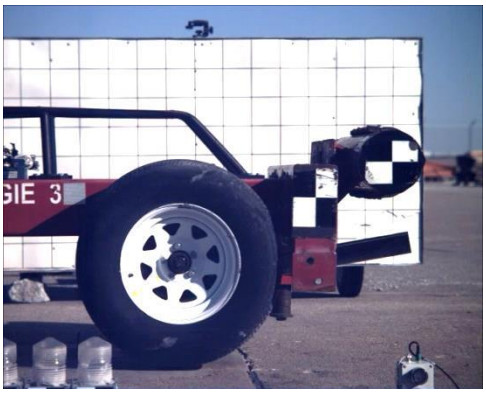

0.120 sec

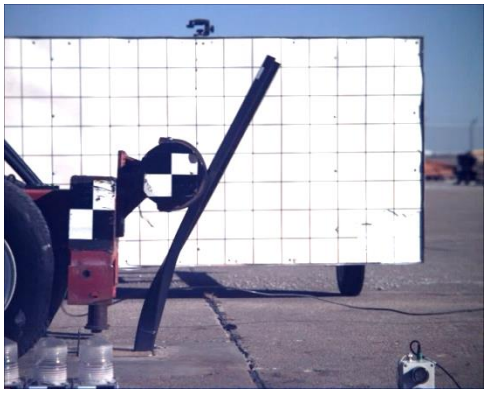
0.030 sec

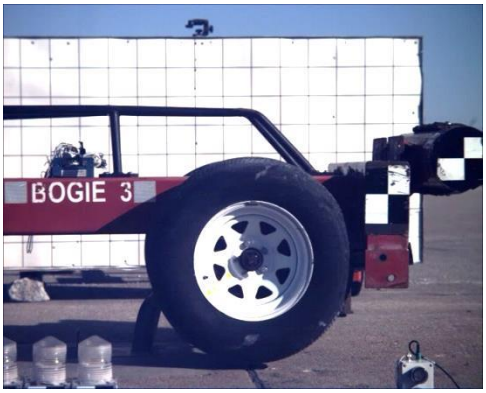

0.150 sec

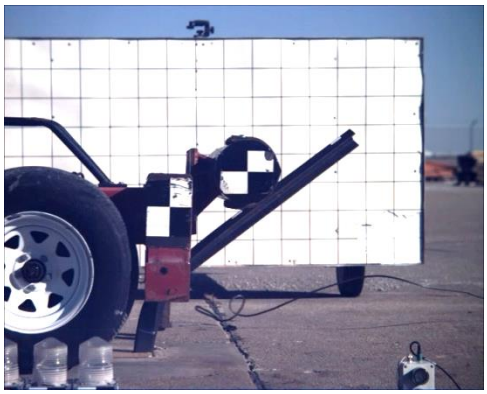
0.060 sec

0.180 sec

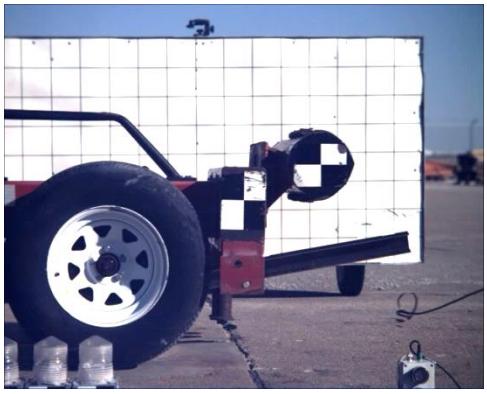
0.090 sec

0.210 sec

Figure 39. Sequential Photographs, Test No. 4CMBC-11

5.2.12 Test No. 4CMBC-12

During test no. 4CMBC-12, the bogie impacted the 7-gauge C-Section steel post in a rigid sleeve at a speed of 20.9 mph (33.6 km/h). As a result of the strong-axis impact, the post bent backward, twisted, and buckled approximately 11 in. (279 mm) above the groundline. The bogie overrode the post at a maximum deflection of 20.2 in. (513 mm).

Force vs. deflection and energy vs. deflection curves created from the DTS accelerometer data are shown in Figure 40. The forces quickly rose to a peak force of 6.2 kips (27.6 kN) at 2.3 in. (58 mm) of deflection. The post provided an average resistive force of 2.7 kips (12.0 kN) through 10 in. (254 mm) of deflection and 2.1 kips (9.3 kN) through 15 in. (381 mm) of deflection. The energy absorbed by the post was 26.9 kip-in. (3.0 kJ) through 10 in. (254 mm) of deflection and 31.6 kip-in. (3.6 kJ) through 15 in. (381 mm) of deflection. Post-test photographs are shown in Figure 41. Time-sequential photographs are shown in Figure 42.

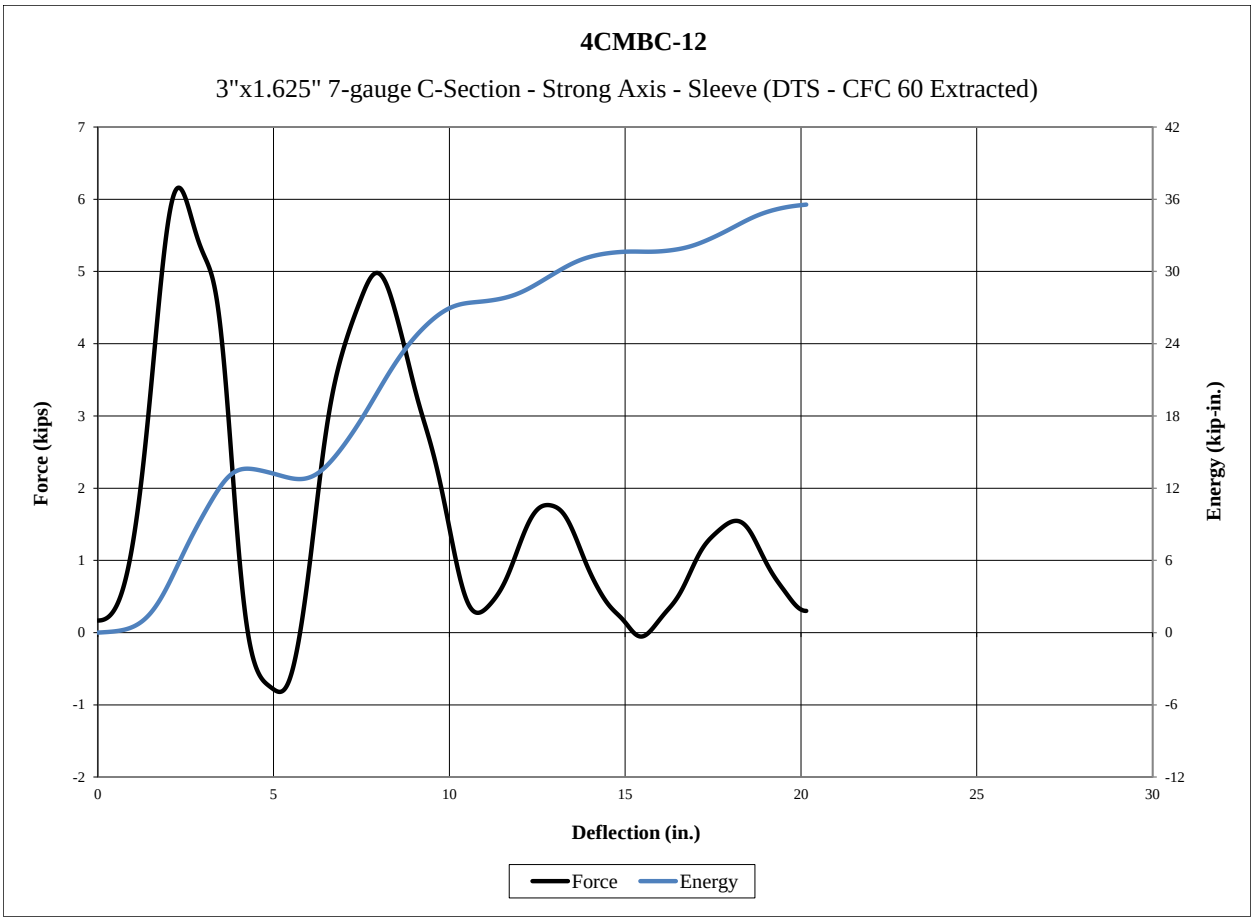

Figure 40. Force vs. Deflection and Energy vs. Deflection, Test No. 4CMBC-12

Post-Test

Figure 41. Post-Test Photograph, Test No. 4CMBC-12

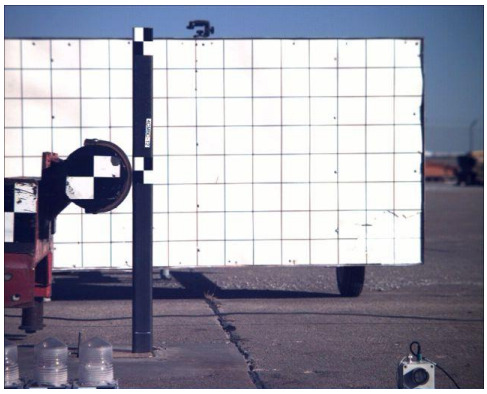
0.000 sec

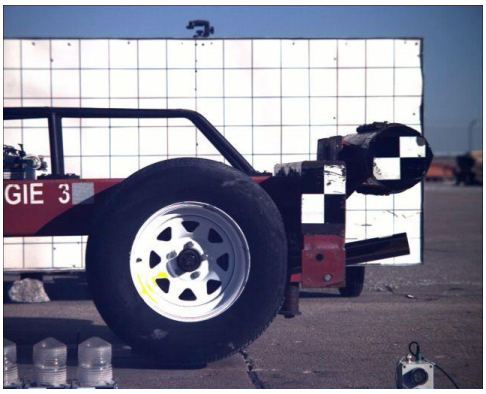

0.120 sec

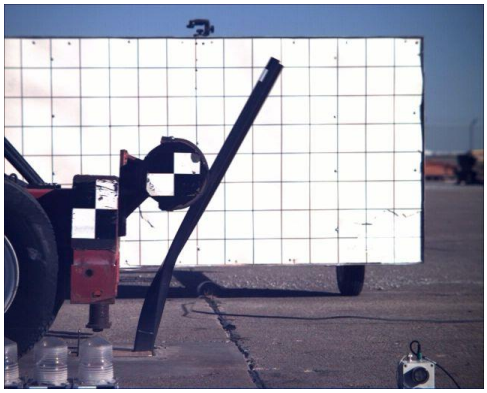
0.030 sec

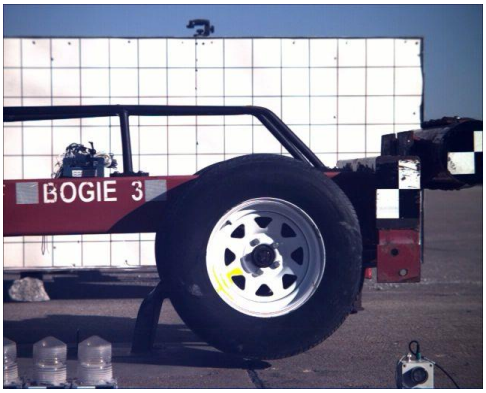

0.150 sec

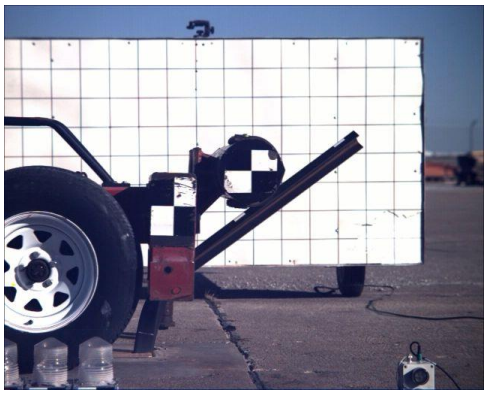
0.060 sec

0.180 sec

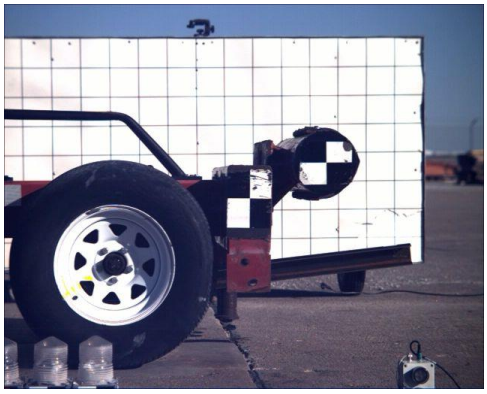
0.090 sec

0.210 sec

Figure 42. Sequential Photographs, Test No. 4CMBC-12

5.2.13 Test No. 4CMBC-13

During test no. 4CMBC-13, the bogie impacted the 10-gauge C-Section steel post in a rigid sleeve at a speed of 20.3 mph (32.7 km/h). As a result of the weak-axis impact, the post bent backward and yielded near the groundline. The bogie overrode the post at a maximum deflection of 20.4 in. (518 mm).

Force vs. deflection and energy vs. deflection curves created from the DTS accelerometer data are shown in Figure 43. The forces quickly rose to a peak force of 3.7 kips (16.5 kN) at 3.0 in. (76 mm) of deflection. The post provided an average resistive force of 0.7 kips (3.1 kN) through both 10 in. (254 mm) and 15 in. (381 mm) of deflection. The energy absorbed by the post was 7.1 kip-in. (0.8 kJ) through 10 in. (254 mm) of deflection and 10.0 kip-in. (1.1 kJ) through 15 in. (381 mm) of deflection. Pre-test and post-test photographs are shown in Figure 44. Time-sequential photographs are shown in Figure 45.

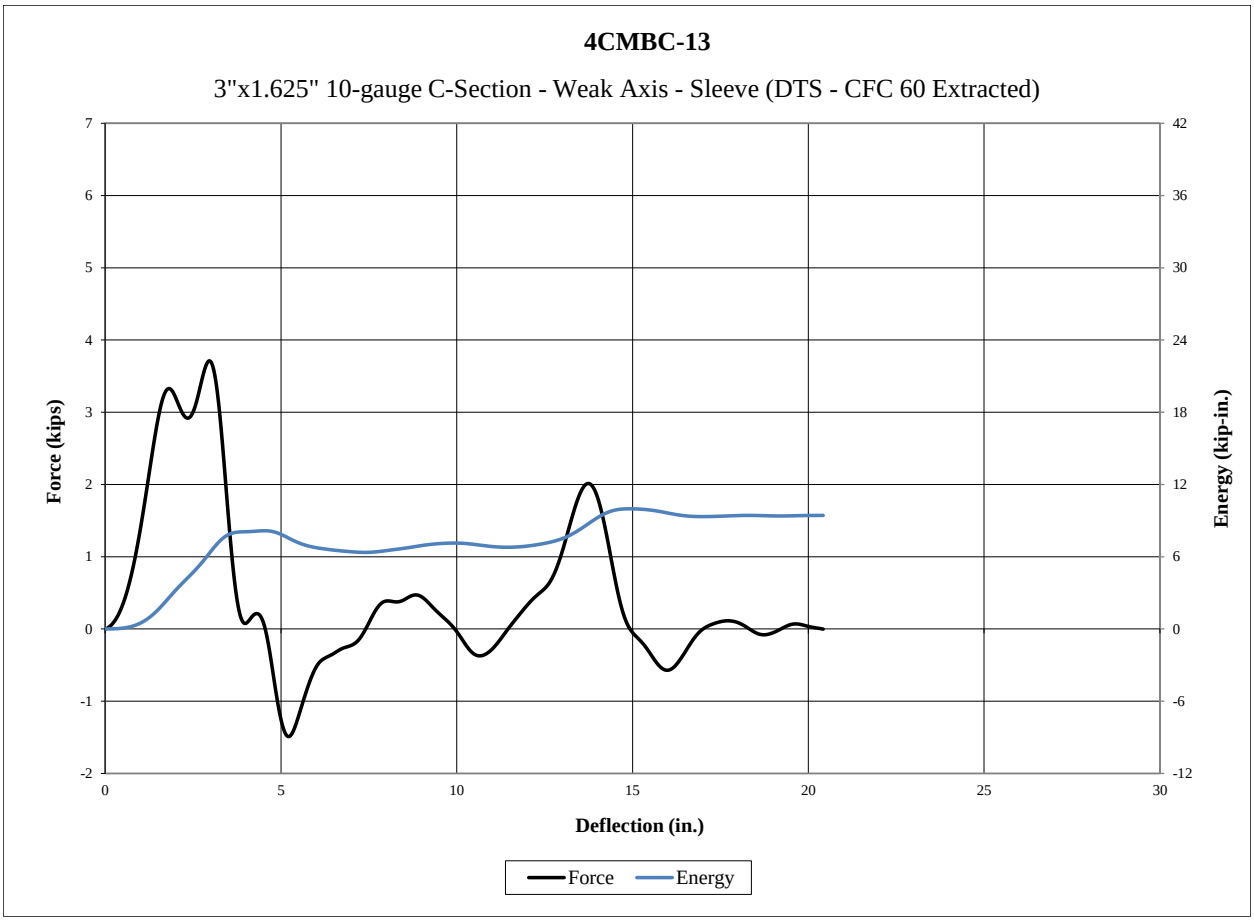

Figure 43. Force vs. Deflection and Energy vs. Deflection, Test No. 4CMBC-13

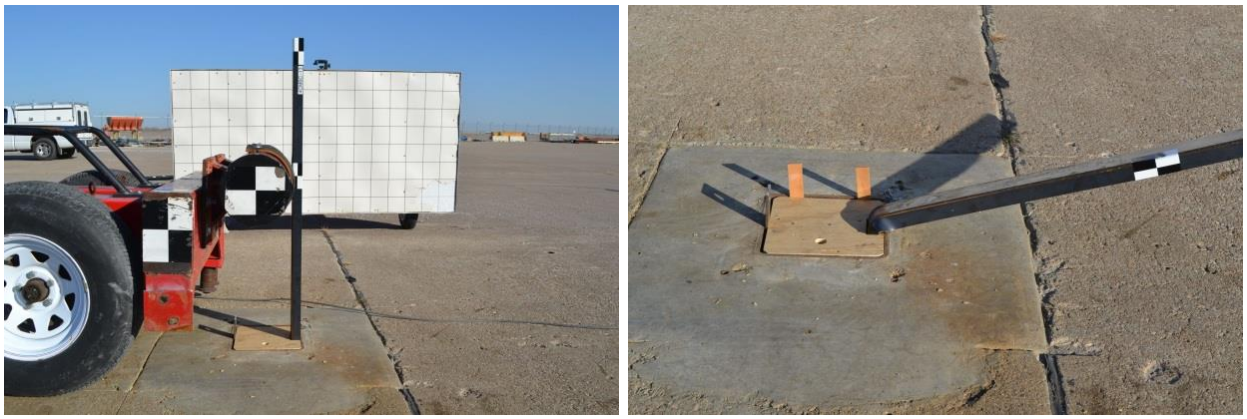

Pre-Test Post-Test

Figure 44. Pre-Test and Post-Test Photographs, Test No. 4CMBC-13

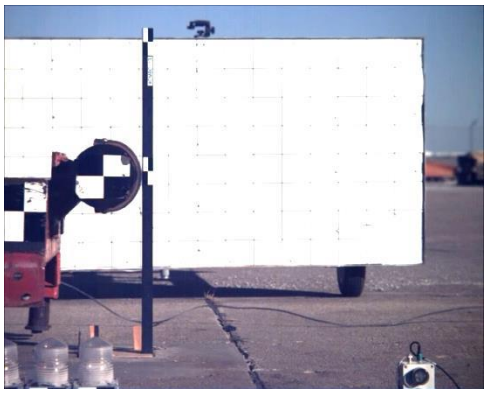
0.000 sec

0.120 sec

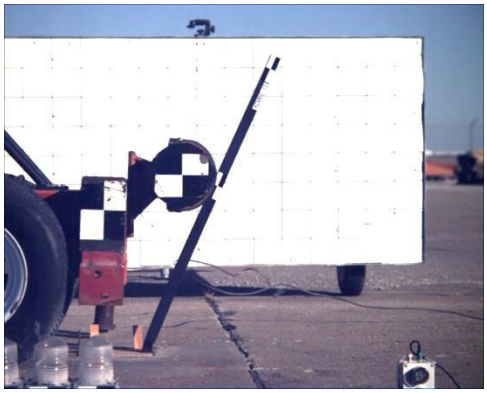
0.030 sec

0.150 sec

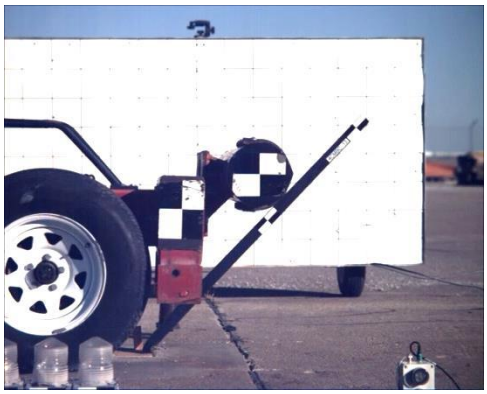
0.060 sec

0.180 sec

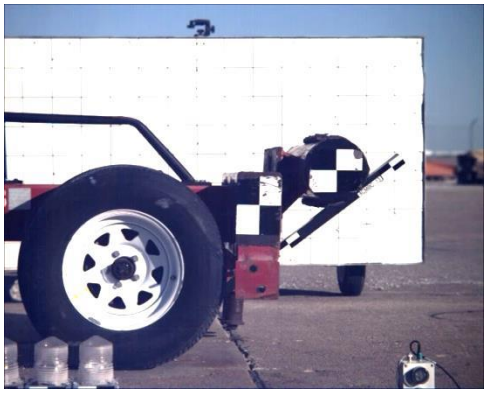
0.090 sec

0.210 sec

Figure 45. Sequential Photographs, Test No. 4CMBC-13

5.2.14 Test No. 4CMBC-14

During test no. 4CMBC-14, the bogie impacted the 10-gauge C-Section steel post in a rigid sleeve at a speed of 21.0 mph (33.8 km/h). As a result of the weak-axis impact, the post bent backward and yielded near the groundline. The bogie overrode the post at a maximum deflection of 21.6 in. (549 mm).

Force vs. deflection and energy vs. deflection curves created from the DTS accelerometer data are shown in Figure 46. The forces quickly rose to a peak force of 3.8 kips (16.9 kN) at 3.2 in. (81 mm) of deflection. The post provided an average resistive force of 1.0 kips (4.4 kN) through 10 in. (254 mm) of deflection and 0.9 kips (4.0 kN) through 15 in. (381 mm) of deflection. The energy absorbed by the post was 10.1 kip-in. (1.1 kJ) through 10 in. (254 mm) of deflection and 13.9 kip-in. (1.6 kJ) through 15 in. (381 mm) of deflection. Pre-test and post-test photographs are shown in Figure 47. Time-sequential photographs are shown in Figure 48.

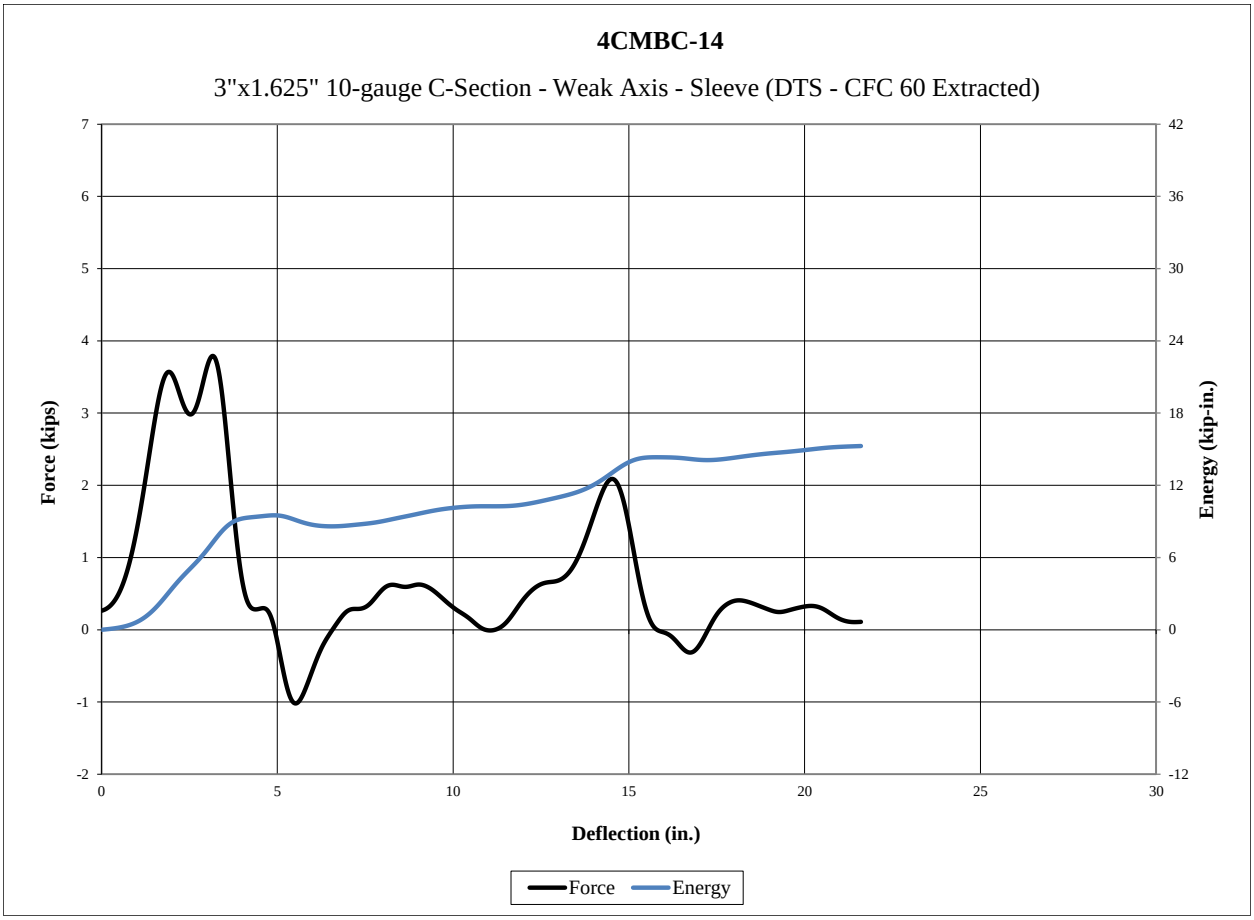

Figure 46. Force vs. Deflection and Energy vs. Deflection, Test No. 4CMBC-14

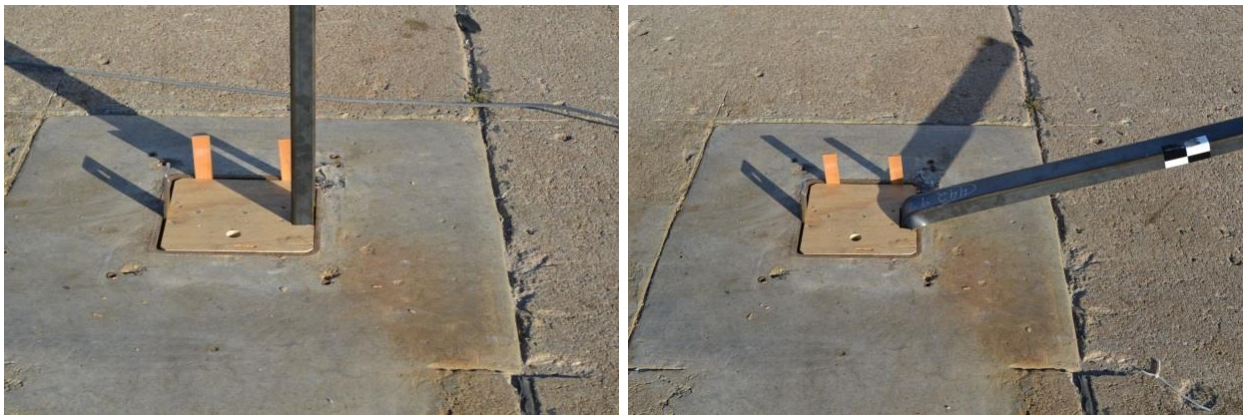

Pre-Test Post-Test

Figure 47. Pre-Test and Post-Test Photographs, Test No. 4CMBC-14

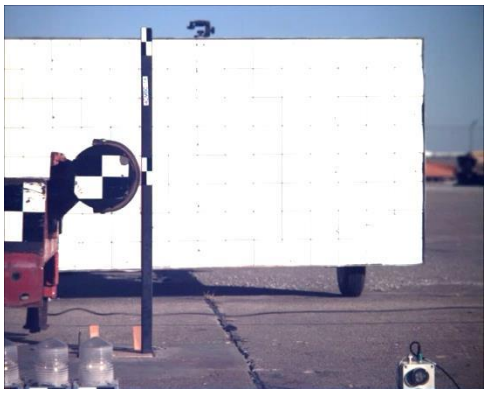
0.000 sec

0.120 sec

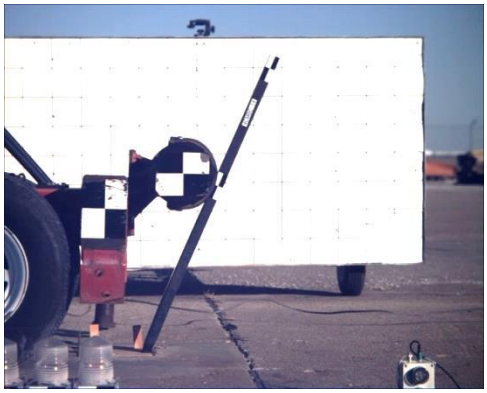
0.030 sec

0.150 sec


0.060 sec

0.180 sec

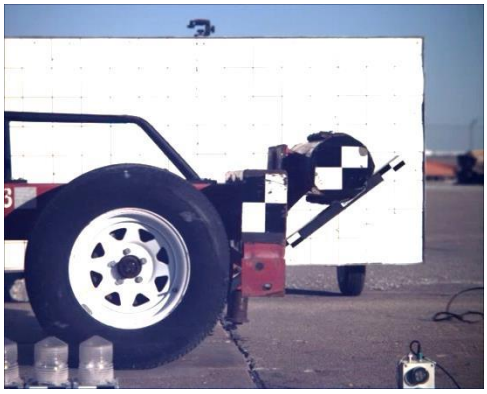
0.090 sec

0.210 sec

Figure 48. Sequential Photographs, Test No. 4CMBC-14

5.2.15 Test No. 4CMBC-15

During test no. 4CMBC-15, the bogie impacted the 10-gauge C-Section steel post in a rigid sleeve at a speed of 20.7 mph (33.3 km/h). As a result of the weak-axis impact, the post bent backward and yielded near the groundline. The bogie overrode the post at a maximum deflection of 19.7 in. (500 mm).

Force vs. deflection and energy vs. deflection curves created from the DTS accelerometer data are shown in Figure 49. The forces quickly rose to a peak force of 5.2 kips (23.1 kN) at 3.4 in. (86 mm) of deflection. The post provided an average resistive force of 1.6 kips (7.1 kN) through 10 in. (254 mm) of deflection and 1.3 kips (5.8 kN) through 15 in. (381 mm) of deflection. The energy absorbed by the post was 16.3 kip-in. (1.8 kJ) through 10 in. (254 mm) of deflection and 19.8 kip-in. (2.2 kJ) through 15 in. (381 mm) of deflection. Pre-test and post-test photographs are shown in Figure 50. Time-sequential photographs are shown in Figure 51.

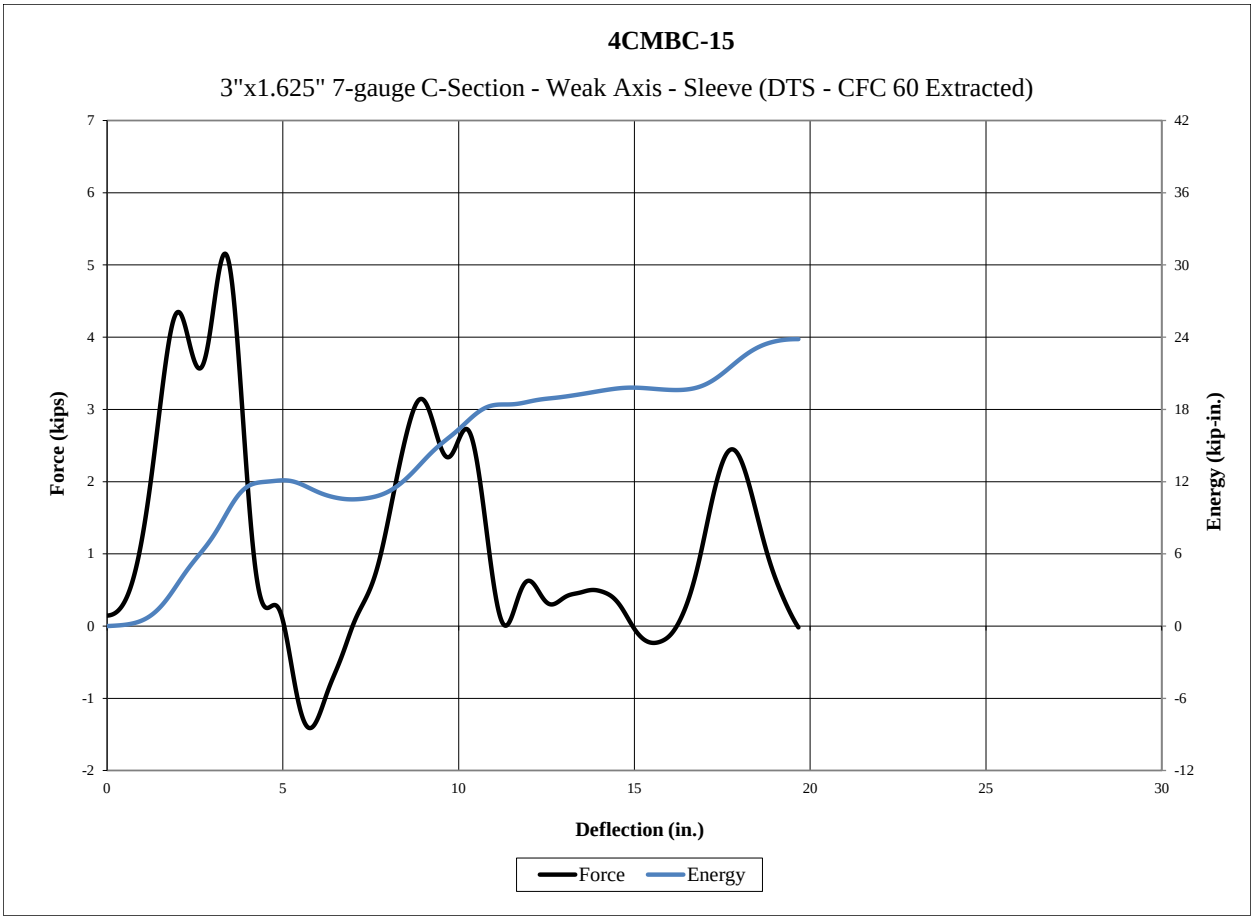

Figure 49. Force vs. Deflection and Energy vs. Deflection, Test No. 4CMBC-15

Pre-Test Post-Test

Figure 50. Pre-Test and Post-Test Photographs, Test No. 4CMBC-15

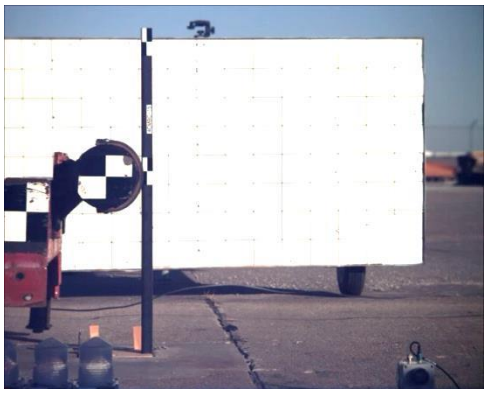
0.000 sec

0.120 sec

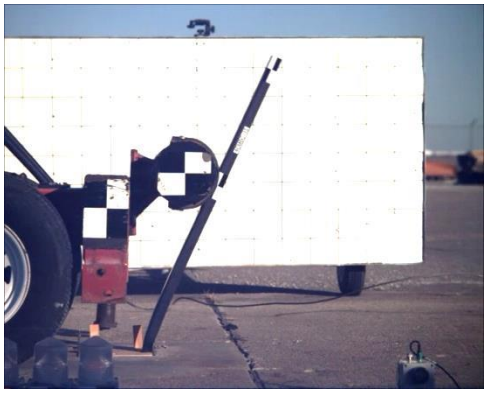
0.030 sec

0.150 sec

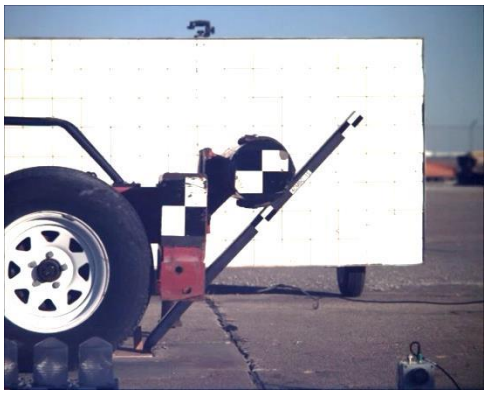
0.060 sec

0.180 sec

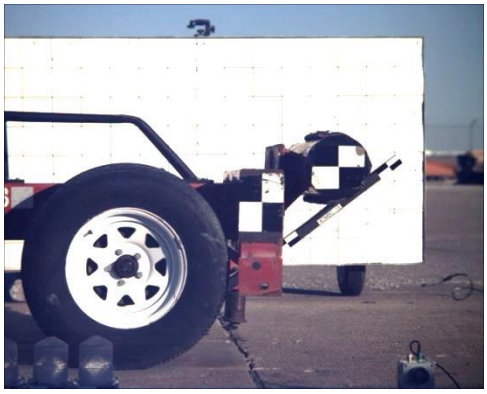
0.090 sec

0.210 sec

Figure 51. Sequential Photographs, Test No. 4CMBC-15

5.2.16 Test No. 4CMBC-16

During test no. 4CMBC-16, the bogie impacted the 7-gauge C-Section steel post in a rigid sleeve at a speed of 20.7 mph (33.3 km/h). As a result of the weak-axis impact, the post bent backward and yielded near the groundline. The bogie overrode the post at a maximum deflection of 23.6 in. (599 mm).

Force vs. deflection and energy vs. deflection curves created from the DTS accelerometer data are shown in Figure 52. The forces quickly rose to a peak force of 5.5 kips (24.5 kN) at 3.5 in. (89 mm) of deflection. The post provided an average resistive force of 1.6 kips (7.1 kN) through 10 in. (254 mm) of deflection and 1.4 kips (6.2 kN) through 15 in. (381 mm) of deflection. The energy absorbed by the post was 16.0 kip-in. (1.8 kJ) through 10 in. (254 mm) of deflection and 21.2 kip-in. (2.4 kJ) through 15 in. (381 mm) of deflection. Pre-test and post-test photographs are shown in Figure 53. Time-sequential photographs are shown in Figure 54.

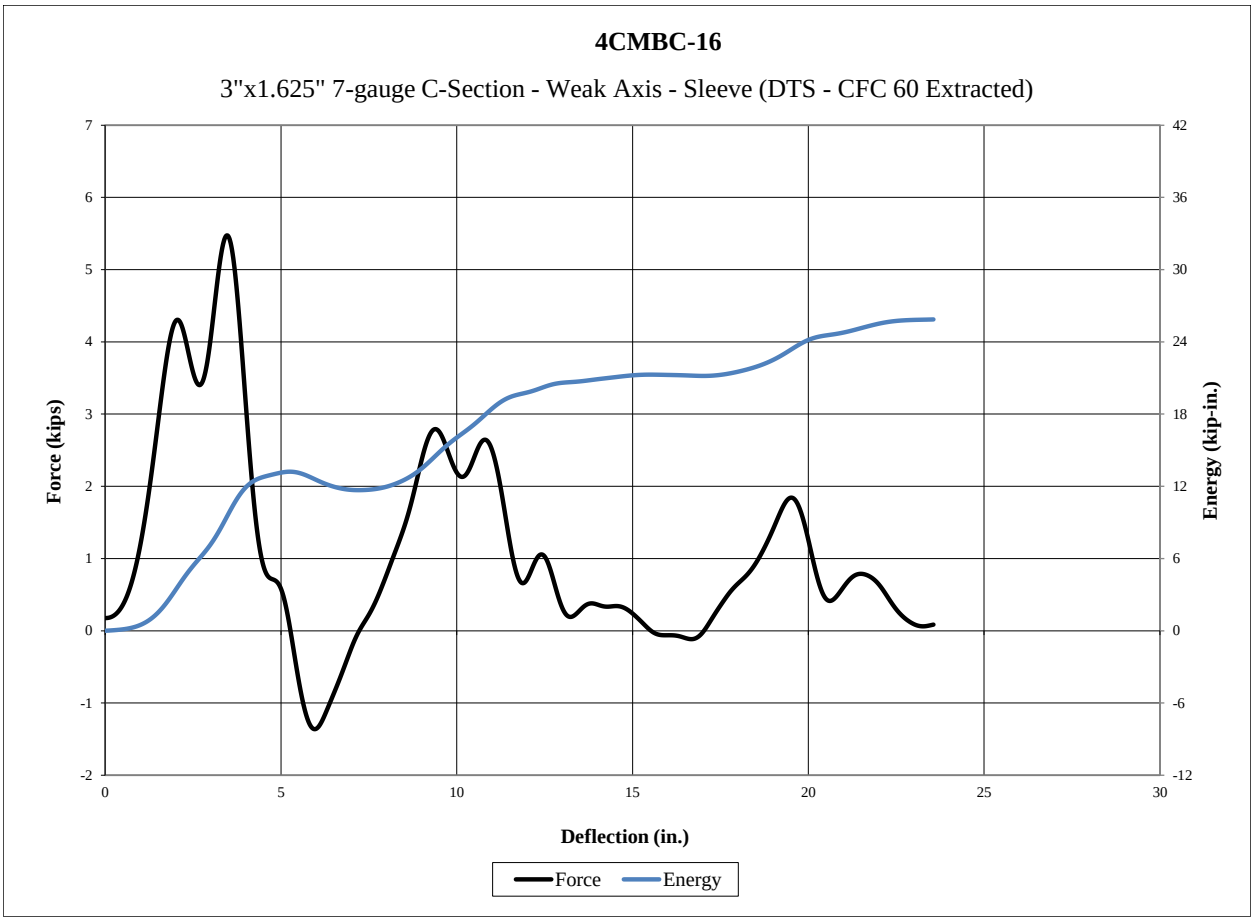

Figure 52. Force vs. Deflection and Energy vs. Deflection, Test No. 4CMBC-16

Pre-Test Post-Test

Figure 53. Pre-Test and Post-Test Photographs, Test No. 4CMBC-16

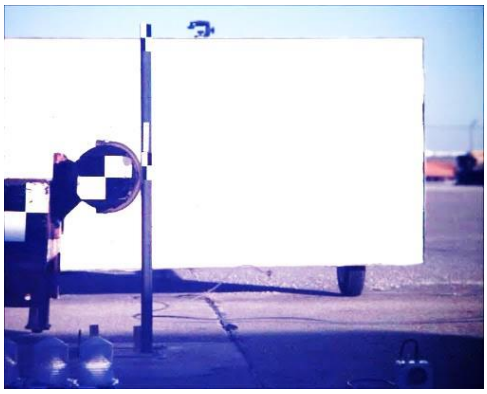
0.000 sec

0.120 sec

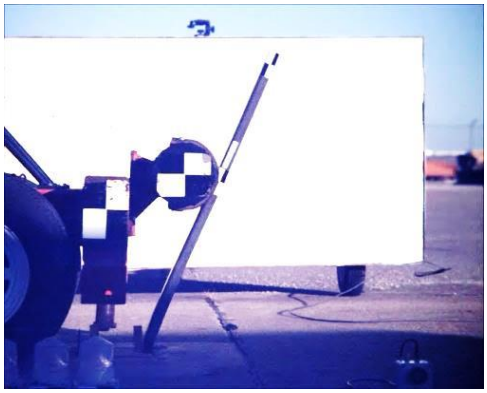
0.030 sec

0.150 sec


0.060 sec

0.180 sec


0.090 sec

0.210 sec

Figure 54. Sequential Photographs, Test No. 4CMBC-16

5.3 Discussion

Sixteen dynamic component tests were conducted on bent C-Section steel posts with two different thicknesses, two different impact axes, and two different foundations to establish the force vs. deflection and energy vs. deflection characteristics. The results from the bogie testing matrix are summarized in Tables 2 and 3. The C-Section steel posts were compared using force vs. displacement comparison curves that are shown in Figures 55 through 61, and energy vs. displacement curves that are shown in Figures 56 through 62.

5.3.1 10-Gauge C-Section Posts

Test nos. 4CMBC-1 and 4CMBC-2 were conducted striking the post at an angle of 90 degrees in soil with a 42-in. (1,067-mm) embedment depth. Test no. 4CMBC-1 appeared to be an outlier, as its force versus deflection behavior was not consistent with the other strong axis testing conducted as part of the research. Thus, this test was judged to be not representative of the post behavior. It was left out from the calculation of the averages and was not used in comparisons, as noted in Table 2.

Based on these tests, it appeared that the 10-gauge (3.4 mm) bent C-section post provided similar peak loads and energy dissipation when installed in a soil foundation or a rigid sleeve. Weak-axis impacts on the post tended to yield the post near the groundline. Strong-axis impacts tended to twist and buckle the post above the groundline due to the asymmetry of the C-section.

5.3.2 7-Gauge C-Section Posts

Testing of the 7-gauge (4.6 mm) bent C-section post provided similar peak loads and energy dissipation when installed in a soil foundation or a rigid sleeve. Weak-axis impacts on the post tended to yield the post near the groundline. Strong-axis impacts tended to twist and buckle the post above the groundline due to the asymmetry of the C-section. As expected, the 7-gauge (4.6 mm) bent C-section post provided higher resistance forces than the 10-gauge (3.4 mm)

posts. These higher forces resulted in increased absorbed energy as well, generally around 30-45 percent greater.

Table 2. Dynamic Testing Results, 10-Gauge Posts

Test No.	Impact Axis	Foundation Type	Impact Velocity mph (km/h)	Peak		Average Force kips (kN)		Maximum Deflection in. (mm)	Absorbed Energy kip-in. (kJ)		Post Behavior	Location of Plastic Hinge above groundline in. (mm)
				Deflection in. (mm)	Force kips (kN)	at 10" (254 mm)	at 15" (381 mm)		at 10" (254 mm)	at 15" (381 mm)		
4CMCB-1	Strong	Soil	20.2 (32.5)	8.8 (224)	1.8 (8.0)	1.0 (4.4)	0.9 (4.0)	14.4 (366)	10.2 (1.2)	13.6 (1.5)	Bending and Twisting	6 (152)
4CMCB-2	Strong	Soil	20.4 (32.8)	1.5 (38)	4.4 (19.6)	1.8 (8.0)	1.4 (6.2)	19.1 (485)	17.9 (2.0)	21.0 (2.4)	Bending and Twisting	6 (152)
Averages*				**1.5 (38)**	**4.4 (19.6)**	**1.8 (8.0)**	**1.4 (6.2)**	**19.1 (485)**	**17.9 (2.0)**	**21.0 (2.4)**		**6 (152)**
4CMCB-3	Weak	Soil	20.2 (32.5)	2.0 (51)	3.7 (16.5)	1.0 (4.4)	0.9 (4.0)	24.7 (627)	10.5 (1.2)	13.6 (1.5)	Bending	-2 (-51)
4CMCB-4	Weak	Soil	21.1 (34.0)	2.3 (58)	3.7 (16.5)	0.9 (4.0)	0.9 (4.0)	22.1 (561)	8.6 (1.0)	13.5 (1.5)	Bending	-2 (-51)
Averages				**2.2 (56)**	**3.7 (16.5)**	**1.0 (4.4)**	**0.9 (4.0)**	**23.4 (594)**	**9.6 (1.1)**	**13.6 (1.5)**		**-2 (-51)**
4CMCB-9	Strong	Sleeve	21.1 (34.0)	2.3 (58)	4.5 (20.0)	1.9 (8.5)	1.5 (6.7)	18.2 (462)	19.0 (2.1)	21.8 (2.5)	Bending and Twisting	13 (330)
4CMCB-10	Strong	Sleeve	20.0 (32.2)	1.8 (46)	4.3 (19.1)	1.8 (8.0)	1.3 (5.8)	18.5 (470)	18.4 (2.1)	20.2 (2.3)	Bending and Twisting	13 (330)
Averages				**2.1 (53)**	**4.4 (19.6)**	**1.9 (8.5)**	**1.4 (6.2)**	**18.4 (467)**	**18.7 (2.1)**	**21.0 (2.4)**		**13 (330)**
4CMCB-13	Weak	Sleeve	20.3 (32.7)	3.0 (76)	3.7 (16.5)	0.7 (3.1)	0.7 (3.1)	20.4 (518)	7.1 (0.8)	10.0 (1.1)	Bending	0 (0)
4CMCB-14	Weak	Sleeve	21.0 (33.8)	3.2 (81)	3.8 (16.9)	1.0 (4.4)	0.9 (4.0)	21.6 (549)	10.1 (1.1)	13.9 (1.6)	Bending	0 (0)
Averages				**3.1 (79)**	**3.8 (16.9)**	**0.9 (4.0)**	**0.8 (3.6)**	**21.0 (533)**	**8.6 (1.0)**	**12.0 (1.4)**		**0 (0)**

*Test No. 4CMBC-1 was not used in calculation of the average

Table 3. Dynamic Testing Results, 7-Gauge Posts

Test No.	Impact Axis	Foundation Type	Impact Velocity mph (km/h)	Peak		Average Force kips (kN)		Maximum Deflection in. (mm)	Absorbed Energy kip-in. (kJ)		Post Behavior	Location of Plastic Hinge above groundline in. (mm)
				Deflection in. (mm)	Force kips (kN)	at 10" (254 mm)	at 15" (381 mm)		at 10" (254 mm)	at 15" (381 mm)		
4CMCB-5	Strong	Soil	19.4 (31.2)	2.1 (53)	5.4 (24.0)	2.1 (9.3)	1.8 (8.0)	18.7 (475)	20.6 (2.3)	27.7 (3.1)	Bending and Twisting	6 (152)
4CMCB-6	Strong	Soil	20.4 (32.8)	2.2 (56)	5.9 (26.2)	2.4 (10.7)	1.9 (8.5)	19.3 (490)	24.3 (2.7)	28.1 (3.2)	Bending and Twisting	6 (152)
Averages				**2.2 (56)**	**5.7 (25.4)**	**2.3 (10.2)**	**1.9 (8.5)**	**19.0 (483)**	**22.5 (2.5)**	**27.9 (3.2)**		**6 (152)**
4CMCB-7	Weak	Soil	21.9 (35.2)	1.8 (46)	4.7 (20.9)	1.5 (6.7)	1.4 (6.2)	24.0 (610)	15.2 (1.7)	21.0 (2.4)	Bending	0 (0)
4CMCB-8	Weak	Soil	21.0 (33.8)	1.7 (43)	4.2 (18.7)	1.3 (5.8)	1.1 (4.9)	26.7 (678)	12.6 (1.4)	17.2 (1.9)	Bending	0 (0)
Averages				**1.8 (46)**	**4.5 (20.0)**	**1.4 (6.2)**	**1.3 (5.8)**	**25.4 (645)**	**13.9 (1.6)**	**19.1 (2.2)**		**0 (0)**
4CMCB-11	Strong	Sleeve	20.5 (33.0)	1.9 (48)	5.5 (24.5)	2.5 (11.1)	1.9 (8.5)	19.5 (495)	24.8 (2.8)	29.1 (3.3)	Bending and Twisting	11 (279)
4CMCB-12	Strong	Sleeve	20.9 (33.6)	2.3 (58)	6.2 (27.6)	2.7 (12.0)	2.1 (9.3)	20.2 (513)	26.9 (3.0)	31.6 (3.6)	Bending and Twisting	11 (279)
Averages				**2.1 (53)**	**5.9 (26.2)**	**2.6 (11.6)**	**2.0 (8.9)**	**19.9 (505)**	**25.9 (2.9)**	**30.4 (3.4)**		**11 (279)**
4CMCB-15	Weak	Sleeve	20.7 (33.3)	3.4 (86)	5.2 (23.1)	1.6 (7.1)	1.3 (5.8)	19.7 (500)	16.3 (1.8)	19.8 (2.2)	Bending	0 (0)
4CMCB-16	Weak	Sleeve	20.7 (33.3)	3.5 (89)	5.5 (24.5)	1.6 (7.1)	1.4 (6.2)	23.6 (599)	16.1 (1.8)	21.2 (2.4)	Bending	0 (0)
Averages				**3.5 (89)**	**5.4 (24.0)**	**1.6 (7.1)**	**1.4 (6.2)**	**21.7 (551)**	**16.2 (1.8)**	**20.5 (2.3)**		**0 (0)**

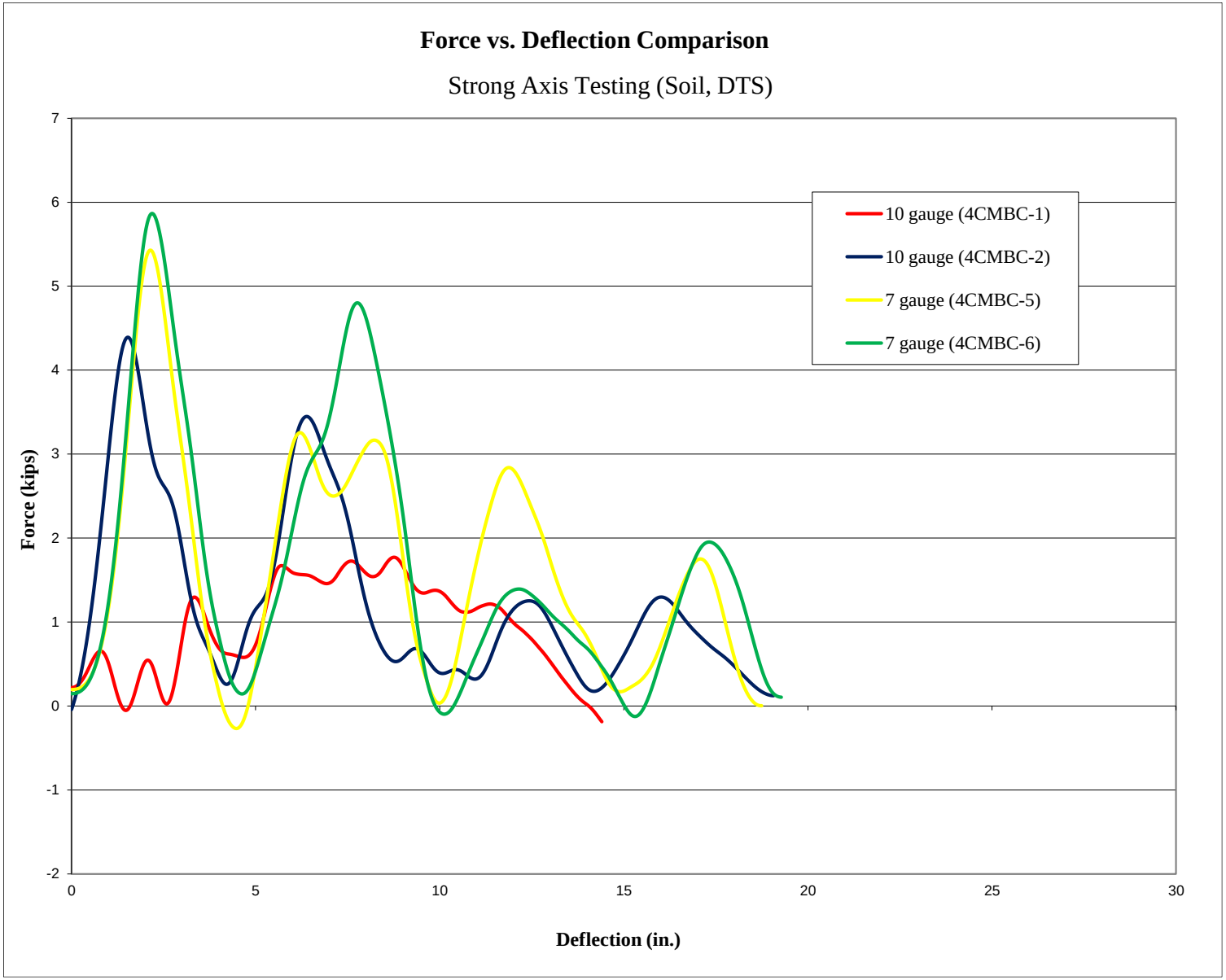

Figure 55. Force vs. Deflection Comparison, Strong Axis, Soil

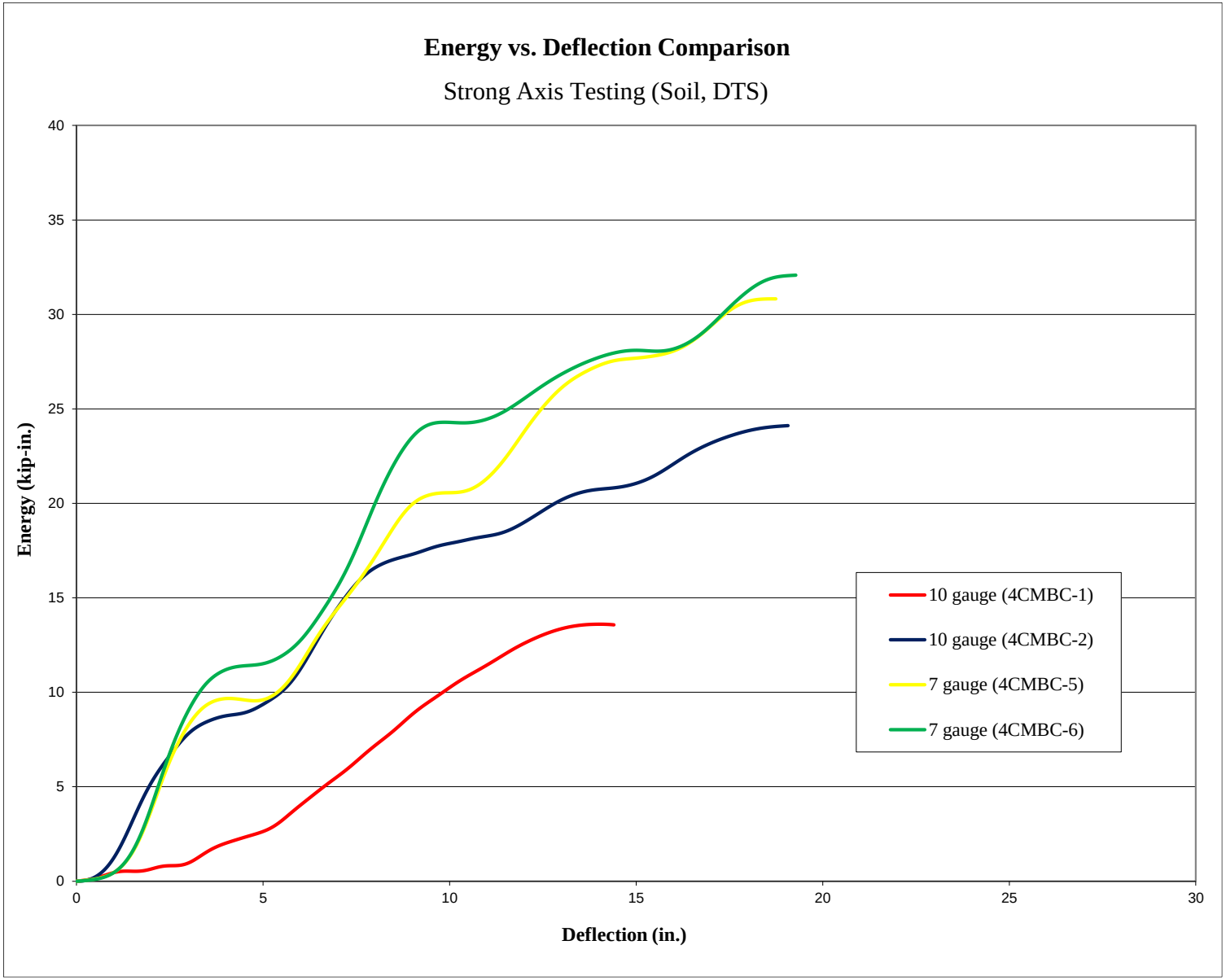

Figure 56. Energy vs. Deflection Comparison, Strong Axis, Soil

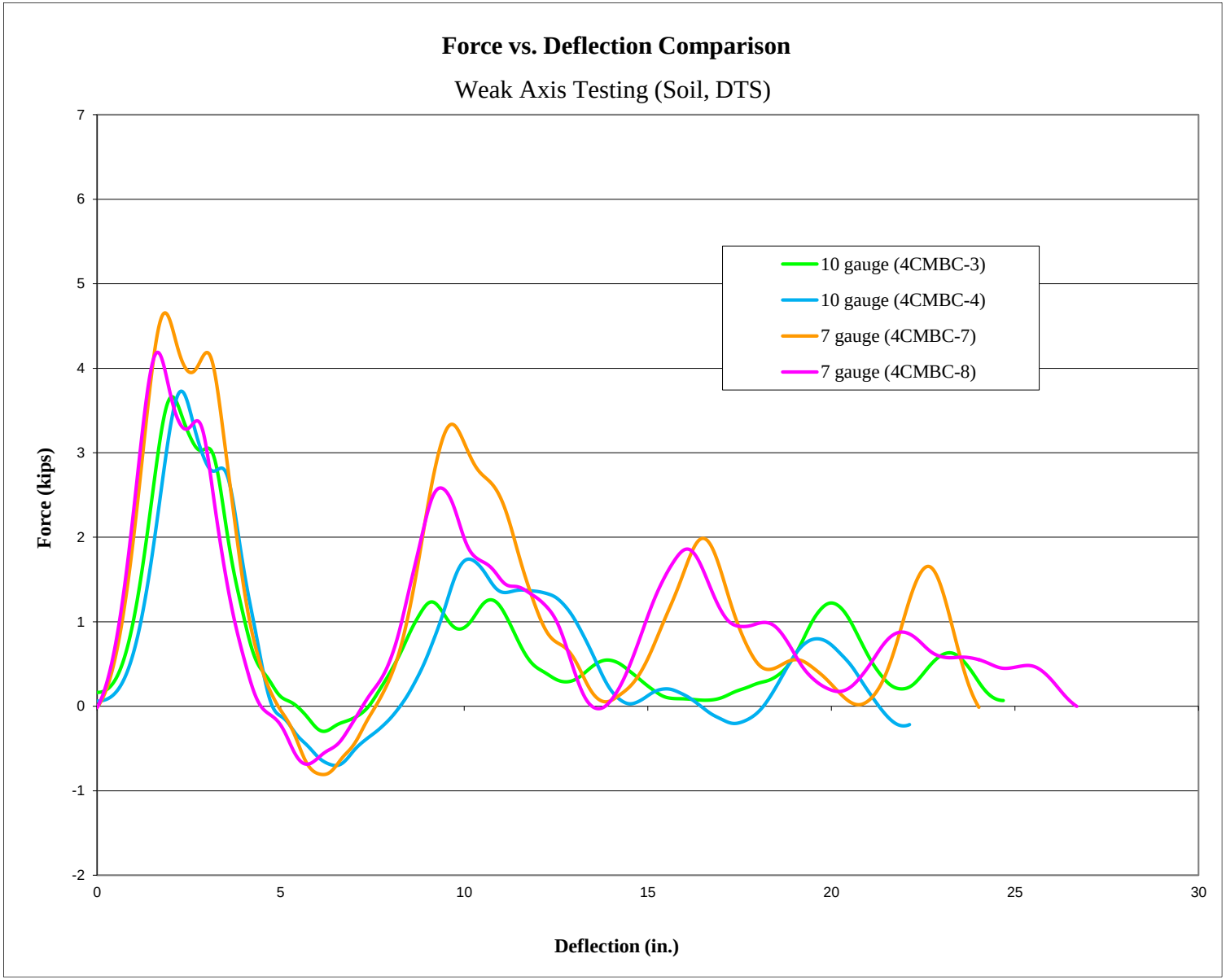

Figure 57. Force vs. Deflection Comparison, Weak Axis, Soil

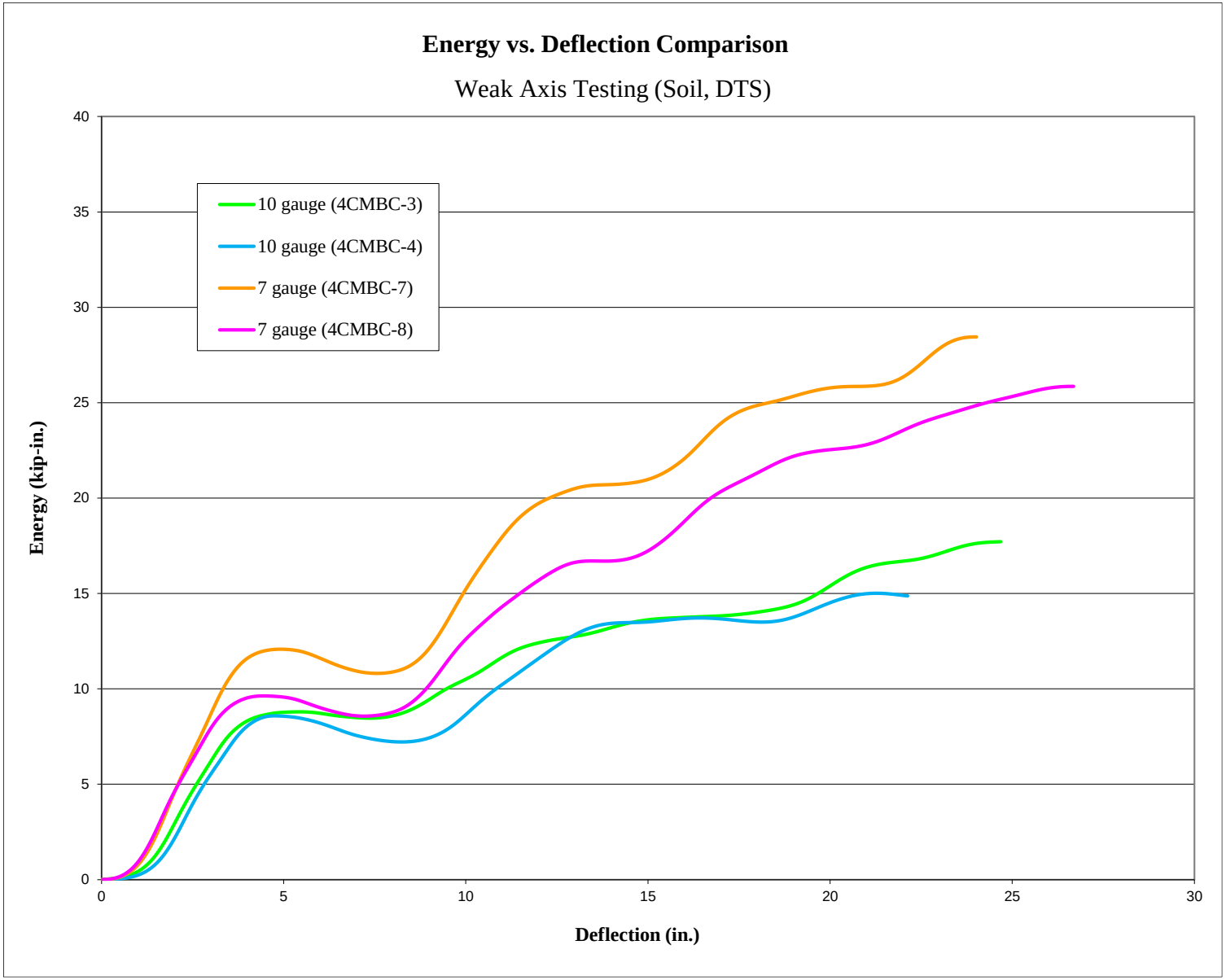

Figure 58. Energy vs. Deflection Comparison, Weak Axis, Soil

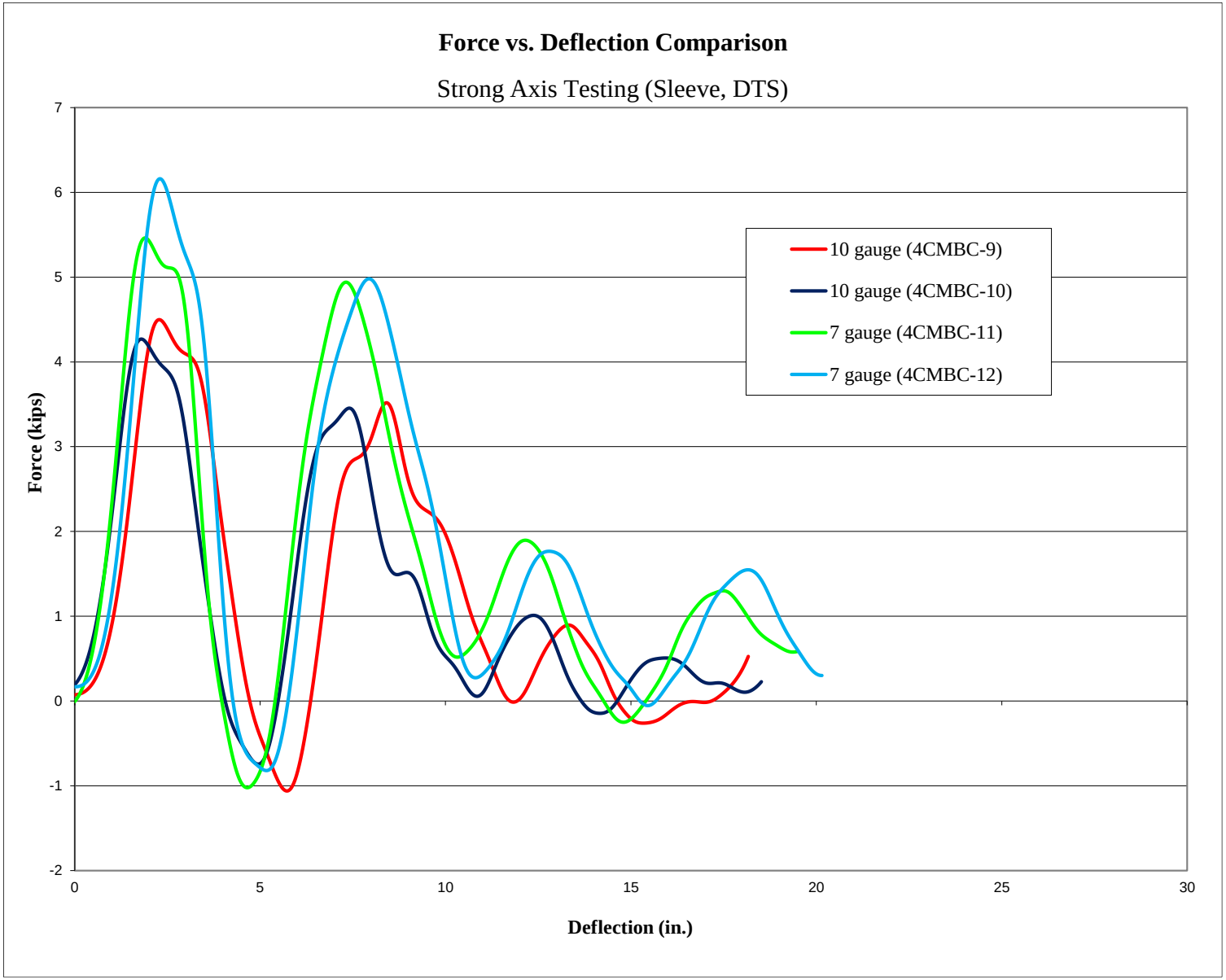

Figure 59. Force vs. Deflection Comparison, Strong Axis, Sleeve

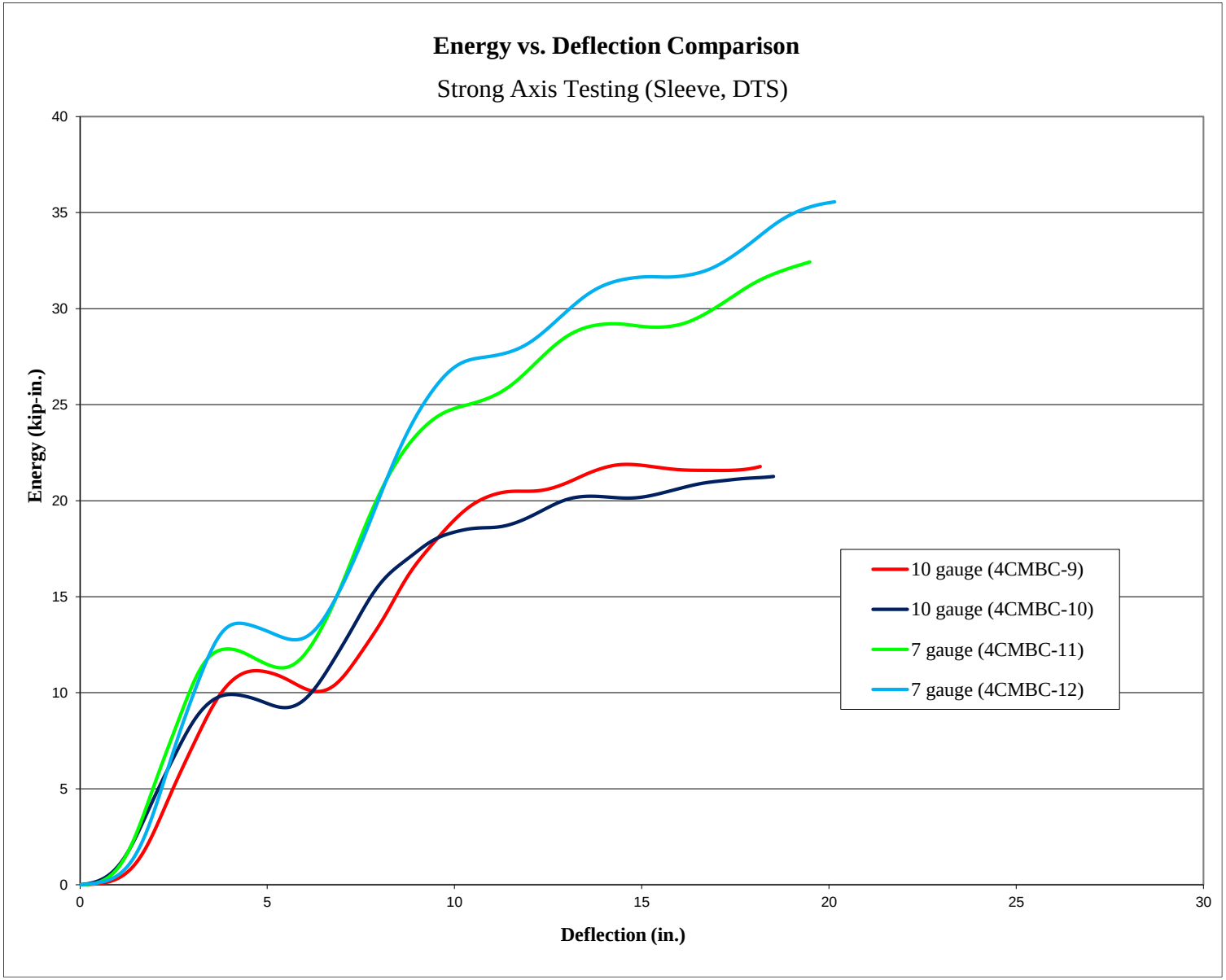

Figure 60. Energy vs. Deflection Comparison, Strong Axis, Sleeve

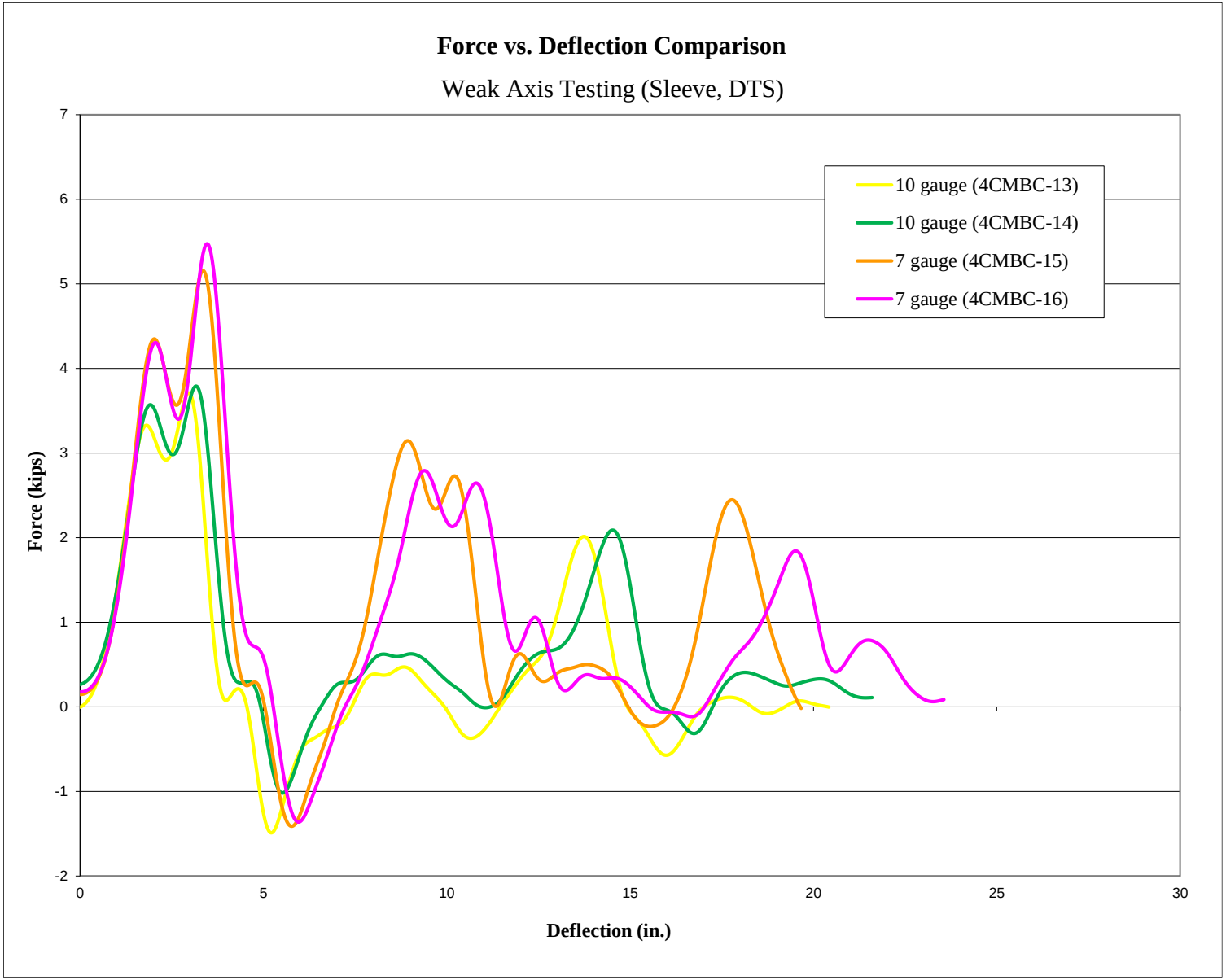

Figure 61. Force vs. Deflection Comparison, Weak Axis, Sleeve

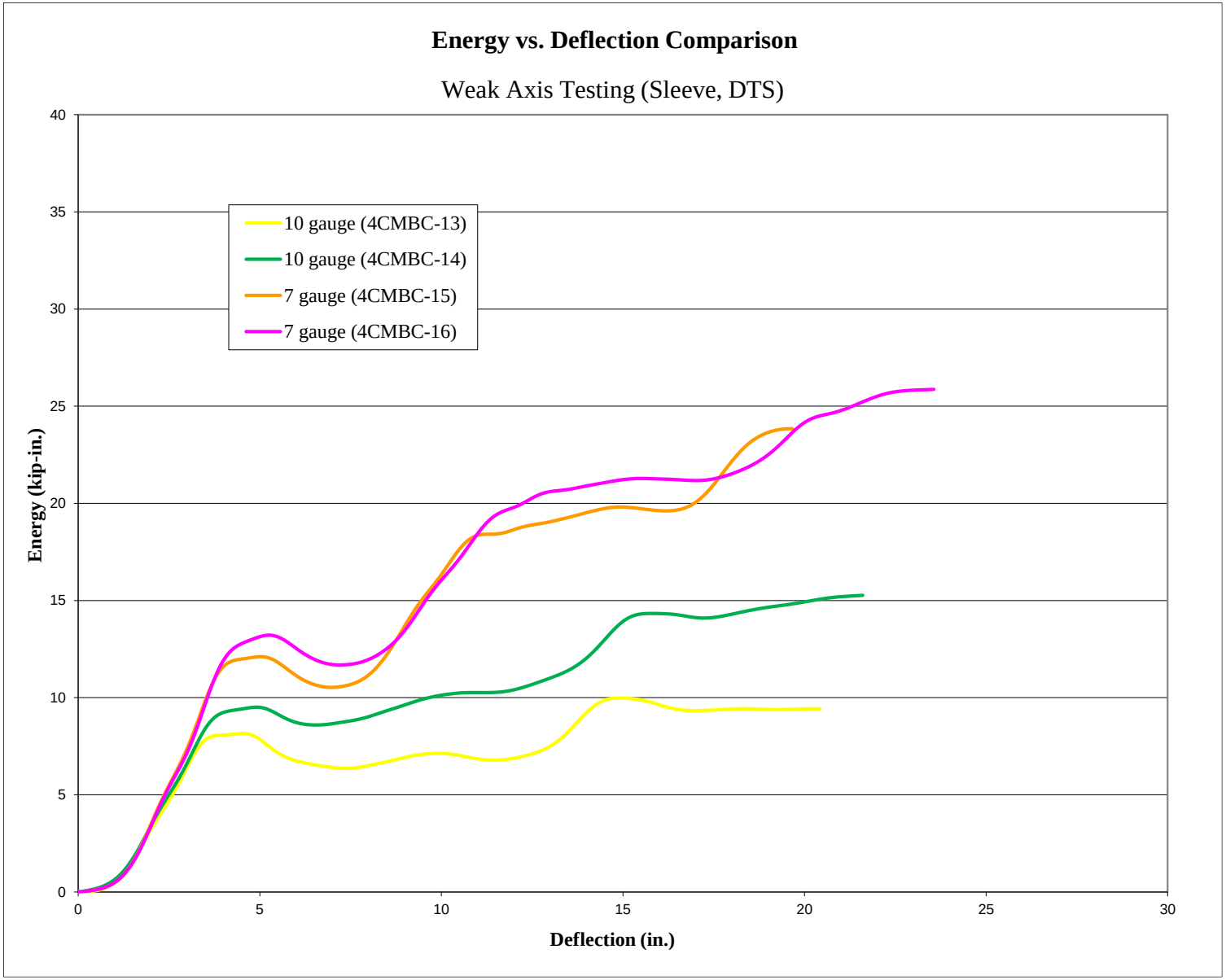

Figure 62. Energy vs. Deflection Comparison, Weak Axis, Sleeve

5.4 Comparison of S3x5.7 (S76x8.5) Steel Posts

The S3x5.7 (S76x8.5) steel post used in the previous design iteration of the non-proprietary high-tension cable median barrier was used as the baseline for evaluating the C-section posts. As noted previously, the primary goal of the new post section was to lower the lateral or strong-axis strength of the post. The results from previous bogie tests of S3x5.7 (S76x8.5) steel posts are summarized in Table 4. The force comparison between the tested C-section posts and previous S3x5.7 (S76x8.5) posts are shown in Table 5. The force vs. deflection and energy vs. deflection comparison curves for the S3x5.7 (S76x8.5) steel posts at a 27-in. (686-mm) impact height and C-section posts are shown in Figures 63 through 70.

Due to some of the S3x5.7 (S76x8.5) steel post tests being conducted at lower impact heights of either $21^{13}/_{20}$ in. (550 mm) or 25 in. (635 mm) as opposed to 27 in. (686 mm), modifications were made to adjust the force vs. deflection curves of the previous tests to represent the impact height at 27 in. (686 mm). This made it possible to compare the results of the C-section posts to the modified S3x5.7 (S76x8.5) forces and energies. Equations utilizing a ratio of the change in heights were used to determine the deflections and forces for an impact height of 27 in. (686 mm). The equations are:

$$D_2 = D_1\left(\frac{L_2}{L_1}\right) \qquad \text{(Eq-1)}$$

$$F_2 = F_1\left(\frac{L_1}{L_2}\right) \qquad \text{(Eq-2)}$$

Where:

D = Deflection

L = Load Height

F = Force

Comparison of the strong-axis testing of the bent C-section posts to the S3x5.7 (S76x8.5) posts when installed in a soil foundation found that the 10-gauge C-section posts provided 37.9 percent and 56.3 percent reduced forces through deflections of 10 in. (254 mm) and 15 in. (381 mm), respectively. The 7-gauge C-section posts provided 20.7 percent and 40.6 percent reduced forces over the same 10 in. (254 mm) and 15 in. (381 mm) displacements, as shown in Figures 63 and 64.

Comparison of the strong-axis testing of the bent C-section posts to the S3x5.7 (S76x8.5) posts when installed in a rigid foundation found that the 10-gauge C-Section posts provided 58.7 percent and 72.0 percent reduced forces through deflections of 10 in. (254 mm) and 15 in. (381 mm), respectively. The 7-gauge C-Section posts provided 43.5 percent and 60.0 percent reduced forces over the same 10 in. (254 mm) and 15 in. (381 mm) displacements, as shown in Figures 65 and 66.

Comparison of the weak-axis testing of the bent C-section posts to the S3x5.7 (S76x8.5) posts when installed in a soil foundation found that the 10-gauge C-section posts provided 47.4 percent and 52.6 percent reduced forces through deflections of 10 in. (254 mm) and 15 in. (381 mm), respectively. The 7-gauge C-Section posts provided 26.3 percent and 31.6 percent reduced forces over the same 10 in. (254 mm) and 15 in. (381 mm) displacements, as shown in Figures 67 and 68.

Comparison of the weak-axis testing of the bent C-section posts to the S3x5.7 (S76x8.5) posts when installed in a rigid foundation found that the 10-gauge C-section posts provided 35.7 percent and 46.7 percent reduced forces through deflections of 10 in. (254 mm) and 15 in. (381 mm) with a 90 degree impact angle in a sleeve. The 7-gauge C-section posts provided a 14.3 percent increase and a 6.7 percent decrease in forces over the same displacements, as shown in Figures 69 and 70.

Based on these comparisons of the bent C-section post and the S3x5.7 (S76x8.5) post, it was evident that both the 7 -and 10-gauge C-section posts successfully met the desired design goals. Both posts reduced the lateral (or strong-axis) capacity of the post significantly. In addition, both posts reduced the longitudinal (or weak-axis) capacity of the post and were easier and less expensive to fabricate than the S-post. However, some concerns arose that the force reductions associated with the 10-gauge C-section post may be too extreme and may negatively affect the performance of the system without greatly reducing the post spacing. In addition, there was some concern that the thinner-gauge post may be difficult to drive without damaging and might be susceptible to localized deformation when the cable-to-post attachments were placed under load. Thus, the 7-gauge post was chosen for further evaluation as it reduced the lateral capacity of the post section approximately 50 percent and did not present the same concerns with respect to drivability and localized deformations.

Table 4. Previous S3x5.7 (S76x8.5) Test Results Scaled to Reflect 27 in. Impact Heights

Test No.	Reference Number	Embedment Depth in. (mm)	Impact Speed mph (km/h)	Peak Force kips (kN)	Average Force kips (kN)		Maximum Deflection in. (mm)	Absorbed Energy kip-in. (kJ)	
					at 10" (254 mm)	at 15" (381 mm)		at 10" (254 mm)	at 15" (381 mm)
Strong Axis in Soil									
CMPB-14	8	30.0 (762)	21.6 (34.8)	4.2 (18.7)	3.1 (13.8)	3.4 (15.1)	47.5 (1,207)	31.3 (3.5)	50.2 (5.7)
CMPB-21	9	42.0 (1,067)	13.5 (21.7)	4.0 (17.8)	2.7 (12.0)	2.9 (12.9)	40.1 (1,019)	27.3 (3.1)	44.1 (5.0)
Averages			**17.6 (28.3)**	**4.1 (18.2)**	**2.9 (12.9)**	**3.2 (14.2)**	**43.8 (1,113)**	**29.3 (3.3)**	**47.2 (5.3)**
Strong Axis in Sleeve									
CMPB-6	8	30.0 (762)	19.8 (31.9)	5.3 (23.6)	4.2 (18.7)	4.6 (20.5)	43.4 (1,102)	42.2 (4.8)	68.6 (7.8)
CP-1	10	14.0 (356)	22.5 (36.2)	7.8 (34.7)	4.5 (20.0)	4.9 (21.8)	34.0 (864)	44.9 (5.1)	73.7 (8.3)
CP-2	10	14.0 (356)	22.3 (35.9)	7.6 (33.8)	4.5 (20.0)	4.9 (21.8)	31.7 (805)	44.9 (5.1)	73.3 (8.3)
CP-3	10	14.0 (356)	22.0 (35.4)	6.6 (29.4)	4.8 (21.4)	5.0 (22.2)	31.5 (800)	47.9 (5.4)	75.5 (8.5)
CP-4	10	14.0 (356)	21.8 (35.1)	6.6 (29.4)	4.5 (20.0)	5.0 (22.2)	32.7 (831)	45.4 (5.1)	75.5 (8.5)
CP-5	10	14.0 (356)	20.5 (33.0)	7.3 (32.5)	5.3 (23.6)	5.5 (24.5)	41.8 (1,062)	53.1 (6.0)	82.4 (9.3)
Averages			**21.5 (34.6)**	**6.9 (30.7)**	**4.6 (20.5)**	**5.0 (22.2)**	**35.9 (912)**	**46.4 (5.2)**	**74.8 (8.5)**
Weak Axis in Soil									
CPB-6*	11	30.0 (762)	20.0 (32.2)	4.0 (17.8)	1.9 (8.5)	1.9 (8.5)	36.0 (914)	17.6 (2.0)	28.2 (3.2)
Averages			**20.0 (32.2)**	**4.0 (17.8)**	**1.9 (8.5)**	**1.9 (8.5)**	**36.0 (914)**	**17.6 (2.0)**	**28.2 (3.2)**
Weak Axis in Sleeve									
CCP-5	12	38.0 (965)	20.1 (32.3)	2.0 (8.9)	1.4 (6.2)	1.5 (6.7)	35.9 (912)	14.0 (1.6)	22.6 (2.6)
Averages			**20.1 (32.3)**	**2.0 (8.9)**	**1.4 (6.2)**	**1.5 (6.7)**	**35.9 (912)**	**14.0 (1.6)**	**22.6 (2.6)**

*Data was re-processed from the report [11]

Table 5. Force Comparisons Between S3x5.7 (S76x8.5) and C-Section Posts

Post Type	Peak Force		Average Force @ 10 in. (254 mm)		Average Force @ 15 in. (381 mm)	
	kips (kN)	% of S3x5.7	kips (kN)	% of S3x5.7	kips (kN)	% of S3x5.7
Strong Axis in Soil						
S3x5.7	4.1 (18.2)	-	2.9 (12.9)	-	3.2 (14.2)	-
10-Gauge C	4.4 (19.6)	107.3%	1.8 (8.0)	62.1%	1.4 (6.2)	43.8%
7-Gauge C	5.7 (25.4)	139.0%	2.3 (10.2)	79.3%	1.9 (8.5)	59.4%
Strong Axis in Sleeve						
S3x5.7	6.9 (30.7)	-	4.6 (20.5)	-	5.0 (22.2)	-
10-Gauge C	4.4 (19.6)	63.8%	1.9 (8.5)	41.3%	1.4 (6.2)	30.0%
7-Gauge C	5.9 (26.2)	85.5%	2.6 (11.6)	56.5%	2.0 (8.9)	40.0%
Weak Axis in Soil						
S3x5.7	4.0 (17.8)	-	1.9 (8.5)	-	1.9 (8.5)	-
10-Gauge C	3.7 (16.5)	92.5%	1.0 (4.4)	52.6%	0.9 (4.0)	47.4%
7-Gauge C	4.5 (20.0)	112.5%	1.4 (6.2)	73.7%	1.3 (5.8)	68.4%
Weak Axis in Sleeve						
S3x5.7	2.0 (8.9)	-	1.4 (6.2)	-	1.5 (6.7)	-
10-Gauge C	3.8 (16.9)	190.0%	0.9 (4.0)	64.3%	0.8 (3.6)	53.3%
7-Gauge C	5.4 (24.0)	270.0%	1.6 (7.1)	114.3%	1.4 (6.2)	93.3%

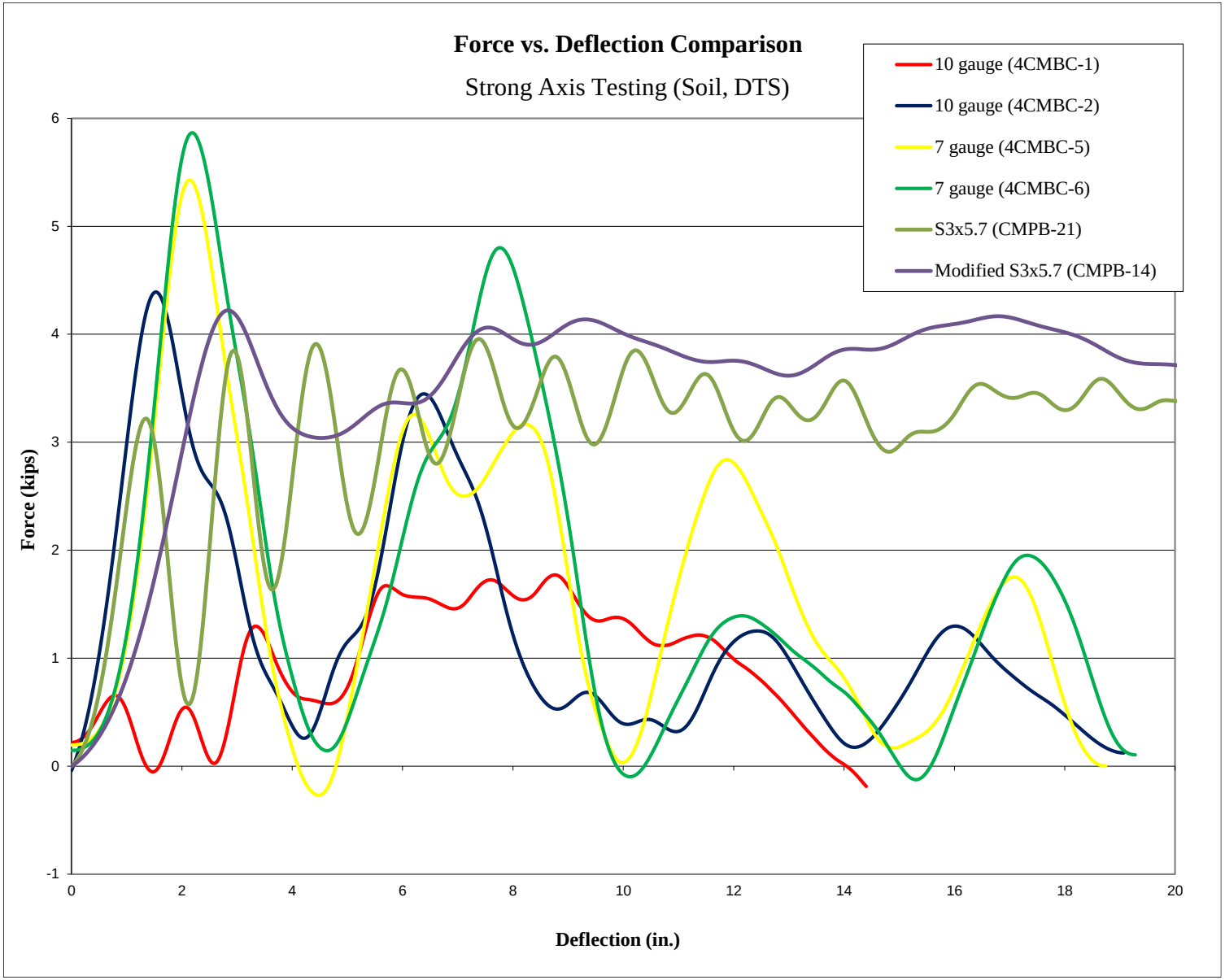

Figure 63. Force vs. Deflection Post Comparison, Strong Axis Testing in Soil

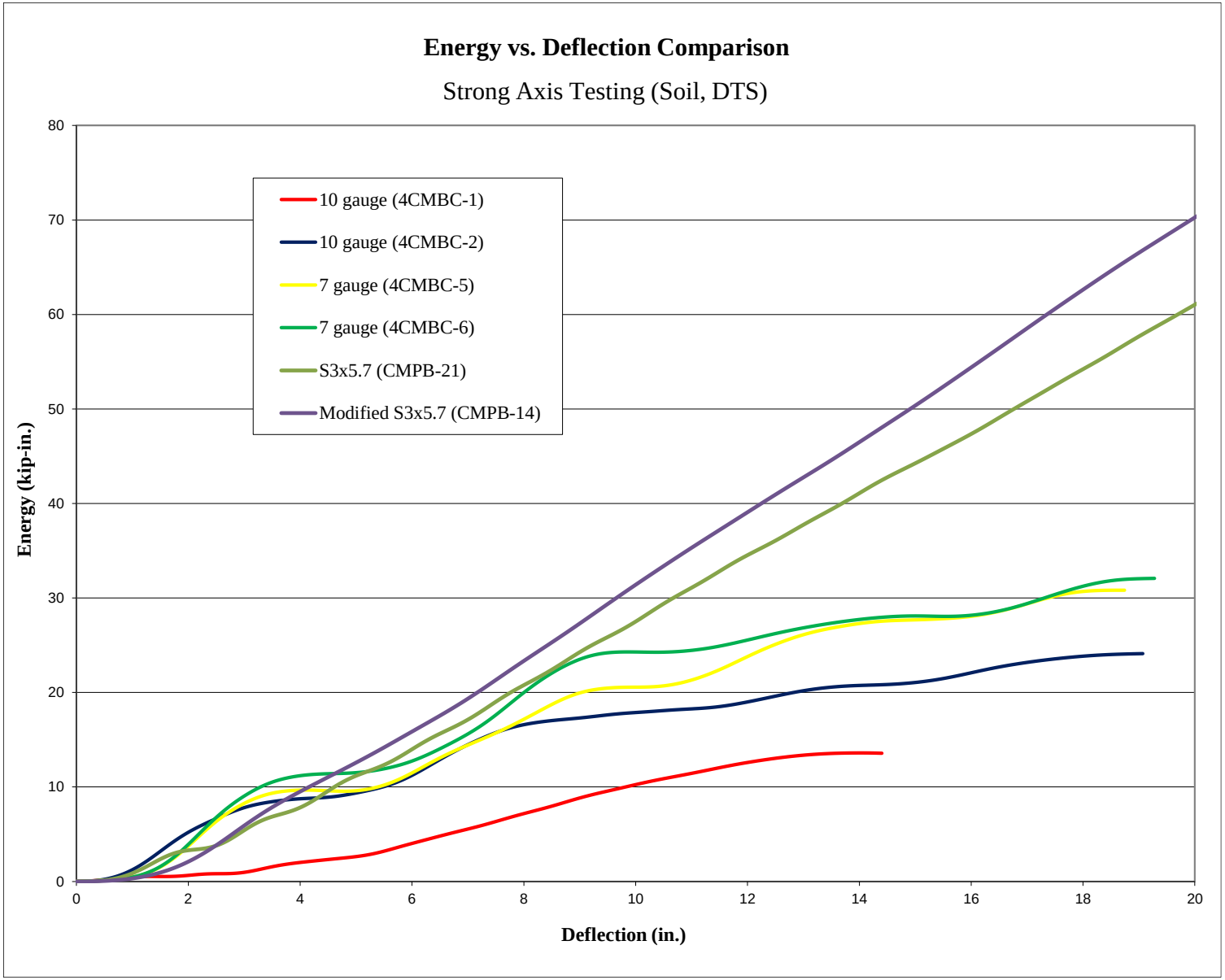

Figure 64. Energy vs. Deflection Post Comparison, Strong Axis Testing in Soil

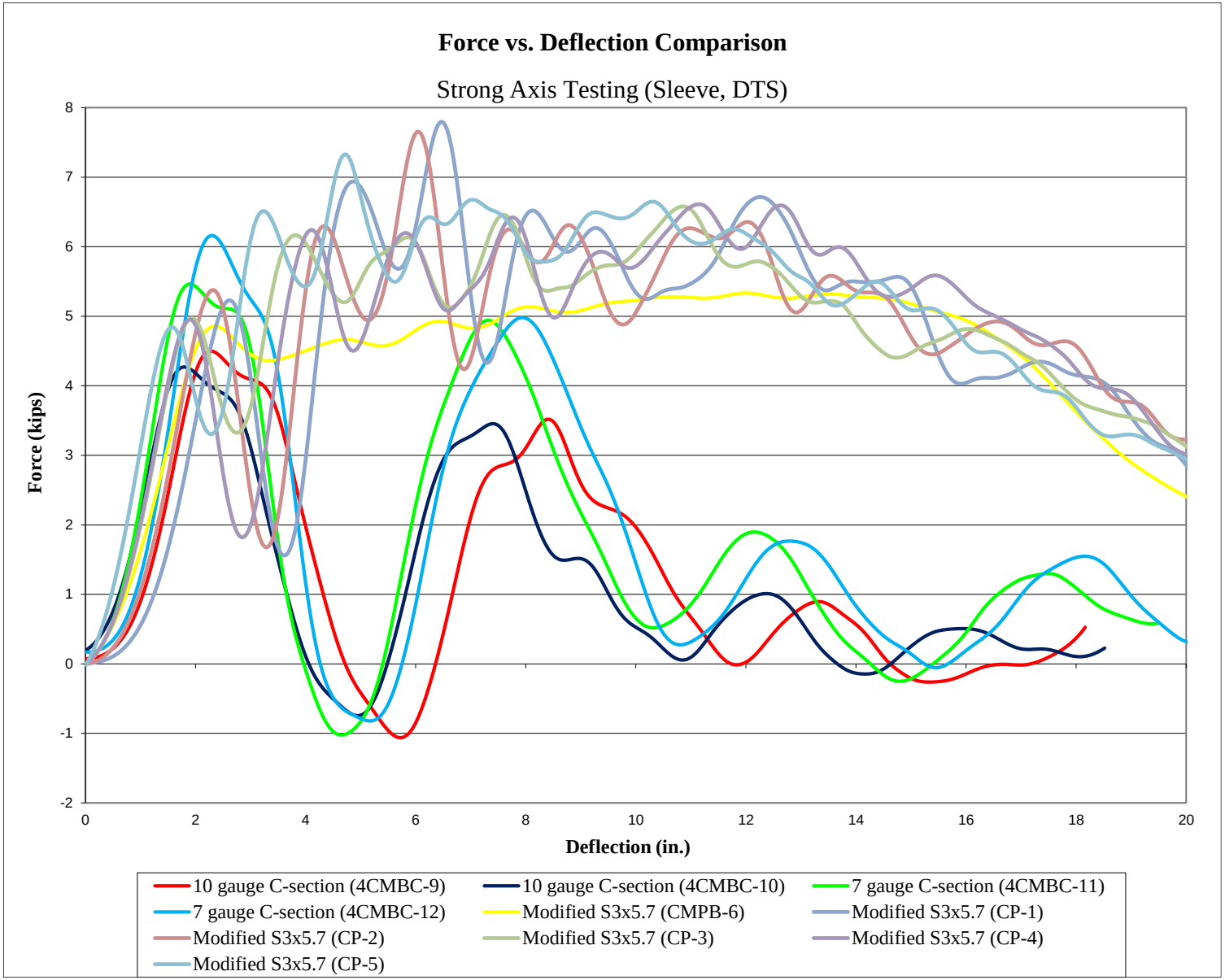

Figure 65. Force vs. Deflection Post Comparison, Strong Axis Testing in Sleeve

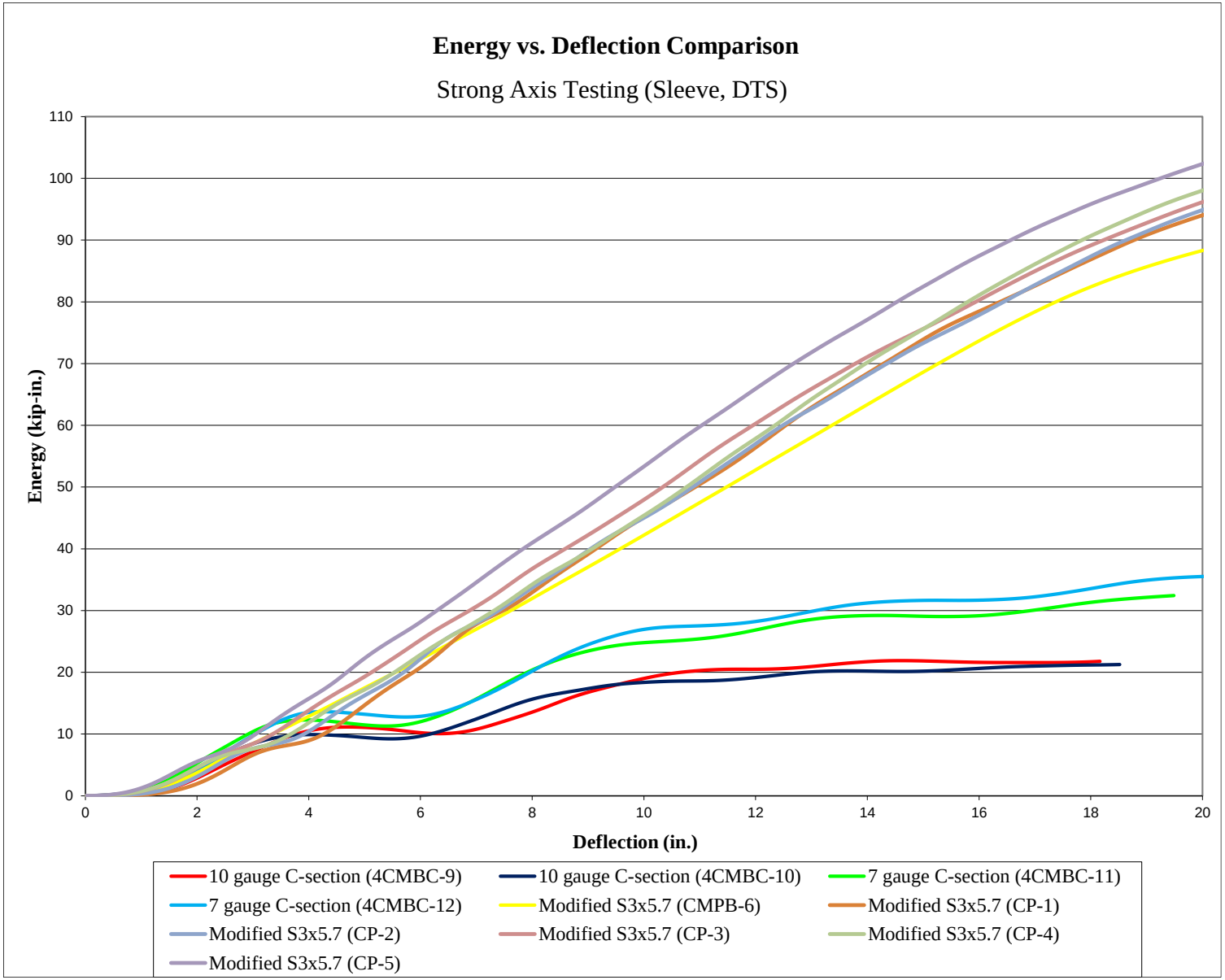

Figure 66. Energy vs. Deflection Post Comparison, Strong Axis Testing in Sleeve

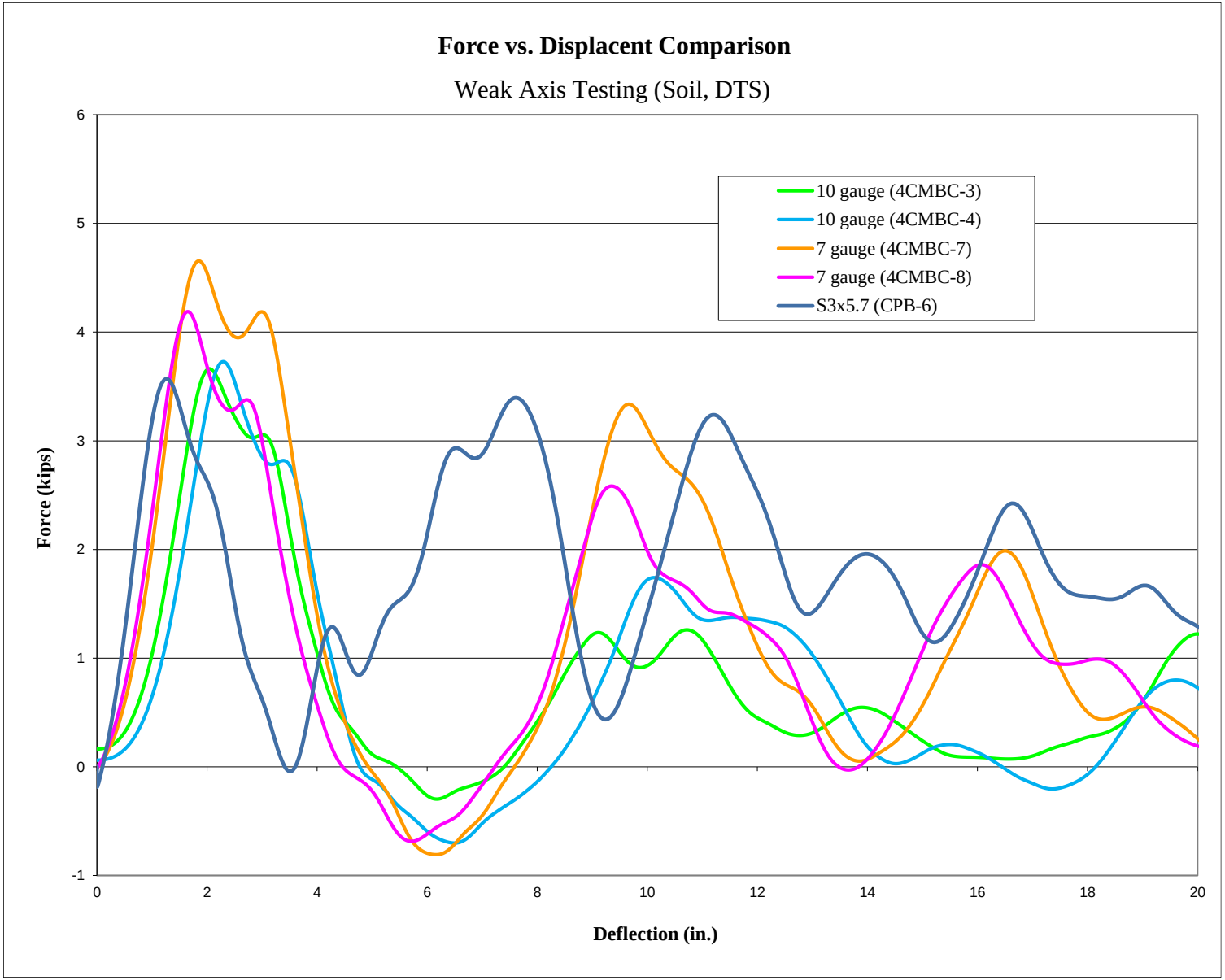

Figure 67. Force vs. Deflection Post Comparison, Weak Axis Testing in Soil

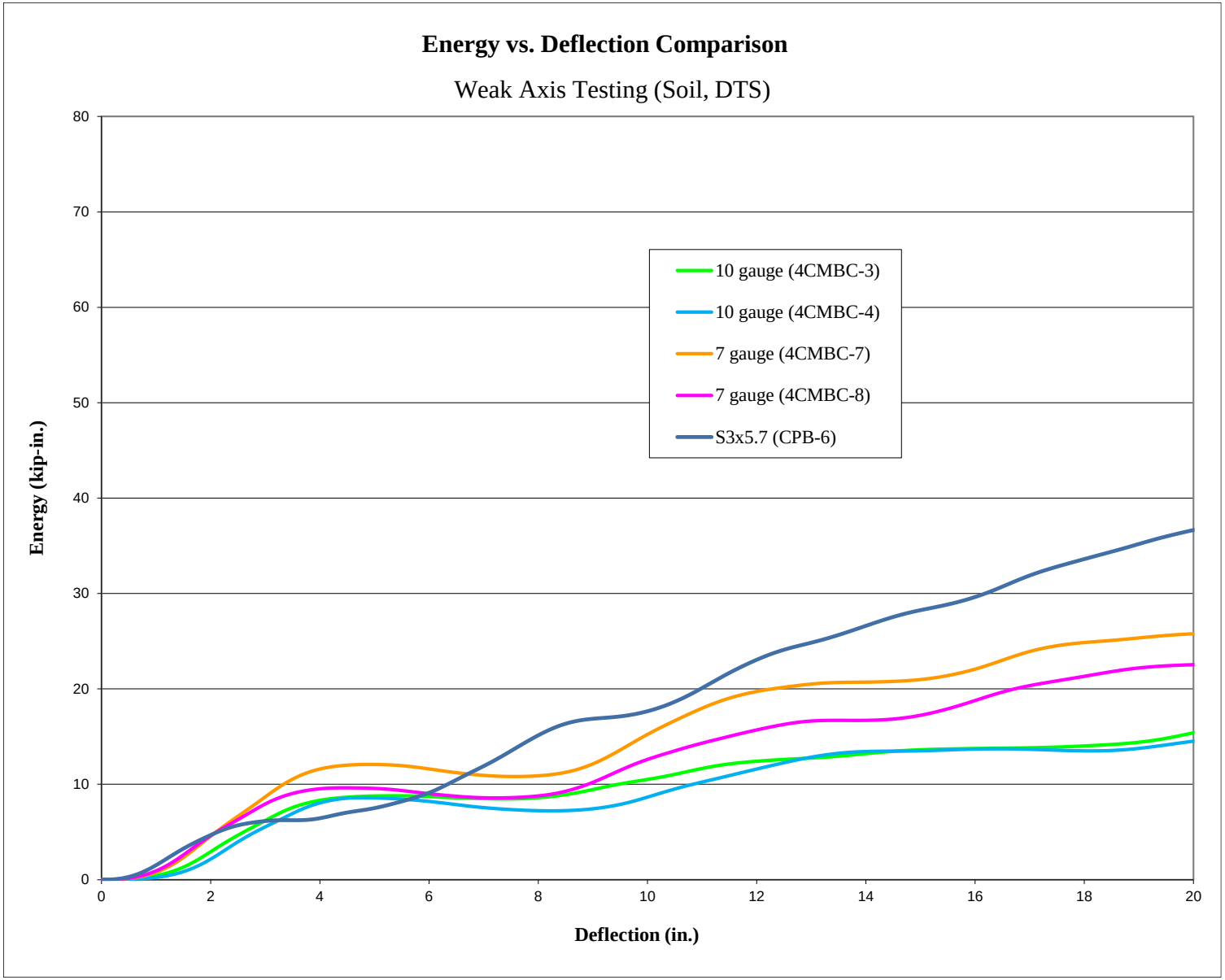

Figure 68. Energy vs. Deflection Post Comparison, Weak Axis Testing in Soil

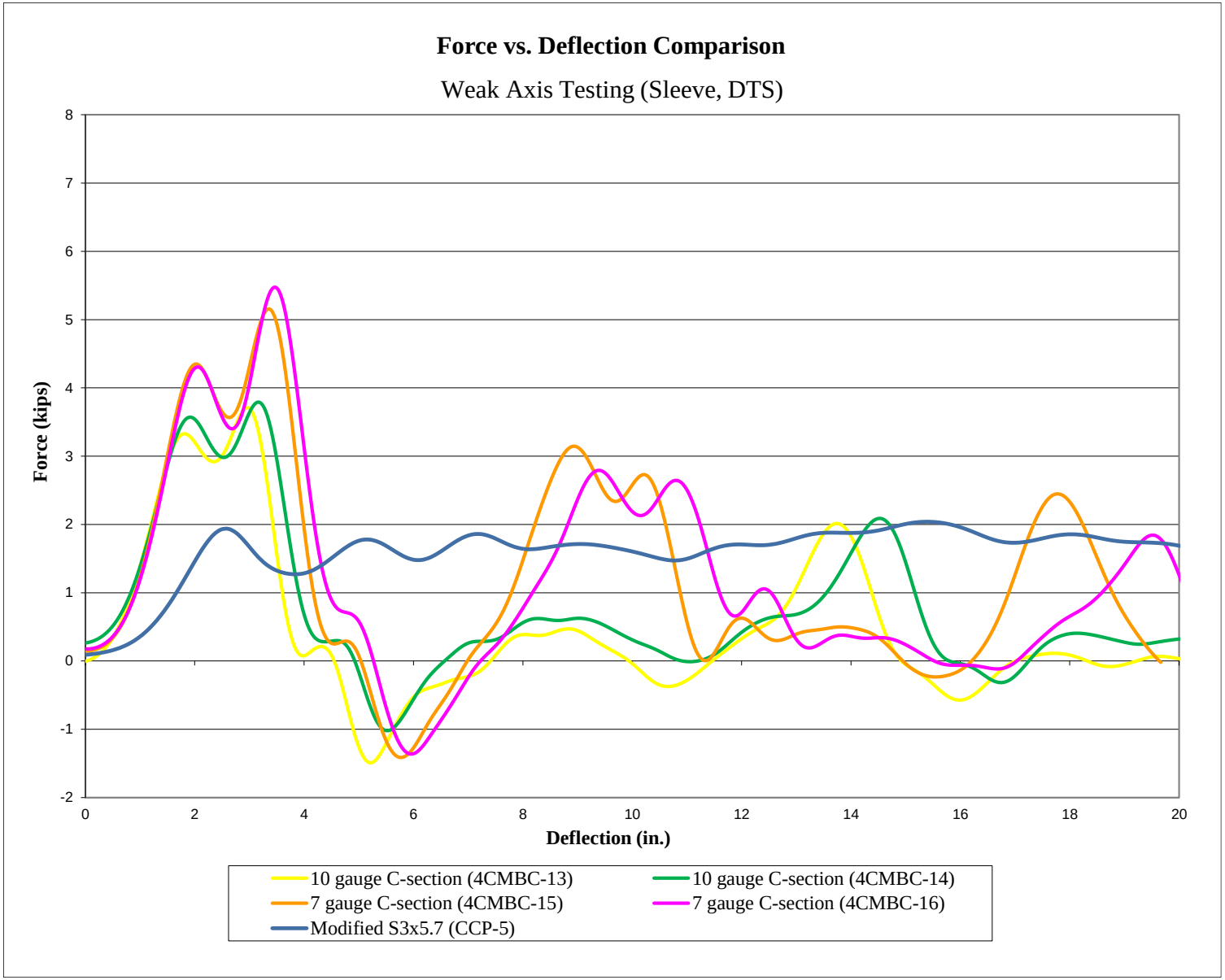

Figure 69. Force vs. Deflection Post Comparison, Weak Axis Testing in Sleeve

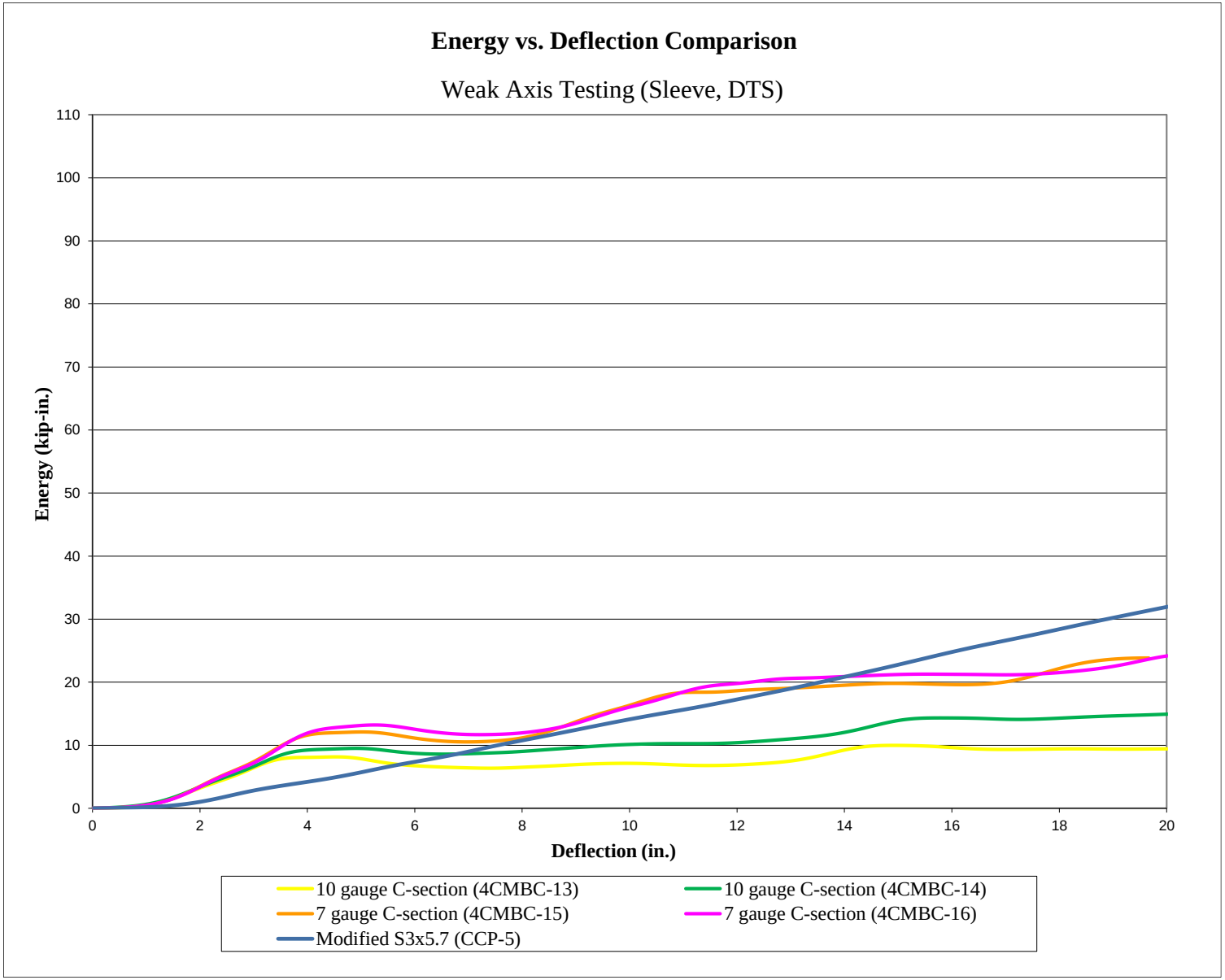

Figure 70. Energy vs. Deflection Post Comparison, Weak Axis Testing in Sleeve

6 DYNAMIC TESTING – KEYWAY WITH C-SECTION POST

6.1 Scope

The 7-gauge bent C-section post was selected for further evaluation following test nos. 4CMBC-1 through 4CMBC-16 and comparison of its performance with the 10-gauge C-section post and S3x5.7 (S76x8.5) steel posts. All of the testing of the bent C-section posts described up to this point focused on post sections without the keyway and hole configuration required for the cable-to-post attachments. There was some concern that the new post design may behave differently under load with these features included. Thus, a second round of component testing of the 7-gauge bent C-section post was conducted. For these tests, a keyway was added to the 7-gauge C-section post 16 in. (406 mm) above the groundline.

Two dynamic component tests were conducted on long, bent 7-gauge C-section posts with keyway holes. The target impact speed was 20 mph (32 km/h) for both tests. The posts were placed in a rigid sleeve. One test was conducted on the weak axis and the other was conducted on the strong axis. The dynamic component test matrix is show in Table 6. The test setup and bent C-section post are shown in Figures 71 and 72, respectively. Material specifications, mill certificates, and certificates of conformity for the post materials used in both tests are shown in Appendix A.

Table 6. Dynamic Post Testing Matrix, Test Nos. CPK-1 and CPK-2

Test No.	Post Type	Gauge	Impact Axis	Foundation Type	Post Length in. (mm)	Embedment Depth in. (mm)	Target Impact Velocity mph (km/h)
CPK-1	Bent C-Section with Keyway Holes	7	Strong	Sleeve	90 (2,286)	42 (1,067)	20 (32)
CPK-2	Bent C-Section with Keyway Holes	7	Weak	Sleeve	90 (2,286)	42 (1,067)	20 (32)

Test Quantity	Post Type	Bogie No.	Embedment Depth in. [mm]	Load Height in. [mm]	Impact Speed mph [km/h]	Impact Axis
1	7–Gauge C–Section Post	3	42 [1067]	27 [686]	20 [32.2]	Strong
1	7–Gauge C–Section Post	3	42 [1067]	27 [686]	20 [32.2]	Weak

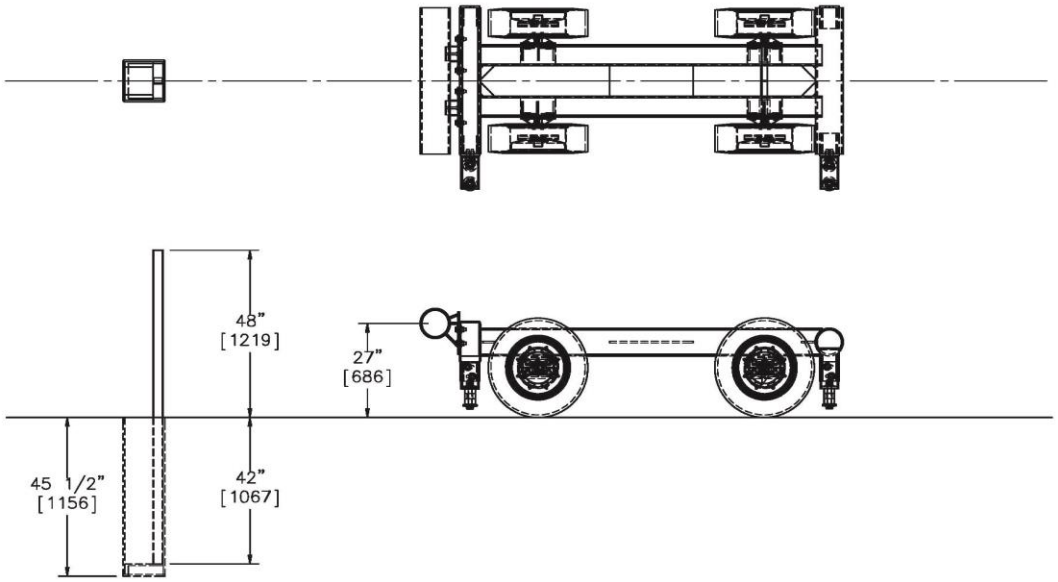

Notes: (1) Drawing shows strong–axis test setup only. For weak axis, the post shall be rotated 90 degrees to its closed face.

(2) A 3–in. (76–mm) spacer is placed at the bottom of the rigid sleeve to raise the post to the correct height.

(3) Shim material to fit. Posts must be placed in holes with wood and steel shims and made tight (i.e., no gaps).

Midwest Roadside Safety Facility	Cable Median Barrier Bent C–Section with Keyway C–Section Rigid Sleeve Test	SHEET: 1 of 2 DATE: 11/4/2014 DRAWN BY: JGP/SDB
	DWG. NAME. CPostKeyway_R2 SCALE: 1:40 UNITS: in.[mm]	REV. BY: –

Figure 71. Bogie Test Setup, Test Nos. CPK-1 and CPK-2

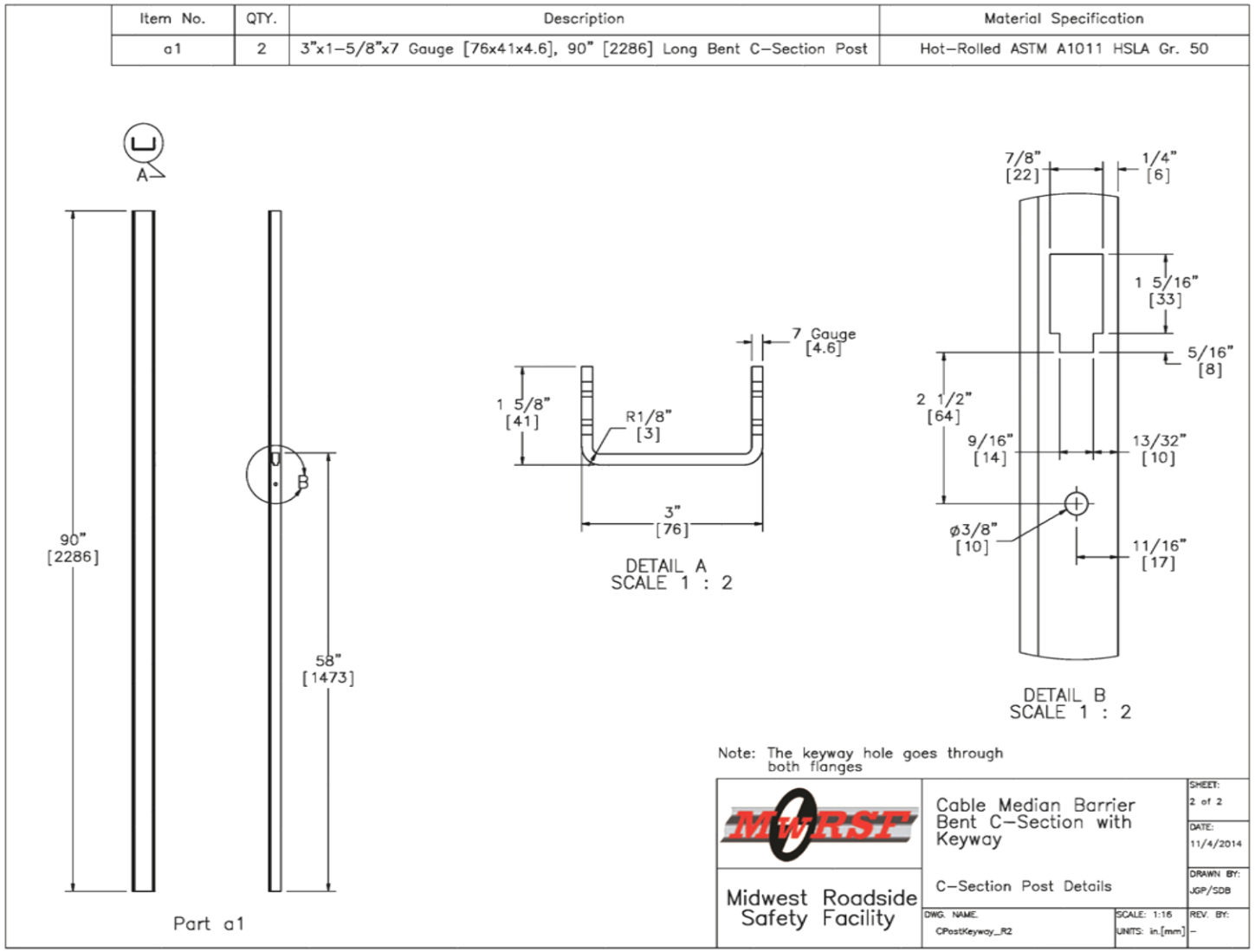

Figure 72. Post Details, Test Nos. CPK-1 and CPK-2

6.2 Dynamic Testing Results

Results of each test are discussed in the following sections. Individual results for all accelerometers used during each test are provided in Appendix C. The values described were calculated from the DTS-SLICE data curves.

6.2.1 Test No. CPK-1

During test no. CPK-1, the bogie impacted the 7-gauge C-section steel post at a speed of 20.5 mph (33.0 km/h). As a result of the strong-axis impact, the post began to deflect, twisted, and then yielded and produced a hinge at the keyway approximately 14½ in. (368 mm) above the groundline. The bogie overrode the post at a maximum deflection of 12.1 in. (307 mm).

Force vs. deflection and energy vs. deflection curves created from the DTS-SLICE accelerometer data are shown in Figure 73. The forces quickly rose to a peak force of 7.0 kips (31.1 kN) at 2.5 in. (64 mm) of deflection. The post provided an average resistive force of 2.1 kips (9.3 kN) through 5 in. (127 mm) of deflection and 2.0 kips (8.9 kN) through 10 in. (254 mm) of deflection. The energy absorbed by the post was 10.5 kip-in. (1.2 kJ) through 5 in. (127 mm) of deflection and 20.4 kip-in. (2.3 kJ) through 10 in. (254 mm) of deflection. Pre-test and post-test photographs are shown in Figure 74. Time-sequential photographs are shown in Figure 75.

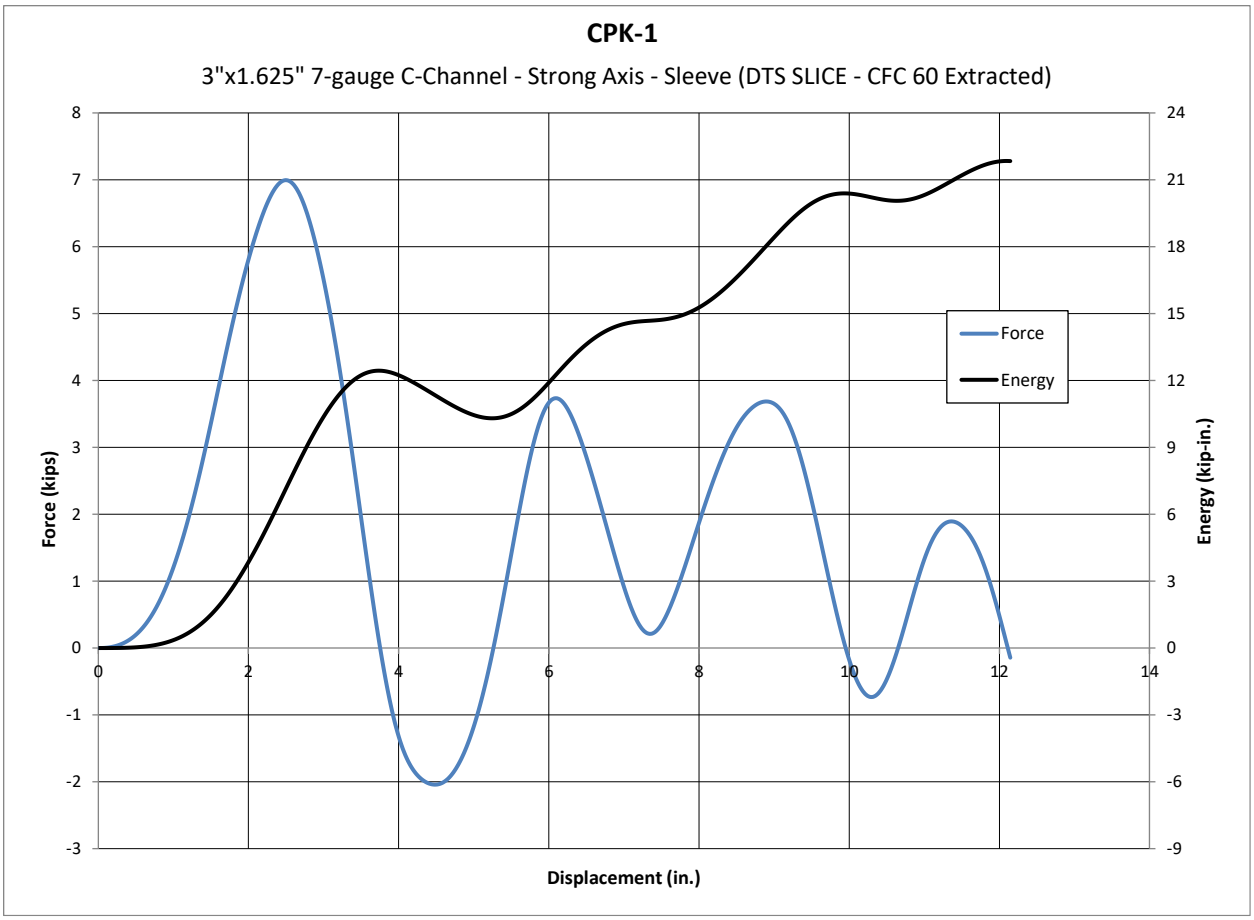

Figure 73. Force vs. Deflection and Energy vs. Deflection, Test No. CPK-1

Pre-Test Post-Test

Figure 74. Pre-Test and Post-Test Photographs, Test No. CPK-1


0.000 sec


0.040 sec


0.010 sec


0.050 sec


0.020 sec

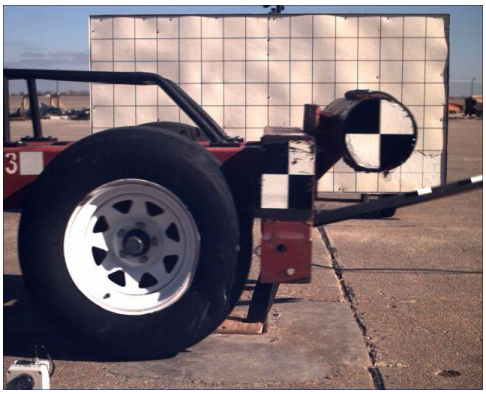
0.060 sec


0.030 sec


0.070 sec

Figure 75. Sequential Photographs, Test No. CPK-1

6.2.2 Test No. CPK-2

During test no. CPK-2, the bogie impacted the 7-gauge C-section steel post at a speed of 20.6 mph (33.2 km/h). As a result of the weak-axis impact, the post deflected backward, yielded, and produced a hinge at the keyway approximately 14 ½ in. (368 mm) above the groundline. The bogie overrode the post at a maximum deflection of 10.8 in. (274 mm).

Force vs. deflection and energy vs. deflection curves created from the DTS-SLICE accelerometer data are shown in Figure 76. The forces quickly rose to a peak force of 5.2 kips (23.1 kN) at 2.3 in. (58 mm) of deflection. The post provided an average resistive force of 2.3 kips (10.2 kN) through 5 in. (127 mm) of deflection and 1.5 kips (6.7 kN) through 10 in. (254 mm) of deflection. The energy absorbed by the post was 11.5 kip-in. (1.3 kJ) through 5 in. (127 mm) of deflection and 15.4 kip-in. (1.7 kJ) through 10 in. (254 mm) of deflection. Pre-test and post-test photographs are shown in Figure 77. Time-sequential photographs are shown in Figure 78.

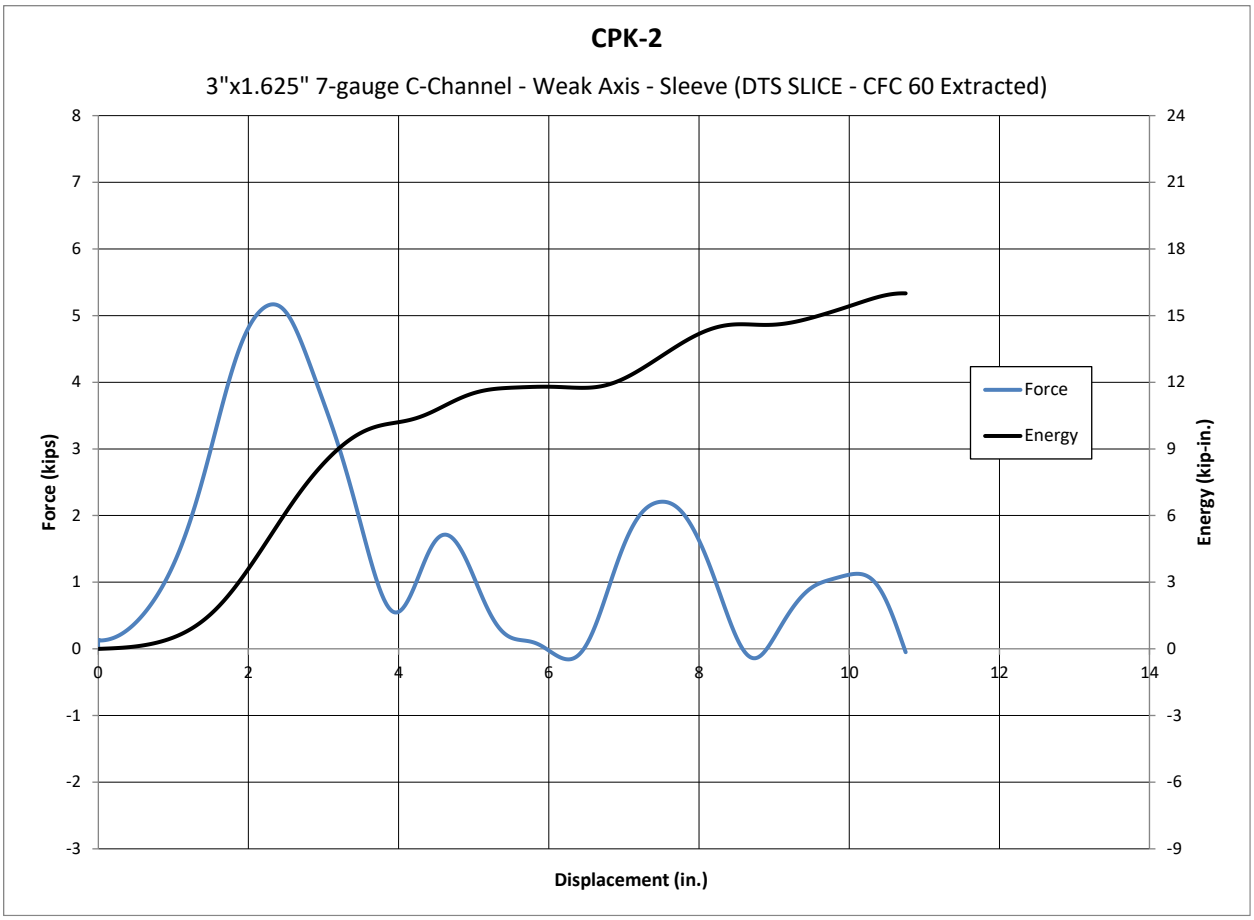

Figure 76. Force vs. Deflection and Energy vs. Deflection, Test No. CPK-2

Pre-Test Post-Test

Figure 77. Pre-Test and Post-Test Photographs, Test No. CPK-2

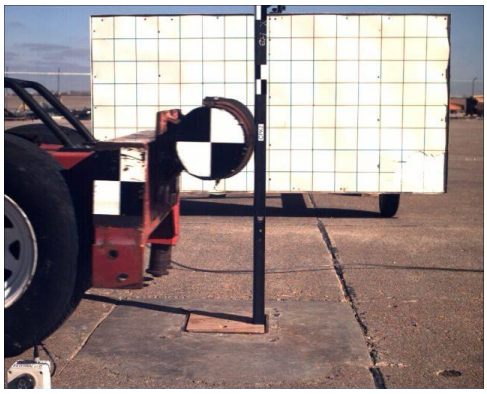
0.000 sec

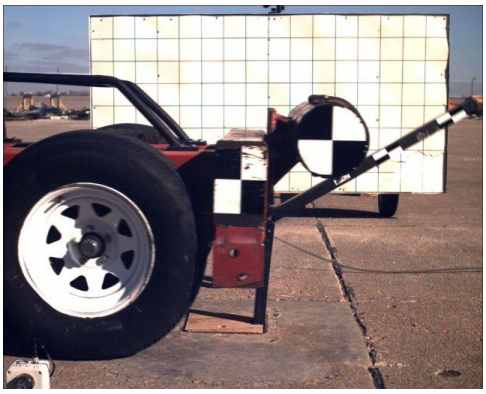
0.040 sec

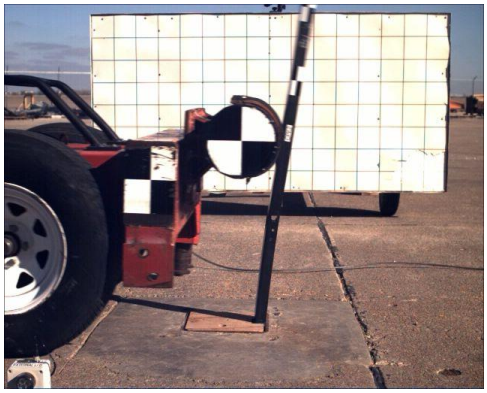
0.010 sec

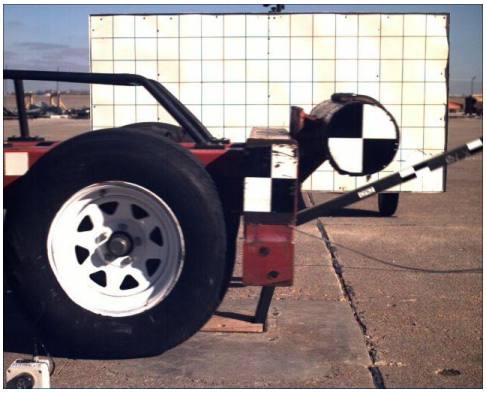
0.050 sec


0.020 sec

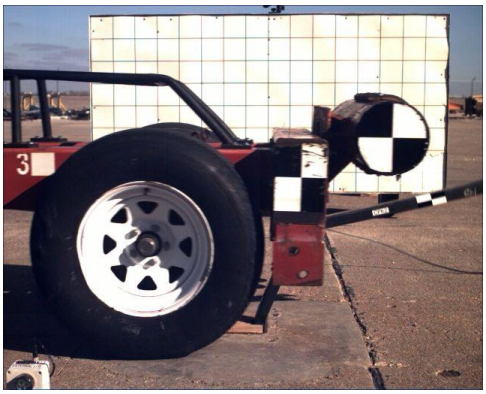

0.060 sec

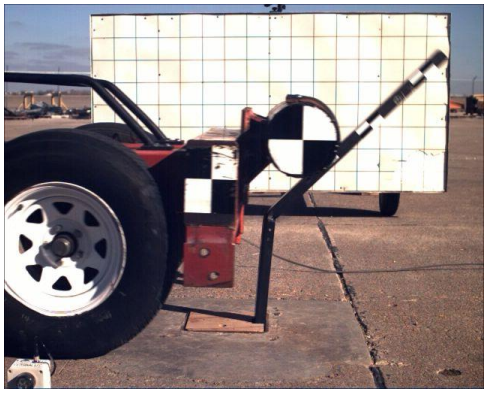
0.030 sec

0.070 sec

Figure 78. Sequential Photographs, Test No. CPK-2

6.3 Summary of Dynamic Testing

Two dynamic component tests were conducted on long, bent 7-gauge C-section posts with cable-to-post attachment keyways and holes placed with the top of the keyway 16 in. (406 mm) above the groundline. The posts were impacted on both the strong and weak axes to establish the force vs. deflection and energy vs. deflection characteristics of the post with the keyways in place. The results from the bogie testing matrix and comparisons to the C-section posts are summarized in Table 7. The C-section posts were compared using force vs. deflection and energy vs. deflection comparison curves, as shown in Figures 79 through 82.

Comparison of the strong-axis testing of the bent C-section post with keyways to the posts without keyways showed reductions in average forces, as shown in Figures 79 and 80. When installed in a rigid foundation, the posts with keyways provided 23.1 percent lower forces through 10 in. (254 mm) of deflection.

Similar results were obtained for the weak-axis testing, as shown in Figures 79 and 80. However, the keyways provided only a 6.3 percent reduction in forces through 10 in. (254 mm) of deflection.

Due to the addition of the keyway, both posts failed at the keyway by buckling, reducing the force and energies. The buckling at the keyway also limited the effective energy absorption of the posts as the post hinged around the keyway, giving the posts approximately 50 percent less deflection. After impact, there was also a large post stub left below the keyway, which could potentially penetrate into the occupant compartment during an impact event. Therefore, the post was needed to be redesigned to improve the performance.

Table 7. Dynamic Testing Results, Keyway Posts

Test No.	Impact Axis	Impact Velocity mph (km/h)	Peak		Average Force kips (kN)		Maximum Deflection in. (mm)	Absorbed Energy kip-in. (kJ)		Post Behavior	Location of Plastic Hinge Above Groundline in. (mm)
			Deflection in. (mm)	Force kips (kN)	at 5" (127 mm)	at 10" (254 mm)		at 5" (127 mm)	at 10" (254 mm)		
C-Section Keyway Posts in Sleeve											
CPK-1	Strong	20.5 (33.0)	2.5 (64)	7.0 (31.1)	2.1 (9.3)	2.0 (8.9)	12.1 (307)	10.5 (1.2)	20.4 (2.3)	Bending	14.5 (368)
CPK-2	Weak	20.6 (33.2)	2.3 (58)	5.2 (23.1)	2.3 (10.2)	1.5 (6.7)	10.8 (274)	11.5 (1.3)	15.4 (1.7)	Bending	14.5 (368)
C-Section Posts in Sleeve											
4CMCB-11	Strong	20.5 (33.0)	1.9 (48)	5.5 (24.5)	2.3 (10.2)	2.5 (11.1)	19.5 (495)	11.5 (1.3)	24.8 (2.8)	Bending, Twisting	11 (279)
4CMCB-12	Strong	20.9 (33.6)	2.3 (58)	6.2 (27.6)	2.6 (11.6)	2.7 (12.0)	20.2 (513)	13.2 (1.5)	26.9 (3.0)	Bending, Twisting	11 (279)
Averages			**2.1 (53)**	**5.9 (26.2)**	**2.5 (11.1)**	**2.6 (11.6)**	**19.9 (505)**	**12.4 (1.4)**	**25.9 (2.9)**		**11 (279)**
4CMCB-15	Weak	20.7 (33.3)	3.4 (86)	5.2 (23.1)	2.4 (10.7)	1.6 (7.1)	19.7 (500)	12.1 (1.4)	16.3 (1.8)	Bending	0 (0)
4CMCB-16	Weak	20.7 (33.3)	3.5 (89)	5.5 (24.5)	2.6 (11.6)	1.6 (7.1)	23.6 (599)	13.1 (1.5)	16.1 (1.8)	Bending	0 (0)
Averages			**3.5 (89)**	**5.4 (24.0)**	**2.5 (11.1)**	**1.6 (7.1)**	**21.7 (551)**	**12.6 (1.4)**	**16.2 (1.8)**		**0 (0)**

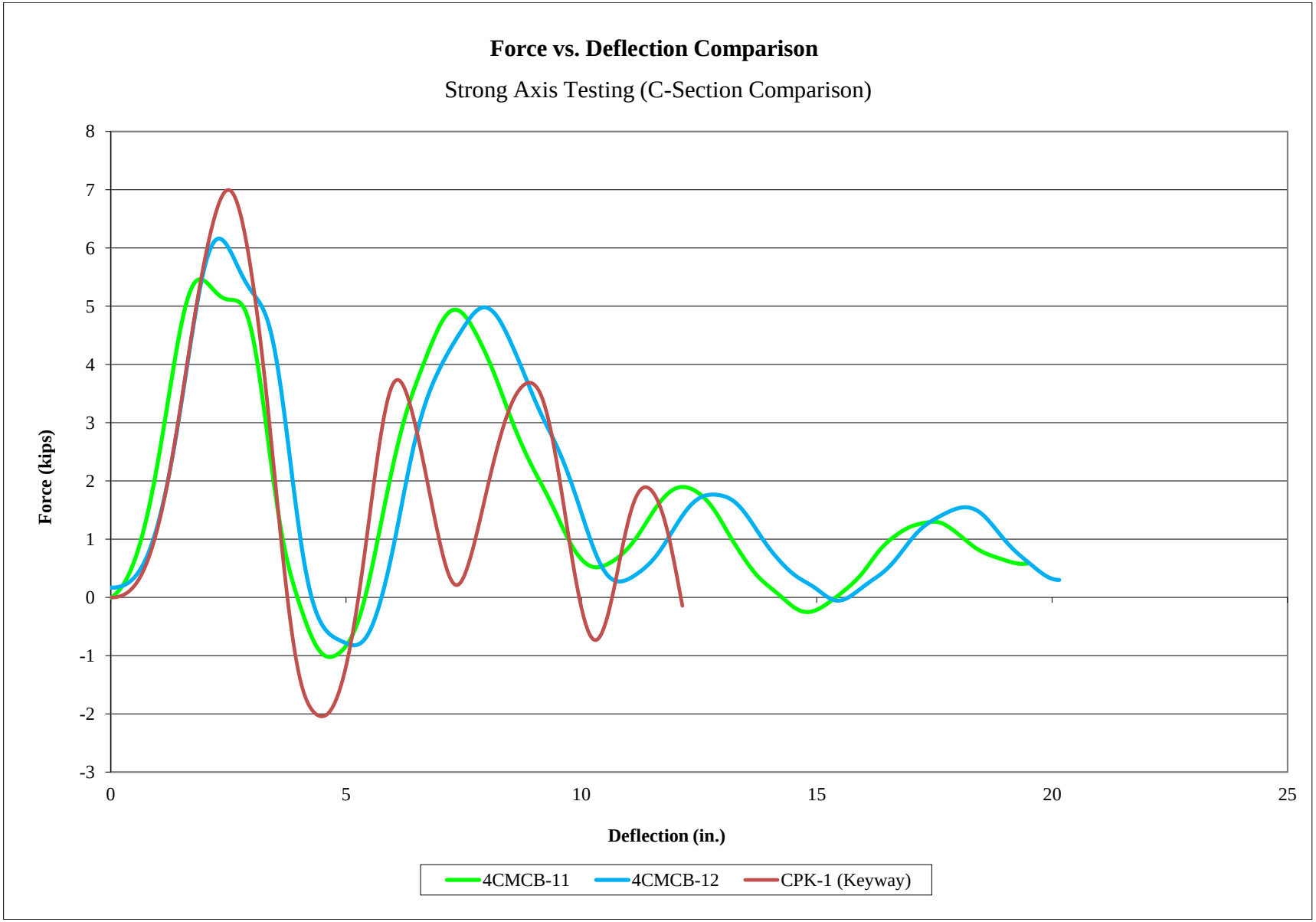

Figure 79. Force vs. Deflection Comparison, Strong Axis

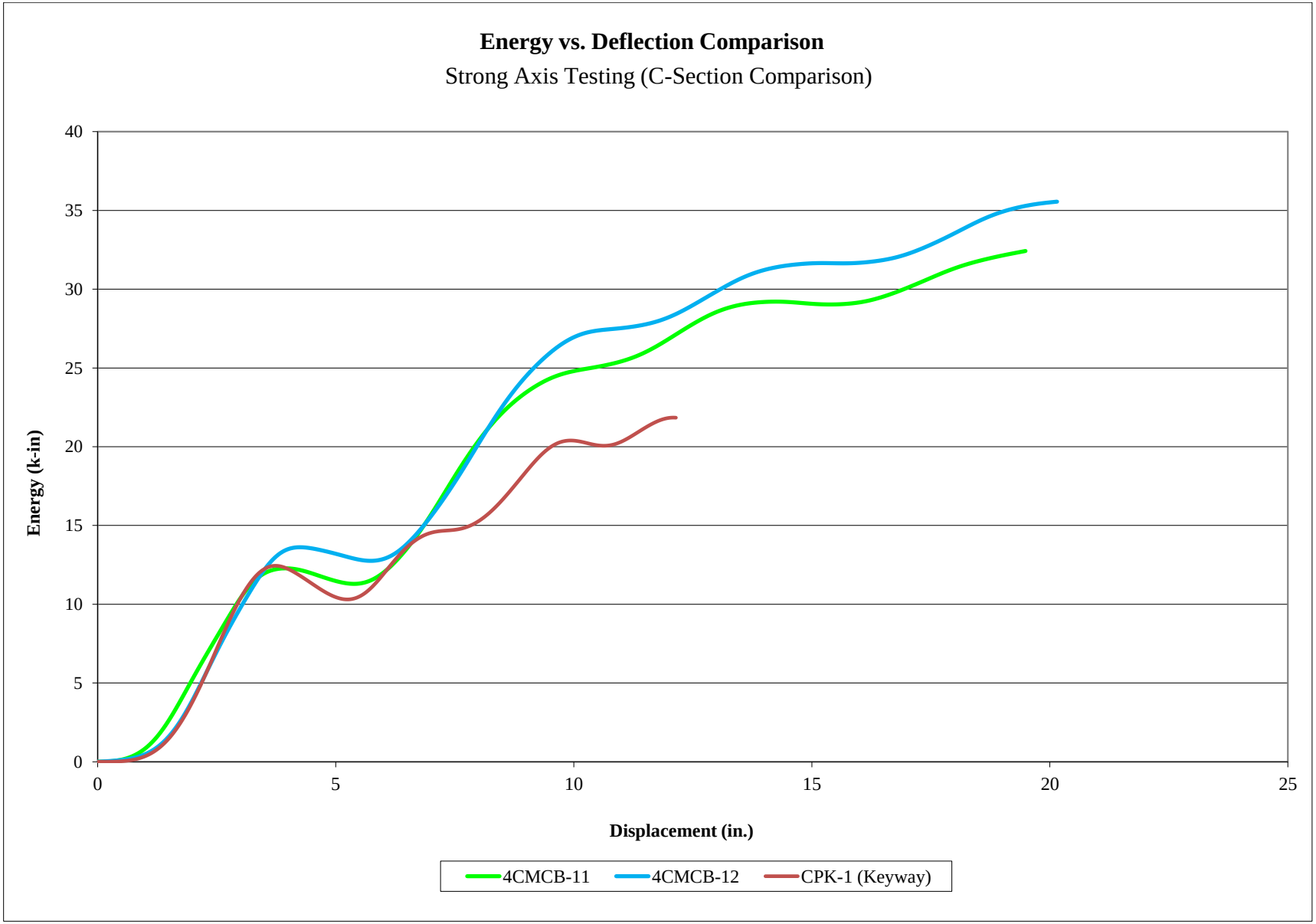

Figure 80. Energy vs. Deflection Comparison, Strong Axis

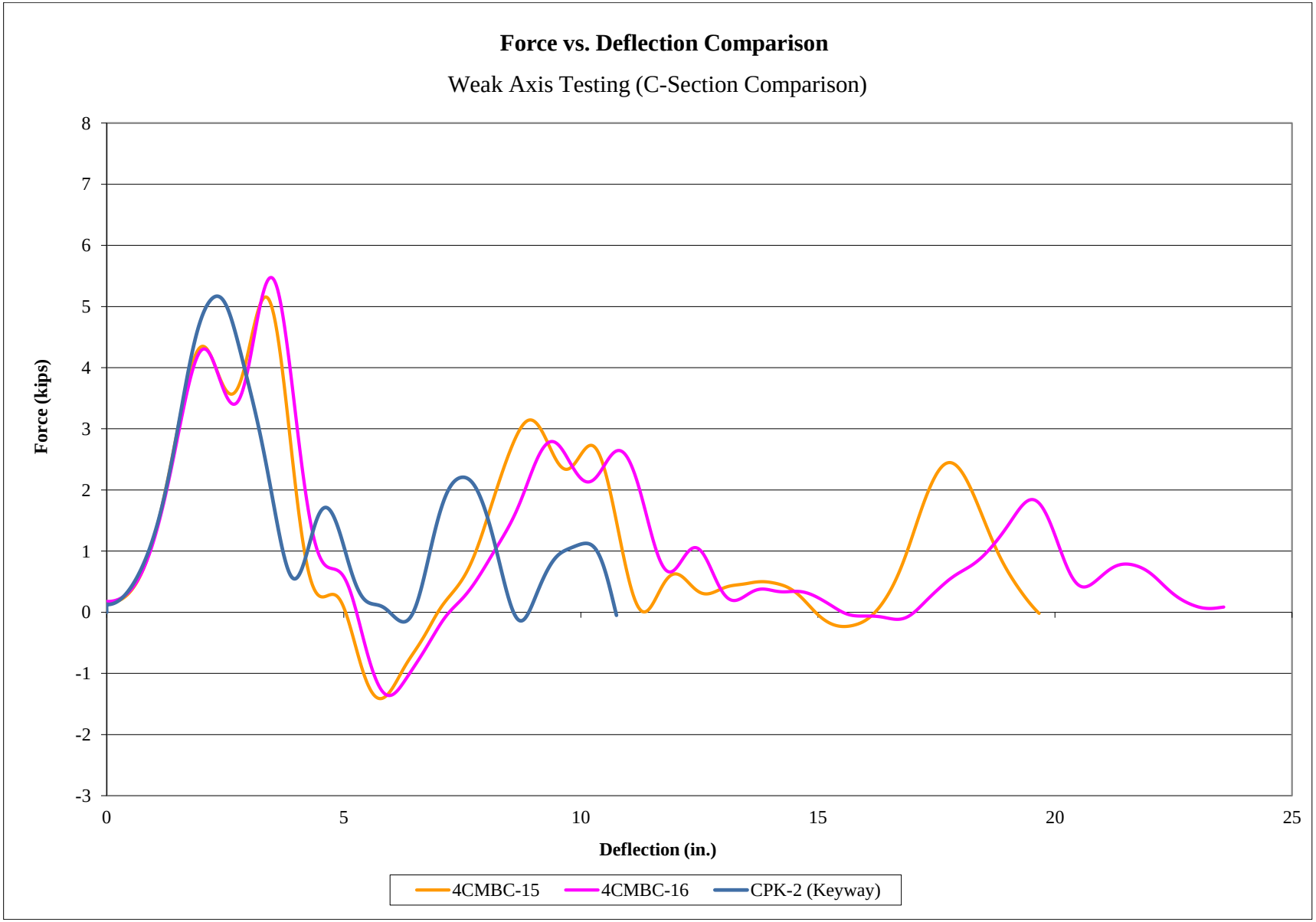

Figure 81. Force vs. Deflection Comparison, Weak Axis

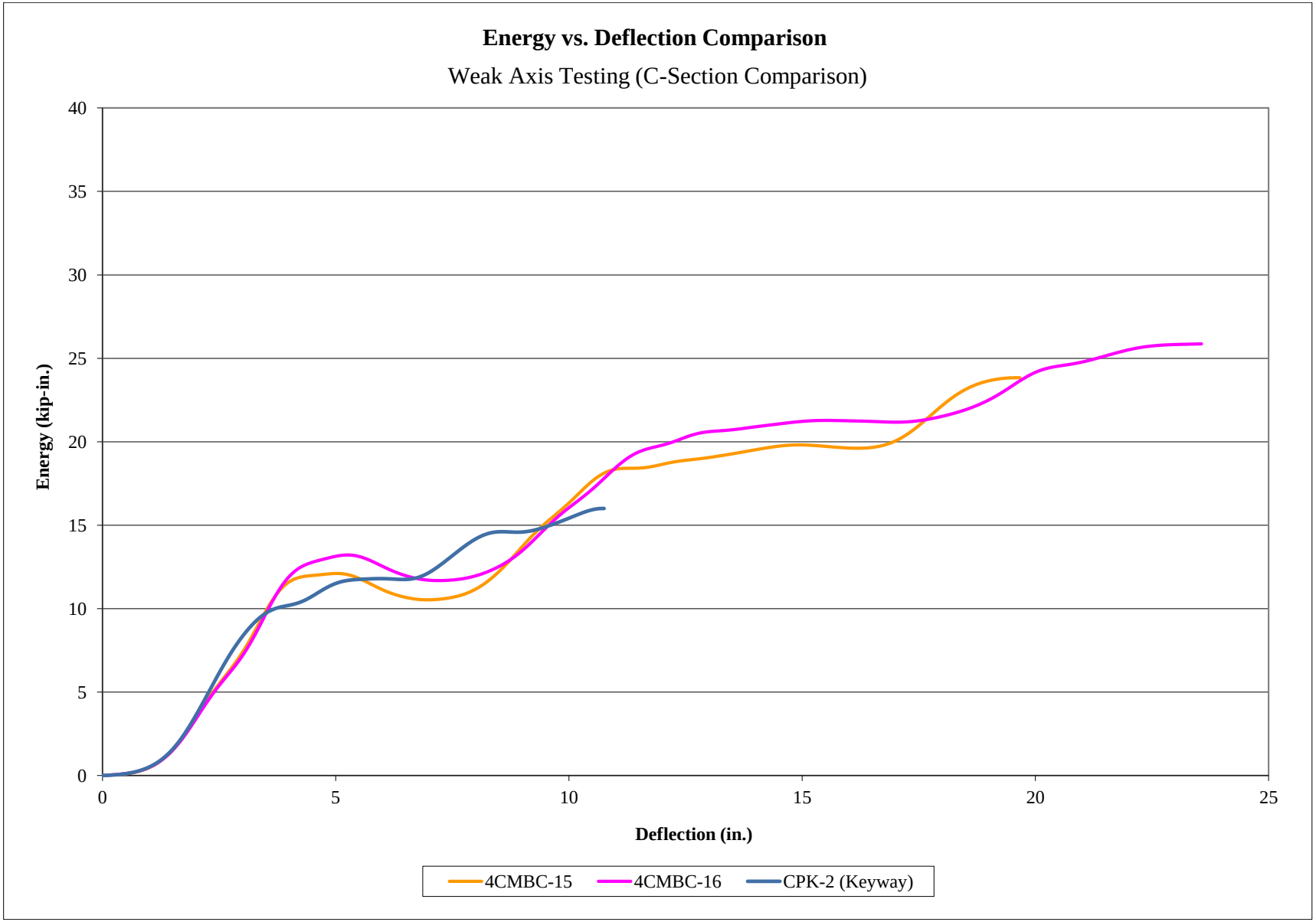

Figure 82. Energy vs. Deflection Comparison, Weak Axis

7 DESIGN AND SIMULATION OF REVISED POST SECTION

Following the testing of the bent C-section posts, the researchers turned to finite element computer simulation with LS-DYNA [13] to design and evaluate improved post sections for the non-proprietary high-tension cable median barrier system. The goal of the simulation effort was to develop a post section that met the original design criteria set forth in Chapter 2 and would prevent the buckling of the post section above the groundline near the keyway used for the cable-to-post attachment. Redesign of the post section was performed in three steps. First, the researchers developed a computer simulation model of the bent C-section post that was capable of reproducing the loading and buckling behaviors observed in the component testing. Next, modifications were made to the C-section post design to alleviate the buckling of the post at the keyway, including modifying the section dimensions and weakening the base of the post. Finally, alternative post cross sections that were not C-shaped were modeled to develop a more effective post section.

7.1 Simulation of 7-Gauge Bent C-Section Posts

The development of a revised and improved post section began with the creation of baseline models of the 7-gauge bent C-section posts that were evaluated in the previous component testing in a rigid foundation with and without keyways. The posts were modeled based on the rigid sleeve, strong-axis tests to isolate the performance of the steel post section and attempt to replicate the buckling observed in the physical tests. A simple model of the component testing was set up using a rigid impact head equipped with the mass of the original bogie vehicle and prescribed to impact the simulated post at the same speed and impact height as the 4CMBC and CPK test series. A model of the 7-gauge bent C-section post was created using shell elements and embedded in a rigid sleeve similar to the component testing. The post was formed with Belytschko-Tsay elements with hourglass control, and the material properties were

defined using MAT_PIECEWISE_LINEAR_PLASTICITY and material data taken from the mill certs of the ASTM A1011 HSLAS Grade 50 sheet steel used in the tests.

7.1.1 C-Section Post Without Keyways

An initial model of the 7-gauge bent C-section post was created without keyways for comparison with test nos. 4CMBC-11 and 4CMBC-12 in order to verify that the model produced representative force and energy levels and similar deformation to the strong axis component tests, as shown in Figure 83. Sequential comparisons between the results from the simulation and the component tests are shown in Figure 84. The force vs. deflection and energy vs. deflection plots from the simulation and testing are shown in Figure 85, and the deformation and failure mode of the deformed post following the test are shown in Figure 86.

Review of the simulation results found that the simulation model provided a reasonable prediction of the performance of the post without keyways. The sequential images of the two component tests and the simulation demonstrated similar post behavior during the impact, with the post deflecting, twisting, and yielding in a very similar manner. The force vs. deflection curves of the physical testing and the simulation showed very similar peak loads and overall shapes, but the secondary force peak and average forces were lower for the simulated post. This discrepancy was due to some extent on the simple impactor used in the simulation, in lieu of the actual bogie vehicle, which did not register secondary impacts with the bogie frame that were observed in the physical test. Comparison of the energy curves further demonstrated this trend, as energy levels were very similar through the first 6 in. to 8 in. (152 mm to 203 mm) of deflection, and then were reduced for the simulated post. Thus, the loading behavior of the simulated post was considered a reasonable representation of the physical tests in the absence of the complete bogie vehicle. Finally, comparison of the deformed posts from the simulation and testing found that the simulated post developed similar twisting and yielding to the tested posts.

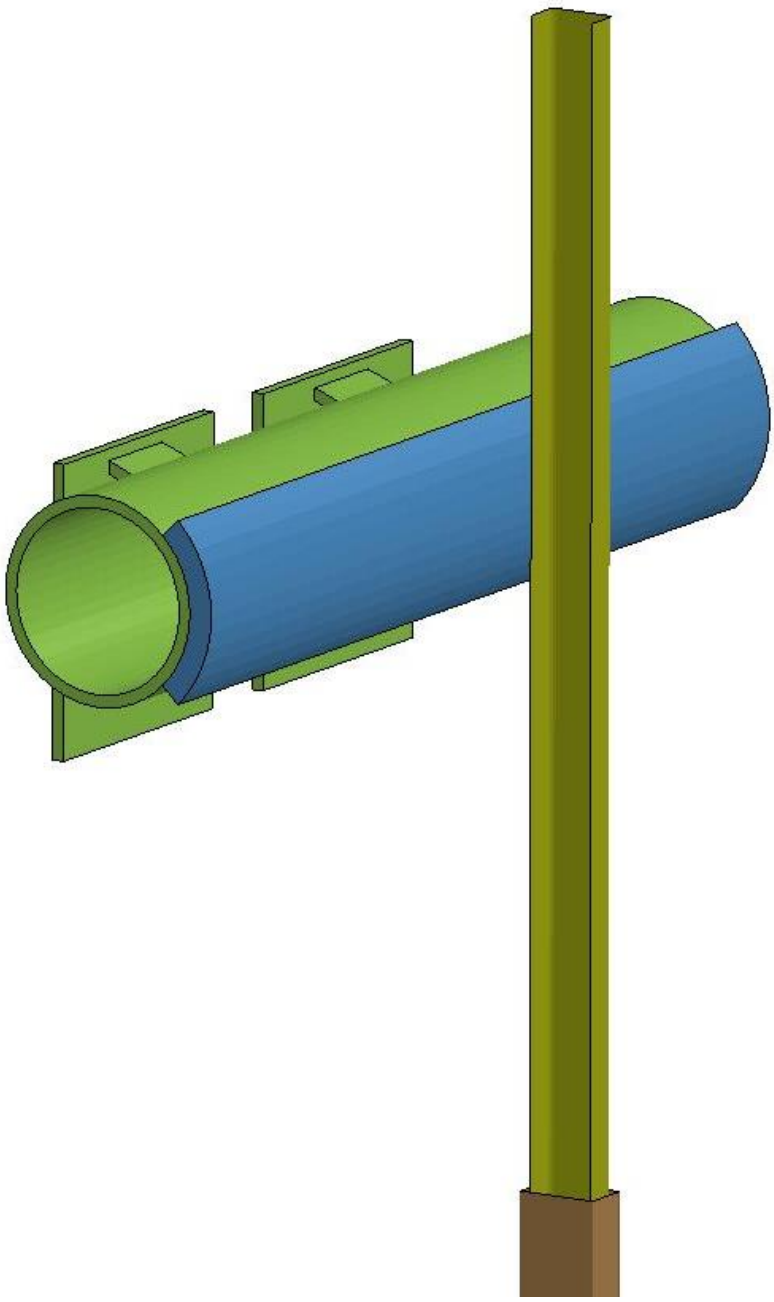

Figure 83. LS-DYNA Simulation of 7-Gauge Bent C-Section Post Strong-Axis Impact

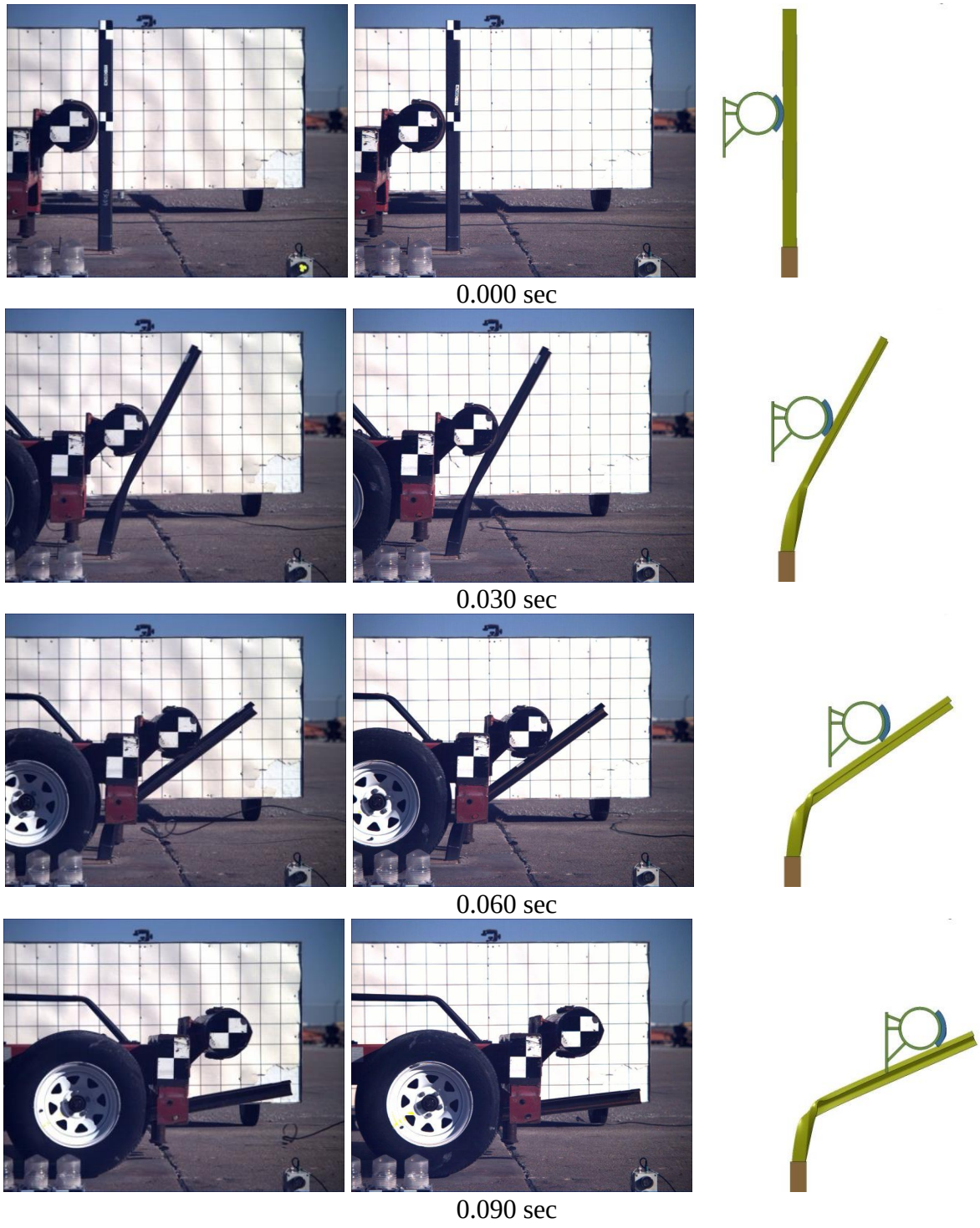

Figure 84. Sequential Images, Test Nos. 4CMBC-11 and 4CMBC-12, and LS-DYNA Simulation

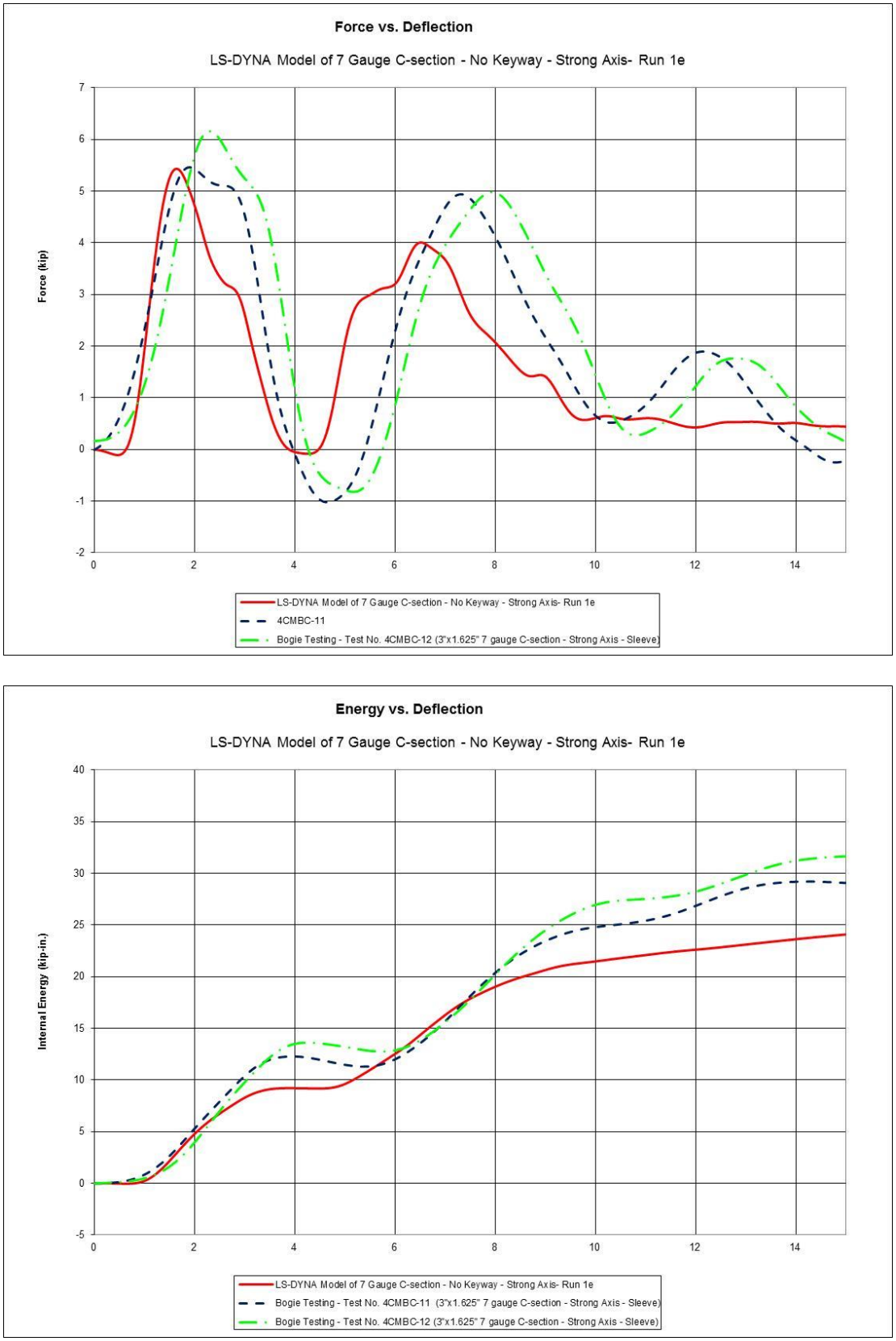

Figure 85. Force and Energy vs. Deflection, Test Nos. 4CMBC-11 and 4CMBC-12, and LS-DYNA Simulation

Test No. 4CMBC-11

Test No. 4CMBC-12

Figure 86. Deformed Post Shape, Test Nos. 4CMBC-11 and 4CMBC-12, and LS-DYNA Simulation

Based on these comparisons, the researchers believed that the simulated post was capable of reproducing the behavior from the physical tests and providing similar loads and failure mechanisms. The next step was to model the post with the keyways for the cable-to-post attachments included to ensure that the model could capture the buckling failure observed in tests of that configuration prior to investigating design modifications.

7.1.2 C-Section Post With Keyways

A second model of the 7-gauge bent C-section post was created with the keyways and holes for the cable-to-post attachments, as shown previously in test nos. CPK-1 and CPK-2. The simulation model used the same general setup and model parameters as the previous C-section post model except for the addition of the keyways, as shown in Figure 87. The objective of the simulation model was to verify that the simulation model could capture the buckling of the post near the keyway that the researcher desired to eliminate. Once the model proved capable of replicating that failure mode, there would be high confidence that simulation of revised post sections would be able to indicate potential solutions.

Sequential comparison of the results from the simulation and test no. CPK-1 are shown in Figure 88. The force vs. deflection and energy vs. deflection plots from the simulation and testing are shown in Figure 89, and the deformation and failure mode of the deformed post following the test are shown in Figure 90.

Review of the simulation results found that the simulation model provided a reasonable prediction of the performance of the bent C-section post with keyways. The sequential images of the component test and the simulation demonstrated similar post behavior during the impact, with the post deflecting, and buckling near the lowest keyway on the backside of the post in both the test and the simulation. The force vs. deflection curves of the physical testing and the simulation showed very similar peak loads between the simulation and the data taken from the

Figure 87. LS-DYNA Simulation of 7-Gauge Bent C-Section Post Strong-Axis Impact

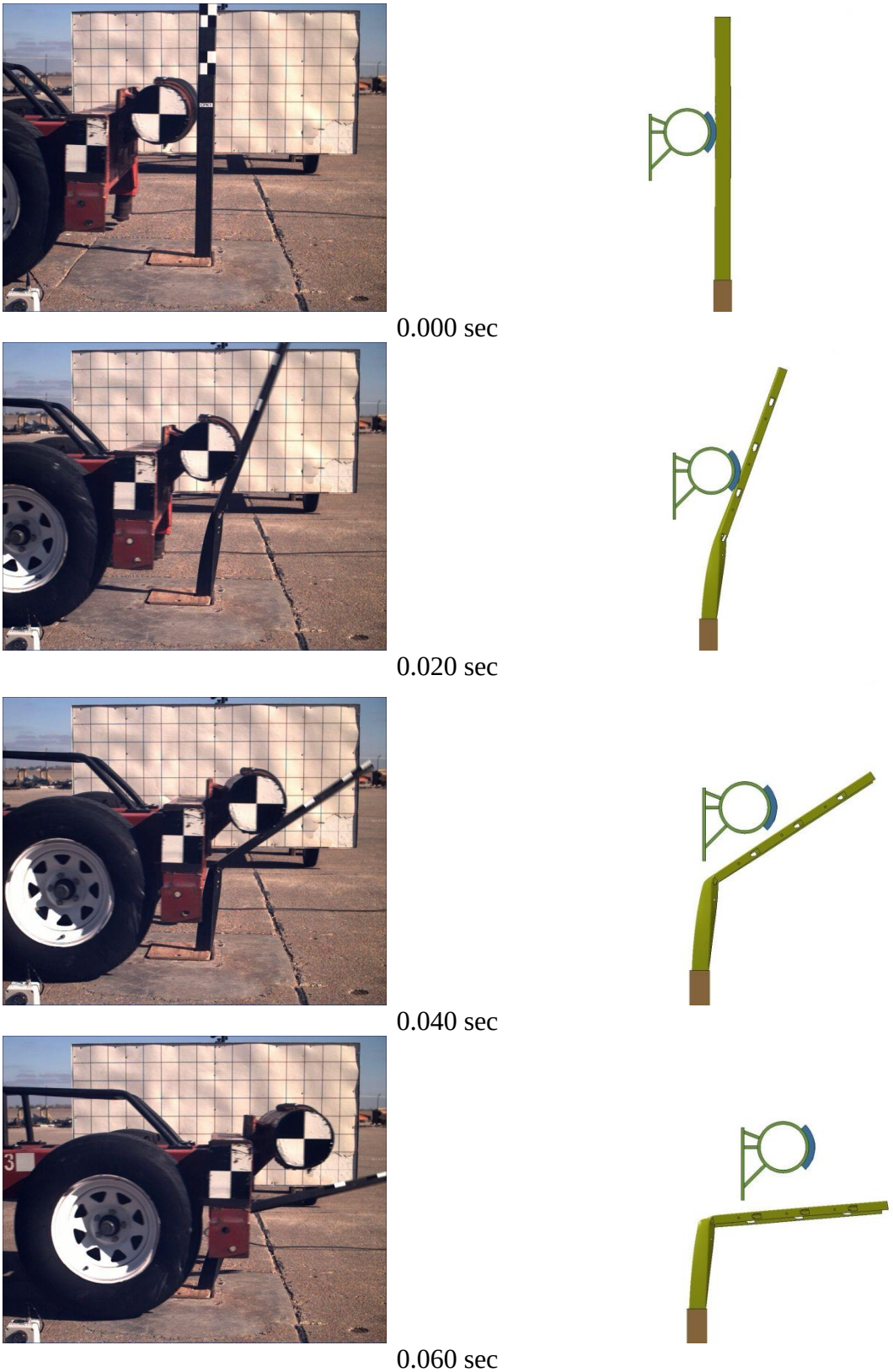

Figure 88. Sequential Images, Test No. CPK-1 and LS-DYNA Simulation

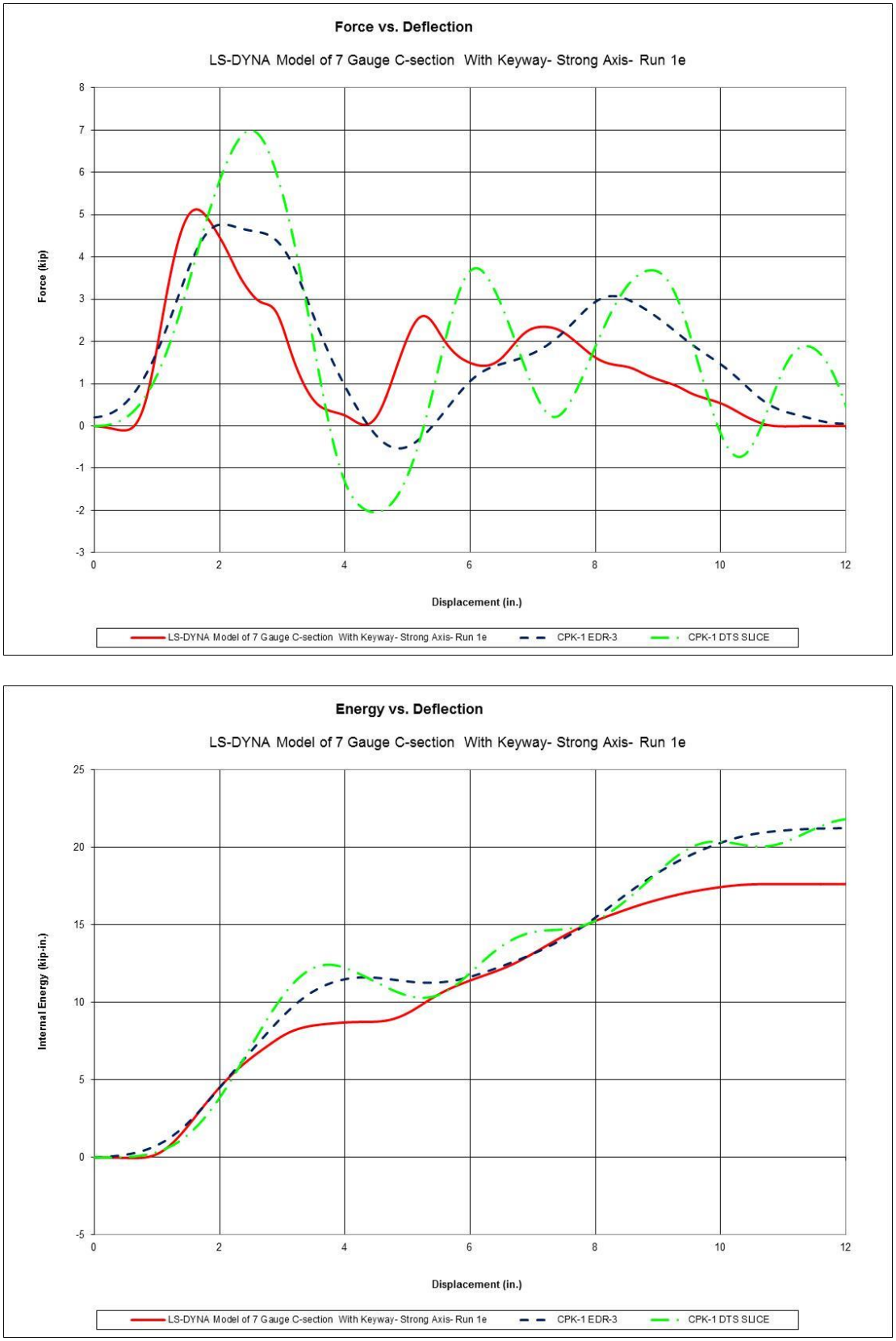

Figure 89. Force and Energy vs. Deflection, Test No. CPK-1 and LS-DYNA Simulation

Test No. CPK-1

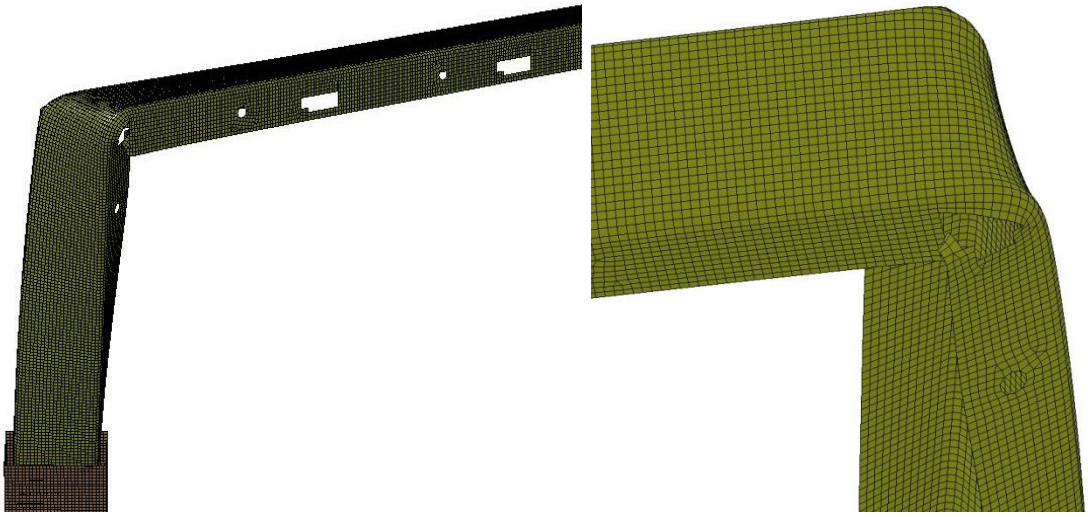

Figure 90. Deformed Post Shape, Test No. CPK-1 and LS-DYNA Simulation

EDR-3 unit and test no. CPK-1. The DTS-SLICE system found higher peak loads. The overall shapes for the force vs. deflection curves demonstrated similar trends, but the timing and duration of the loads varied somewhat between the simulation and each of the transducers used in test no. CPK-1. Again, this may have been partially due to the simple impactor used in the simulation not registering secondary impacts with the bogie frame that were observed in the physical test. Comparison of the energy curves further found that the energy levels were very similar through the first 6 in. to 8 in. (152 mm to 203 mm) of deflection, and then were reduced for the simulated post. Finally, comparison of the deformed posts from the simulation and testing found that the simulated post developed the same buckling failure mode observed near the lowest keyway. Thus, the comparisons of the C-post models with and without keyways to the physical testing found that the simulation was capable of capturing the behavior and failure modes of the posts.

7.2 Simulation of Modified 7-Gauge Bent C-Section Posts

The next step in the redesign of the post section for the non-proprietary high-tension cable median barrier was to use LS-DYNA computer simulation modeling to evaluate potential modifications to the previously tested bent C-section post in order to alleviate the buckling that was caused by the keyways used for the cable-to-post attachment. Two modifications were proposed and simulated in order to improve the performance of the post:

1. The width of the post flange was increased from $1^{5}/_{8}$ in. (41 mm) to 2 in. (51 mm), 2½ in. (64 mm), and 3 in. (76 mm), while maintaining the location of the keyway with respect to the web of the post. It was hoped that the increased flange width and the associated increase in material adjacent to the keyway would reduce the propensity for localized buckling at this location.

2. The C-section of the post was modified to include additional flange tabs on the open side of the section, as shown in Figure 91. The addition of the flange tabs was anticipated to provide additional strength and stability to the post and prevent buckling near the keyway.

Both of the proposed post section modifications were simulated, and the results for the increased flange length and the additional flange tabs are shown in Figure 92 and Figure 93, respectively. In both cases, the failure mode of the post remained buckling of the post flange near the lower keyway. This was undesirable due to the exposed post stub and the inadequate energy absorption caused by the buckling.

Further analysis using engineering calculations of the C-section post found that the asymmetry of the post moved the shear center of the section far from the center of the post section. Application of loads to the post that do not act through the shear center, such as those produced in strong-axis loading, cause the formation of a moment due to the eccentricity of the load with respect to the shear center. Thus, loading of the post along the strong axis causes the bending and twisting of the post observed in testing of the C-section post with and without keyways. When coupled with the weakened section near the keyway, this induced the buckling of the post. Based on this analysis and the simulations of the modified C-sections, it was determined that a more symmetric post section would be required in order to achieve a more stable design.

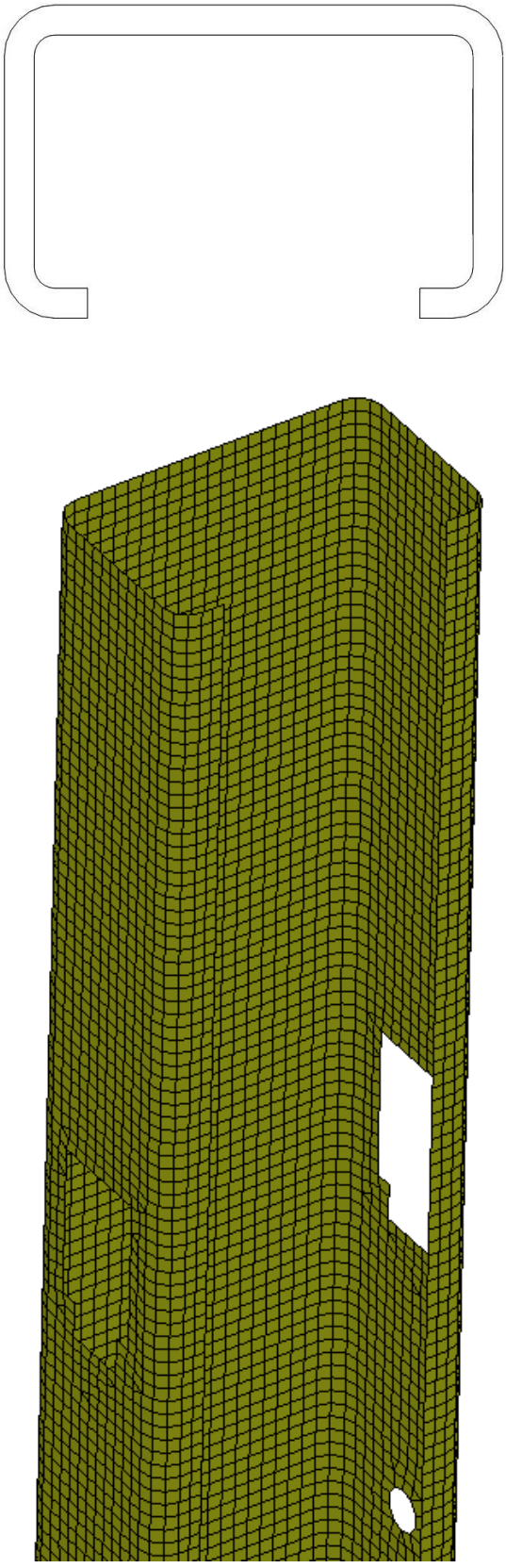

Figure 91. Proposed C-Section Post Modification, Additional Flange Tabs

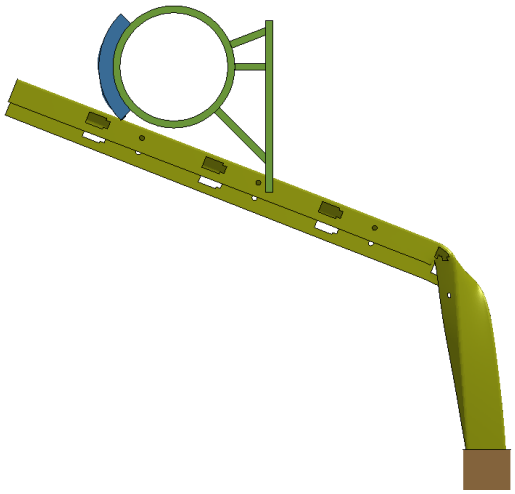

2-in. (51 mm) Flange

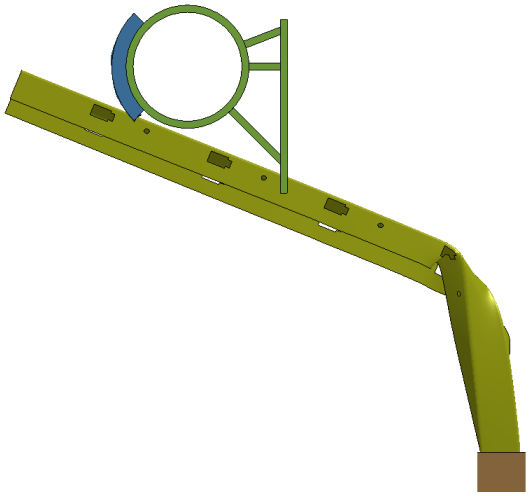

2 ½ in. (64 mm) Flange

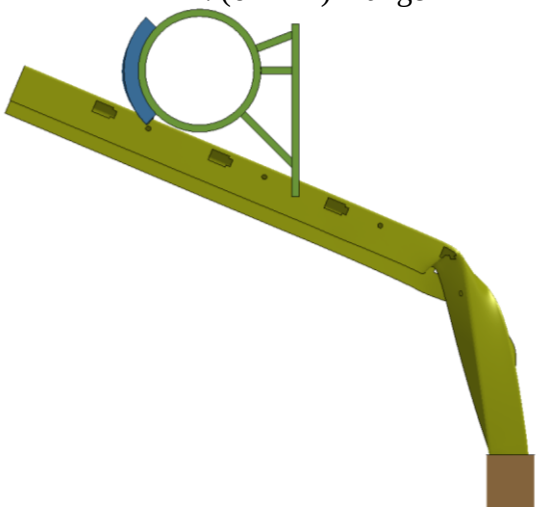

3 in. (76 mm) Flange

Figure 92. Simulation of Modified C-section Posts, Increased Flange Length

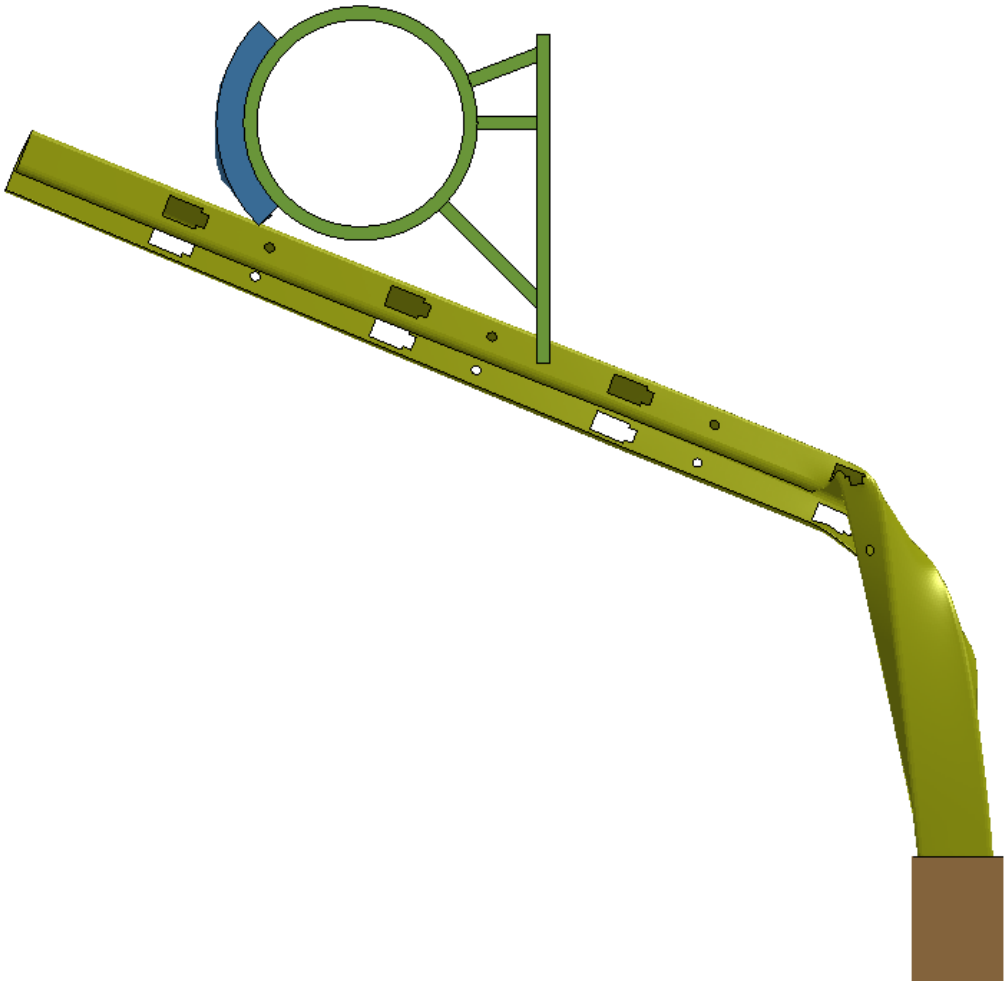

Figure 93. Simulation of Modified C-section Posts, Additional Flange Tabs

7.3 Design and Simulation 7-Gauge Bent Z-Section Posts

Following the simulation and analysis of the modified C-section posts, the researchers focused on development of a post section that could be fabricated from folded sheet steel like the C-section post but would retain the shear center in the center of the post section to prevent eccentric loading and buckling. In order to meet that goal, new post section designs were proposed and LS-DYNA computer simulations were conducted on the new sections to determine if they would perform as desired.

7.3.1 Design of Post Section

The researchers began with development of new, rotationally symmetric post cross sections that could be created from folded sheet steel. The requirement to fold the steel eliminated closed sections and the desire for rotational symmetry eliminated a majority of other section shapes such as L-sections. One shape that seemed to fit the design needs was a Z-shape post section as the shear center was located at the center of the post. Thus, a Z-section post was selected for the new post cross section.

Three versions of a Z-section post were developed for simulation and analysis, as shown in Figure 94. All three designs were selected to develop a strong-axis capacity near that of the 7-gauge bent C-section post tested previously, while maintaining a weak-axis capacity at or below that of an S3x5.7 (S76x8.5) post. Two different versions of traditional Z-sections were developed based on different versions of the cable-to-post attachments that were developed in parallel with the post study detailed herein [4]. The first option was developed and sized to allow for attachment of tabbed bracket V8, and the second option was developed and sized to allow for attachment of tabbed bracket V10. Tabbed bracket V8 extended slightly longer into the body of the post and thus required a slightly larger post section to accommodate the bracket. A third post design was developed that modified a standard Z-shape to optimize the attachment of the cable-

to-post bracket. The third design option had short sections of perpendicular web connected by a diagonal web section. This geometry allowed for placement of the cable-to-post attachment at the center of post section and reduced the width of the section considerably. All three sections were simulated using LS-DYNA to evaluate their effectiveness.

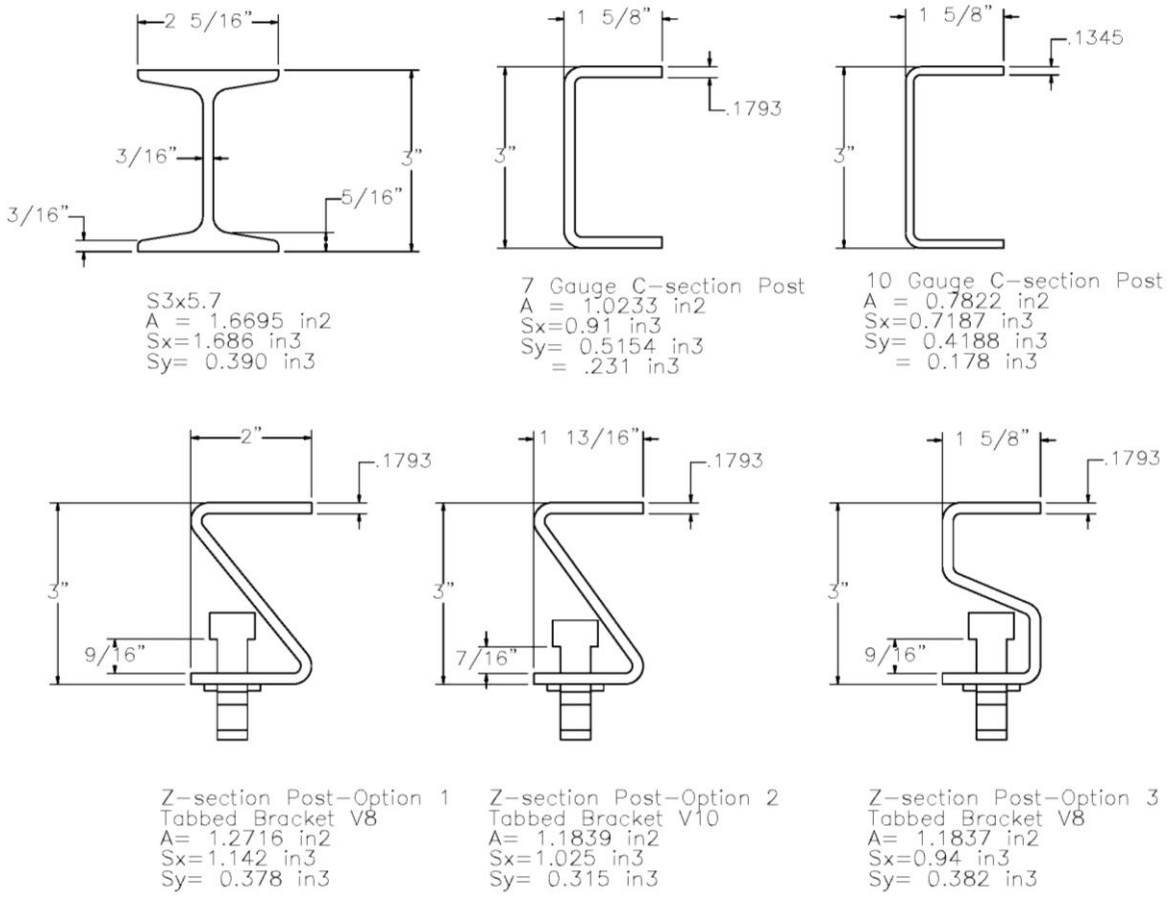

Sx=Strong-axis section modulus
Sy=Weak-axis section modulus

Figure 94. Z-Section Post Designs

7.3.2 Simulation of Proposed Post Sections

In order to evaluate the proposed Z-section post designs, LS-DYNA simulations were conducted on the strong and weak axes of the posts with all of the keyways in the post flanges in place. The simulated impacts were analyzed to determine if the new post sections eliminated the stability and buckling issues identified in the C-section post testing.

The results from the strong- and weak-axis impact simulations of the Z-section post Option 1, Option 2, and Option 3 are shown in Figures 95, 96, and 97, respectively. All three of the post section designs exhibited much improved stability and eliminated the buckling observed in the C-section post designs. Peak loads and average loads for all three sections were very similar. Option 3 demonstrated slightly lower loads in the strong-axis impact and slightly higher loads in the weak axis impact as compared with the other two designs. However, the differences were minor and were consistent with the calculated section moduli of the post sections. The weak-axis loads for all three sections were significantly less than that of an S3x5.7 (S76x8.5) post. The Option 3 design was selected for further development over the other two design options based on its lower strong-axis loads and the modified Z-section's ability to align the cable-to-post attachment at the centerline of the post section.

In order to further evaluate the post, additional simulation and force vs. deflection comparisons were made with the Option 3 design. First, simulation of the post impacted at 25-degree and 45-degree angles was conducted to ensure that the presence of the keyways did not induce buckling of the post when impacted at oblique angles. Figure 98 displays the performance of the Option 3 post design when impacted at 25-degree and 45-degree angles, respectively. In both impacts, the Option 3 post design yielded and bent at the groundline and did not exhibit any tendency to buckle near the keyways in the post.

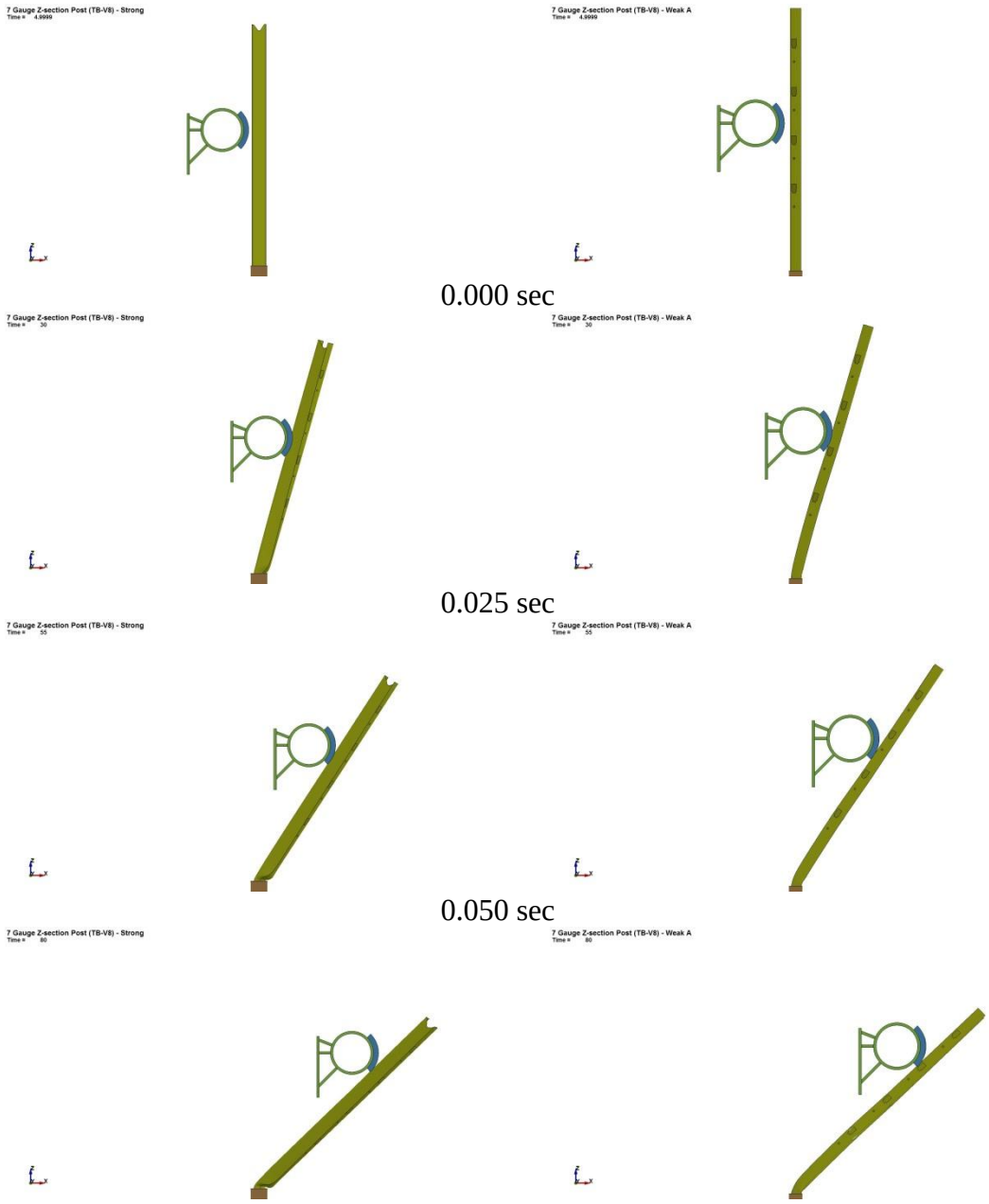

Figure 95. Z-Section Post Option 1 Simulation, Strong and Weak Axis

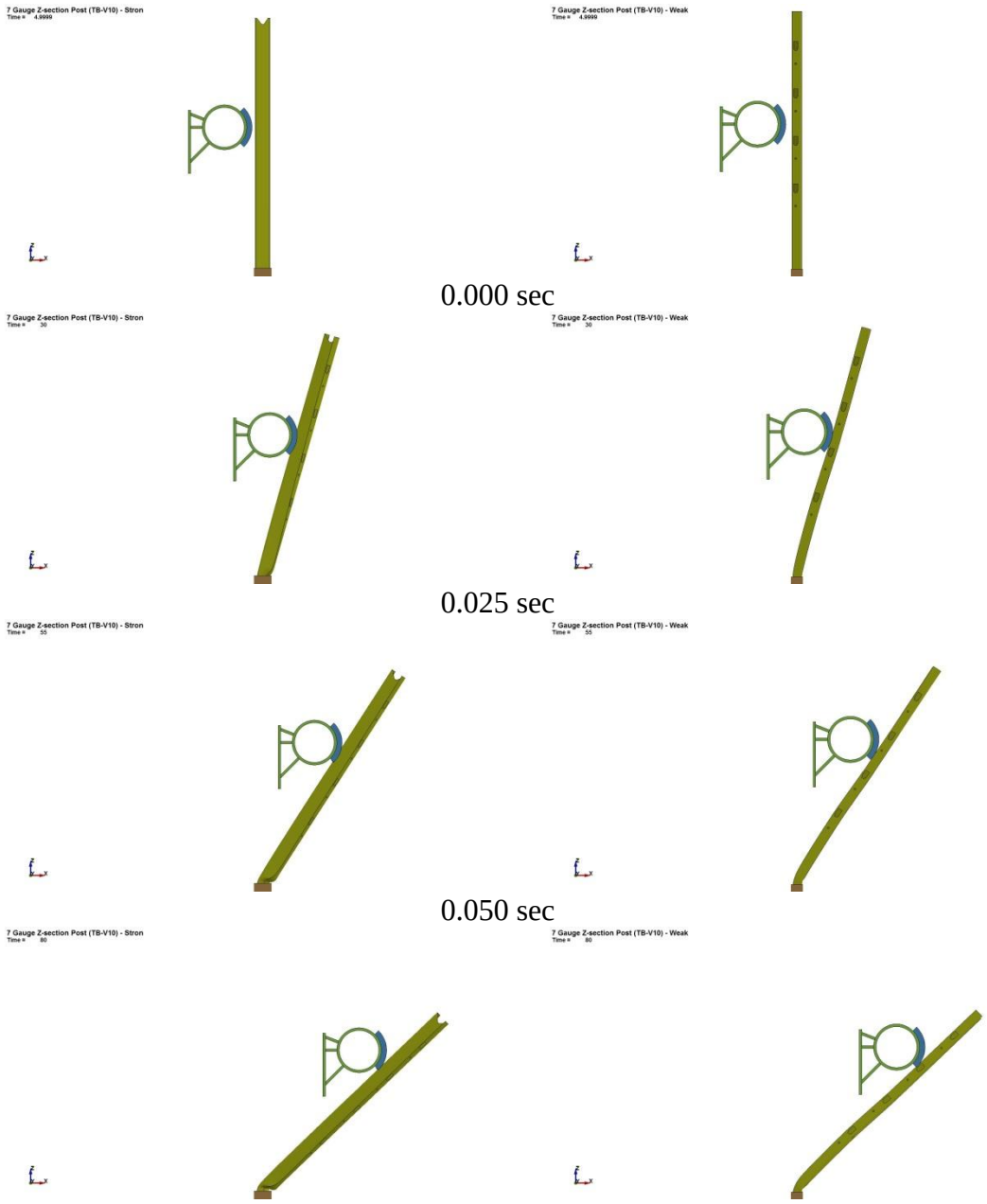

Figure 96. Z-Section Post Option 2 Simulation, Strong and Weak Axis

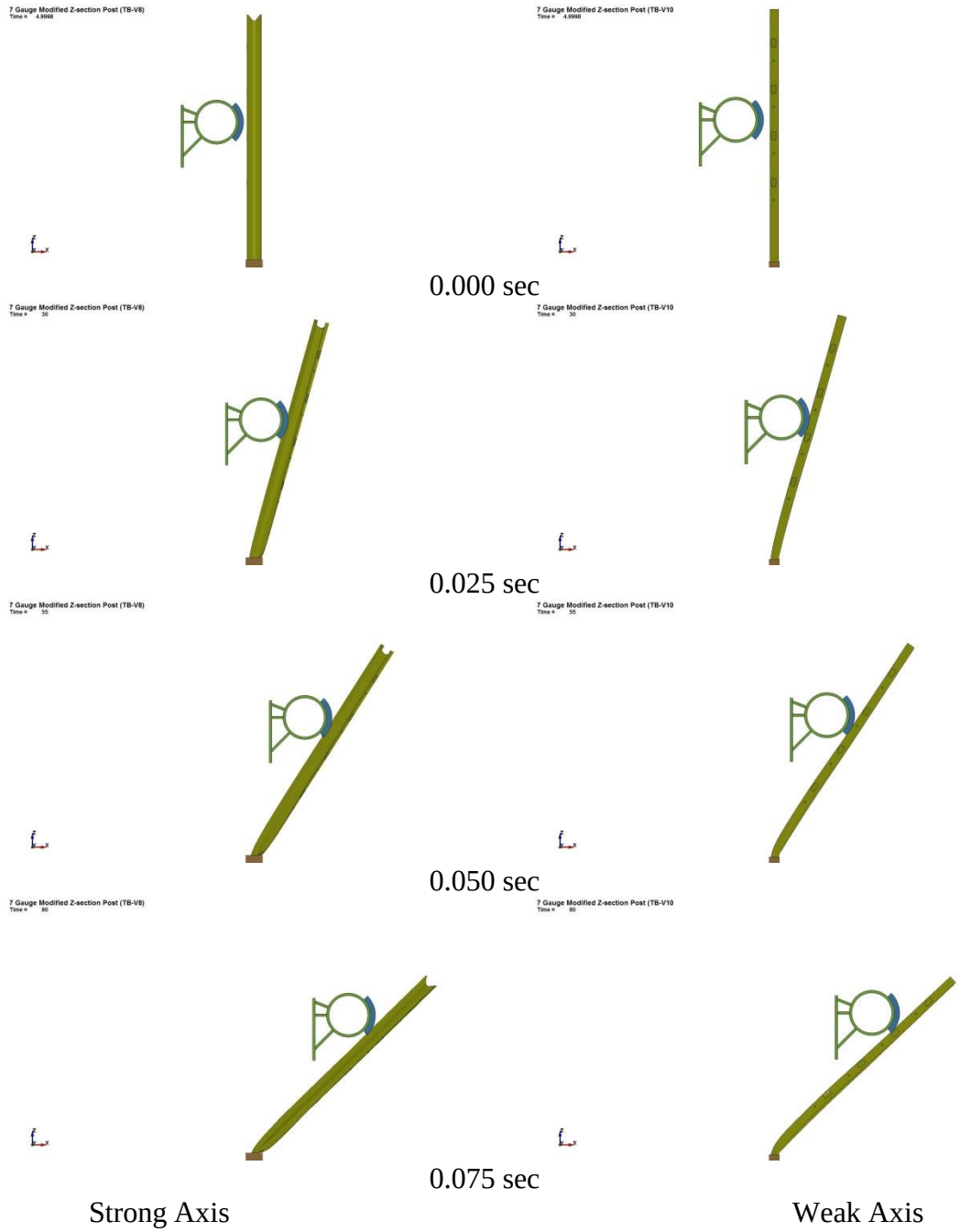

Figure 97. Z-Section Post Option 3 Simulation, Strong and Weak Axis

Comparisons were also made between the strong-axis force and energy vs. deflection behavior of the 7-gauge bent C-section post component testing with and without keyways and the Option 3 post design simulation, as shown in Figure 99. Comparison of the new post section with the previous component testing indicated that the new post design developed more consistent load during the deflection of the post due to the elimination of the twisting and buckling behavior. However, average forces and energy levels were consistent with the 7-gauge bent C-section post design.

Based on these comparisons, the researchers decided to proceed with the development of the Option 3 post section. The post design was renamed the Midwest Weak Post, or MWP. The final step in the development of the post was dynamic component testing to verify the simulation effort.

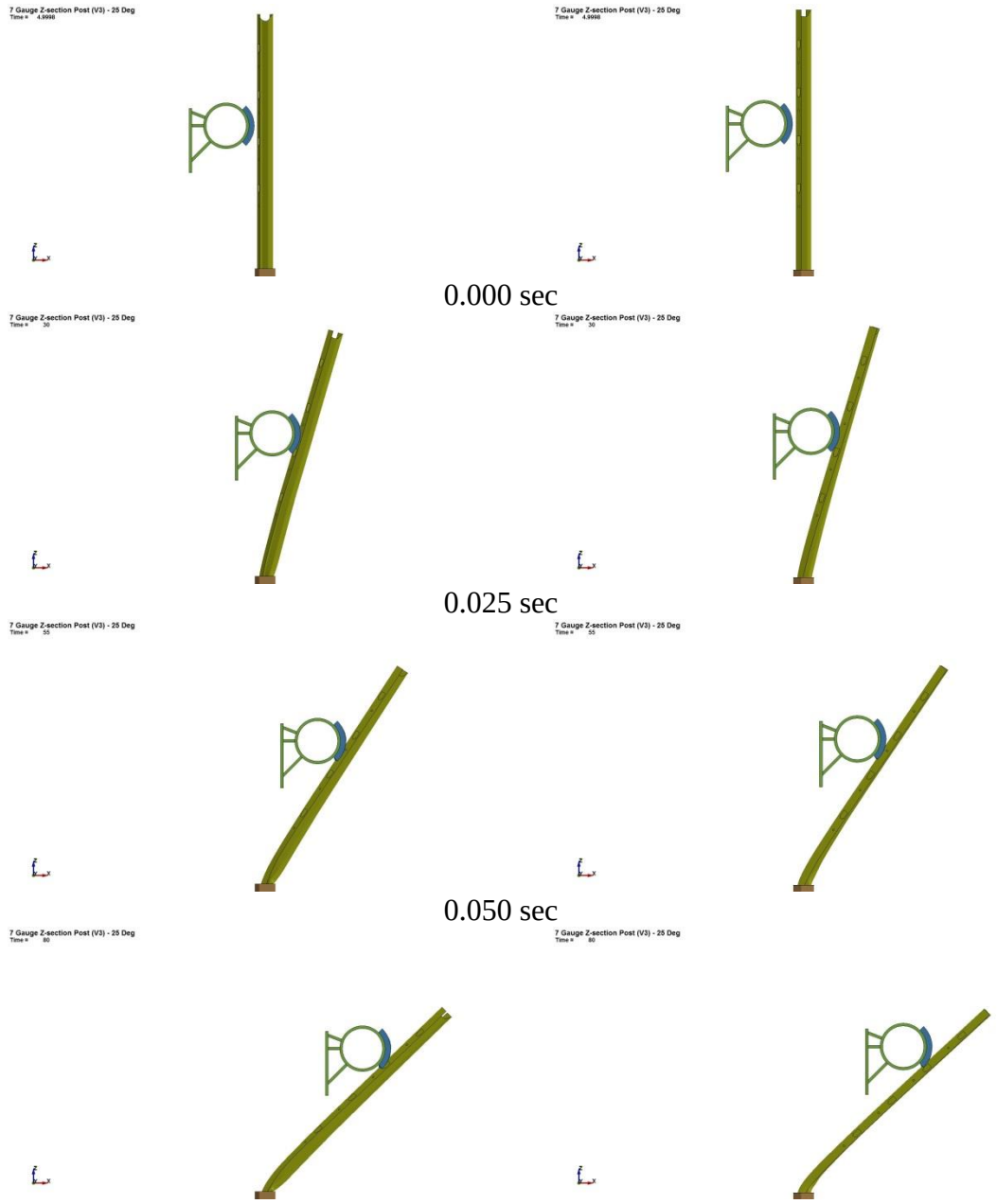

Figure 98. Z-Section Post Option 3 Simulation, 25-Degree and 45-Degree Impact Angles

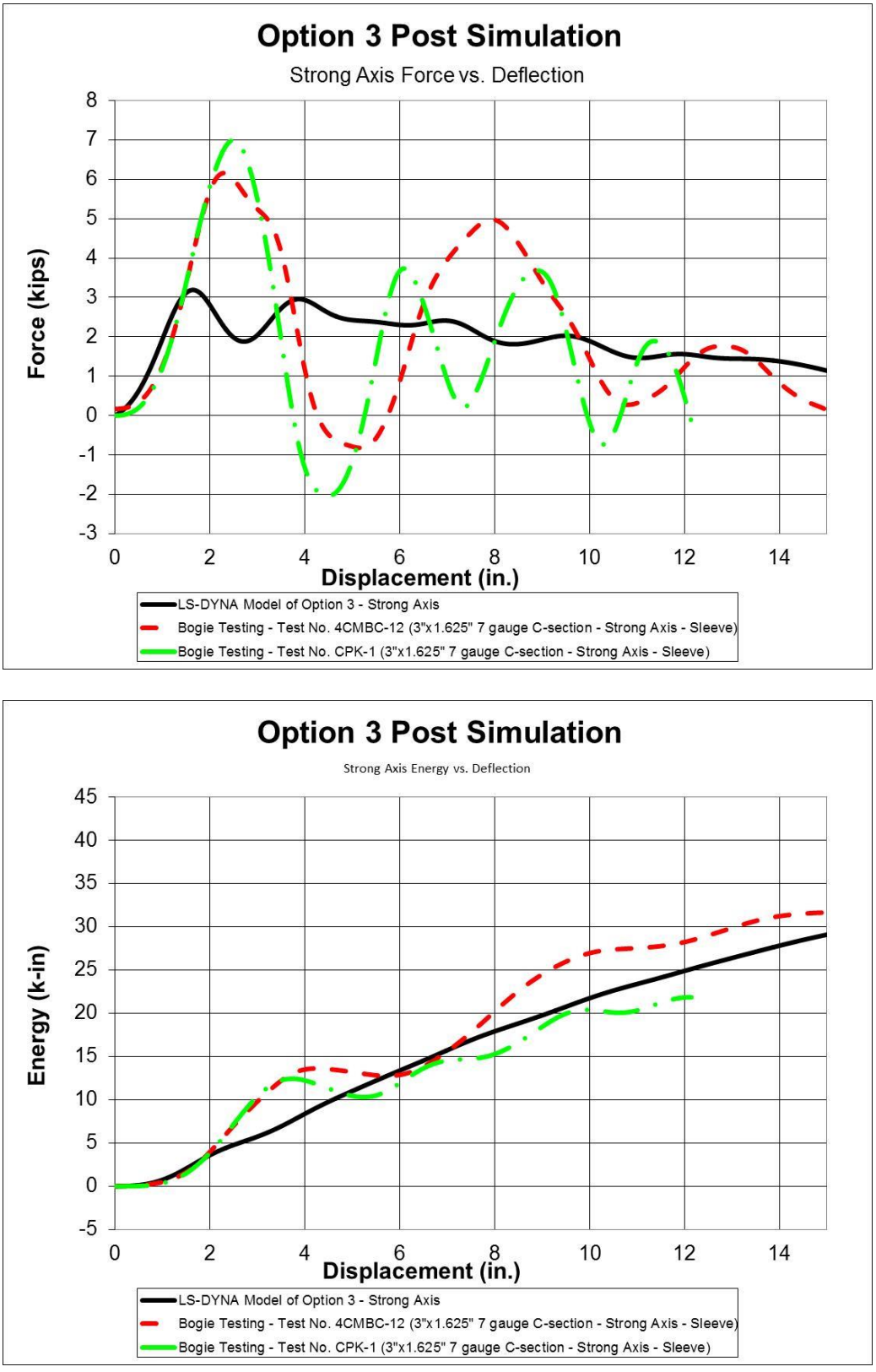

Figure 99. Force and Energy Versus Deflection, Test Nos. 4CMBC-12 and CPK-1, and LS-DYNA Simulation

8 MIDWEST WEAK POST TESTING

The design and simulation effort for the MWP indicated that the new post section would provide improved post stability and meet the original design goals for the non-proprietary high-tension cable barrier system line posts. However, dynamic component testing of the new post section was desired in order to develop further confidence in the design and confirm the simulation results prior to implementing the post into the cable system. Thus, component tests were conducted to evaluate the new post section in the strong and weak axes as well as to evaluate the behavior of the new post and the cable-to-post attachment when loaded by a cable.

8.1 Scope

Two dynamic component tests were conducted on the 7-gauge MWP with keyway holes, as well as one cable pull test on the MWP using a bracket and keyway [4]. The target impact speed was 20 mph (32 km/h) for test nos. CPZ-1 and CPZ-2 and 15 mph (24 km/h) for test no. CPZ-3. All three posts were $80^{7}/_{8}$ in. (2,054 mm) long with a 42-in. (1,067-mm) embedment, tested in a rigid sleeve. Test no. CPZ-1 was impacted on the weak axis and test no. CPZ-2 was impacted on the strong axis. Test no. CPZ-3 loaded the cable-to-post attachment in the direction of the strong axis of the post. The dynamic component test matrix is shown in Table 8. The test setup and MWP details are shown in Figures 100 through 108. Material specifications, mill certificates, and certificates of conformity for the post materials used in all three tests are shown in Appendix A.

Table 8. Dynamic Post Testing Matrix, Test Nos. CPZ-1 through CPK-3

Test No.	Post Type	Loading Parameter	Impact Axis	Foundation Type	Post Length in. (mm)	Impact Height in. (mm)	Target Impact Velocity mph (km/h)
CPZ-1	Midwest Weak Post	Bogie Impact	Weak	Rigid Sleeve	$80^{7}/_{8}$ (2,054)	27 (686)	20(32)
CPZ-2	Midwest Weak Post	Bogie Impact	Strong	Rigid Sleeve	$80^{7}/_{8}$ (2,054)	27 (686)	20 (32)
CPZ-3	Midwest Weak Post	Cable Pull Test	Strong	Rigid Sleeve	$80^{7}/_{8}$ (2,054)	27 (686)	15 (24)

Test Qty.	Post Type	Bogie No.	Embedment Depth in. [mm]	Load Height in. [mm]	Impact Speed mph [km/h]	Impact Axis
1	7-Gauge Z-Section Post	3	42 [1067]	27 [686]	20 [32.2]	Strong
1	7-Gauge Z-Section Post	3	42 [1067]	27 [686]	20 [32.2]	Weak

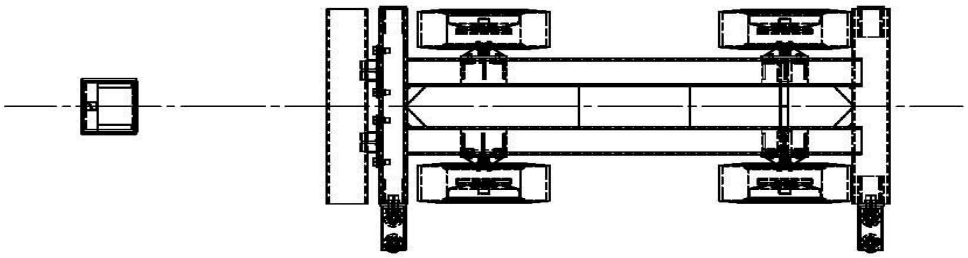

PLAN VIEW

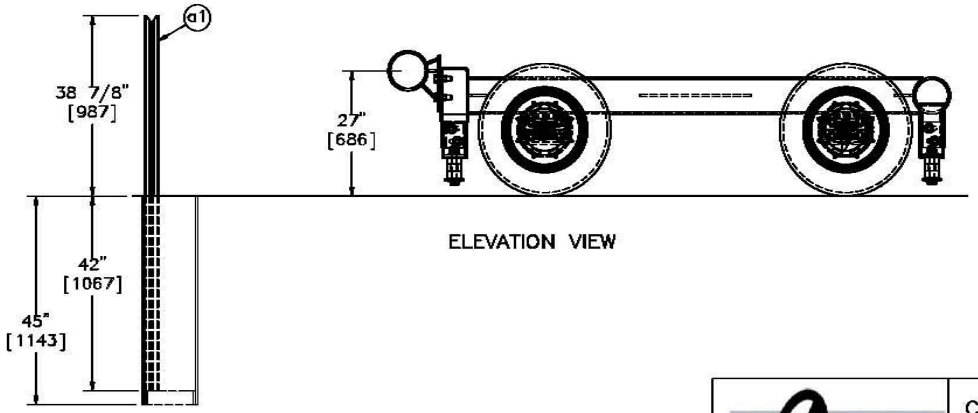

ELEVATION VIEW

Notes: (1) Drawing shows strong-axis test setup only. For weak axis, the post shall be rotated 90 degrees.

(2) A 3 in. [76] spacer is placed at the bottom of the rigid sleeve to raise the post to the correct height.

(3) Shim material to fit. Posts must be placed in holes with wood and steel shims and made tight (i.e., no gaps).

Midwest Roadside Safety Facility	Cable Median Barrier Bent Z-Section Post Test Setup	SHEET: 1 of 3 DATE: 7/2/2013 DRAWN BY: JGP/CWP/RJB
DWG. NAME: Z-Post_R3	SCALE: 1:30 UNITS: in.[mm]	REV. BY: KAL/RJB/TLS

Figure 100. Bogie Test Setup, Test Nos. CPZ-1 and CPZ-2

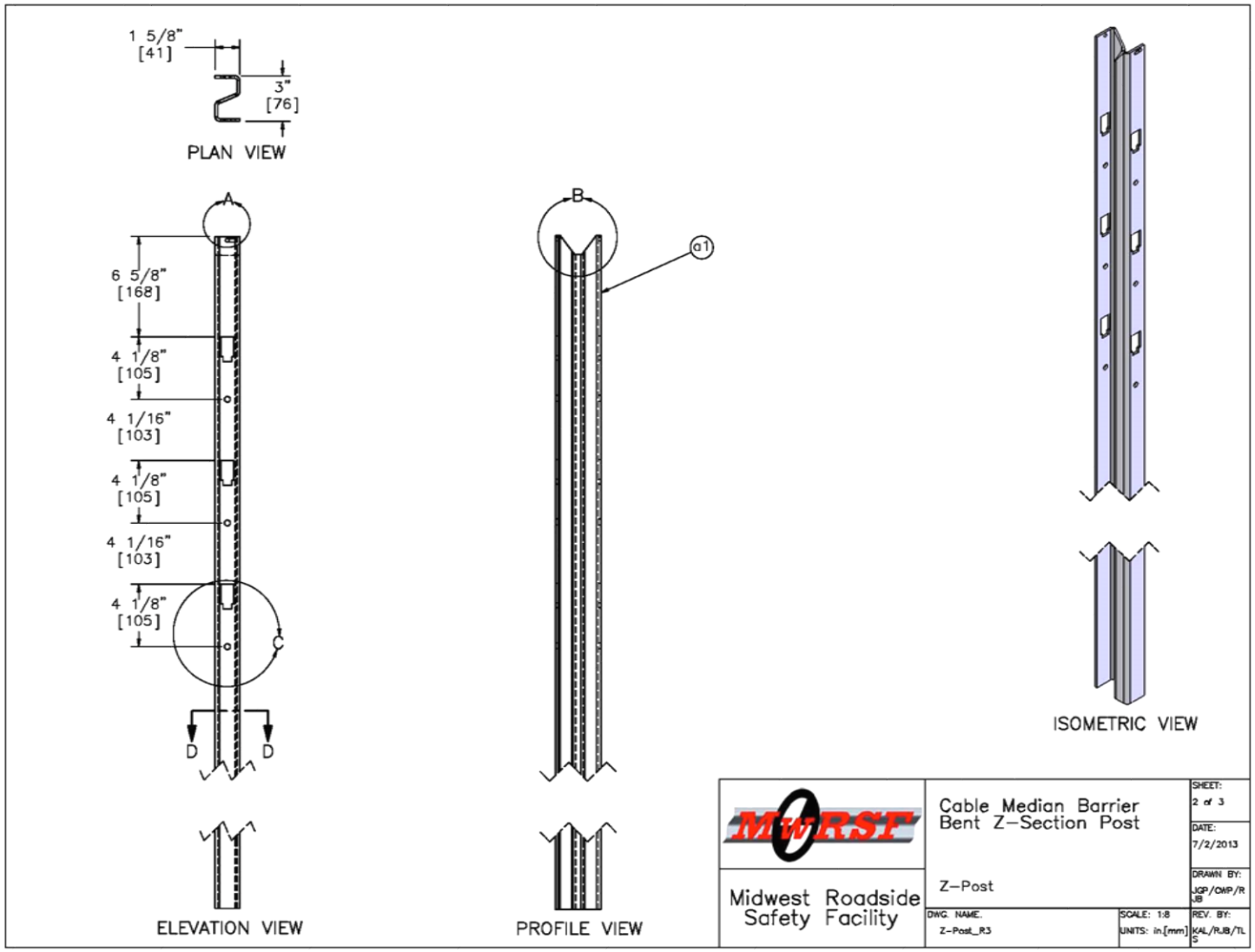

Figure 101. Midwest Weak Post Details, Test Nos. CPZ-1 and CPZ-2

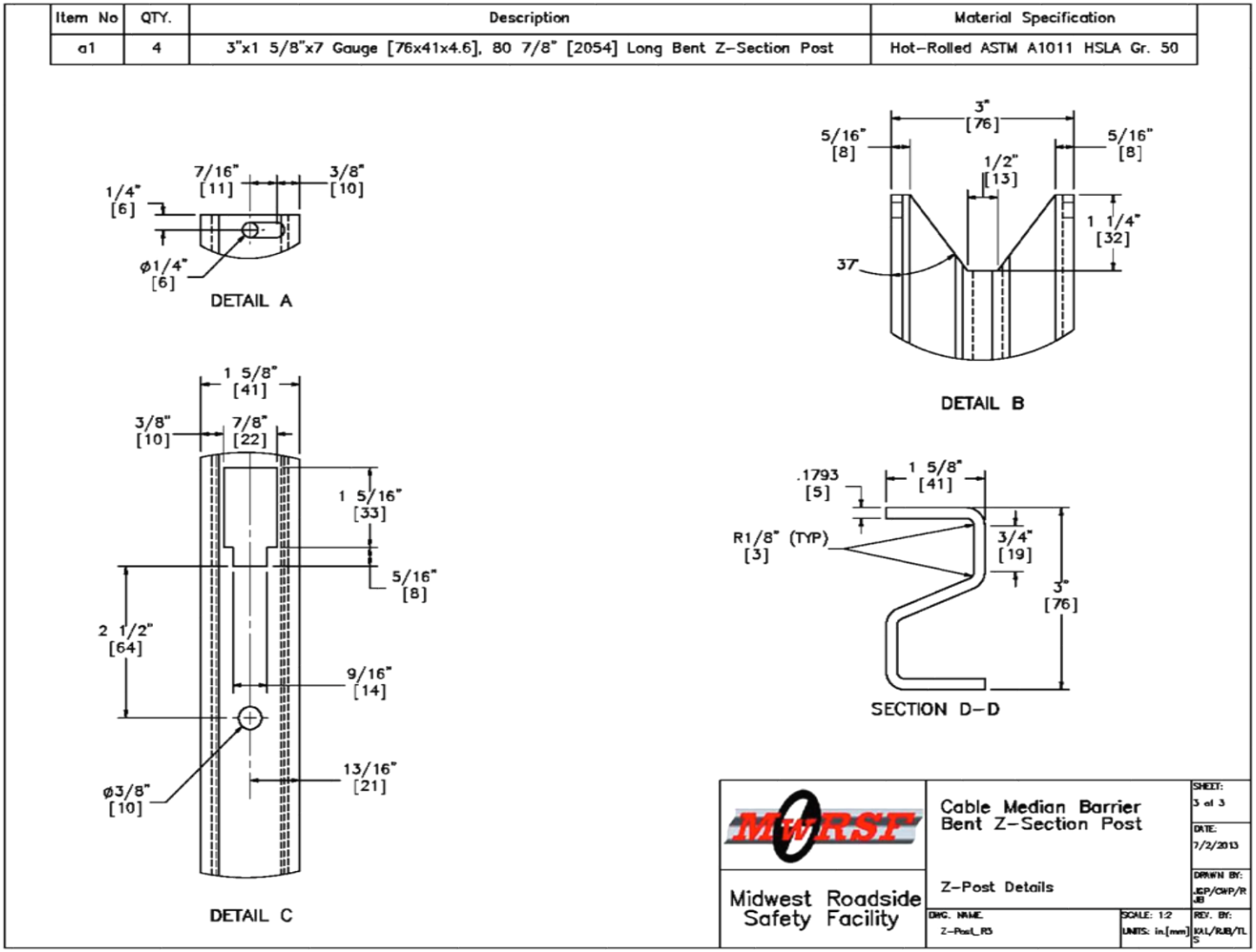

Figure 102. Midwest Weak Post Details, Test Nos. CPZ-1 and CPZ-2

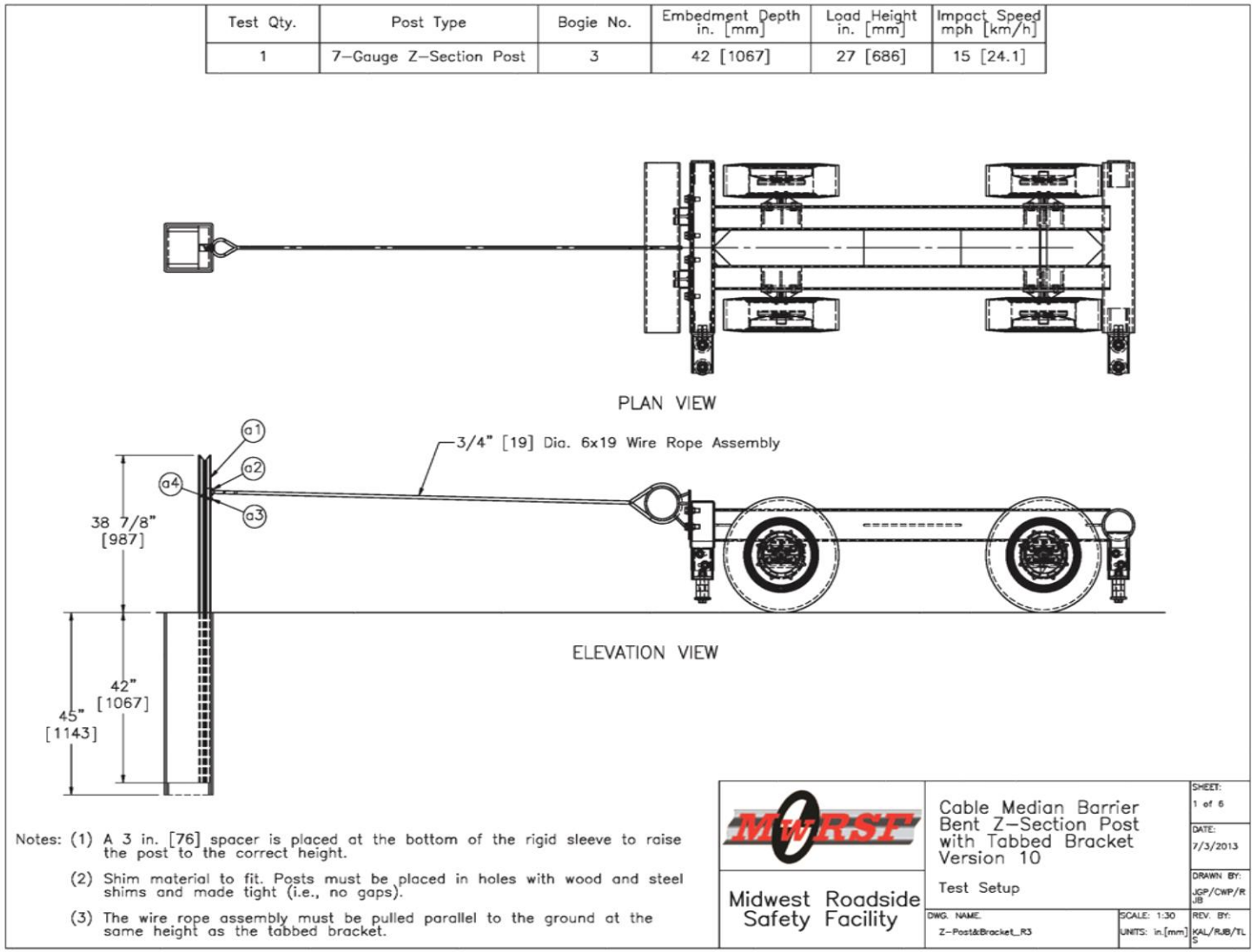

Figure 103. Bogie Test Setup, Test No. CPZ-3

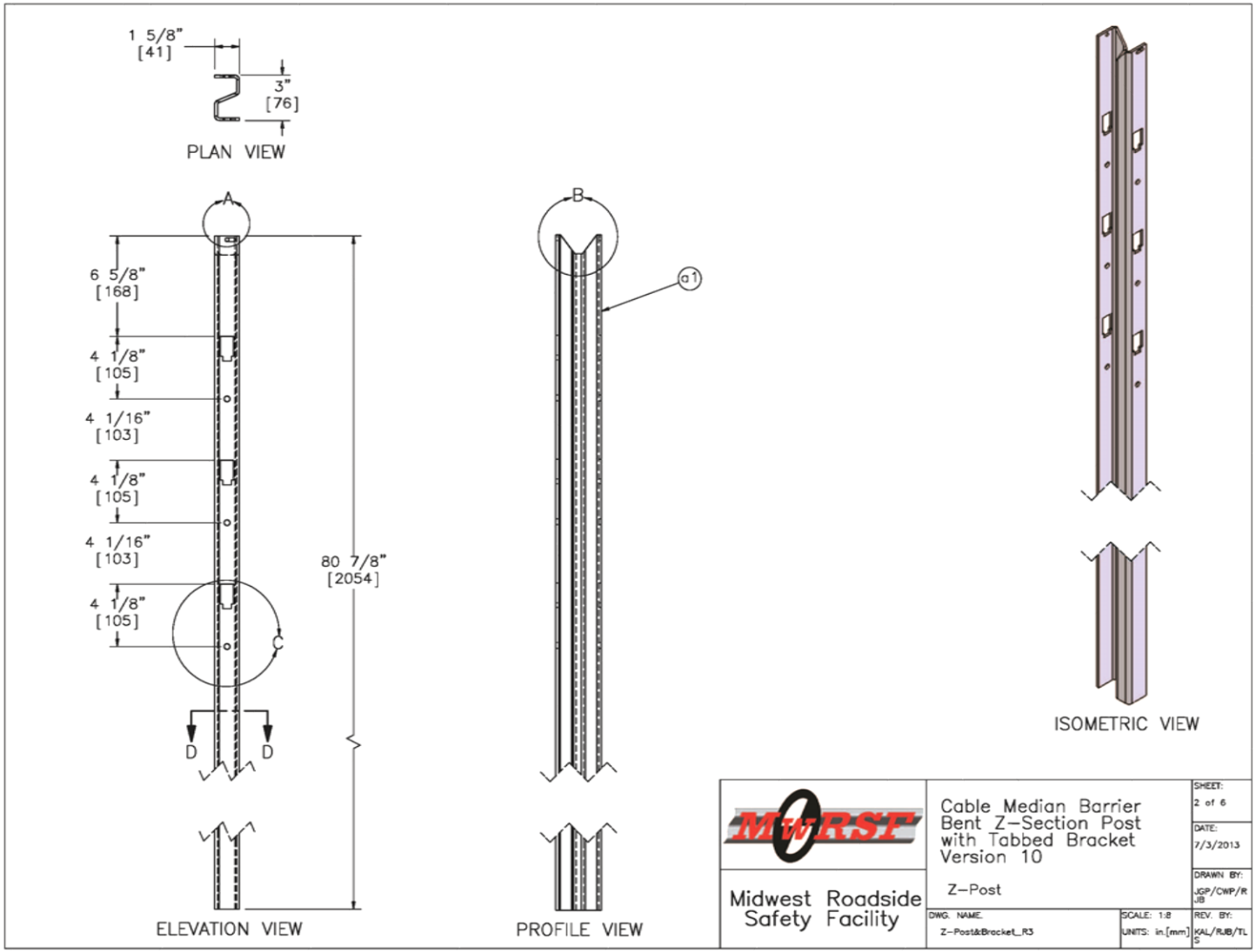

Figure 104. Midwest Weak Post Details, Test No. CPZ-3

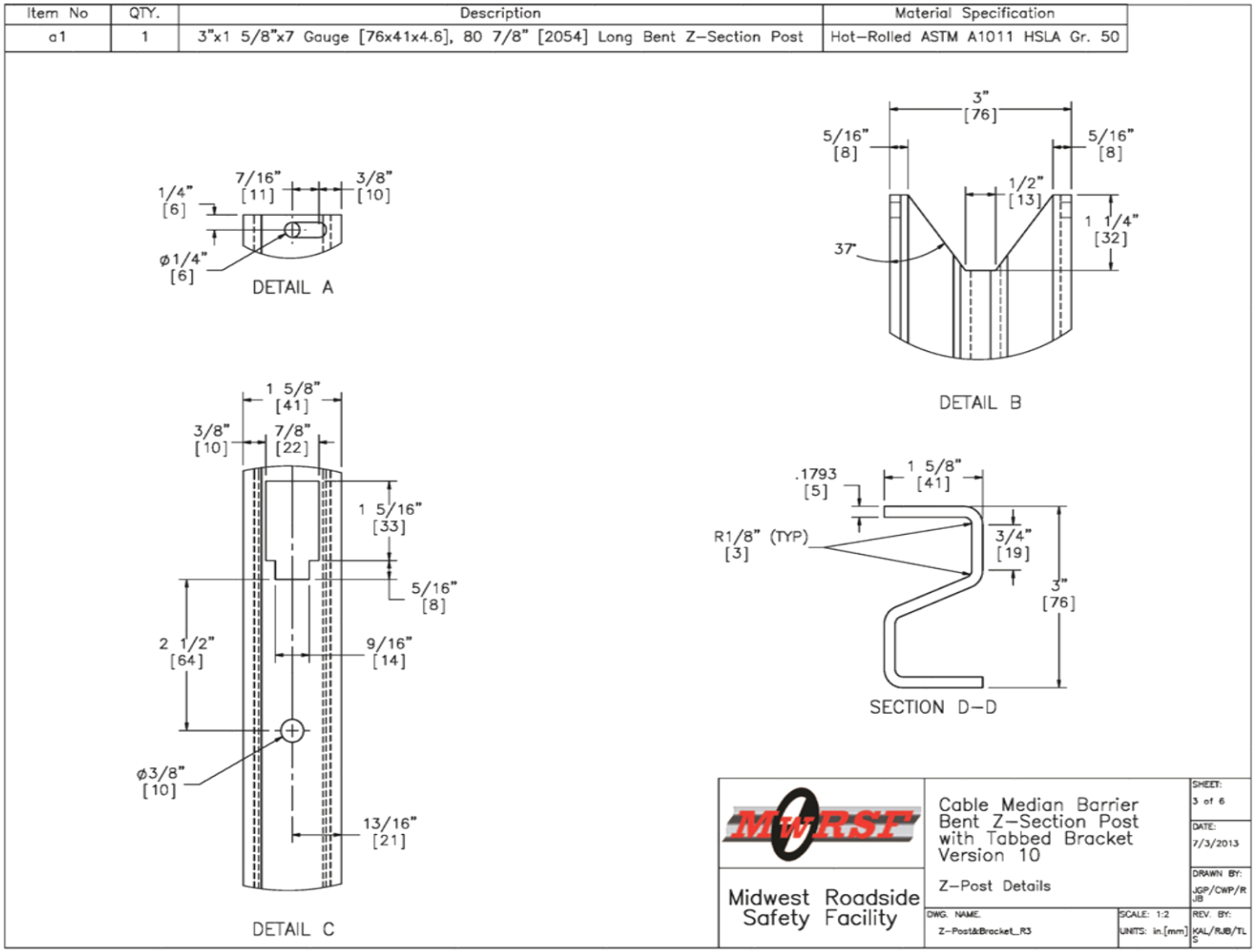

Figure 105. Midwest Weak Post Details, Test No. CPZ-3

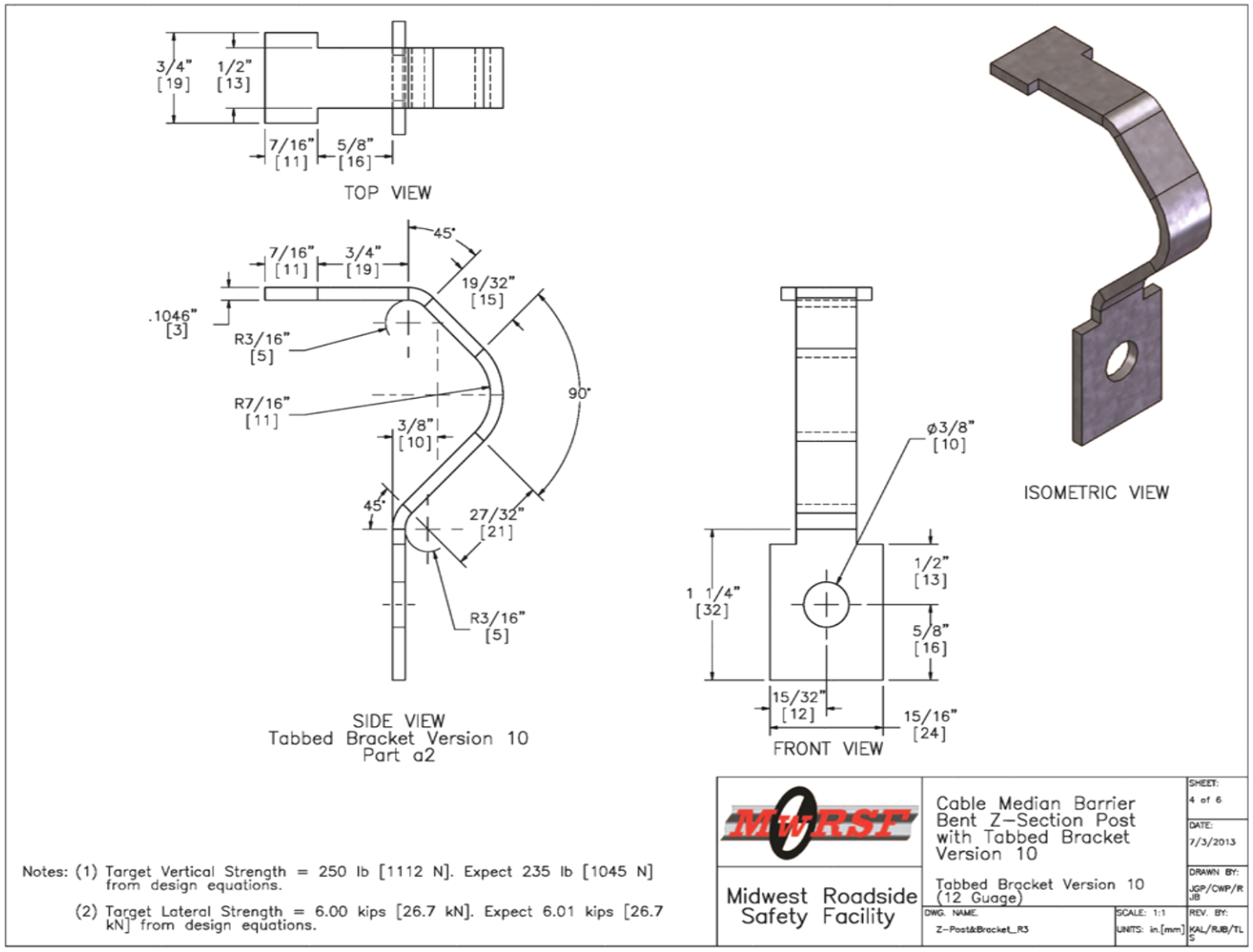

Figure 106. Midwest Weak Post Details, Test No. CPZ-3

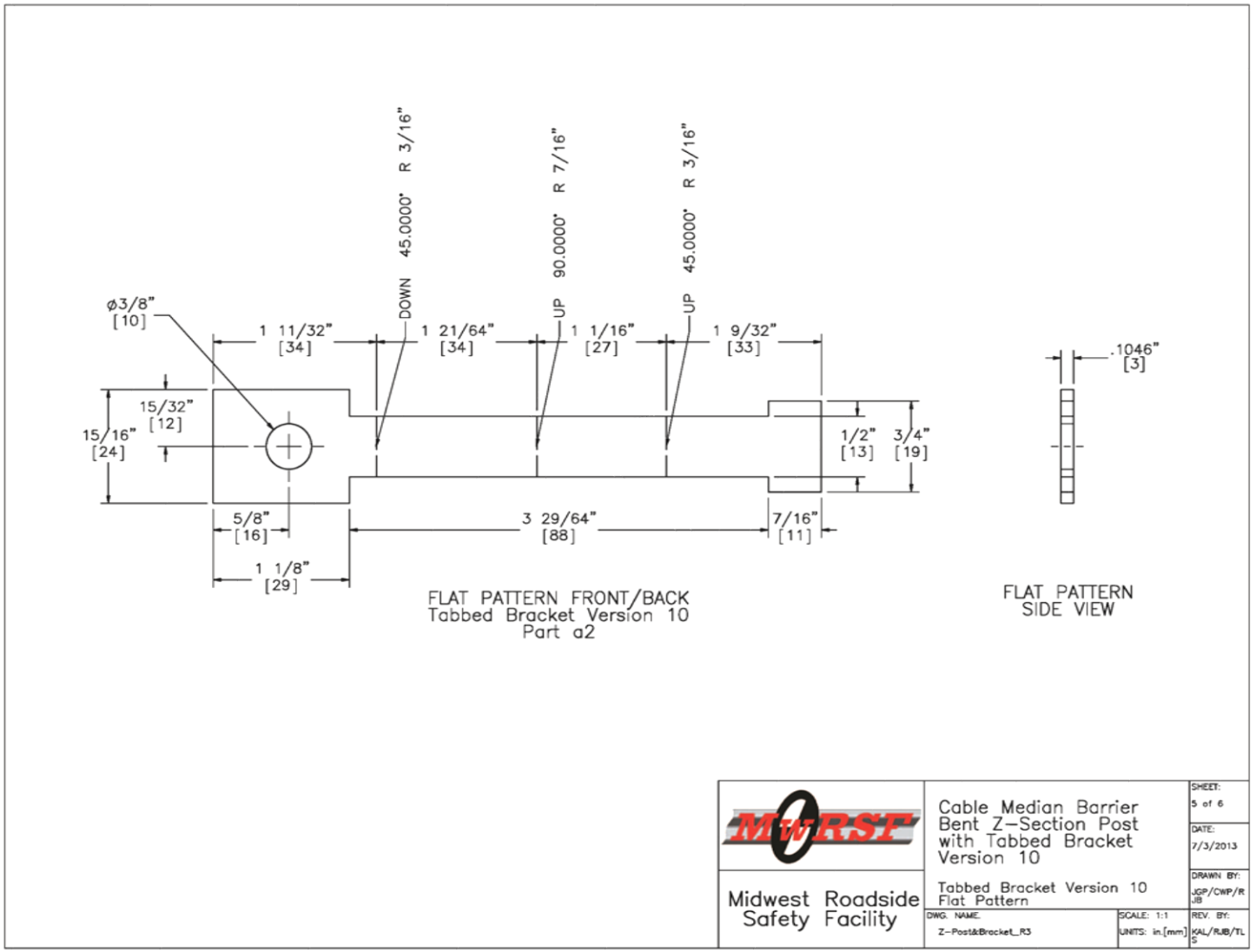

Figure 107. Midwest Weak Post Details, Test No. CPZ-3

Item No.	QTY.	Description	Material Specification
a1	1	3"x1 5/8"x7 Gauge [76x41x4.6], 80 7/8" [2054] Long Bent Z-Section Post	Hot-Rolled ASTM A1011 HSLA Gr. 50
a2	1	Tabbed Bracket – Version 10	12 Gauge Hot-Rolled ASTM A1011 HSLA Grade 50
a3	1	5/16" [8] Dia. UNC, 1" [25] Long Hex Cap Screw	SAE Grade 5
a4	1	5/16" [8] Dia. Heavy Hex Nut	ASTM A563 DH Galv.

Midwest Roadside Safety Facility

Cable Median Barrier
Bent Z-Section Post
with Tabbed Bracket
Version 10

Bill of Materials

SHEET: 6 of 6
DATE: 7/3/2013
DRAWN BY: JGP/CWP/RJB
REV. BY: KAL/RJB/TLS

DWG. NAME: Z-Post&Bracket_R3
SCALE: 1:64
UNITS: in.[mm]

Figure 108. Bill of Materials, Test No. CPZ-3

8.2 Dynamic Testing Results

Results of each test are discussed in the following sections. Individual results for all accelerometers used during each test are provided in Appendix C. The values described were calculated from the DTS-SLICE data curves.

8.2.1 Test No. CPZ-1

During test no. CPZ-1, the bogie impacted the 7-gauge MWP at a speed of 20.4 mph (32.8 km/h). As a result of the weak-axis impact, the post bent backward and hinged near the groundline. The bogie overrode the post at a maximum deflection of 22.8 in. (579 mm).

Force vs. deflection and energy vs. deflection curves created from the DTS-SLICE accelerometer data are shown in Figure 109. The forces quickly rose to a peak force of 4.2 kips (18.7 kN) at 1.7 in. (43 mm) of deflection. The post provided an average resistive force of 1.6 kips (7.1 kN) through both 10 in. (254 mm) and 15 in. (381 mm) of deflection. The energy absorbed by the post was 16.3 kip-in. (1.8 kJ) through 10 in. (254 mm) of deflection and 24.4 kip-in. (2.8 kJ) through 15 in. (381 mm) of deflection. Pre-test and post-test photographs are shown in Figure 110. Time-sequential photographs are shown in Figure 111.

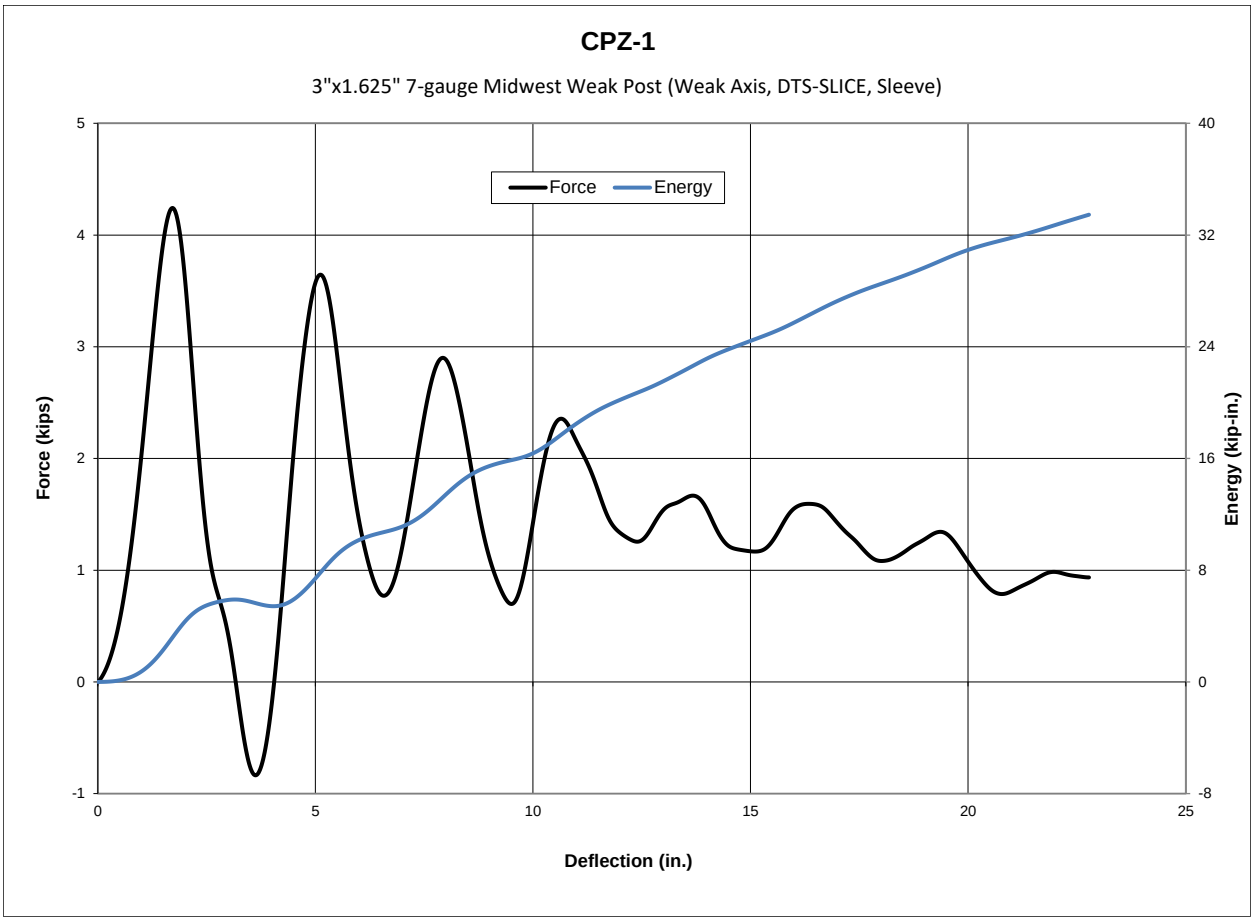

Figure 109. Force vs. Deflection and Energy vs. Deflection, Test No. CPZ-1

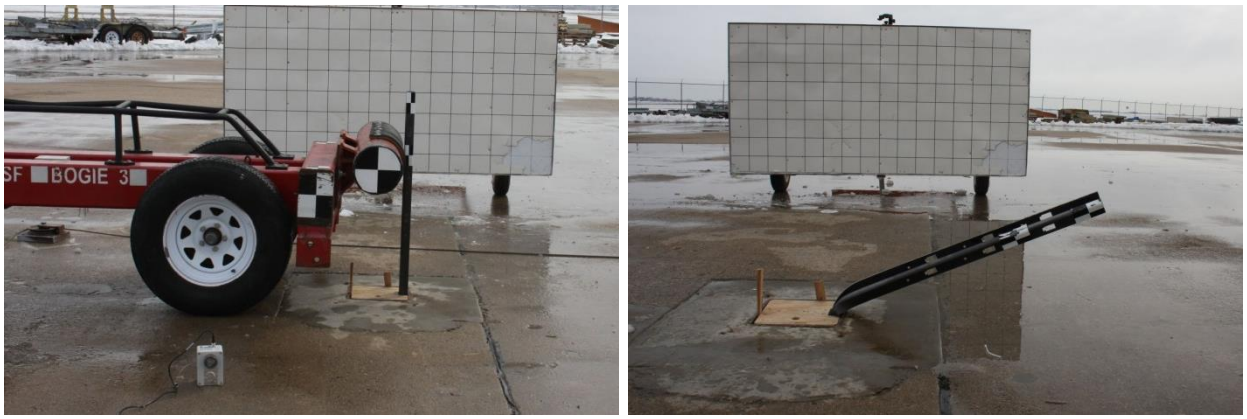

Pre-Test Post-Test

Figure 110. Pre-Test and Post-Test Photographs, Test No. CPZ-1

0.000 sec

0.120 sec

0.030 sec

0.150 sec

0.060 sec

0.180 sec

0.090 sec

0.210 sec

Figure 111. Sequential Photographs, Test No. CPZ-1

8.2.2 Test No. CPZ-2

During test no. CPZ-2, the bogie impacted the 7-gauge MWP at a speed of 19.5 mph (31.4 km/h). As a result of the strong-axis impact, the post yielded and hinged near the groundline. The bogie overrode the post at a deflection of 23.0 in. (584 mm).

Force vs. deflection and energy vs. deflection curves created from the DTS-SLICE accelerometer data are shown in Figure 112. The forces quickly rose to a peak force of 4.4 kips (19.6 kN) at 1.9 in. (48 mm) of deflection. The post provided an average resistive force of 2.1 kips (9.3 kN) through 10 in. (254 mm) of deflection and 1.8 kips (8.0 kN) through 15 in. (381 mm) of deflection. The energy absorbed by the post was 20.8 kip-in. (2.4 kJ) through 10 in. (254 mm) of deflection and 27.7 kip-in. (3.1 kJ) through 15 in. (381 mm) of deflection. Pre-test and post-test photographs are shown in Figure 113. Time-sequential photographs are shown in Figure 114.

Review of the damage to the MWP post following test no. CPZ-2 found that there was some local deformation of the post in the area between the uppermost keyway and the outer edge of the post, as shown in Figure 115. This deformation of the keyway posed a potential concern that excess deformation of the post near the keyway could prevent proper function of the cable-to-post attachments due to narrowing of the keyway exit area. Thus, it was noted that a slight widening of the post flange might be warranted to strengthen that area of the post while not drastically increasing the strong and weak axis section properties of the post.

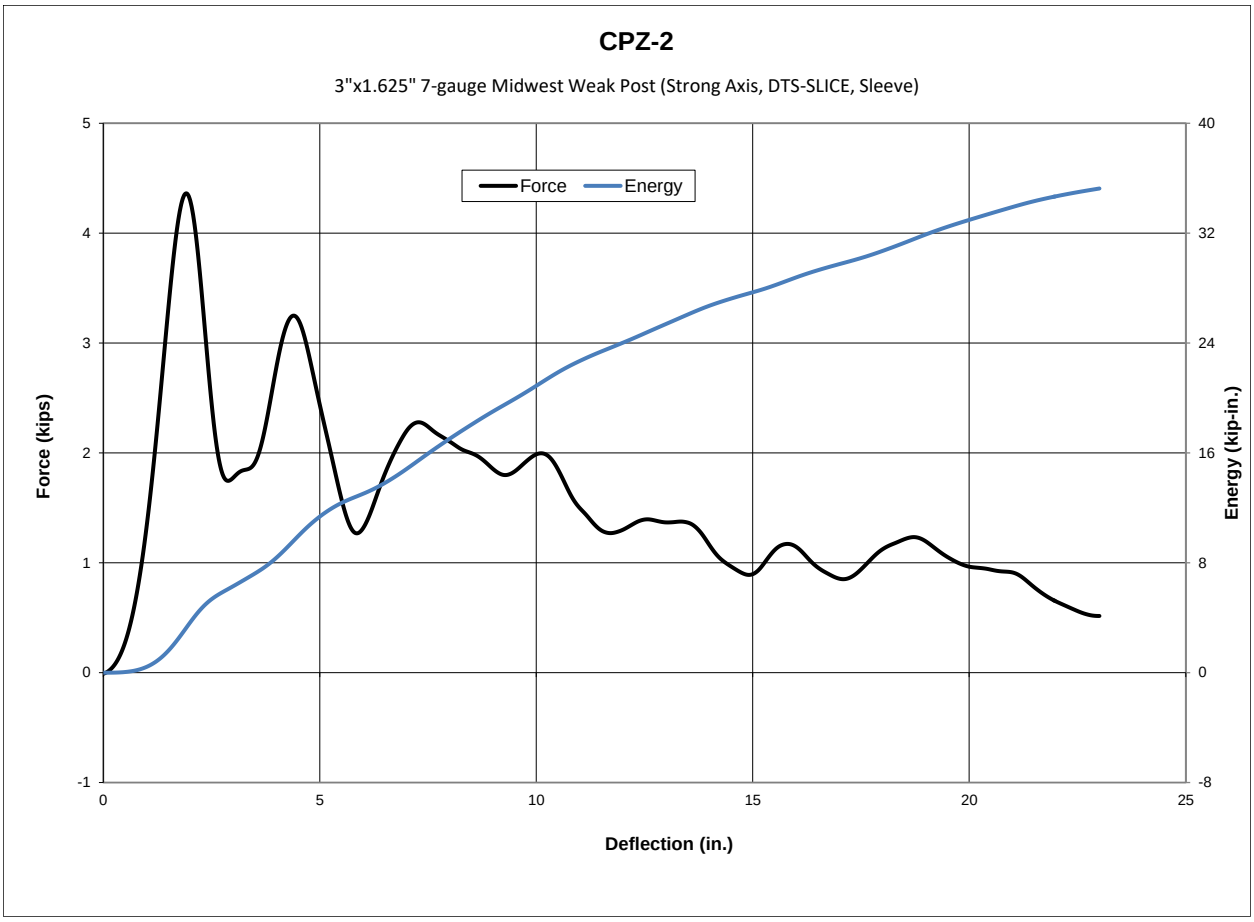

Figure 112. Force vs. Deflection and Energy vs. Deflection, Test No. CPZ-2

Pre-Test Post-Test

Figure 113. Pre-Test and Post-Test Photographs, Test No. CPZ-2


0.000 sec


0.120 sec


0.030 sec


0.150 sec


0.060 sec


0.180 sec


0.090 sec


0.210 sec

Figure 114. Sequential Photographs, Test No. CPZ-2

Figure 115. Localized Deformation of MWP Post Near Upper Keyway, Test No. CPZ-2

8.2.3 Test No. CPZ-3

Test no. CPZ-3 was conducted as a cable pull test, utilizing the version 10 tabbed bracket [1] on the 7-gauge MWP at a speed of 21.1 mph (34.0 km/h). As a result of the strong axis test, the post yielded and produced a hinge near the groundline. The cable was released from the post when the top of the cable bracket pulled through the upper part of the keyway as the post rotated. The post had a maximum deflection of 43.7 in. (1,110 mm).

Force vs. deflection data from the DTS-SLICE accelerometer data are shown in Figure 116. Due to the gradual tensioning and stretch in the cable, the deflections measured by the bogie vehicle acceleration were difficult to correlate with the actual deflection of the MWP. Thus, while the loads measured in the test were accurate, the accelerometer deflections do not align directly with the post deflections. The deflection over the first 5 in. (127 mm) to 8 in. (203 mm) was due to the bogie picking up and tensioning the cable used to load the bracket and post. The forces gradually rose to a peak force of 3.5 kips (15.6 kN). Average forces and energies for the post were not calculated, due to the deflection measurement difficulties noted above. The cable was released from the post after the post bent to approximately 56 degrees at a time of 102 msec, and no indications of buckling or post instability were noted. Pre-test and post-test photographs are shown in Figure 117. Time-sequential photographs are shown in Figure 118.

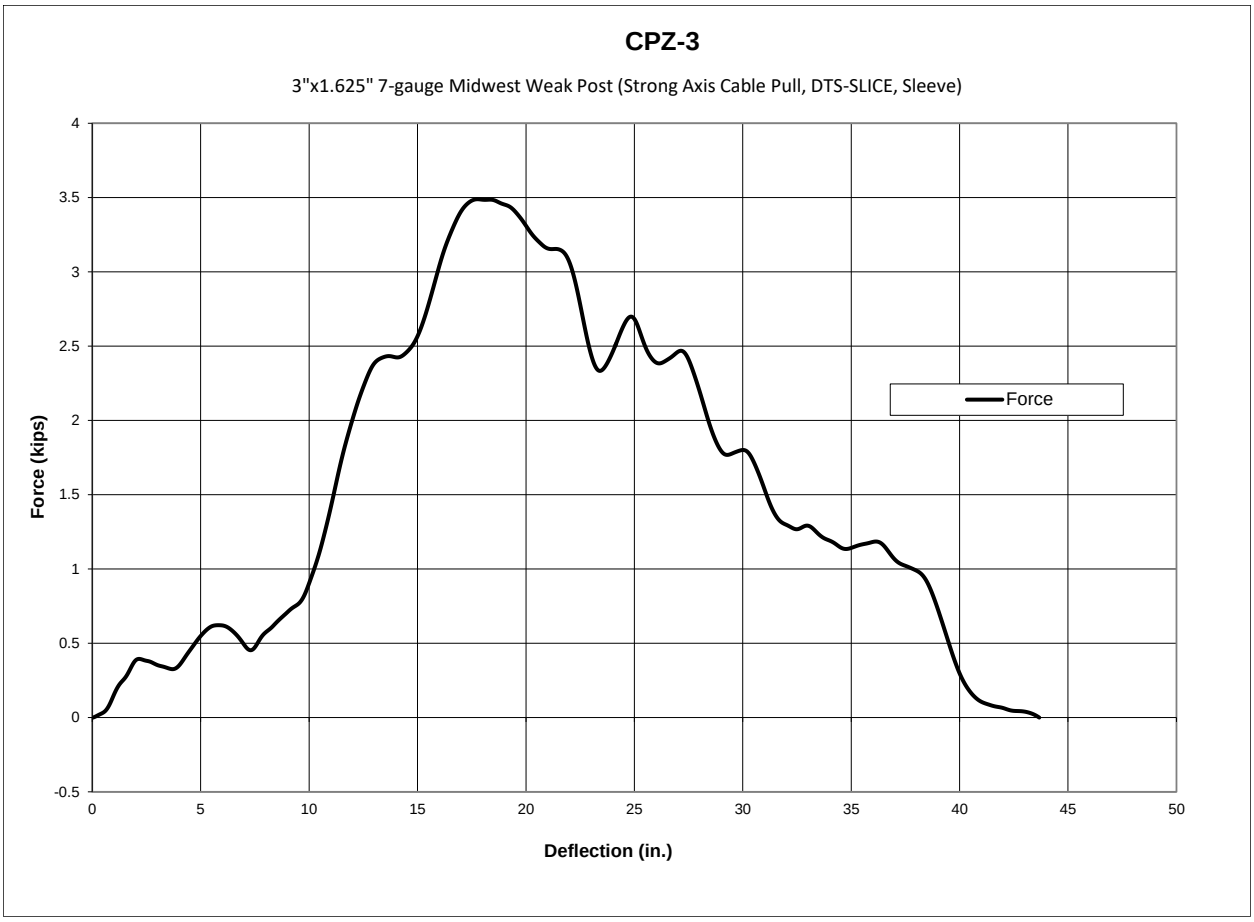

Figure 116. Force vs. Deflection, Test No. CPZ-3

Pre-Test Post-Test

Figure 117. Pre-Test and Post-Test Photographs, Test No. CPZ-3


0.000 sec


0.120 sec


0.040 sec


0.140 sec


0.080 sec


0.160 sec

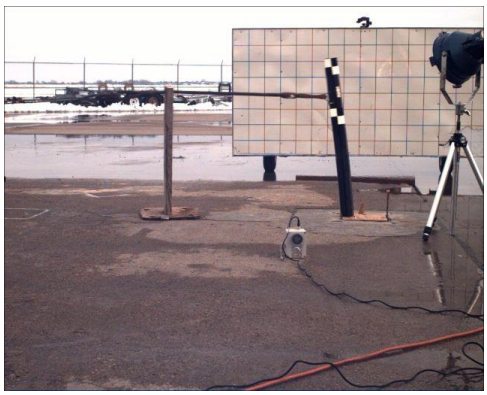
0.100 sec


0.180 sec

Figure 118. Sequential Photographs, Test No. CPZ-3

8.3 Summary of Dynamic Testing

Two dynamic component tests and one cable pull test were conducted on MWPs loading two different impact axes to establish the force vs. deflection and energy vs. deflection characteristics and examine the stability of the post section. The results from the bogie testing matrix are summarized in Table 9, and a comparison of the MWP to the C-section steel posts and S3x5.7 (S76x8.5) posts is summarized in Table 10. The force vs. deflection comparison curves are shown in Figures 119 and 120, and the energy vs. displacement curves are shown in Figures 121 and 122. Note that the modified height scaling was used in calculation of the forces and energies, as described in Chapter 5.

The weak axis performance of the MWP was compared with previous testing of S3x5.7 (S76x8.5) posts and the 7-gauge C-section post without keyways to evaluate if it met the design goals. Test No. CPZ-1, which involved a MWP impacted along the weak axis, resulted in average forces of 1.6 kips (7.1 kN) through both 10 in. (254 mm) and 15 in. (381 mm) of deflection. The S3x5.7 (S76x8.5) steel posts resulted in average forces of 1.4 kips (6.2 kN) and 1.5 kips (6.7 kN) through displacements of 10 in. (254 mm) and 15 in. (381 mm), respectively. This corresponded to 14.3 and 6.7 percent increases in average weak-axis forces for the MWP post when compared to the S3x5.7 (S76x8.5) post. The 7-gauge bent C-section steel posts resulted in average forces of 1.6 kips (7.1 kN) and 1.4 kips (6.2 kN) through displacements of 10 in. (254 mm) and 15 in. (381 mm), respectively, which corresponded to 0 and 14.3 percent increases in average weak-axis forces for the MWP post when compared to the 7-gauge bent C-section posts. Subsequently, energy levels for the weak axis impacts of the MWP, the 7-gauge, bent C-section post, and the S3x5.7 (S76x8.5) post were very similar. This indicated that the MWP post met the design goal of having approximately the same weak-axis capacity as the S3x5.7 (S76x8.5) post the 7-gauge bent C-section post.

Similarly, the strong-axis performance of the MWP was compared with previous testing of S3x5.7 (S76x8.5) posts and the 7-gauge bent C-section post without keyways. Test no. CPZ-2, which evaluated the strong-axis of the MWP, resulted in average forces of 2.1 kips (9.3 kN) and 1.8 kips (8.0 kN) through 10 in. (254 mm) and 15 in. (381 mm) of deflection, respectively. The S3x5.7 (S76x8.5) steel posts resulted in average forces of 4.7 kips (20.9 kN) and 5.0 kips (22.2 kN) through displacements of 10 in. (254 mm) and 15 in. (381 mm), respectively. This corresponded to 55.3 and 64.0 percent reductions in average strong-axis forces for the MWP when compared to the S3x5.7 (S76x8.5) post. The 7-gauge bent C-section posts resulted in average forces of 2.6 kips (11.6 kN) and 2.0 kips (8.9 kN) through displacements of 10 in. (254 mm) and 15 in. (381 mm), respectively. This corresponded to 19.2 and 10.0 percent reductions in average strong-axis forces for the MWP compared to the 7-gauge bent C-section post. Energy levels for the weak axis impacts of the MWP and the 7-gauge bent C-section post were very similar, and the energy levels for both posts were approximately half of the S3x5.7 (S76x8.5) posts. These comparisons indicated that the strong-axis performance of the MWP was similar to the previously designed C-section post, and that the new post section had significantly reduced strong-axis capacity as compared to the S3x5.7 (S76x8.5) post, as intended. It was noted that the flange of the post may need to be widened slightly to prevent the local deformation of the keyway slot observed in this test.

Test no. CPZ-3, a cable pull test, was conducted to evaluate the stability of the post section when it was loaded by the cable-to-post attachment bracket and to determine if the cable-to-post attachment bracket would release the cable as designed when used with the new post section. Results from that test indicated that the MWP had adequate stability under the cable loading, and the cable-to-post attachment bracket V10 released the cable as intended as the post rotated.

Table 9. Test Summary Matrix, Test Nos. CPZ-1 through CPZ-3

Test No.	Impact Axis	Impact Speed mph (km/h)	Peak Force kips (kN)	Average Force kips (kN)		Maximum Deflection in. (mm)	Absorbed Energy kip-in. (kJ)		Results
				at 10" (254 mm)	at 15" (381 mm)		at 10" (254 mm)	at 15" (381 mm)	
Midwest Weak 7 gauge post									
CPZ-1	Weak	20.4 (32.8)	4.2 (18.7)	1.6 (7.1)	1.6 (7.1)	22.8 (579)	16.3 (1.8)	24.4 (2.8)	Bent at Groundline
CPZ-2	Strong	19.5 (31.4)	4.4 (19.6)	2.1 (9.3)	1.8 (8.0)	23.0 (584)	20.8 (2.4)	27.7 (3.1)	Bent at Groundline
CPZ-3	Strong	21.1 (34.0)	3.5 (15.6)	0.5 (2.2)	1.0 (4.4)	43.7 (1,110)	4.6 (0.5)	14.5 (1.6)	Bent at Groundline

Table 10. Testing Comparison Matrix

Post Type	Peak Force		Average Force @ 10 in. (254 mm)		Average Force @ 15 in. (381 mm)	
	kips (kN)	% of S3x5.7	kips (kN)	% of S3x5.7	kips (kN)	% of S3x5.7
Strong Axis in Sleeve						
S3x5.7	6.9 (30.7)	-	4.6 (20.5)	-	5.0 (22.2)	-
10-Gauge C	4.4 (19.6)	63.8%	1.9 (8.5)	41.3%	1.4 (6.2)	30.0%
7-Gauge C	5.9 (26.2)	85.5%	2.6 (11.6)	56.5%	2.0 (8.9)	40.0%
MWP	4.4 (19.6)	63.8%	2.1 (9.3)	45.7%	1.8 (8.0)	36.0%
Weak Axis in Sleeve						
S3x5.7	2.0 (8.9)	-	1.4 (6.2)	-	1.5 (6.7)	-
10-Gauge C	3.8 (16.9)	190.0%	0.9 (4.0)	64.3%	0.8 (3.6)	53.3%
7-Gauge C	5.4 (24.0)	270.0%	1.6 (7.1)	114.3%	1.4 (6.2)	93.3%
MWP	4.2 (18.7)	210.0%	1.6 (7.1)	114.3%	1.6 (7.1)	106.7%

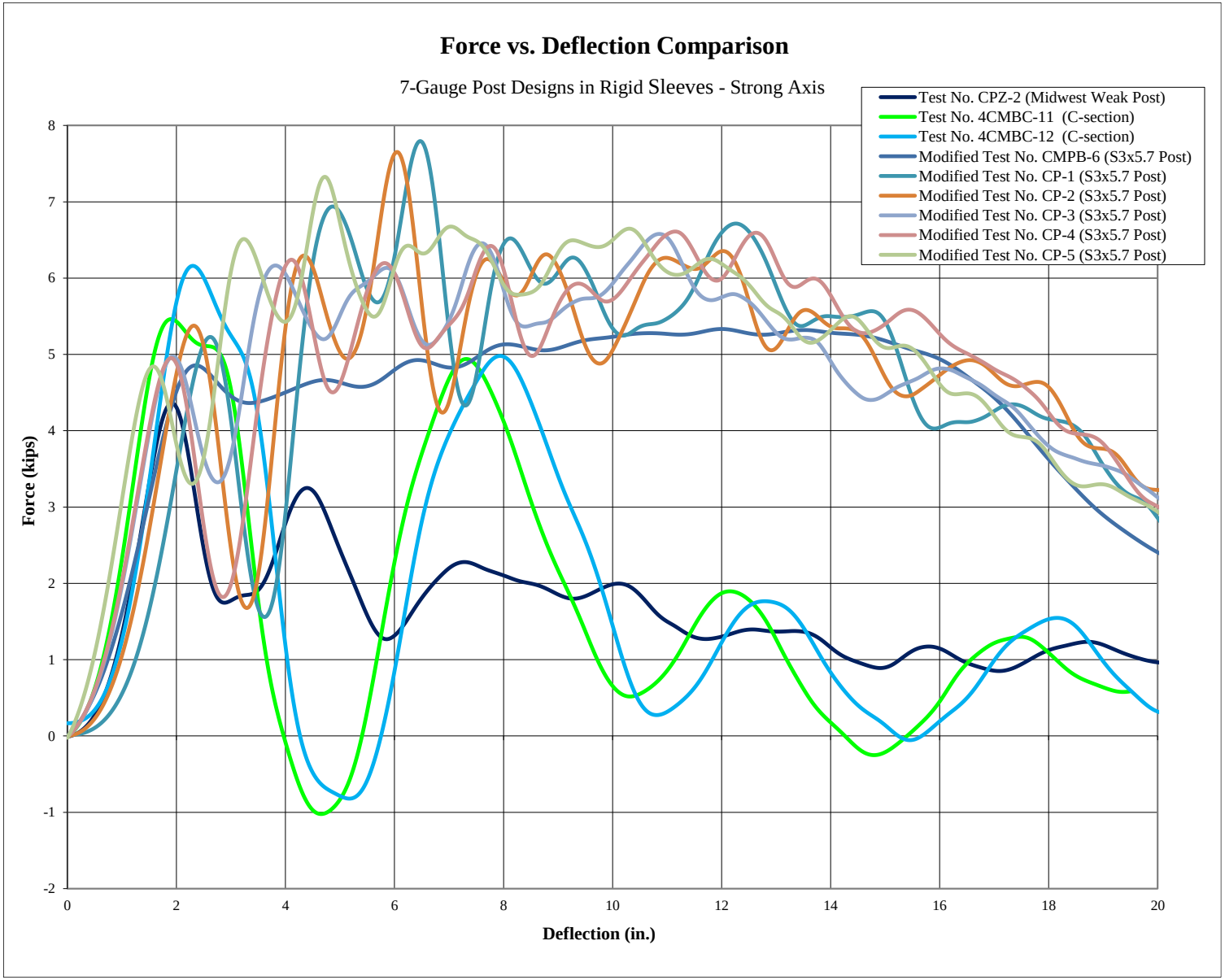

Figure 119. Force vs. Deflection Comparison, Strong Axis, Sleeve

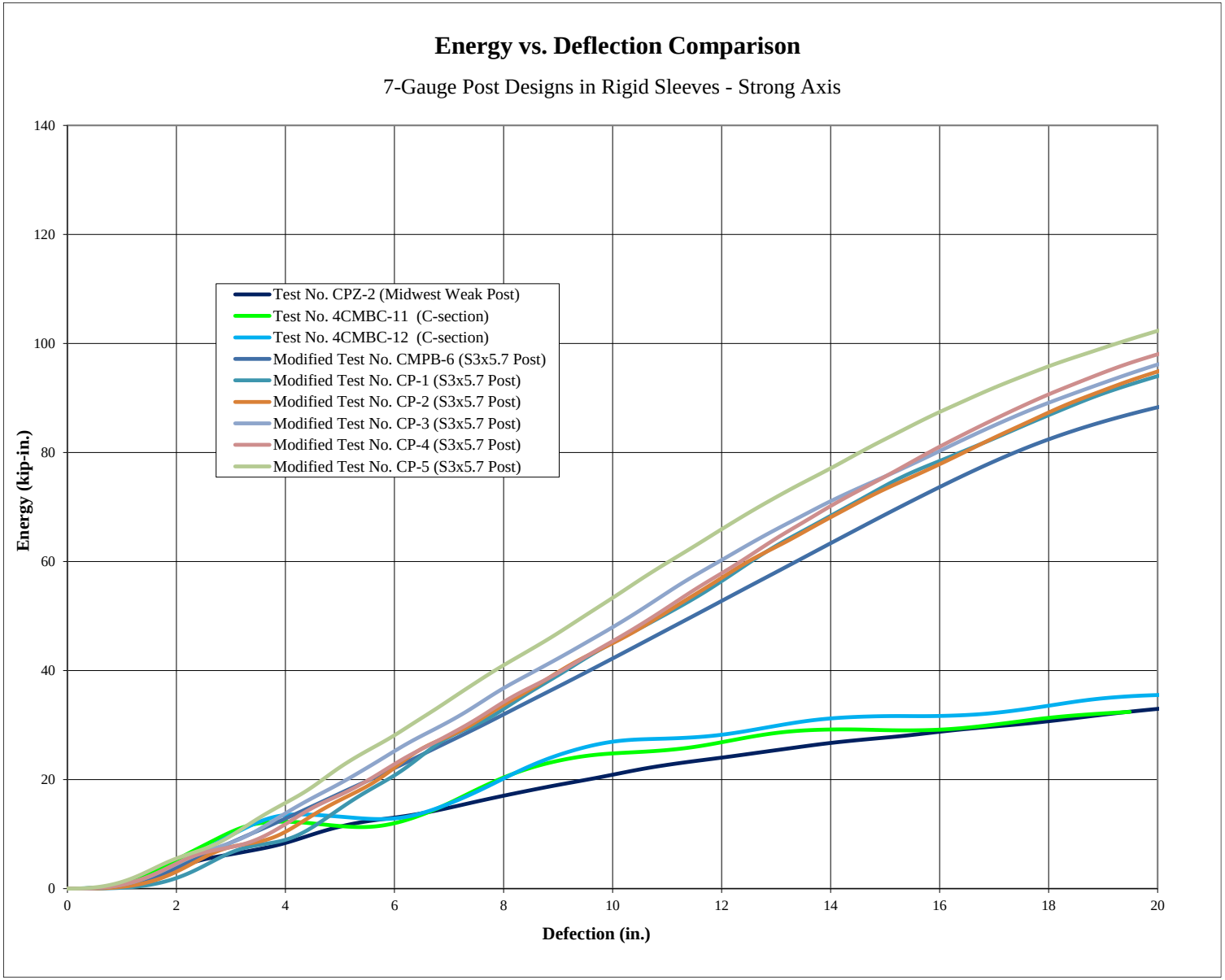

Figure 120. Energy vs. Deflection Comparison, Strong Axis, Sleeve

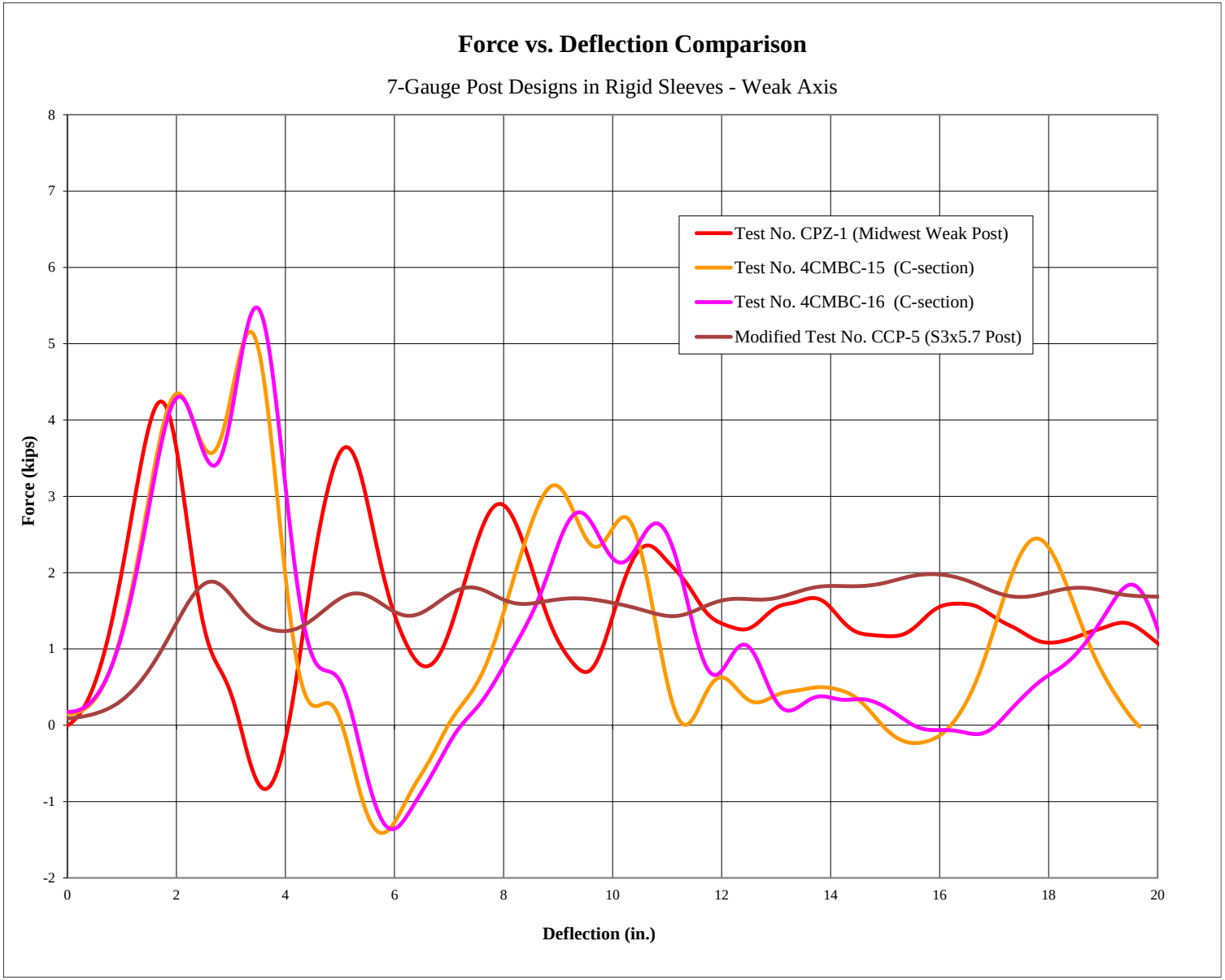

Figure 121. Force vs. Deflection Comparison, Weak Axis, Sleeve

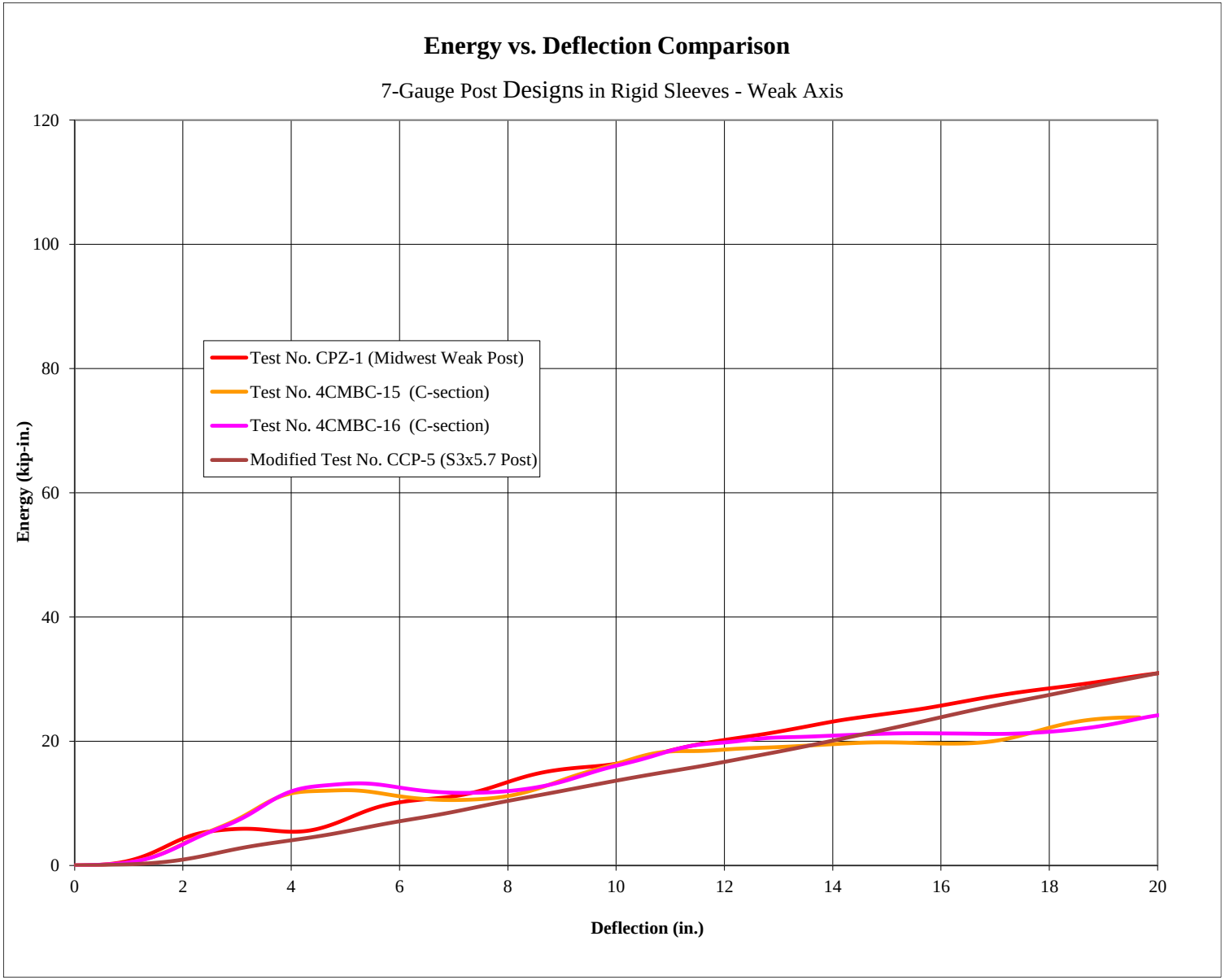

Figure 122. Energy vs. Deflection Comparison, Weak Axis, Sleeve

It should be noted that the researchers revisited the original simulation of the MWP to evaluate its ability to predict the performance of the new post section. Comparisons of the post behavior during the test, the force and energy levels, and the deformed shape and failure modes of the post were conducted, as shown in Figures 123 through 128. Review of the simulation results found that the simulation model provided an accurate prediction of the performance of the strong- and weak-axis behavior of the post. The sequential images of the component tests and the simulations demonstrated similar post behavior during impact, with the post deflecting and yielding in a very similar manner. The force vs. deflection curves of the physical testing and the simulation correlated very well for the strong-axis impact. The weak-axis impact correlated reasonably well, with the simulation predicting slightly lower peak forces than those observed in the testing. Comparison of the energy curves further demonstrated this trend as energy levels were nearly identical for the strong-axis impact, but were slightly lower in the weak axis for the simulated post. The overall loading behavior of the simulated post was considered a good representation of the physical tests. Finally, comparison of the deformed posts from the simulation and testing found that the simulated posts developed nearly identical deformation and failure modes as the tested posts in both the strong- and weak-axes.

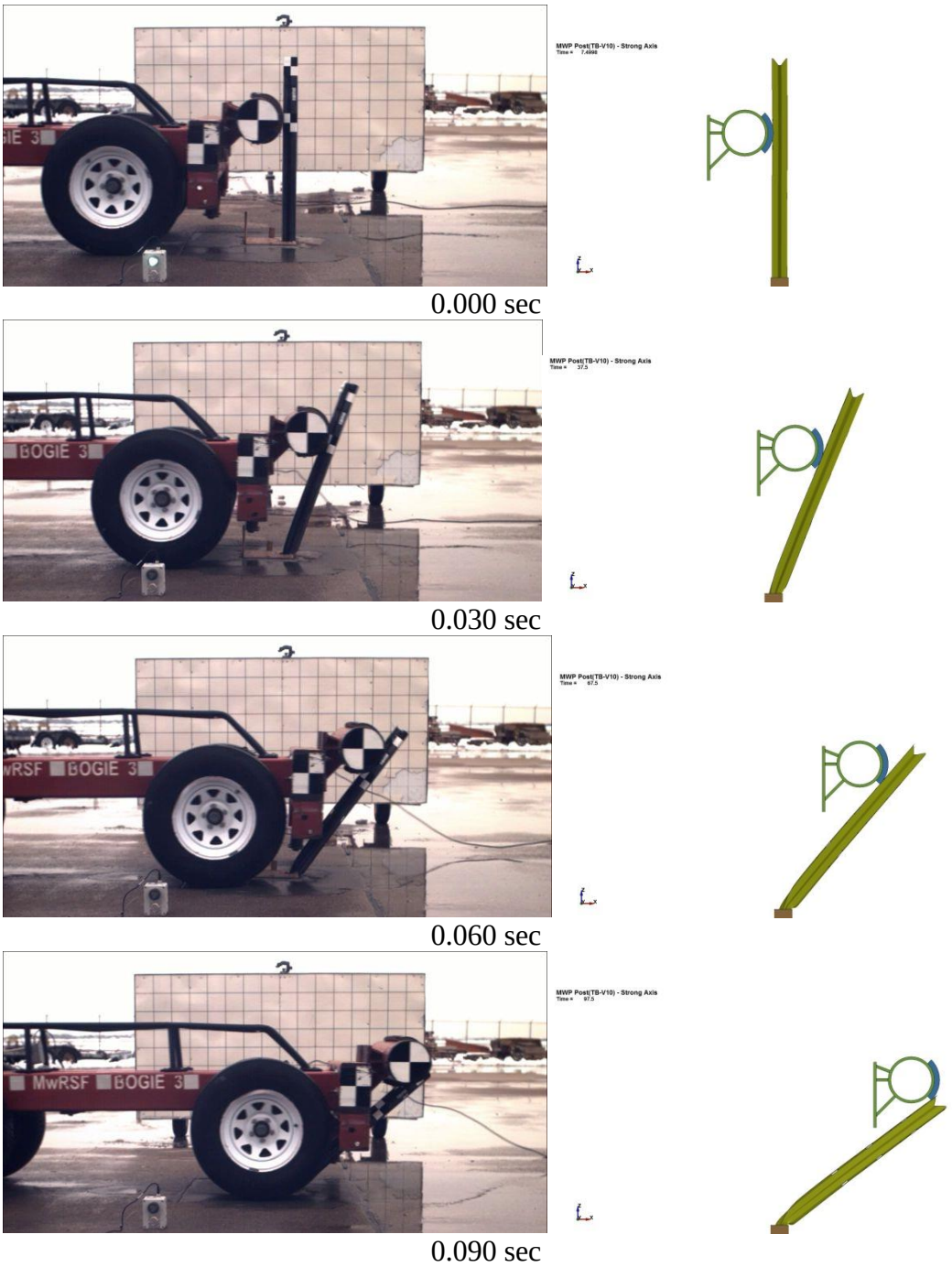

Figure 123. Sequential Images, Strong-Axis Test No. CPZ-2 and LS-DYNA MWP Simulation

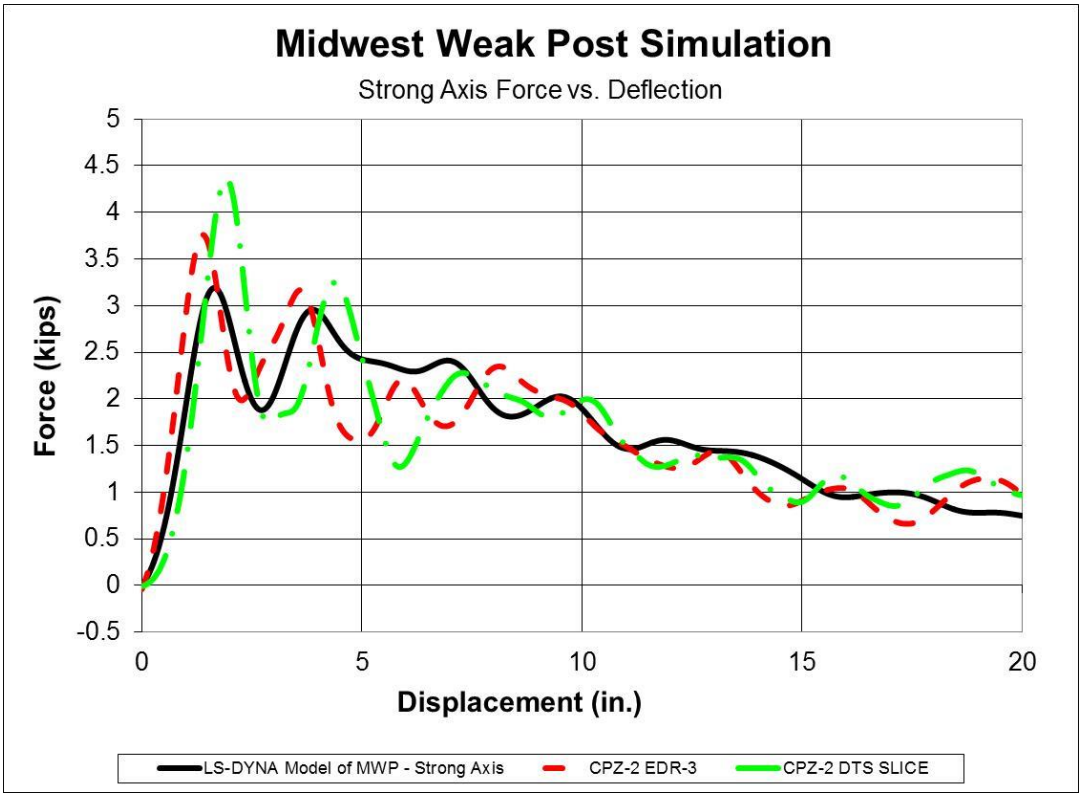

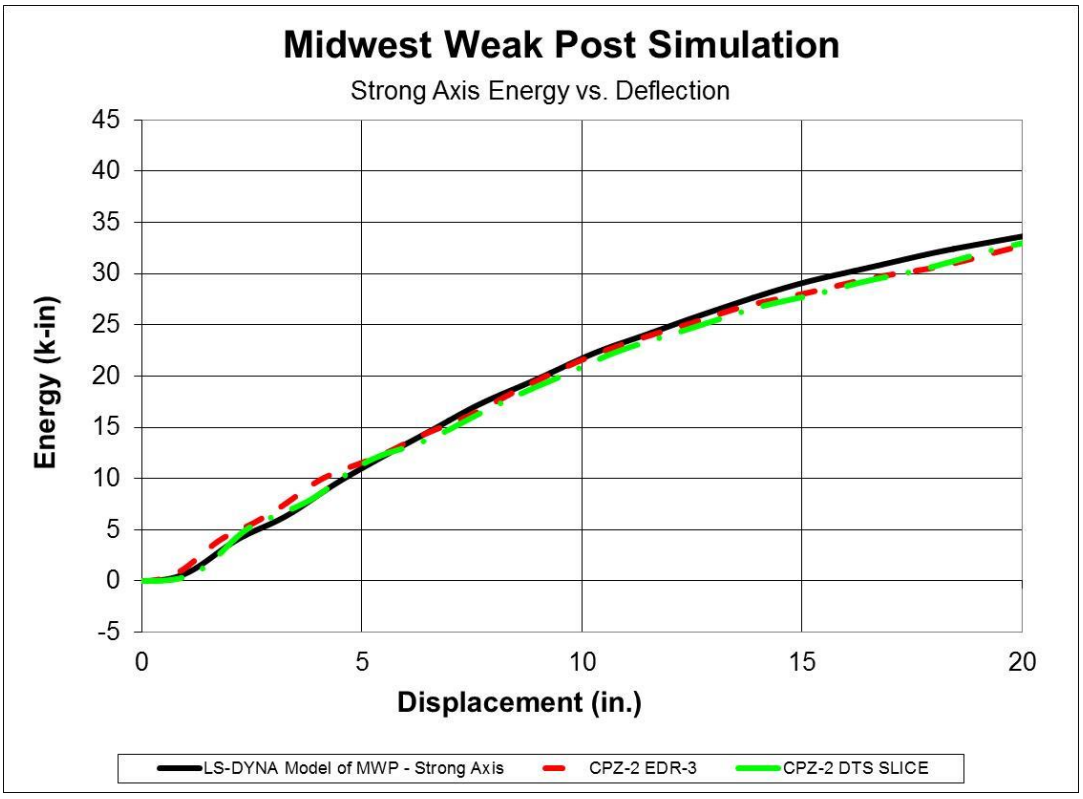

Figure 124. Force and Energy Versus Deflection, Strong-Axis Test No. CPZ-2 and LS-DYNA MWP Simulation

CPZ-2

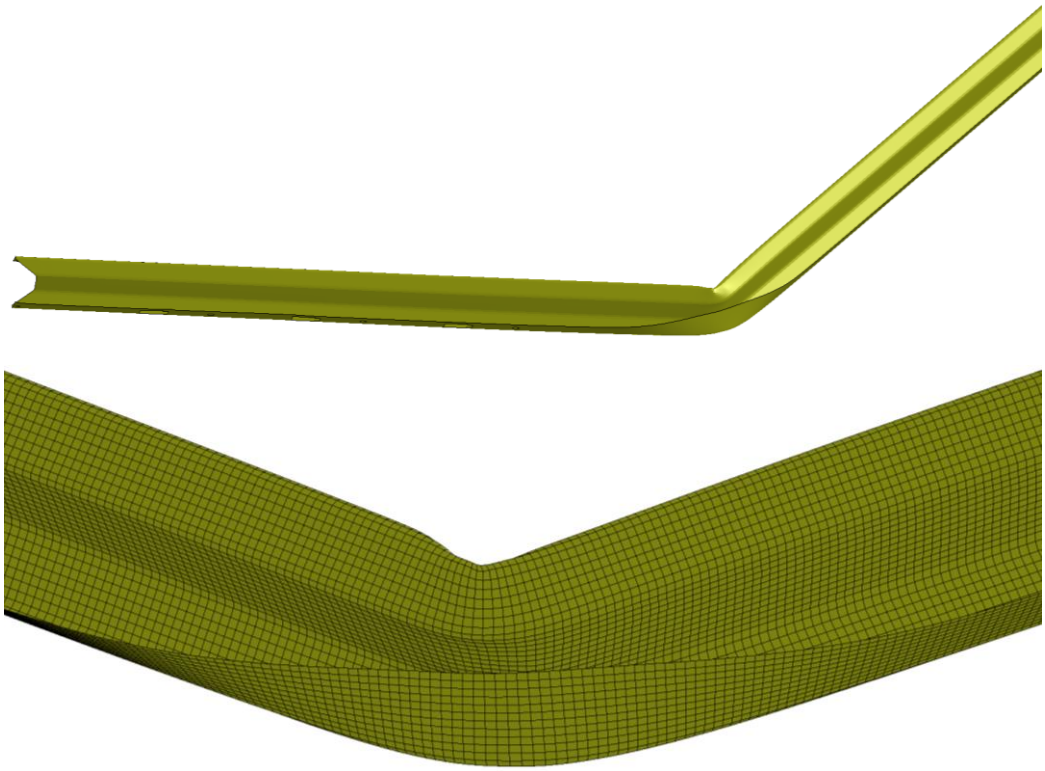

Simulation

Figure 125. Deformed Post Shape, Strong-Axis Test No. CPZ-2 and LS-DYNA MWP Simulation

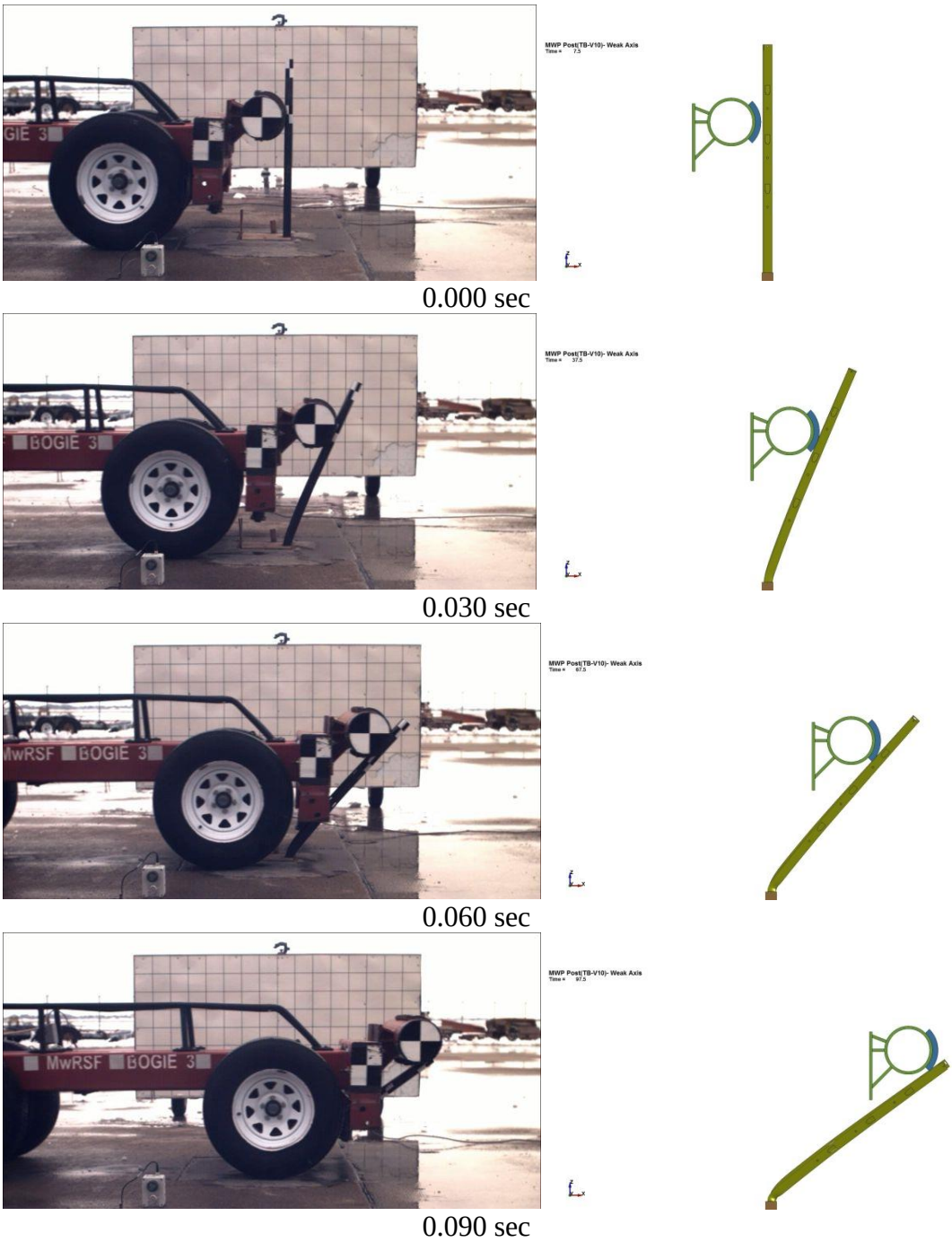

Figure 126. Sequential Images, Weak-Axis Test No. CPZ-1 and LS-DYNA MWP Simulation

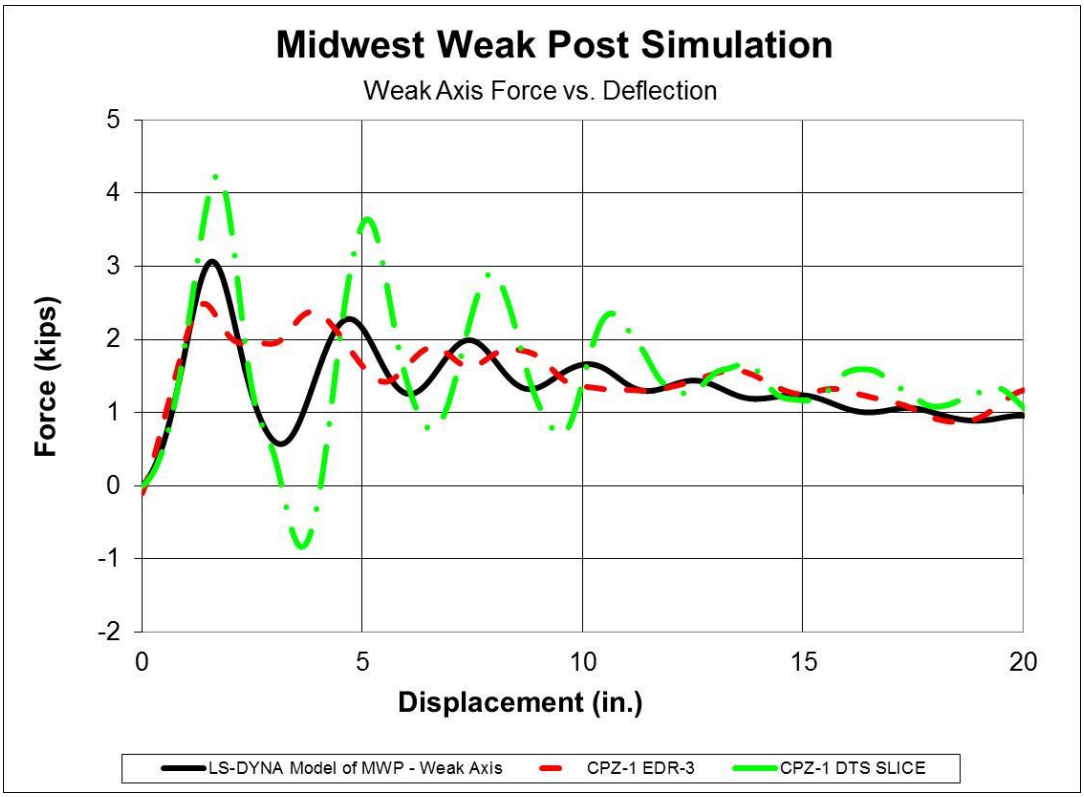

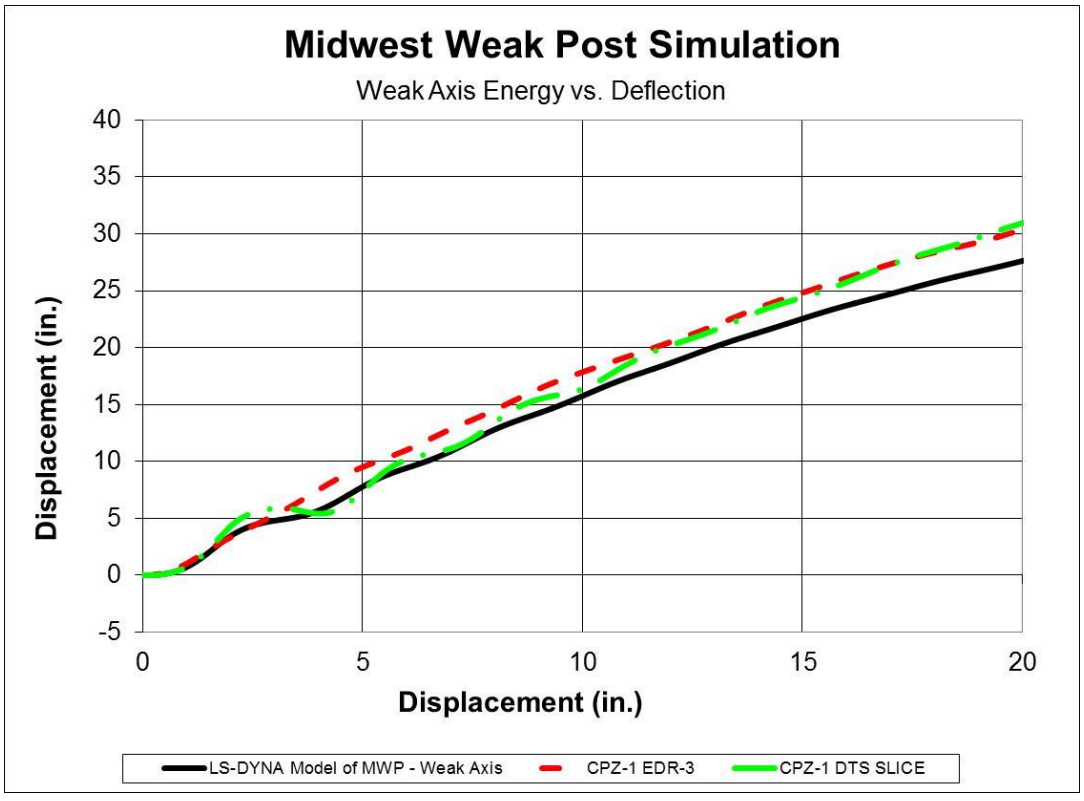

Figure 127. Force and Energy Versus Deflection, Weak-Axis Test No. CPZ-1 and LS-DYNA MWP Simulation

CPZ-1

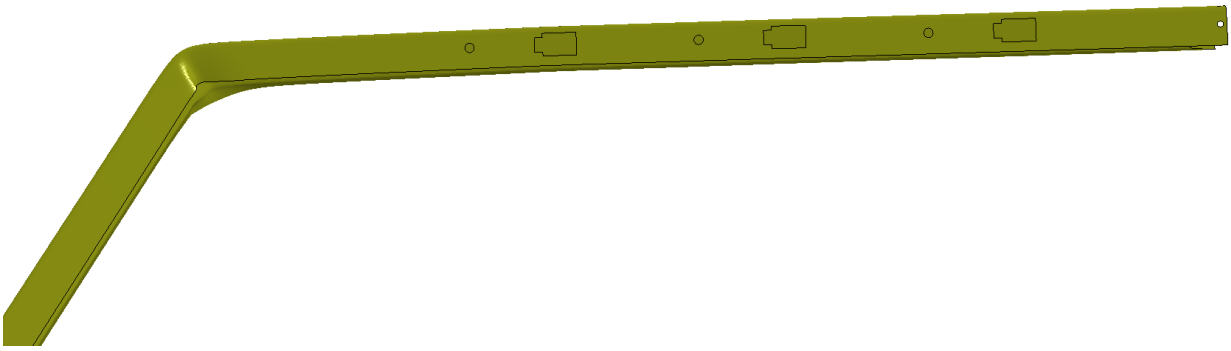

Simulation

Figure 128. Deformed Post Shape, Weak-Axis Test No. CPZ-2 and LS-DYNA MWP Simulation

9 SUMMARY AND CONCLUSIONS

The objective of this research study was to develop a new post section for the non-proprietary high-tension cable median barrier that improved the safety and performance of the barrier system. Several design criteria were identified for the post, including reduction of the lateral, or strong-axis, capacity of the post to limit the loading of the A-pillar by the cables, maintaining a longitudinal, or weak-axis, capacity similar to the current S3x5.7 (S76x8.5) post in order to minimize the potential for vehicle instabilities or snag concerns during vehicle redirection, providing a geometry that allowed for mounting of the cable-to-post attachment brackets developed previously, and utilizing an alternative section that could reduce the costs of post fabrication.

The research effort began with the development of a new post section design. A C-section post formed from folded sheet metal was proposed that met the design criteria. In order to evaluate the new post section, a series of dynamic component tests were conducted on the strong and weak axes of 7-gauge and 10-gauge C-section posts. From these tests, test nos. 4CMBC-1 through 4CMBC-16, it was determined that the 7-gauge C-Section post would be further investigated for the non-proprietary high-tension cable median barrier because it reduced the lateral capacity of the post section approximately 50 percent over the S3x5.7 (S76x8.5) post and did not present the concerns with respect to drivability and localized deformations that were posed by the 10-gauge version of the C-section post.

Following the selection of the 7-gauge C-section post, additional tests of the post were conducted. The C-section posts were originally tested without the keyway and hole configuration required for the cable-to-post attachments, and it was unknown if the post would perform differently under load with these features included. Thus, a second round of component testing was conducted. For these tests, a keyway was added to the 7-gauge C-section post 16 in. (406

mm) above the groundline. In both the strong- and weak-axis tests of the post with the keyways, the posts buckled and hinged at the keyway. This behavior was undesirable, as it left a large exposed post stub and compromised the energy absorption of the post.

LS-DYNA simulation was used to investigate other alternative post sections that did not suffer due to instability of the section. Simulations of modified C-section posts discovered that the natural asymmetry of the post section combined with the keyways in the post flange resulted in post buckling regardless of the modifications to the section. Thus, variations of Z-section posts were investigated. Three versions of Z-section posts were simulated, and a modified Z-section post was selected for further development over the other two design options based on its improvement of the post stability, its lower strong-axis loads, and its ability to align the cable-to-post attachment at the centerline of the post section. The new post section was named the Midwest Weak Post (MWP).

The final phase of the design process was dynamic component testing of the MWP to verify its performance in the strong and weak axis and evaluate its behavior when loaded at the cable-post-attachment. Thus, three additional tests were conducted. Test nos. CPZ-1 and CPZ-2 impacted on the weak- and strong axes of the post, respectively. Test No. CPZ-3 loaded the cable-to-post attachment bracket in the direction of the strong-axis of the post. In all three of the dynamic component tests, the MWP eliminated the instability and buckling observed with the C-section posts, and the new section met all of the design criteria. It was noted that the post flange may need to be widened slightly prior to full-scale testing to prevent localized deformation of the keyway that could adversely affect the release of the cable-to-post attachment brackets. Thus, the MWP was selected for implementation into the non-proprietary high-tension cable median barrier system.

The new steel post section developed in this research formed from folded or rolled steel sheet, dubbed the MWP, has advantages over standard post sections in that it was tuned to provide the desired strong and weak axis capacities while using less material than the standard S-section post it was replacing. In addition, the new post section can be rolled from sheet steel, which makes it economical to fabricate.

It is believed that a similar approach could be applied to the design of a new strong post section for other barrier systems like the Midwest Guardrail System (MGS). Design of a new post for other barrier systems would function similarly to the methodology of this study by optimizing the post capacities in the strong and weak axes, while reducing the cost of the post through reduced material and fabrication effort.

10 REFERENCES

1. Johnson, E.A., Sicking, D.L., Faller, R.K., Lechtenberg, K.A., Rohde, J.R., Bielenberg, R.W., Reid, J.D., and Rosenbaugh, S.K., *Phase I Development of a Non-Proprietary, Four-Cable, High-Tension Median Barrier*, Final Report to the Midwest States' Regional Pooled Fund Program, Transportation Research Report No. TRP-03-213-11, Project No.: SPR-3(017), Project Code: RPFP-04-01 and RPFP-08-02 – Years 14, 16, and 18, Midwest Roadside Safety Facility, University of Nebraska-Lincoln, Lincoln, Nebraska, December 28, 2011.

2. Schmidt, J.D., Sicking, D.L., Faller, R.K., Lechtenberg, K.A., Bielenberg, R.W., Reid, J.D., and Rosenbaugh, S.K., *Phase II Development of a Non-Proprietary, Four-Cable, High-Tension Median Barrier,* Final Report to the Midwest States' Regional Pooled Fund Program, Transportation Research Report No. TRP-03-253-12, Project No. TPF-5(091) Supplement #1, Project Code: RPFP-09-01 – Year 19, Midwest Roadside Safety Facility, University of Nebraska-Lincoln, Lincoln, Nebraska, March 21, 2012.

3. Kampschneider, L.R., Homan, D. H., Lechtenberg, K.A., Faller, R.K., Bielenberg, R.W., Sicking, D.L., Reid, J.D., and Rosenbaugh, S.K., *Evaluation of a Non-Proprietary, High-Tension, 4-Cable Median Barrier on Level Terrain*, Final Report to the Midwest States' Regional Pooled Fund Program, Transportation Research Report No. TRP-03-258-12, Project Nos. TPF-5(091) Supplement #1, TPF-5(193) Supplement #20, #44, and #45, Project Codes: RPFP-09-01, RPFP-10-CABLE-2, and RPFP-12-CABLE-1&2—Years 19, 20 and 22, Midwest Roadside Safety Facility, University of Nebraska-Lincoln, Lincoln, Nebraska, November 29, 2012.

4. Bateman, R.J., Faller, R.K., Bielenberg, R.W., Sicking, D.L., Reid, J.D., Stolle, C.S., Lechtenberg, K.A., and Rosenbaugh, S.K., *Design of Cable-to-Post Attachments for Use in a Non-Proprietary, High-Tension, Cable Median Barrier,* Final Report to the Midwest States' Pooled Fund Program, Transportation Research Report No. TRP-03-285-13, Project Code: RPFP-09-01, and RPFP-12-CABLE 1&2, Years 19 & 22, Midwest Roadside Safety Facility, University of Nebraska-Lincoln, Lincoln, Nebraska, April 23, 2013.

5. Stolle, C.S., *Cable Median Barrier Failure Analysis and Remediation*, Doctoral Dissertation, University of Nebraska-Lincoln, Lincoln, Nebraska, December 2012.

6. Society of Automotive Engineers (SAE), *Instrumentation for Impact Test—Part 1—Electronic Instrumentation,* SAE/J211/1 MAR95, New York City, New York, July, 2007.

7. *Manual for Assessing Safety Hardware (MASH),* American Association of State Highway and Transportation Officials (AASHTO), Washington, D.C., 2009.

8. Kuipers, B.D., and Reid, J.D., *Testing of M203x9.7 (M8x6.5) and S76x8.5 (S3x5.7) Steel Posts-Post Comparison Study for the Cable Median Barrier,* Final Report to the Midwest States' Regional Pooled Fund Program, Transportation Research Report No. TRP-03-143-03, Midwest Roadside Safety Facility, University of Nebraska-Lincoln, Lincoln, Nebraska, October 24, 2003.

9. Stolle, C.S., Faller, R.K., and Polivka, K.A., *Dynamic Impact Testing of S76x8.5 (S3x5.7) Steel Posts for Use in Cable Guardrail Systems*, Final Report to the Midwest States' Regional Pooled Fund Program, Transportation Research Report No. TRP-03-186-07, Project No. SPR-3(017), Project Code: RPFP-04-01, Midwest Roadside Safety Facility, University of Nebraska-Lincoln, Lincoln, Nebraska, December 19, 2007.

10. Schneider, A.J., Rosenbaugh, S.K., Faller, R.K., Reid, J.D., Lechtenberg, K.A., and Sicking, D.L., *Safety Performance Evaluation of MGS Attached to Culvert*, Draft Report to the Midwest States' Regional Pooled Fund Program, Transportation Research Report No. TRP-03-277-12, Midwest Roadside Safety Facility, University of Nebraska-Lincoln, Lincoln, Nebraska, In Progress.

11. Fating, R.M., and Reid, J.D., *Dynamic Impact Testing of S76x8.5 Steel Posts*, Final Report to the Midwest States' Regional Pooled Fund Program, Transportation Research Report No. TRP-03-117-02, Midwest Roadside Safety Facility, University of Nebraska-Lincoln, Lincoln, Nebraska, November 15, 2002.

12. Luttig, M., and Lechtenberg, K.A., *Cut Cable Post Bogie Testing Test Nos. CCP-1 through CCP-11*, Internal Report for the Midwest Roadside Safety Facility, Midwest Roadside Safety Facility, University of Nebraska-Lincoln, Lincoln, Nebraska, February 19, 2012.

13. Hallquist, J.O., LS-DYNA Keyword User's Manual, Volume I, Livermore Software Technology Corporation, Livermore, CA, 2007.

11 APPENDICES

Appendix A. Material Certifications

Item No.	QTY.	Description	Material Specification
a1	8	3"x1 5/8"x6 Gauge [76x41x4.9], 90" [2286] Long Bent C-Channel Post	Hot-Rolled ASTM A1011 HSLA Grade 50
a2	8	3"x1 5/8"x10 Gauge [76x41x3.4], 90" [2286] Long Bent C-Channel Post	Hot-Rolled ASTM A1011 HSLA Grade 50

Figure A-1. Bill of Materials, Test Nos. 4CMBC-1 through 4CMBC-16 and CPK-1 through CPK-2

Norfolk Iron & Metal Co.

3001 North Victory Road
Norfolk, NE 68701
PH: (402) 371-1810

Test Certificate

Document: 01020883

Product Description

Thickness: .1800 Heat: Q3343 Supplier: NLMK INDIANA

Specification(s): A1011 HSLAS-F GR50-12

Chemistry Data

C	MN	P	S	SI	AL	CB	V	CU	CR
.07	.96	.009	.004	.051	.036	.0006	.0876	.13	.05

NI	MO	SN	TI	N	B	ZR
.06	.02	.028	.002	.008	.0001	.00

Mechanical Data

	Yield (PSI)	Tensile (PSI)	Elongation 2in	Reduction Of Area	Sample Taken From
1	67464	80768	35.00	40.3300	Head
2	66414	80603	35.50	42.6800	Center

Produced From Coil

Country of Origin: UNITED STATES

Melted and Manufactured In: UNITED STATES

The Mechanical Data for the product described above reflect the results of tests made by us in accordance with applicable ASTM or ASME standards and our testing procedures, and we certify that the information included in this Test Certificate with respect to such Mechanical Data is accurate to the best of our knowledge.

The Chemistry Data shown above was reported to us by NLMK INDIANA and have been included in this Test Certificate solely for your information.

Figure A-2. C-Channel Post Material Certification, 7-Gauge, Test Nos. 4CMBC-5 through 4CMBC-8, 4CMBC-11 and 4CMBC-12, 4CMBC-15 and 4CMBC-16, and CPK-1 and CPK-2

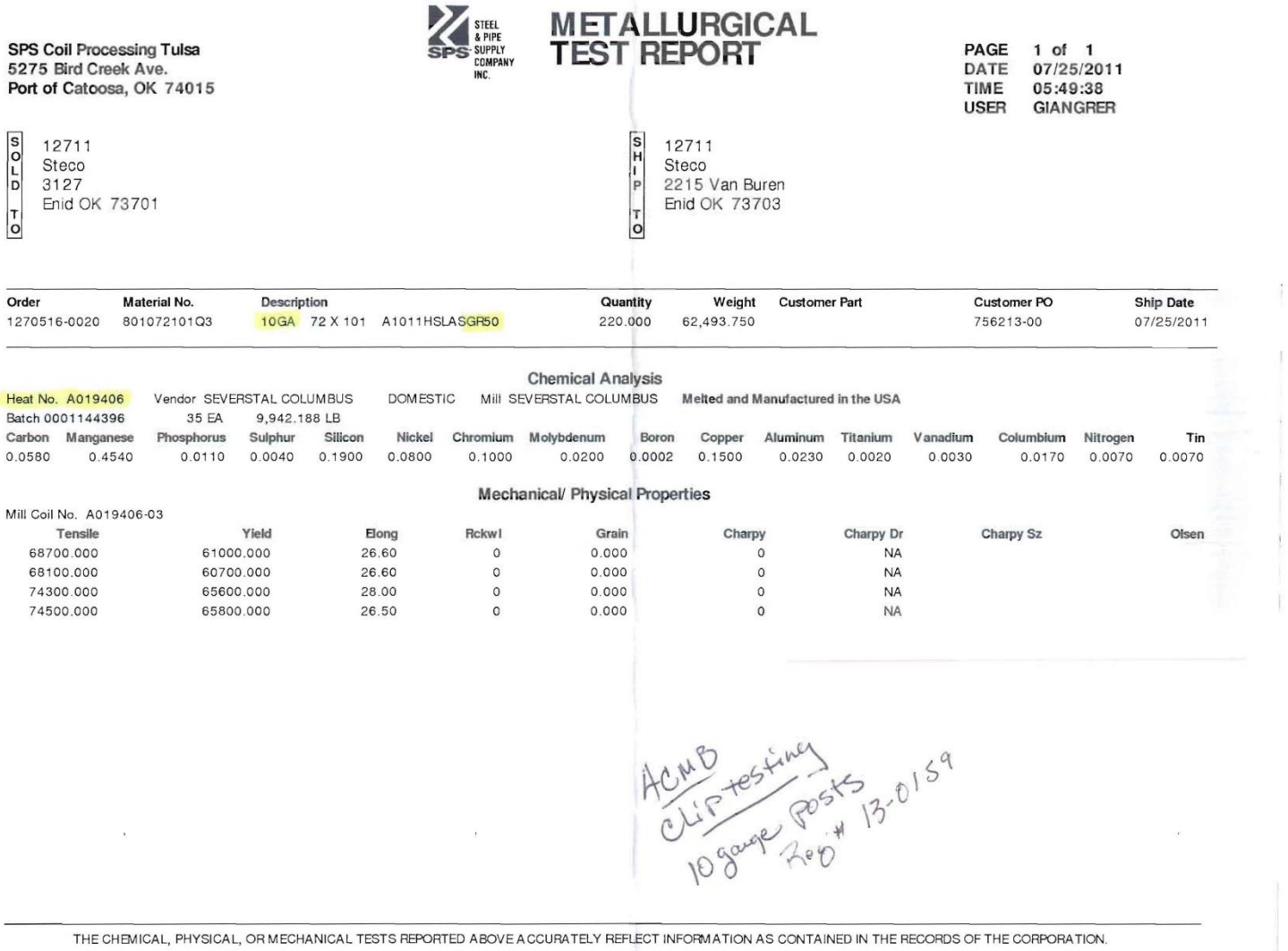

SPS Coil Processing Tulsa
5275 Bird Creek Ave.
Port of Catoosa, OK 74015

STEEL & PIPE SUPPLY COMPANY INC.

METALLURGICAL TEST REPORT

PAGE 1 of 1
DATE 07/25/2011
TIME 05:49:38
USER GIANGRER

SOLD TO
12711
Steco
3127
Enid OK 73701

SHIP TO
12711
Steco
2215 Van Buren
Enid OK 73703

Order	Material No.	Description	Quantity	Weight	Customer Part	Customer PO	Ship Date
1270516-0020	801072101Q3	10GA 72 X 101 A1011HSLASGR50	220.000	62,493.750		756213-00	07/25/2011

Chemical Analysis

Heat No. A019406 Vendor SEVERSTAL COLUMBUS DOMESTIC Mill SEVERSTAL COLUMBUS Melted and Manufactured in the USA
Batch 0001144396 35 EA 9,942.188 LB

Carbon	Manganese	Phosphorus	Sulphur	Silicon	Nickel	Chromium	Molybdenum	Boron	Copper	Aluminum	Titanium	Vanadium	Columbium	Nitrogen	Tin
0.0580	0.4540	0.0110	0.0040	0.1900	0.0800	0.1000	0.0200	0.0002	0.1500	0.0230	0.0020	0.0030	0.0170	0.0070	0.0070

Mechanical/ Physical Properties

Mill Coil No. A019406-03

Tensile	Yield	Elong	Rckwl	Grain	Charpy	Charpy Dr	Charpy Sz	Olsen
68700.000	61000.000	26.60	0	0.000	0	NA		
68100.000	60700.000	26.60	0	0.000	0	NA		
74300.000	65600.000	28.00	0	0.000	0	NA		
74500.000	65800.000	26.50	0	0.000	0	NA		

ACMB
Clip testing
10 gauge posts
Req # 13-0159

THE CHEMICAL, PHYSICAL, OR MECHANICAL TESTS REPORTED ABOVE ACCURATELY REFLECT INFORMATION AS CONTAINED IN THE RECORDS OF THE CORPORATION.

Figure A-3. C-Section Post Material Certification, 10-Gauge, Test Nos. 4CMBC-1 through 4CMBC-4, 4CMBC-9 and 4CMBC-10, and 4CMBC-13 and 4CMBC-14

Test Certificate

Document: 01024973

Norfolk Iron & Metal Co.

3001 North Victory Road
Norfolk, NE 68701
PH: (402) 371-1810

Product Description

Thickness: .1800 Heat: 083707 Supplier: THYSSENKRUPP STEEL USA

Specification(s): A1011 HSLAS-F GR50-12

Chemistry Data

C	MN	P	S	SI	AL	CB	V	CU	CR
.059	.417	.0189	.0026	.017	.0469	.02	.0001	.005	.022

NI	MO	SN	TI	N	B	ZR
.012	.0001	.00	.001	.004	.0002	.00

Mechanical Data

	Yield (PSI)	Tensile (PSI)	Elongation	Reduction Of Area	Sample Taken From
1	59716	68741	37.50 2"	71.9100	Head
2	59522	68267	40.40 2"	76.1700	Center

Produced From Coil

Melted and Manufactured In: Not Provided

The Mechanical Data for the product described above reflect the results of tests made by us in accordance with applicable ASTM or ASME standards and our testing procedures, and we certify that the information included in this Test Certificate with respect to such Mechanical Data is accurate to the best of our knowledge.

The Chemistry Data shown above was reported to us by THYSSENKRUPP STEEL USA and have been included in this Test Certificate solely for your information.

Figure A-4. Midwest Weak Post Material Certification, 7-Gauge, Test Nos. CPZ-1 through CPZ-3

Appendix B. Soil Batch Sieve Analysis

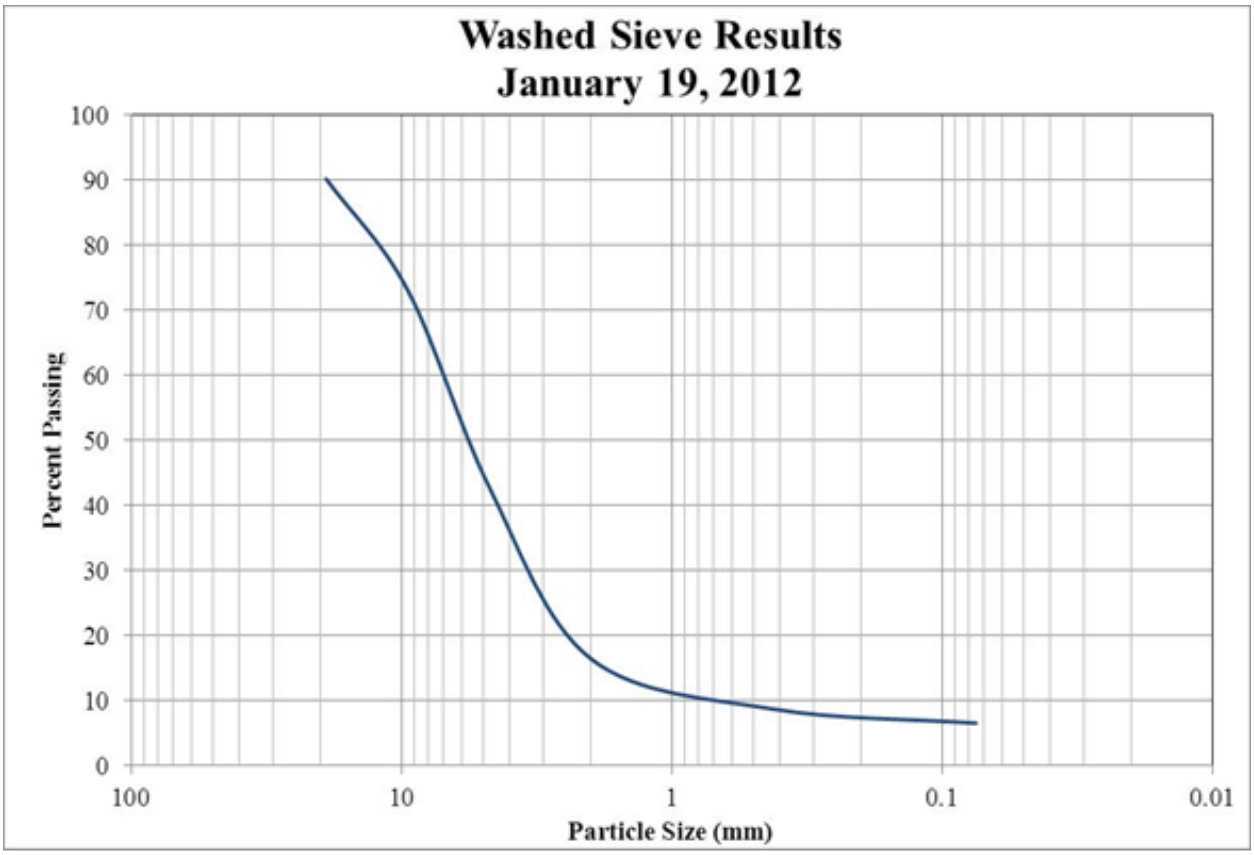

Figure B-1. Soil Gradation for Test Nos. 4CMBC-1 through 4CMBC-8

Appendix C. Bogie Test Results

The results of the recorded data from each accelerometer for every dynamic bogie test are provided in the summary sheets found in this appendix. Summary sheets include acceleration, velocity, and deflection vs. time plots as well, as force vs. deflection and energy vs. deflection plots.

MIDWEST ROADSIDE SAFETY FACILITY

Bogie Test Summary

Test Information	Cable Median Barrier Folded C-Section Post		
Test Number:	4CMBC-1		
Test Date:	2-Nov-2012		
Failure Type:	Post bent and twisted. Data extraction stopped when contact lost with impact head		
Post Properties			
Post Type:	Folded C-Section Post - 10 gauge		
Post Size:	3"x1.625" 10 gauge C-section		
Post Length:	90 in.	228.6 cm	
Embedment Depth:	42 in.	106.7 cm	
Orientation:	Strong		
Soil Properties			
Gradation:	1192012		
Moisture Content:	4.239 @ 15", 4.017 @ 30"		
Compaction Method:	HE8		
Soil Density, γd:	NA		
Bogie Properties			
Impact Velocity:	20.18 mph (29.6 fps)	9.02 m/s	
Impact Height:	27 in.	68.6 cm	
Bogie Mass:	1876 lbs	850.9 kg	
Data Acquired			
Acceleration Data:	DTS		
Camera Data:	AOS-5 Perpendicular		

Test Results Summary			
Max. Deflection:	14.4	in.	
Peak Force:	1.8	k	
Initial Linear Stiffness:	0.3	k/in.	
Total Energy:	13.6	k-in.	

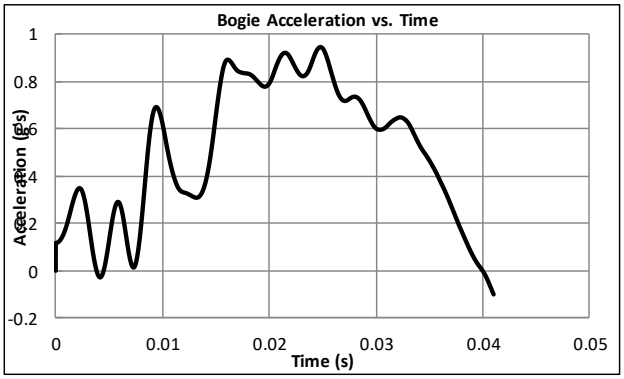

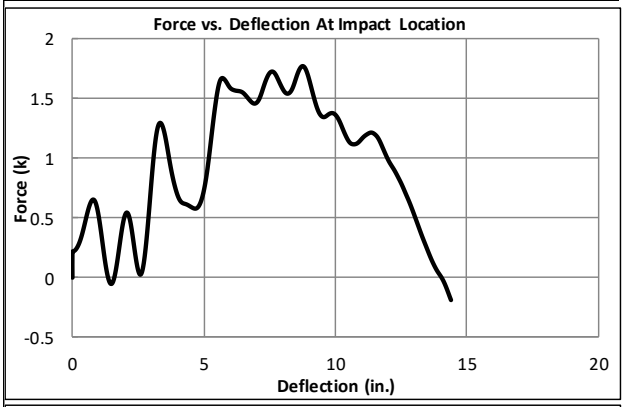

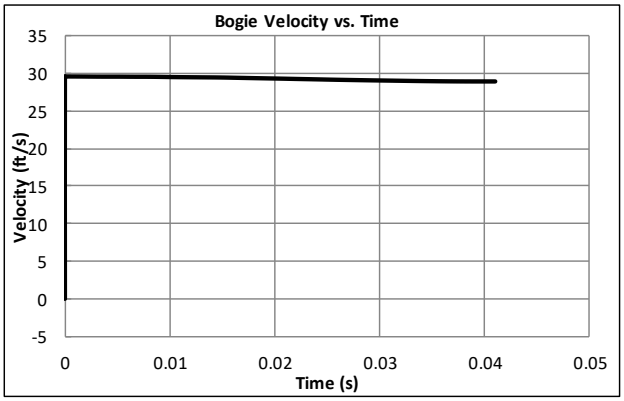

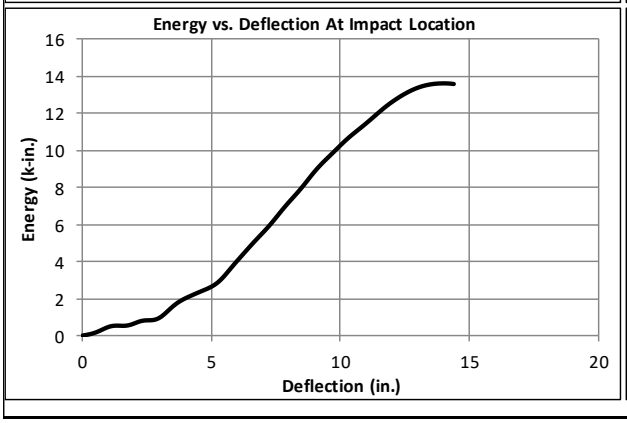

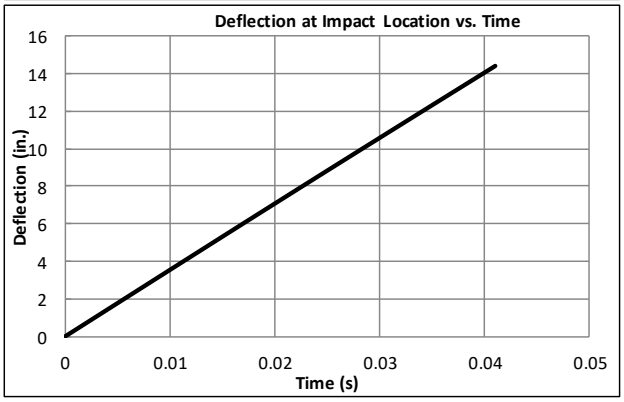

Figure C-1. Test No. 4CMBC-1 Results (DTS)

MIDWEST ROADSIDE SAFETY FACILITY

Bogie Test Summary

Test Information	Cable Median Barrier Folded C-Section Post		
Test Number:	4CMBC-1		
Test Date:	2-Nov-2012		
Failure Type:	Post bent and twisted. Data extraction stopped when contact lost with impact head		
Post Properties			
Post Type:	Folded C-Section Post - 10 gauge		
Post Size:	3"x1.625" 10 gauge C-section		
Post Length:	90 in.	228.6 cm	
Embedment Depth:	42 in.	106.7 cm	
Orientation:	Strong		
Soil Properties			
Gradation:	1192012		
Moisture Content:	4.239 @ 15", 4.017 @ 30"		
Compaction Method:	HE8		
Soil Density, γd:	NA		
Bogie Properties			
Impact Velocity:	20.18 mph (29.6 fps)	9.02 m/s	
Impact Height:	27 in.	68.6 cm	
Bogie Mass:	1876 lbs	850.9 kg	
Data Acquired			
Acceleration Data:	EDR-3		
Camera Data:	AOS-5 Perpendicular		

Test Results Summary		
Max. Deflection:	14.0	in.
Peak Force:	1.5	k
Initial Linear Stiffness:	0.2	k/in.
Total Energy:	12.2	k-in.

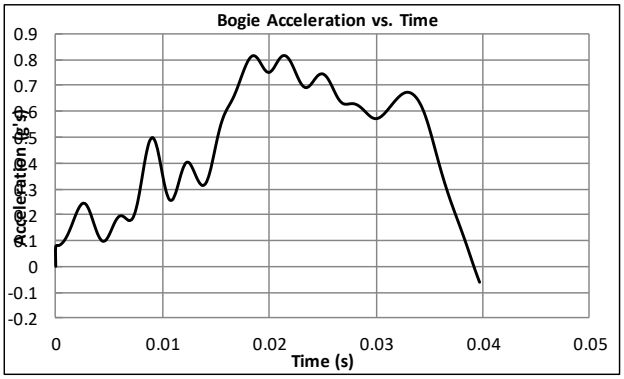

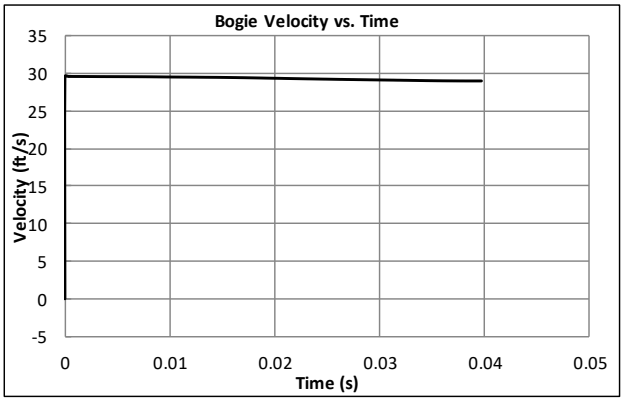

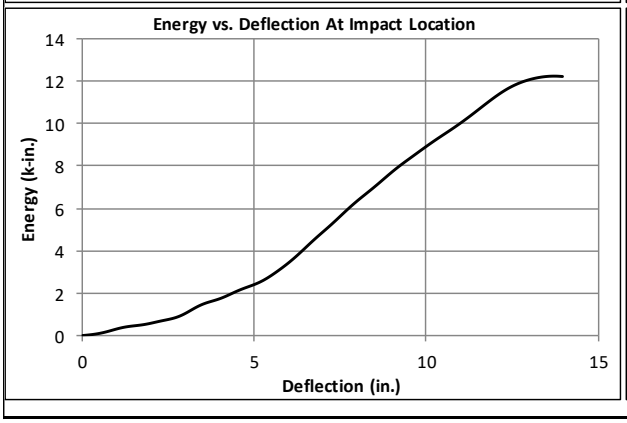

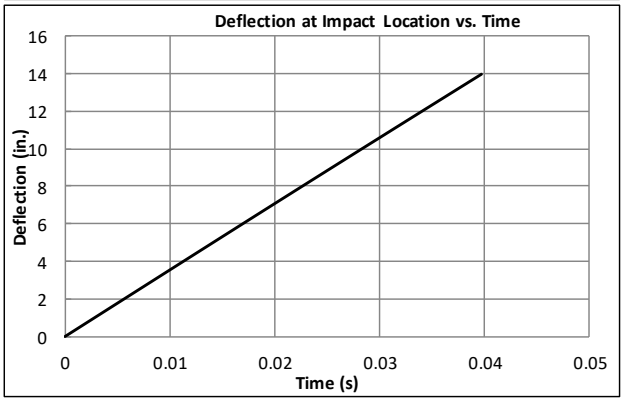

Figure C-2. Test No. 4CMBC-1 Results (EDR-3)

MIDWEST ROADSIDE SAFETY FACILITY

Bogie Test Summary

Test Information	Cable Median Barrier Folded C-Section Post		**Test Results Summary**	
Test Number:	4CMBC-2		Max. Deflection:	19.1 in.
Test Date:	2-Nov-2012		Peak Force:	4.4 k
Failure Type:	Post bent and twisted. Data extraction stopped when contact lost with impact head		Initial Linear Stiffness:	2.9 k/in.
			Total Energy:	24.1 k-in.
Post Properties				
Post Type:	Folded C-Section Post - 10 gauge			
Post Size:	3"x1.625" 10 gauge C-section			
Post Length:	90 in.	228.6 cm		
Embedment Depth:	42 in.	106.7 cm		
Orientation:	Strong			
Soil Properties				
Gradation:	1192012			
Moisture Content:	3.476 @ 15", 3.947 @ 30"			
Compaction Method:	HE8			
Soil Density, γd:	NA			
Bogie Properties				
Impact Velocity:	20.36 mph (29.9 fps)	9.1 m/s		
Impact Height:	27 in.	68.6 cm		
Bogie Mass:	1876 lbs	850.9 kg		
Data Acquired				
Acceleration Data:	DTS			
Camera Data:	AOS-5 Perpendicular			

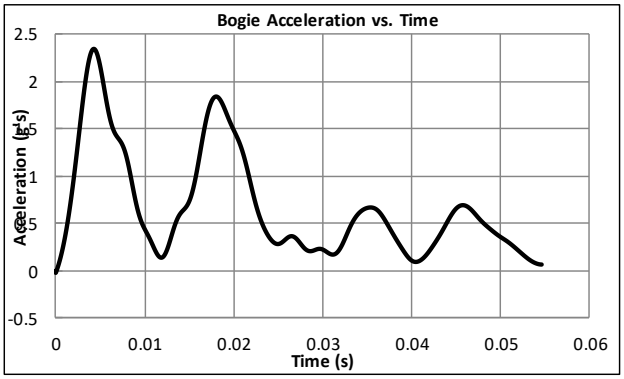

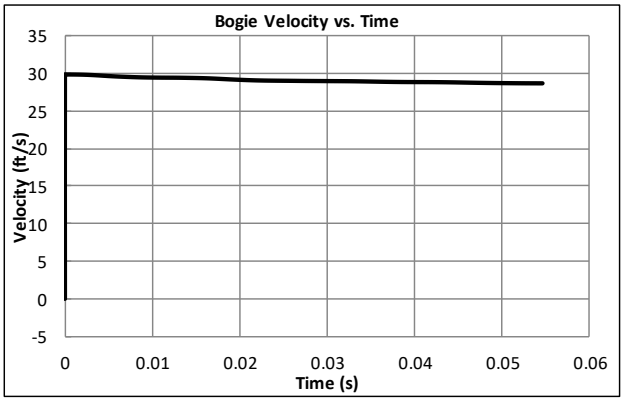

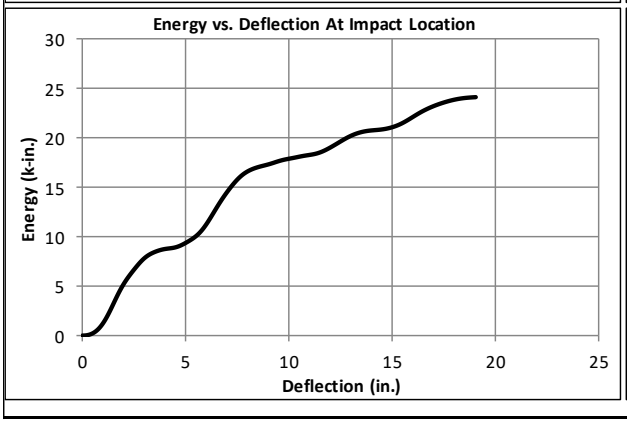

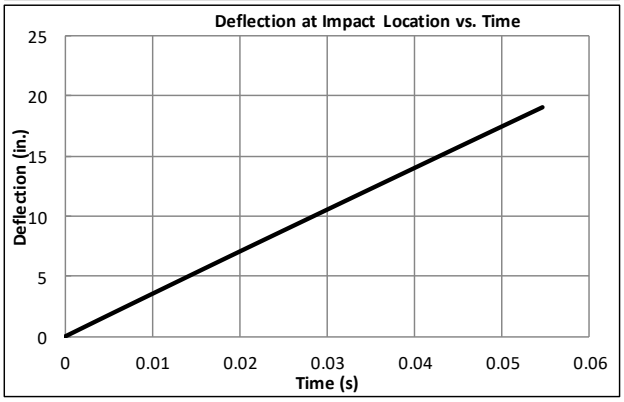

Figure C-3. Test No. 4CMBC-2 Results (DTS)

MIDWEST ROADSIDE SAFETY FACILITY

Bogie Test Summary

Test Information	Cable Median Barrier Folded C-Section Post		**Test Results Summary**	
Test Number:	4CMBC-2		Max. Deflection:	18.0 in.
Test Date:	2-Nov-2012		Peak Force:	3.9 k
Failure Type:	Post bent and twisted. Data extraction stopped when contact lost with impact head		Initial Linear Stiffness:	2.7 k/in.
			Total Energy:	22.9 k-in.
Post Properties				
Post Type:	Folded C-Section Post - 10 gauge			
Post Size:	3"x1.625" 10 gauge C-section			
Post Length:	90 in.	228.6 cm		
Embedment Depth:	42 in.	106.7 cm		
Orientation:	Strong			
Soil Properties				
Gradation:	1192012			
Moisture Content:	3.476 @ 15", 3.947 @ 30"			
Compaction Method:	HE8			
Soil Density, γd:	NA			
Bogie Properties				
Impact Velocity:	20.36 mph (29.9 fps)	9.1 m/s		
Impact Height:	27 in.	68.6 cm		
Bogie Mass:	1876 lbs	850.9 kg		
Data Acquired				
Acceleration Data:	EDR-3			
Camera Data:	AOS-5 Perpendicular			

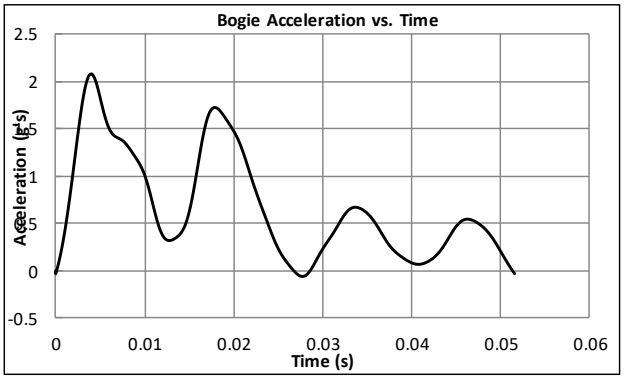

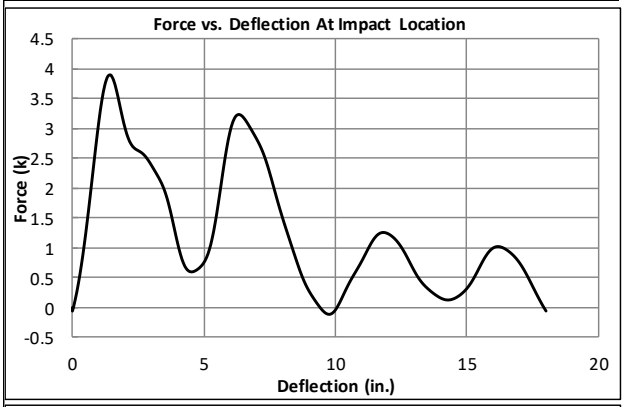

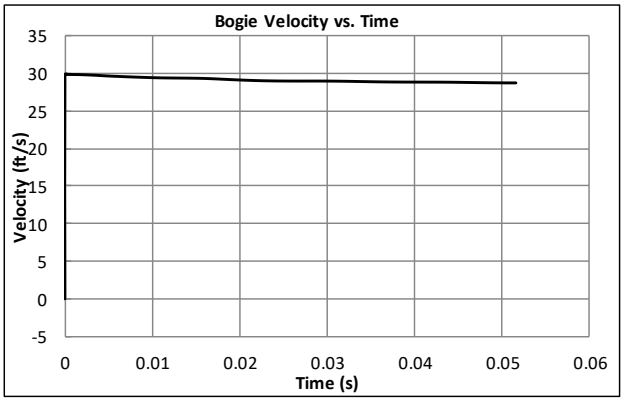

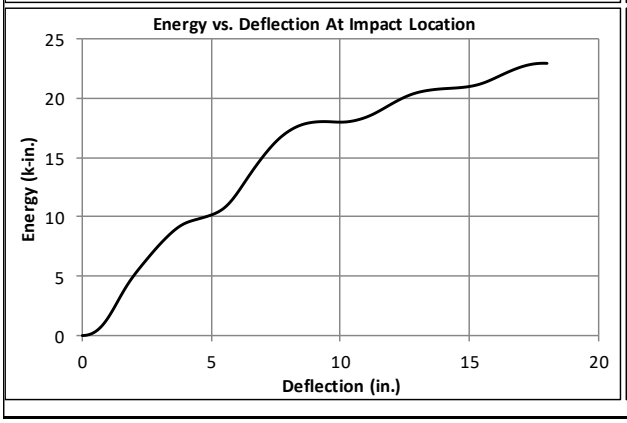

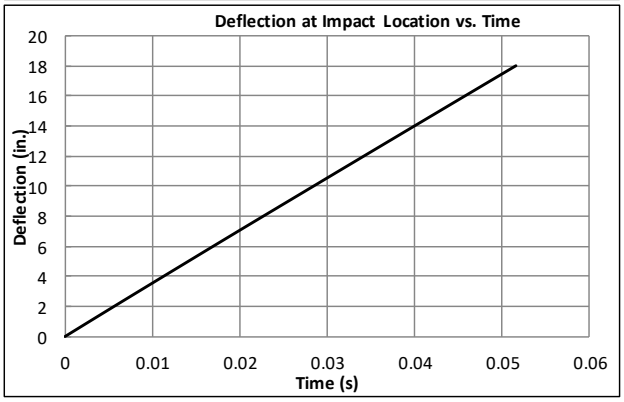

Figure C-4. Test No. 4CMBC-2 Results (EDR-3)

MIDWEST ROADSIDE SAFETY FACILITY

Bogie Test Summary

Test Information	Cable Median Barrier Folded C-Section Post		**Test Results Summary**	
Test Number:	4CMBC-3		Max. Deflection:	24.7 in.
Test Date:	5-Nov-2012		Peak Force:	3.7 k
Failure Type:	Post bent. Data extraction stopped when contact lost with impact head		Initial Linear Stiffness:	1.8 k/in.
			Total Energy:	17.7 k-in.
Post Properties				
Post Type:	Folded C-Section Post - 10 gauge			
Post Size:	3"x1.625" 10 gauge C-section			
Post Length:	90 in.	228.6 cm		
Embedment Depth:	42 in.	106.7 cm		
Orientation:	Weak			
Soil Properties				
Gradation:	1192012			
Moisture Content:	3.295 @ 15", 3.616 @ 30"			
Compaction Method:	HE8			
Soil Density, γd:	NA			
Bogie Properties				
Impact Velocity:	20.22 mph (29.7 fps)	9.04 m/s		
Impact Height:	27 in.	68.6 cm		
Bogie Mass:	1876 lbs	850.9 kg		
Data Acquired				
Acceleration Data:	DTS			
Camera Data:	AOS-5 Perpendicular			

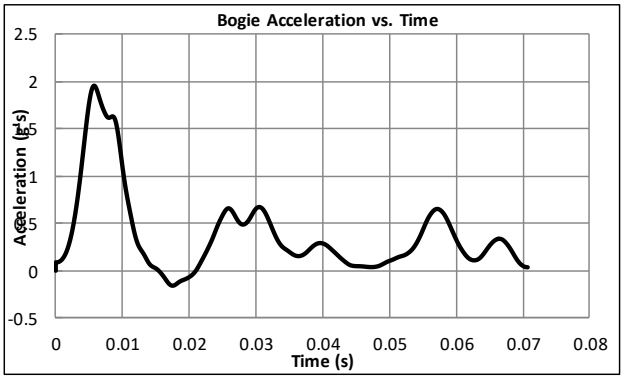

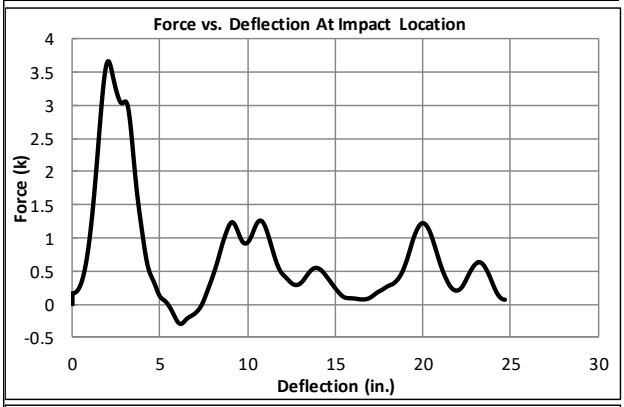

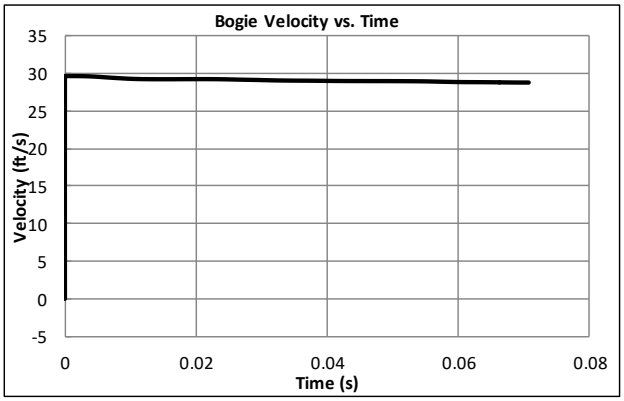

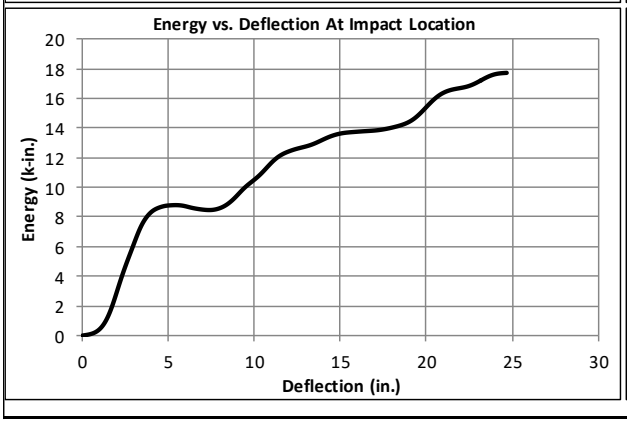

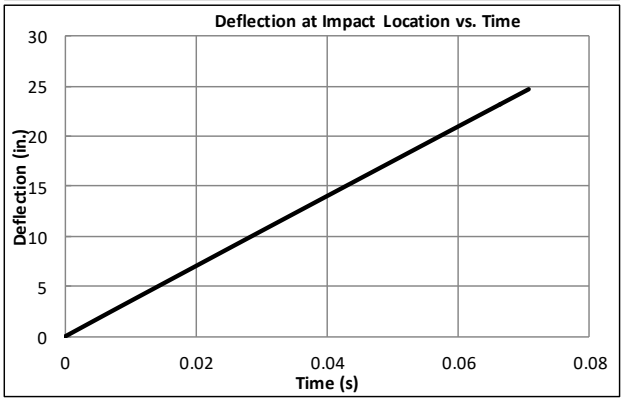

Figure C-5. Test No. 4CMBC-3 Results (DTS)

MIDWEST ROADSIDE SAFETY FACILITY

Bogie Test Summary

Test Information	Cable Median Barrier Folded C-Section Post		
Test Number:	4CMBC-3		
Test Date:	5-Nov-2012		
Failure Type:	Post bent. Data extraction stopped when contact lost with impact head		
Post Properties			
Post Type:	Folded C-Section Post - 10 gauge		
Post Size:	3"x1.625" 10 gauge C-section		
Post Length:	90 in.	228.6 cm	
Embedment Depth:	42 in.	106.7 cm	
Orientation:	Weak		
Soil Properties			
Gradation:	1192012		
Moisture Content:	3.295 @ 15", 3.616 @ 30"		
Compaction Method:	HE8		
Soil Density, γd:	NA		
Bogie Properties			
Impact Velocity:	20.22 mph (29.7 fps)	9.04 m/s	
Impact Height:	27 in.	68.6 cm	
Bogie Mass:	1876 lbs	850.9 kg	
Data Acquired			
Acceleration Data:	EDR-3		
Camera Data:	AOS-5 Perpendicular		

Test Results Summary			
Max. Deflection:	23.0	in.	
Peak Force:	3.1	k	
Initial Linear Stiffness:	1.6	k/in.	
Total Energy:	13.0	k-in.	

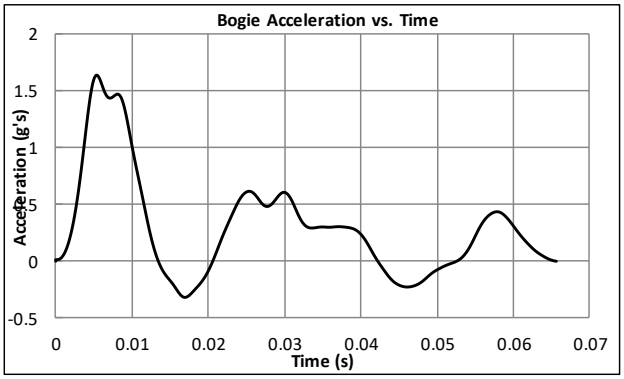

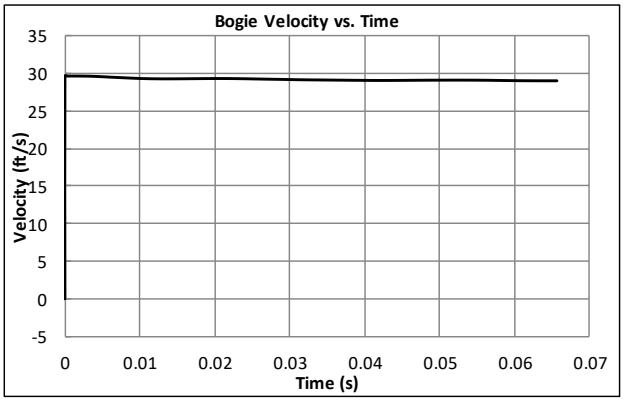

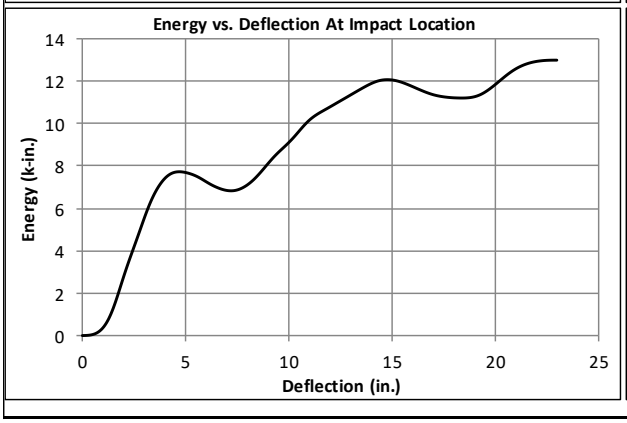

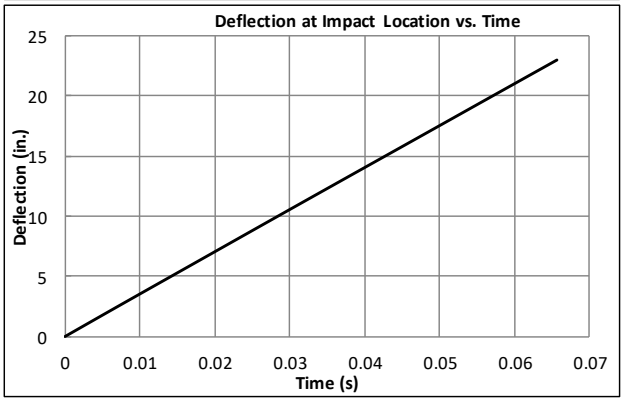

Figure C-6. Test No. 4CMBC-3 Results (EDR-3)

MIDWEST ROADSIDE SAFETY FACILITY

Bogie Test Summary

Test Information	Cable Median Barrier Folded C-Section Post		
Test Number:	4CMBC-4		
Test Date:	5-Nov-2012		
Failure Type:	Post bent. Data extraction stopped when contact lost with impact head		
Post Properties			
Post Type:	Folded C-Section Post - 10 gauge		
Post Size:	3"x1.625" 10 gauge C-section		
Post Length:	90 in.	228.6 cm	
Embedment Depth:	42 in.	106.7 cm	
Orientation:	Weak		
Soil Properties			
Gradation:	1192012		
Moisture Content:	3.846 @ 15", 3.448 @ 30"		
Compaction Method:	HE8		
Soil Density, γd:	NA		
Bogie Properties			
Impact Velocity:	21.14 mph (31.0 fps)	9.45 m/s	
Impact Height:	27 in.	68.6 cm	
Bogie Mass:	1876 lbs	850.9 kg	
Data Acquired			
Acceleration Data:	DTS		
Camera Data:	AOS-5 Perpendicular		

Test Results Summary			
Max. Deflection:	22.1	in.	
Peak Force:	3.7	k	
Initial Linear Stiffness:	1.6	k/in.	
Total Energy:	15.0	k-in.	

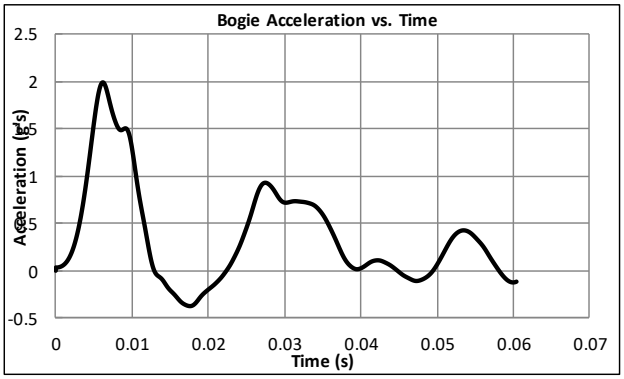

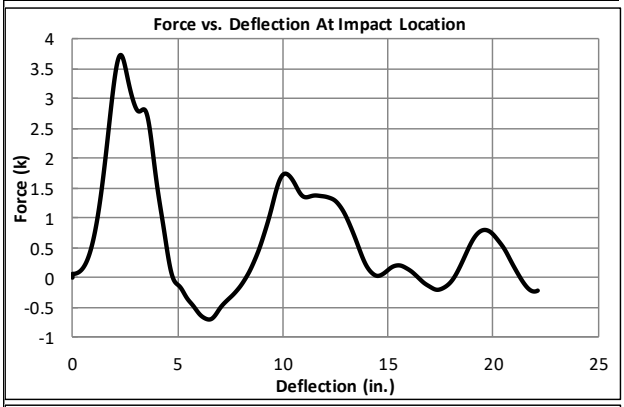

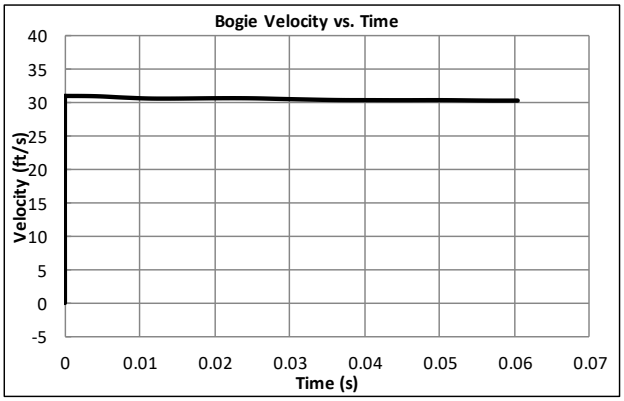

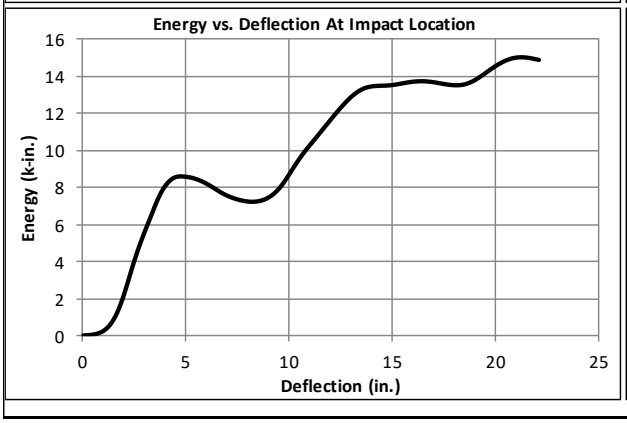

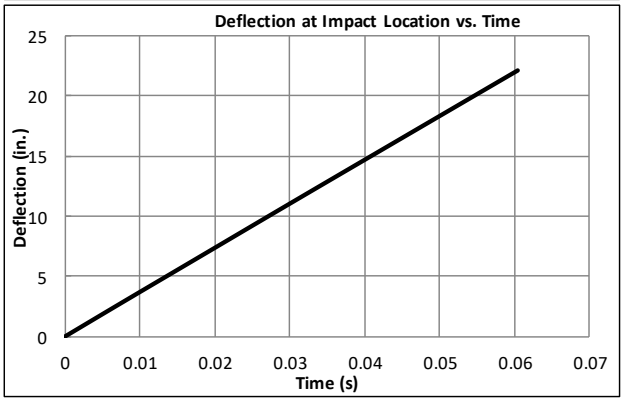

Figure C-7. Test No. 4CMBC-4 Results (DTS)

MIDWEST ROADSIDE SAFETY FACILITY

Bogie Test Summary

Test Information	Cable Median Barrier Folded C-Section Post		
Test Number:	4CMBC-4		
Test Date:	5-Nov-2012		
Failure Type:	Post bent. Data extraction stopped when contact lost with impact head		
Post Properties			
Post Type:	Folded C-Section Post - 10 gauge		
Post Size:	3"x1.625" 10 gauge C-section		
Post Length:	90 in.	228.6 cm	
Embedment Depth:	42 in.	106.7 cm	
Orientation:	Weak		
Soil Properties			
Gradation:	1192012		
Moisture Content:	3.846 @ 15", 3.448 @ 30"		
Compaction Method:	HE8		
Soil Density, γd:	NA		
Bogie Properties			
Impact Velocity:	21.14 mph (31.0 fps)	9.45 m/s	
Impact Height:	27 in.	68.6 cm	
Bogie Mass:	1876 lbs	850.9 kg	
Data Acquired			
Acceleration Data:	EDR-3		
Camera Data:	AOS-5 Perpendicular		

Test Results Summary		
Max. Deflection:	22.2	in.
Peak Force:	3.8	k
Initial Linear Stiffness:	1.5	k/in.
Total Energy:	22.4	k-in.

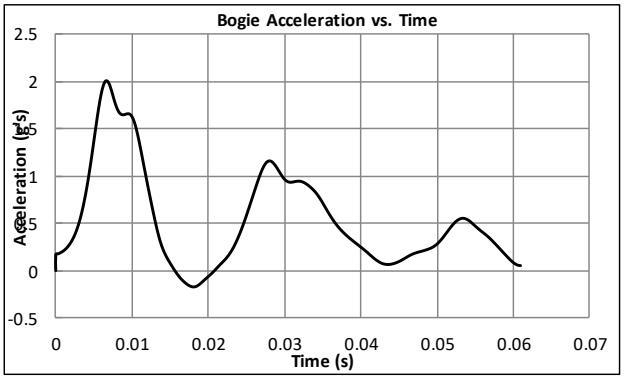

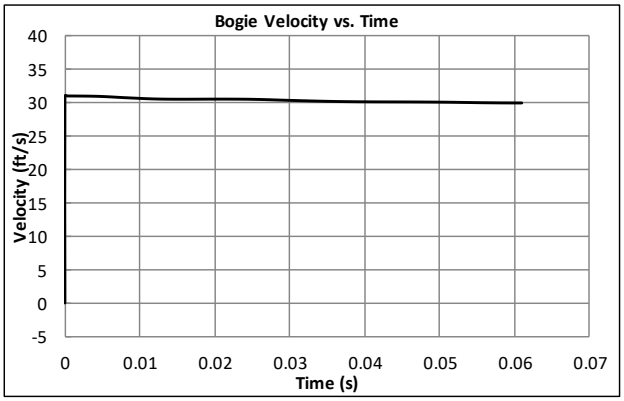

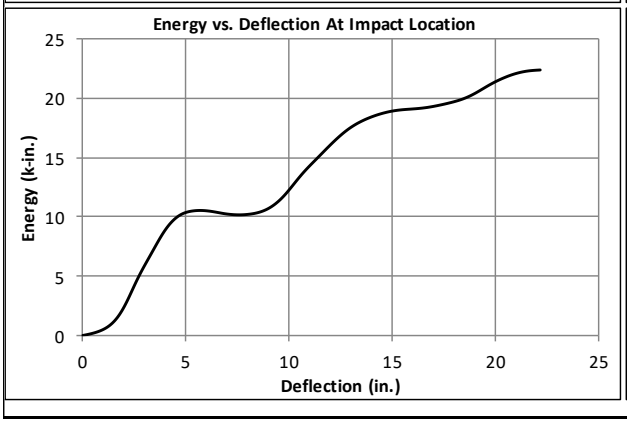

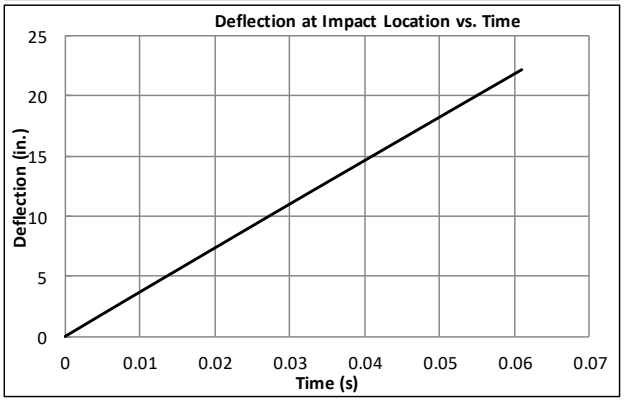

Figure C-8. Test No. 4CMBC-4 Results (EDR-3)

MIDWEST ROADSIDE SAFETY FACILITY

Bogie Test Summary

Test Information	Cable Median Barrier Folded C-Section Post		**Test Results Summary**	
Test Number:	4CMBC-5		Max. Deflection:	18.7 in.
Test Date:	5-Nov-2012		Peak Force:	5.4 k
Failure Type:	Post bent and twisted. Data extraction stopped when contact lost with impact head		Initial Linear Stiffness:	2.5 k/in.
			Total Energy:	30.8 k-in.
Post Properties				
Post Type:	Folded C-Section Post - 7 gauge			
Post Size:	3"x1.625" 7 gauge C-section			
Post Length:	90 in.	228.6 cm		
Embedment Depth:	42 in.	106.7 cm		
Orientation:	Strong			
Soil Properties				
Gradation:	1192012			
Moisture Content:	3,571/3.552			
Compaction Method:	HE8			
Soil Density, γd:	NA			
Bogie Properties				
Impact Velocity:	19.35 mph (28.4 fps)	8.65 m/s		
Impact Height:	27 in.	68.6 cm		
Bogie Mass:	1876 lbs	850.9 kg		
Data Acquired				
Acceleration Data:	DTS			
Camera Data:	AOS-5 Perpendicular			

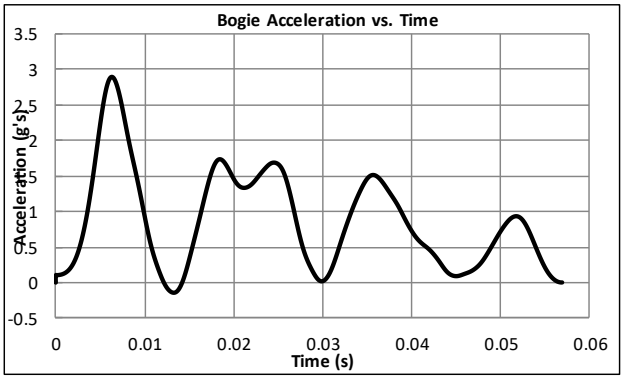

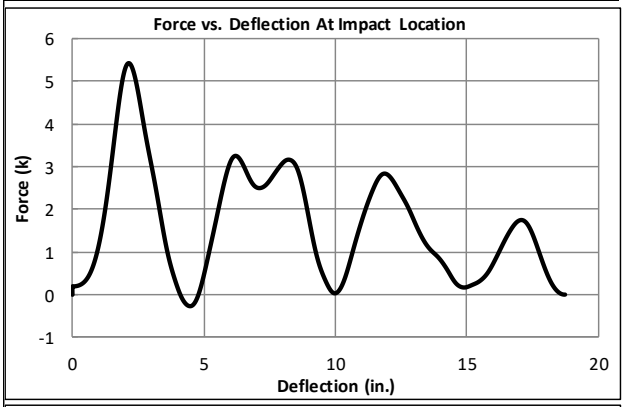

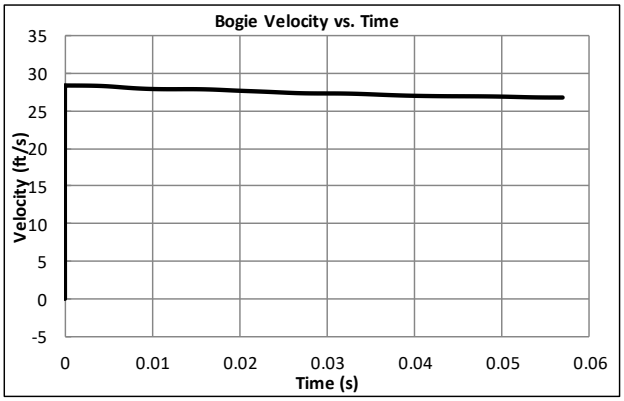

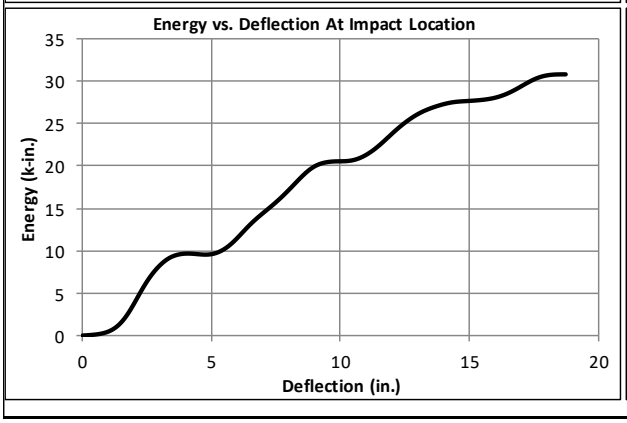

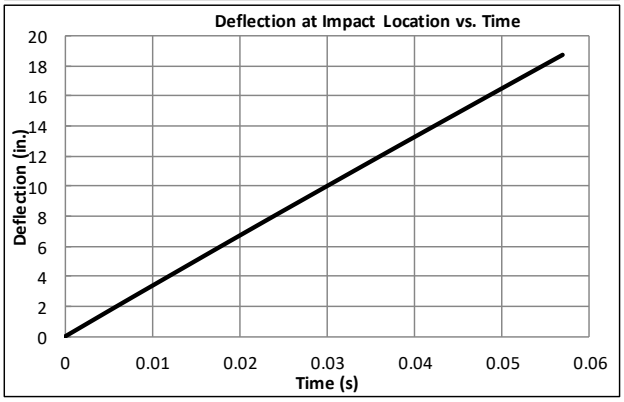

Figure C-9. Test No. 4CMBC-5 Results (DTS)

MIDWEST ROADSIDE SAFETY FACILITY

Bogie Test Summary

Test Information	Cable Median Barrier Folded C-Section Post		
Test Number:	4CMBC-5		
Test Date:	5-Nov-2012		
Failure Type:	Post bent and twisted. Data extraction stopped when contact lost with impact head		
Post Properties			
Post Type:	Folded C-Section Post - 7 gauge		
Post Size:	3"x1.625" 7 gauge C-section		
Post Length:	90 in.	228.6 cm	
Embedment Depth:	42 in.	106.7 cm	
Orientation:	Strong		
Soil Properties			
Gradation:	1192012		
Moisture Content:	3,571/3.552		
Compaction Method:	HE8		
Soil Density, γd:	NA		
Bogie Properties			
Impact Velocity:	19.35 mph (28.4 fps)	8.65 m/s	
Impact Height:	27 in.	68.6 cm	
Bogie Mass:	1876 lbs	850.9 kg	
Data Acquired			
Acceleration Data:	EDR-3		
Camera Data:	AOS-5 Perpendicular		

Test Results Summary		
Max. Deflection:	18.2	in.
Peak Force:	5.6	k
Initial Linear Stiffness:	2.9	k/in.
Total Energy:	40.1	k-in.

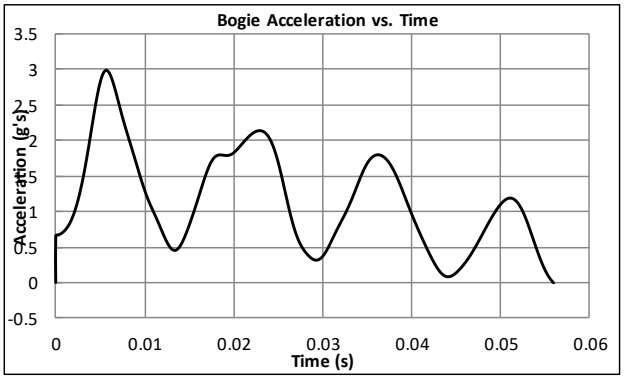

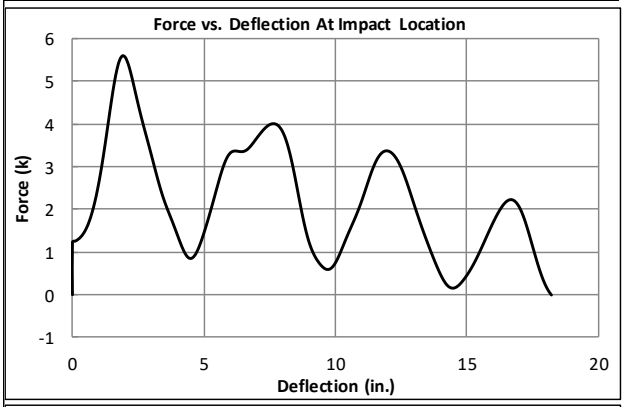

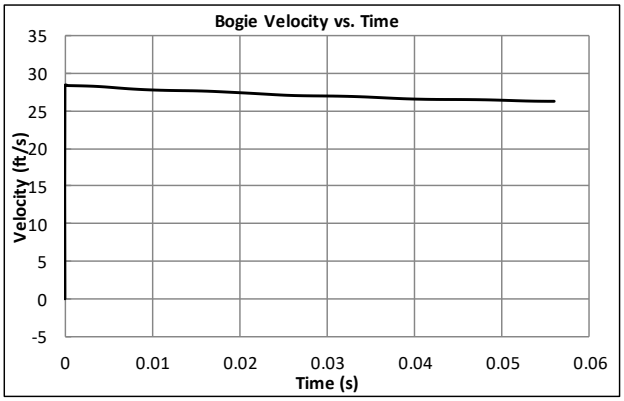

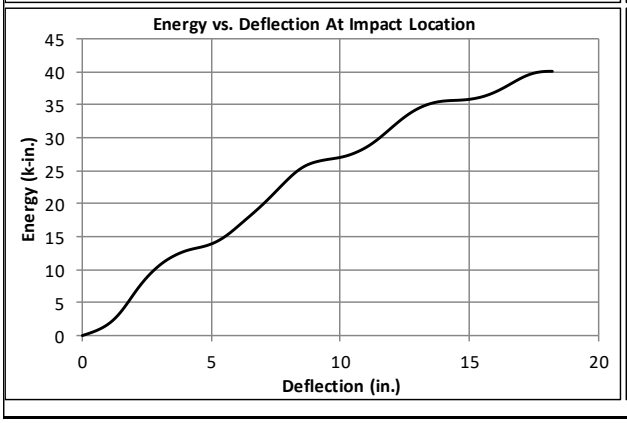

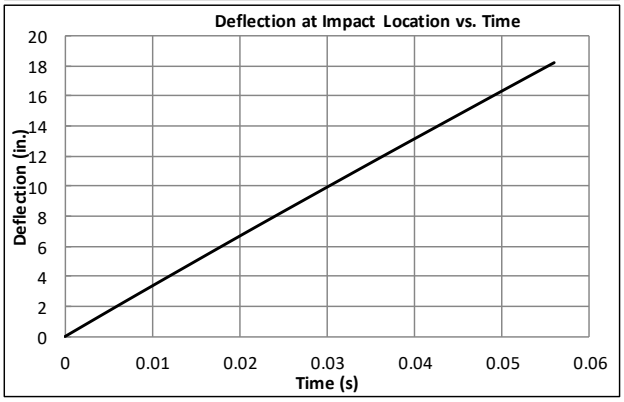

Figure C-10. Test No. 4CMBC-5 Results (EDR-3)

MIDWEST ROADSIDE SAFETY FACILITY

Bogie Test Summary

Test Information	Cable Median Barrier Folded C-Section Post		
Test Number:	4CMBC-6		
Test Date:	5-Nov-2012		
Failure Type:	Post bent and twisted. Data extraction stopped when contact lost with impact head		
Post Properties			
Post Type:	Folded C-Section Post - 7 gauge		
Post Size:	3"x1.625" 7 gauge C-section		
Post Length:	90 in.	228.6 cm	
Embedment Depth:	42 in.	106.7 cm	
Orientation:	Strong		
Soil Properties			
Gradation:	1192012		
Moisture Content:	4.031/3.808		
Compaction Method:	HE8		
Soil Density, γd:	NA		
Bogie Properties			
Impact Velocity:	20.4 mph (29.9 fps)	9.12 m/s	
Impact Height:	27 in.	68.6 cm	
Bogie Mass:	1876 lbs	850.9 kg	
Data Acquired			
Acceleration Data:	DTS		
Camera Data:	AOS-5 Perpendicular		

Test Results Summary		
Max. Deflection:	19.3	in.
Peak Force:	5.9	k
Initial Linear Stiffness:	2.7	k/in.
Total Energy:	32.1	k-in.

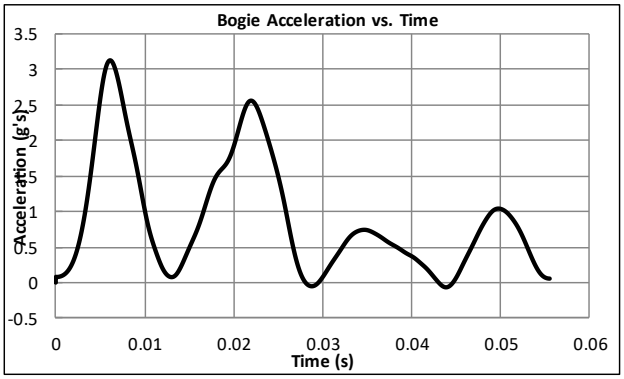

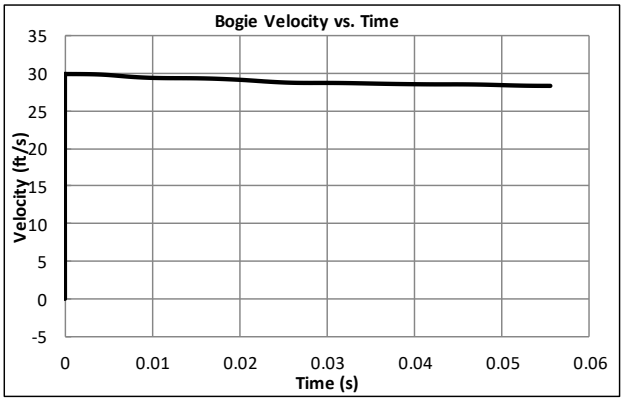

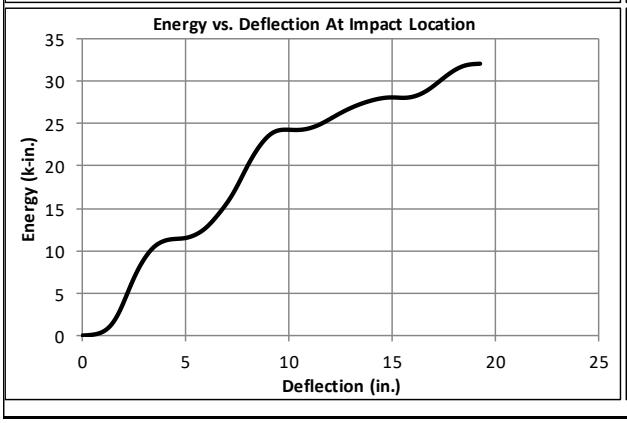

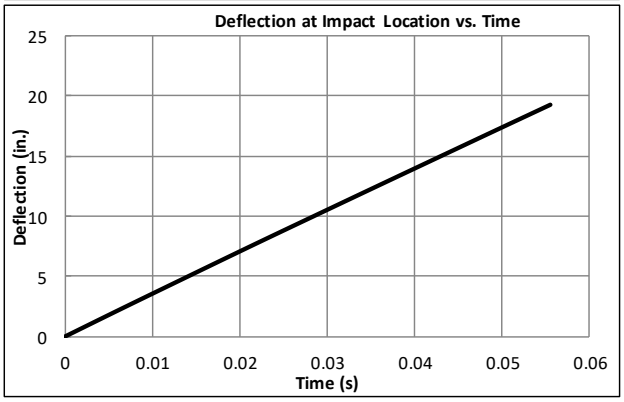

Figure C-11. Test No. 4CMBC-6 Results (DTS)

MIDWEST ROADSIDE SAFETY FACILITY

Bogie Test Summary

Test Information	Cable Median Barrier Folded C-Section Post		
Test Number:	4CMBC-6		
Test Date:	5-Nov-2012		
Failure Type:	Post bent and twisted. Data extraction stopped when contact lost with impact head		
Post Properties			
Post Type:	Folded C-Section Post - 7 gauge		
Post Size:	3"x1.625" 7 gauge C-section		
Post Length:	90 in.	228.6 cm	
Embedment Depth:	42 in.	106.7 cm	
Orientation:	Strong		
Soil Properties			
Gradation:	1192012		
Moisture Content:	4.031/3.808		
Compaction Method:	HE8		
Soil Density, γd:	NA		
Bogie Properties			
Impact Velocity:	20.4 mph (29.9 fps)	9.12 m/s	
Impact Height:	27 in.	68.6 cm	
Bogie Mass:	1876 lbs	850.9 kg	
Data Acquired			
Acceleration Data:	EDR-3		
Camera Data:	AOS-5 Perpendicular		

Test Results Summary		
Max. Deflection:	19.5	in.
Peak Force:	5.5	k
Initial Linear Stiffness:	2.7	k/in.
Total Energy:	33.1	k-in.

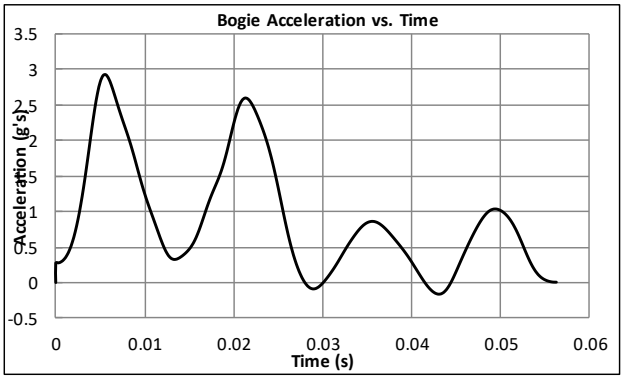

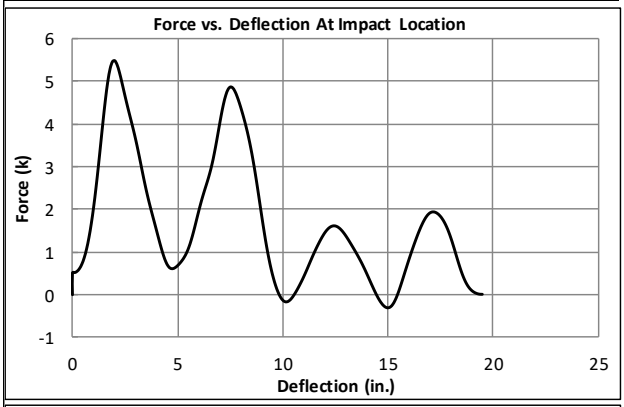

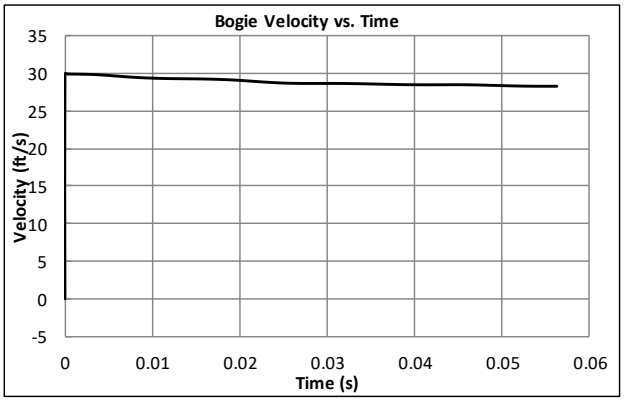

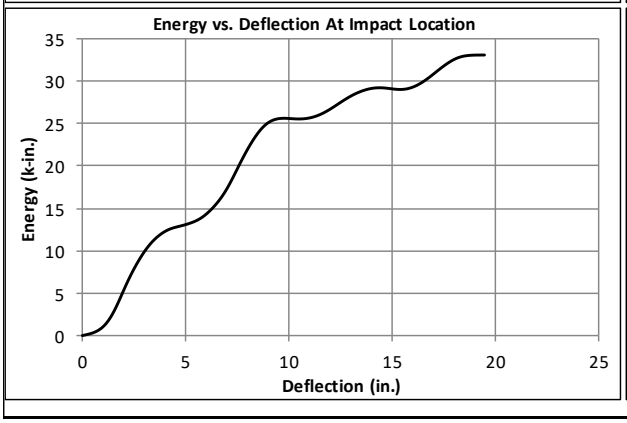

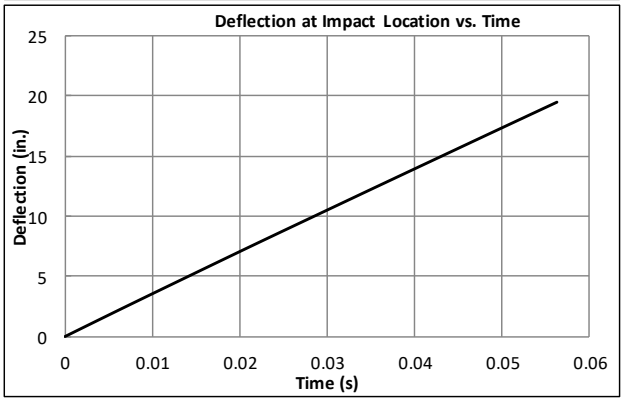

Figure C-12. Test No. 4CMBC-6 Results (EDR-3)

MIDWEST ROADSIDE SAFETY FACILITY

Bogie Test Summary

Test Information	Cable Median Barrier Folded C-Section Post		**Test Results Summary**	
Test Number:	4CMBC-7		Max. Deflection:	24.0 in.
Test Date:	7-Nov-2012		Peak Force:	4.7 k
Failure Type:	Post bent. Data extraction stopped when contact lost with impact head		Initial Linear Stiffness:	2.5 k/in.
			Total Energy:	28.4 k-in.
Post Properties				
Post Type:	Folded C-Section Post - 7 gauge			
Post Size:	3"x1.625" 7 gauge C-section			
Post Length:	90 in.	228.6 cm		
Embedment Depth:	42 in.	106.7 cm		
Orientation:	Weak			
Soil Properties				
Gradation:	1192012			
Moisture Content:	3.197/3.506			
Compaction Method:	HE8			
Soil Density, γd:	NA			
Bogie Properties				
Impact Velocity:	21.92 mph (32.2 fps)	9.8 m/s		
Impact Height:	27 in.	68.6 cm		
Bogie Mass:	1876 lbs	850.9 kg		
Data Acquired				
Acceleration Data:	DTS			
Camera Data:	AOS-5 Perpendicular			

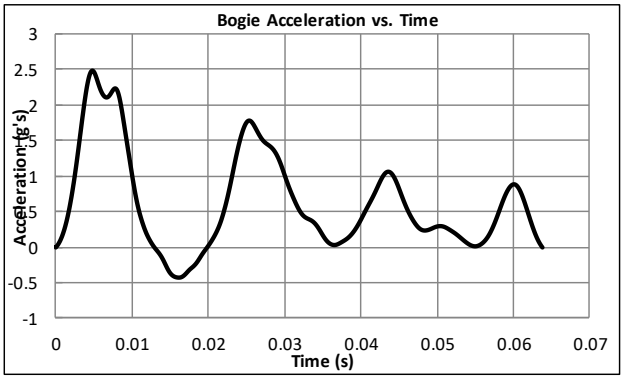

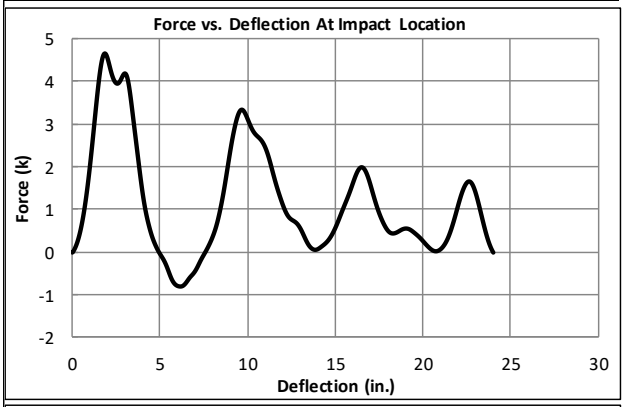

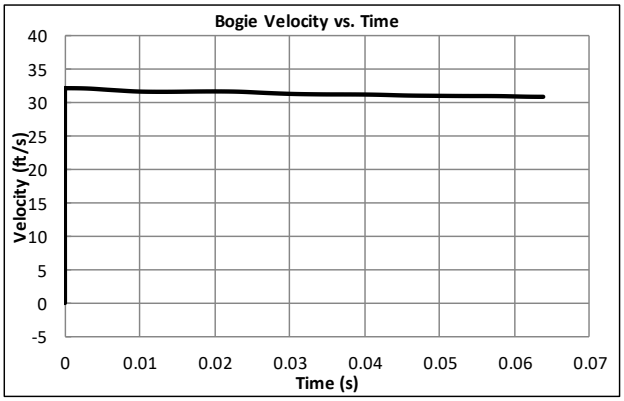

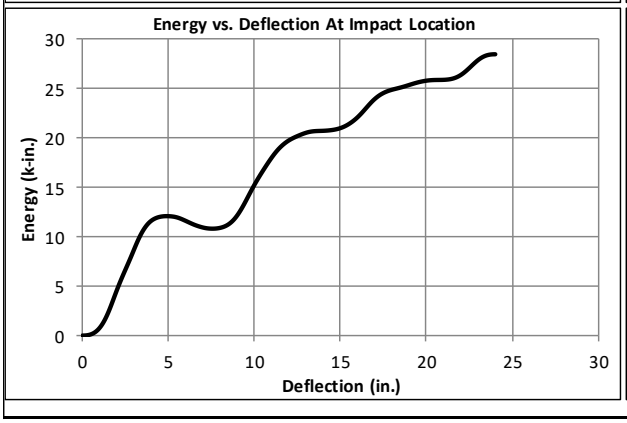

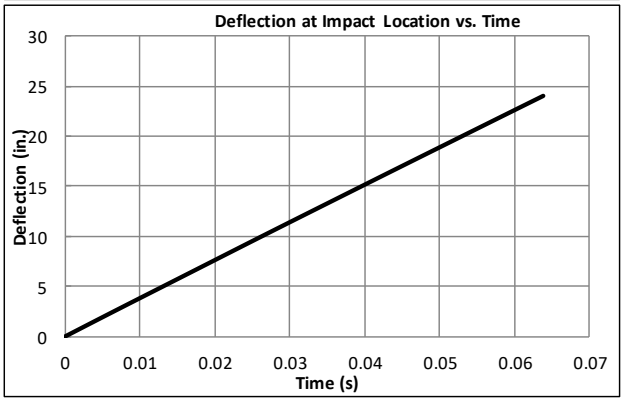

Figure C-13. Test No. 4CMBC-7 Results (DTS)

MIDWEST ROADSIDE SAFETY FACILITY

Bogie Test Summary

Test Information	Cable Median Barrier Folded C-Section Post		
Test Number:	4CMBC-7		
Test Date:	6-Nov-2012		
Failure Type:	Post bent. Data extraction stopped when contact lost with impact head		
Post Properties			
Post Type:	Folded C-Section Post - 7 gauge		
Post Size:	3"x1.625" 7 gauge C-section		
Post Length:	90 in.	228.6 cm	
Embedment Depth:	42 in.	106.7 cm	
Orientation:	Weak		
Soil Properties			
Gradation:	1192012		
Moisture Content:	3.197/3.506		
Compaction Method:	HE8		
Soil Density, γd:	NA		
Bogie Properties			
Impact Velocity:	21.92 mph (32.2 fps)	9.8 m/s	
Impact Height:	27 in.	68.6 cm	
Bogie Mass:	1876 lbs	850.9 kg	
Data Acquired			
Acceleration Data:	EDR-3		
Camera Data:	AOS-5 Perpendicular		

Test Results Summary		
Max. Deflection:	23.9	in.
Peak Force:	4.8	k
Initial Linear Stiffness:	2.4	k/in.
Total Energy:	22.7	k-in.

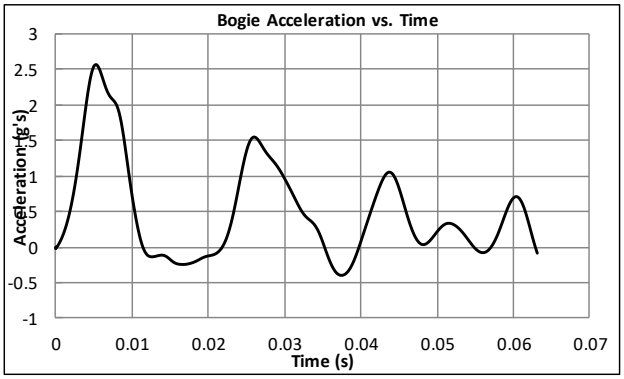

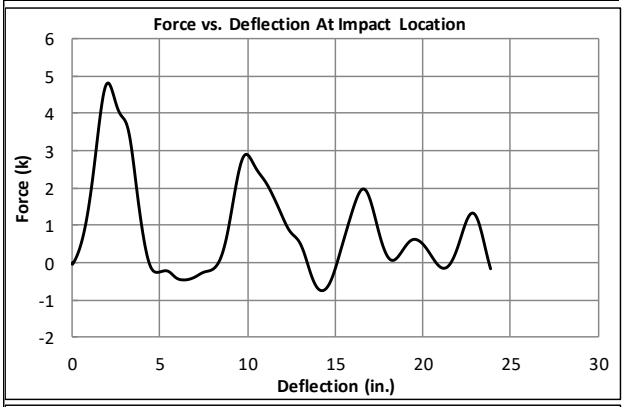

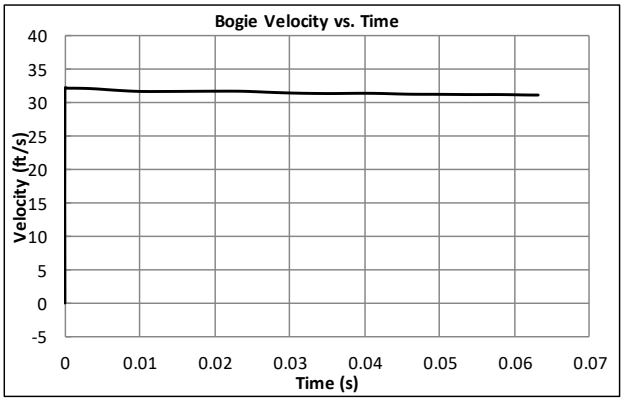

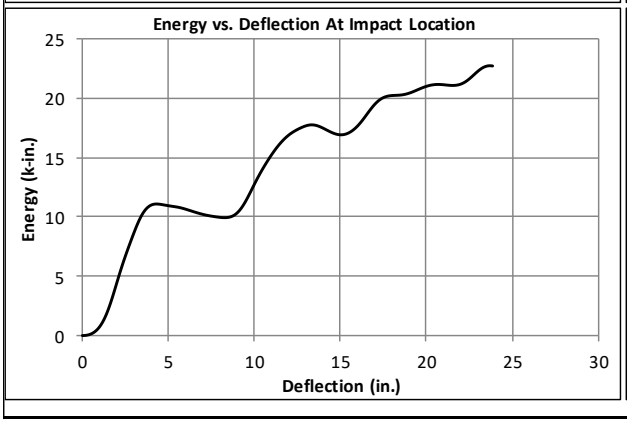

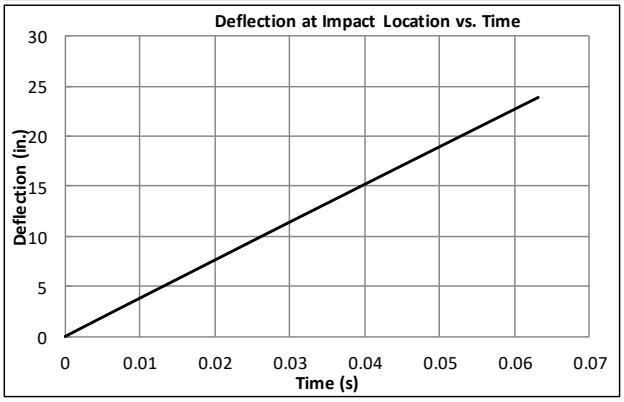

Figure C-14. Test No. 4CMBC-7 Results (EDR-3)

MIDWEST ROADSIDE SAFETY FACILITY

Bogie Test Summary

Test Information	Cable Median Barrier Folded C-Section Post		
Test Number:	4CMBC-8		
Test Date:	7-Nov-2012		
Failure Type:	Post bent. Data extraction stopped when contact lost with impact head		
Post Properties			
Post Type:	Folded C-Section Post - 7 gauge		
Post Size:	3"x1.625" 7 gauge C-section		
Post Length:	90 in.	228.6 cm	
Embedment Depth:	42 in.	106.7 cm	
Orientation:	Weak		
Soil Properties			
Gradation:	1192012		
Moisture Content:	3.5/3.199 @ 15/30" respectively		
Compaction Method:	HE8		
Soil Density, γd:	NA		
Bogie Properties			
Impact Velocity:	21.03 mph (30.8 fps)	9.4 m/s	
Impact Height:	27 in.	68.6 cm	
Bogie Mass:	1876 lbs	850.9 kg	
Data Acquired			
Acceleration Data:	DTS		
Camera Data:	AOS-5 Perpendicular		

Test Results Summary		
Max. Deflection:	26.7	in.
Peak Force:	4.2	k
Initial Linear Stiffness:	2.5	k/in.
Total Energy:	25.9	k-in.

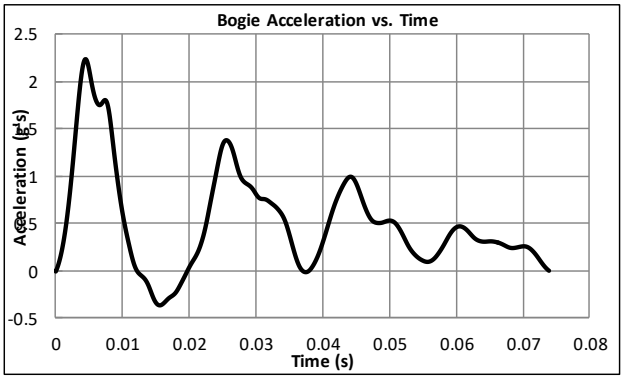

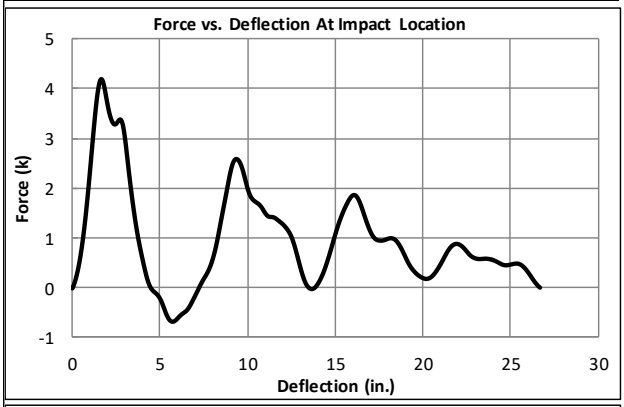

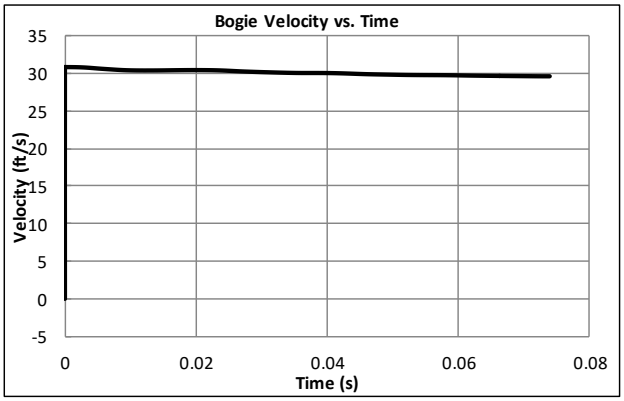

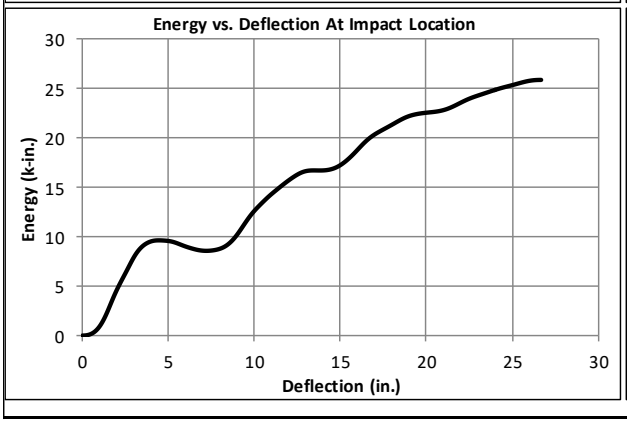

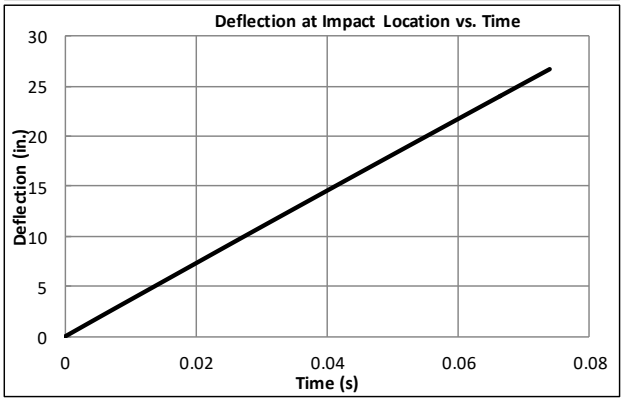

Figure C-15. Test No. 4CMBC-8 Results (DTS)

MIDWEST ROADSIDE SAFETY FACILITY

Bogie Test Summary

Test Information	Cable Median Barrier Folded C-Section Post		**Test Results Summary**	
Test Number:	4CMBC-8		Max. Deflection:	22.9 in.
Test Date:	6-Nov-2012		Peak Force:	4.3 k
Failure Type:	Post bent. Data extraction stopped when contact lost with impact head		Initial Linear Stiffness:	2.8 k/in.
			Total Energy:	12.5 k-in.
Post Properties				
Post Type:	Folded C-Section Post - 7 gauge			
Post Size:	3"x1.625" 7 gauge C-section			
Post Length:	90 in.	228.6 cm		
Embedment Depth:	42 in.	106.7 cm		
Orientation:	Weak			
Soil Properties				
Gradation:	1192012			
Moisture Content:	3.5/3.199 @ 15/30" respectively			
Compaction Method:	HE8			
Soil Density, γd:	NA			
Bogie Properties				
Impact Velocity:	21.03 mph (30.8 fps)	9.4 m/s		
Impact Height:	27 in.	68.6 cm		
Bogie Mass:	1876 lbs	850.9 kg		
Data Acquired				
Acceleration Data:	EDR-3			
Camera Data:	AOS-5 Perpendicular			

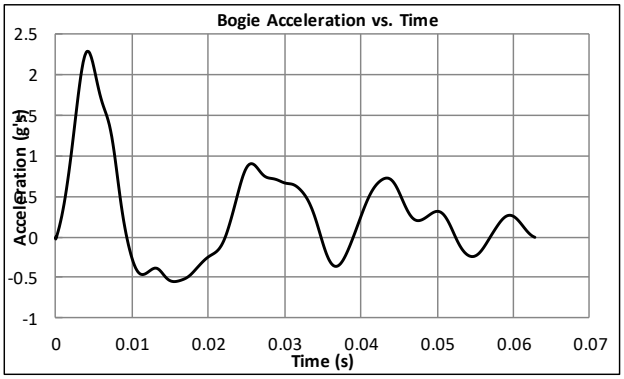

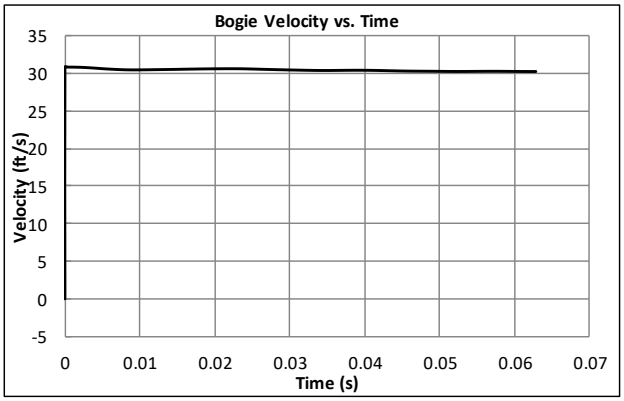

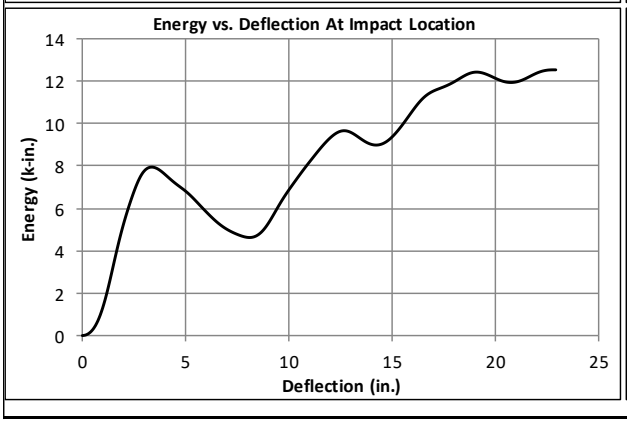

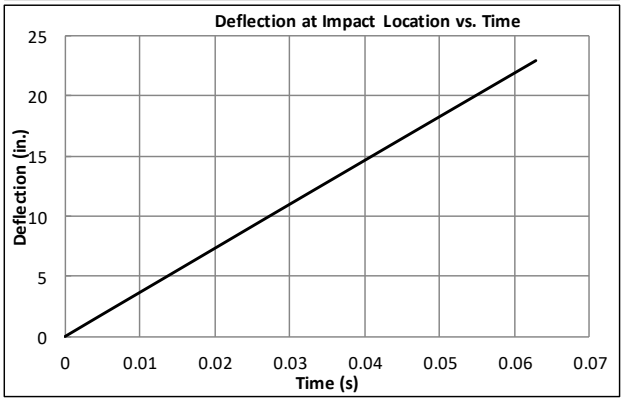

Figure C-16. Test No. 4CMBC-8 Results (EDR-3)

MIDWEST ROADSIDE SAFETY FACILITY

Bogie Test Summary

Test Information	Cable Median Barrier Folded C-Section Post		
Test Number:	4CMBC-9		
Test Date:	7-Nov-2012		
Failure Type:	Post bent and twisted. Data extraction stopped when contact lost with impact head		
Post Properties			
Post Type:	Folded C-Section Post - 10 gauge		
Post Size:	3"x1.625" 10 gauge C-section		
Post Length:	90 in.	228.6 cm	
Embedment Depth:	42 in.	106.7 cm	
Orientation:	Strong		
Soil Properties			
Gradation:	Rigid Sleeve		
Moisture Content:	NA		
Compaction Method:	NA		
Soil Density, γd:	NA		
Bogie Properties			
Impact Velocity:	21.12 mph (31.0 fps)	9.44 m/s	
Impact Height:	27 in.	68.6 cm	
Bogie Mass:	1876 lbs	850.9 kg	
Data Acquired			
Acceleration Data:	DTS		
Camera Data:	AOS-5 Perpendicular		

Test Results Summary		
Max. Deflection:	18.2	in.
Peak Force:	4.5	k
Initial Linear Stiffness:	2.0	k/in.
Total Energy:	21.9	k-in.

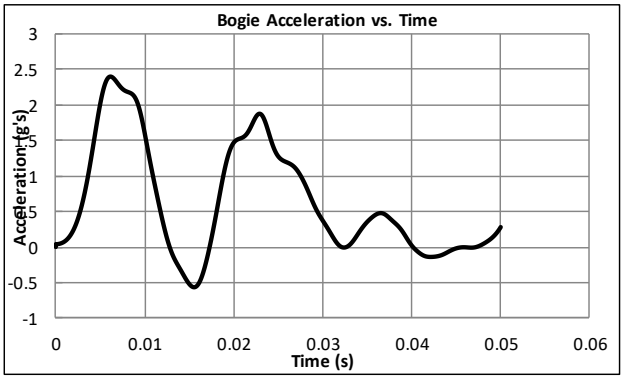

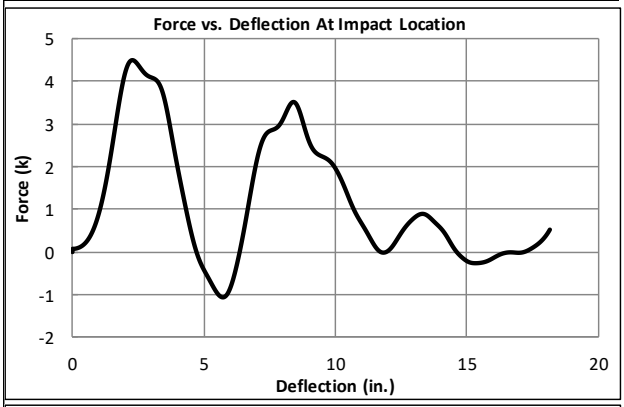

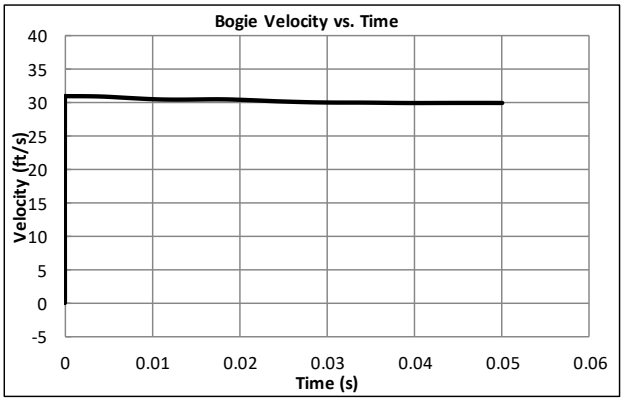

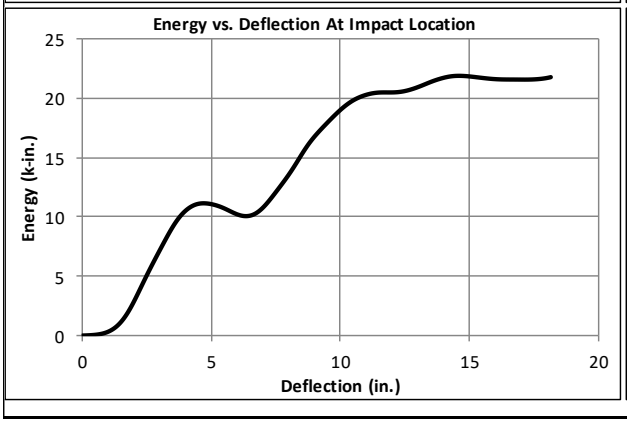

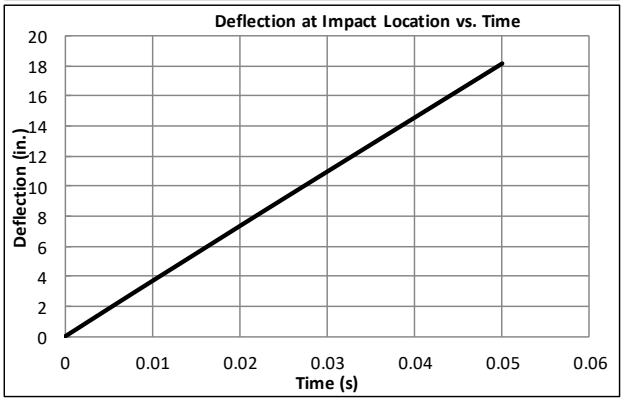

Figure C-17. Test No. 4CMBC-9 Results (DTS)

MIDWEST ROADSIDE SAFETY FACILITY

Bogie Test Summary

Test Information	Cable Median Barrier Folded C-Section Post		
Test Number:	4CMBC-9		
Test Date:	7-Nov-2012		
Failure Type:	Post bent and twisted. Data extraction stopped when contact lost with impact head		
Post Properties			
Post Type:	Folded C-Section Post - 10 gauge		
Post Size:	3"x1.625" 10 gauge C-section		
Post Length:	90 in.	228.6 cm	
Embedment Depth:	42 in.	106.7 cm	
Orientation:	Strong		
Soil Properties			
Gradation:	Rigid Sleeve		
Moisture Content:	NA		
Compaction Method:	NA		
Soil Density, γd:	NA		
Bogie Properties			
Impact Velocity:	21.12 mph (31.0 fps)	9.44 m/s	
Impact Height:	27 in.	68.6 cm	
Bogie Mass:	1876 lbs	850.9 kg	
Data Acquired			
Acceleration Data:	EDR-3		
Camera Data:	AOS-5 Perpendicular		

Test Results Summary		
Max. Deflection:	18.1	in.
Peak Force:	4.5	k
Initial Linear Stiffness:	2.1	k/in.
Total Energy:	28.0	k-in.

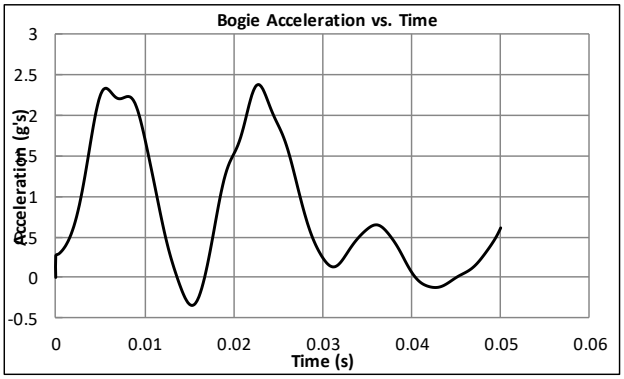

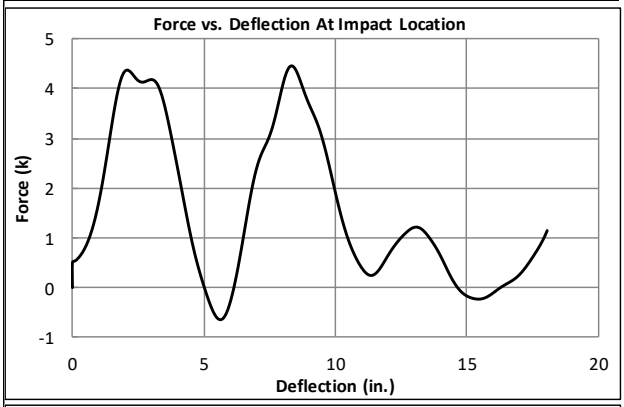

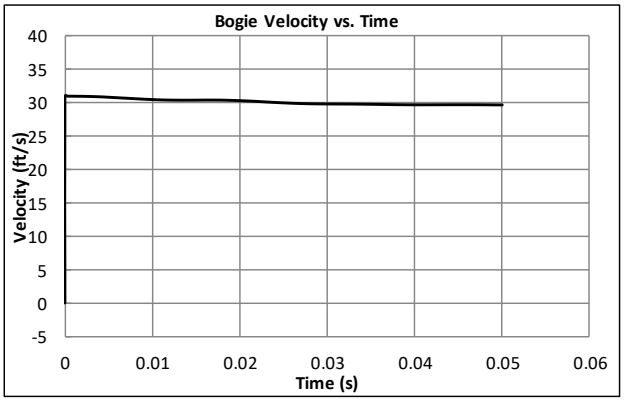

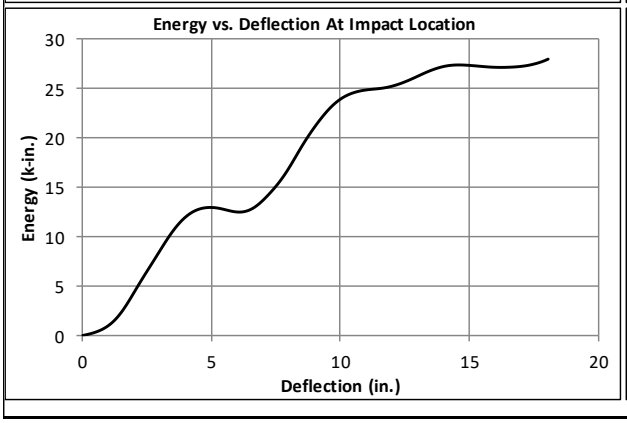

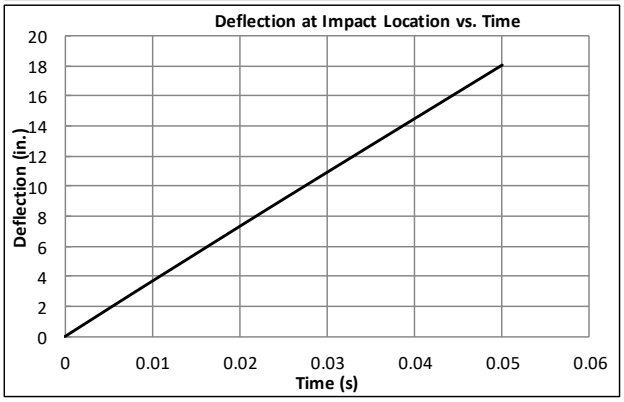

Figure C-18. Test No. 4CMBC-9 Results (EDR-3)

MIDWEST ROADSIDE SAFETY FACILITY

Bogie Test Summary

Test Information	Cable Median Barrier Folded C-Section Post		
Test Number:	4CMBC-10		
Test Date:	7-Nov-2012		
Failure Type:	Post bent and twisted. Data extraction stopped when contact lost with impact head		
Post Properties			
Post Type:	Folded C-Section Post - 10 gauge		
Post Size:	3"x1.625" 10 gauge C-section		
Post Length:	90 in.	228.6 cm	
Embedment Depth:	42 in.	106.7 cm	
Orientation:	Strong		
Soil Properties			
Gradation:	Rigid Sleeve		
Moisture Content:	NA		
Compaction Method:	NA		
Soil Density, γd:	NA		
Bogie Properties			
Impact Velocity:	19.98 mph (29.3 fps)	8.93 m/s	
Impact Height:	27 in.	68.6 cm	
Bogie Mass:	1876 lbs	850.9 kg	
Data Acquired			
Acceleration Data:	DTS		
Camera Data:	AOS-5 Perpendicular		

Test Results Summary		
Max. Deflection:	18.5	in.
Peak Force:	4.3	k
Initial Linear Stiffness:	2.4	k/in.
Total Energy:	21.3	k-in.

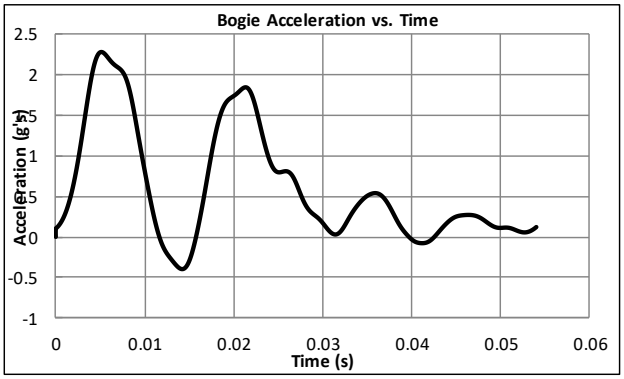

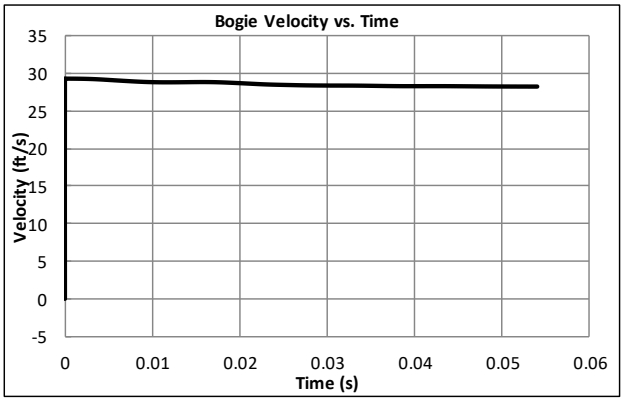

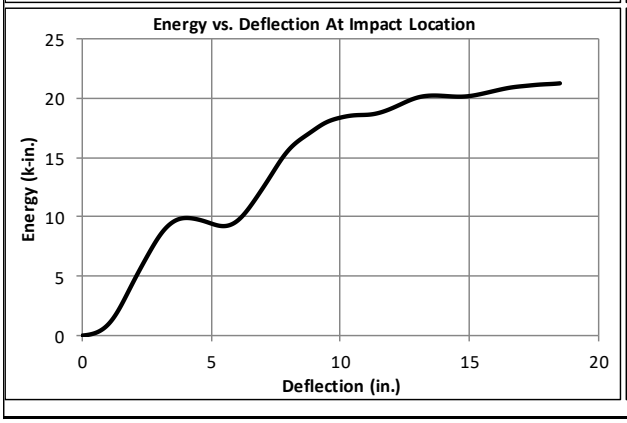

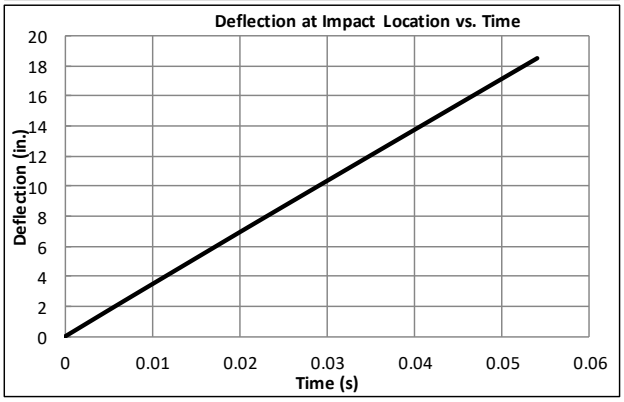

Figure C-19. Test No. 4CMBC-10 Results (DTS)

MIDWEST ROADSIDE SAFETY FACILITY

Bogie Test Summary

Test Information	Cable Median Barrier Folded C-Section Post		**Test Results Summary**	
Test Number:	4CMBC-10		Max. Deflection:	18.5 in.
Test Date:	7-Nov-2012		Peak Force:	4.0 k
Failure Type:	Post bent and twisted. Data extraction stopped when contact lost with impact head		Initial Linear Stiffness:	2.4 k/in.
			Total Energy:	19.6 k-in.
Post Properties				
Post Type:	Folded C-Section Post - 10 gauge			
Post Size:	3"x1.625" 10 gauge C-section			
Post Length:	90 in.	228.6 cm		
Embedment Depth:	42 in.	106.7 cm		
Orientation:	Strong			
Soil Properties				
Gradation:	Rigid Sleeve			
Moisture Content:	NA			
Compaction Method:	NA			
Soil Density, γd:	NA			
Bogie Properties				
Impact Velocity:	19.98 mph (29.3 fps)	8.93 m/s		
Impact Height:	27 in.	68.6 cm		
Bogie Mass:	1876 lbs	850.9 kg		
Data Acquired				
Acceleration Data:	EDR-3			
Camera Data:	AOS-5 Perpendicular			

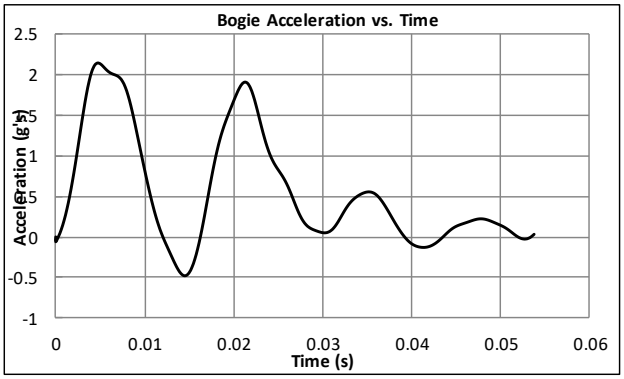

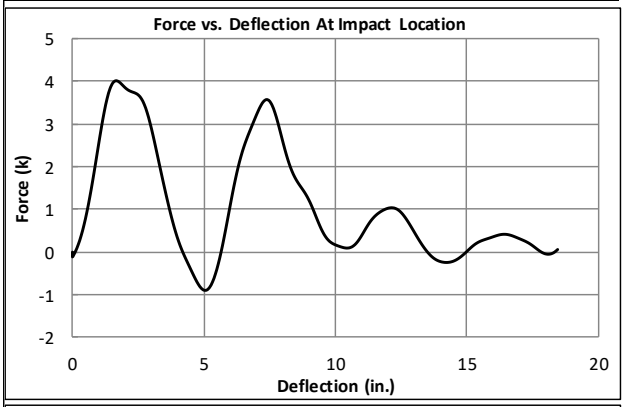

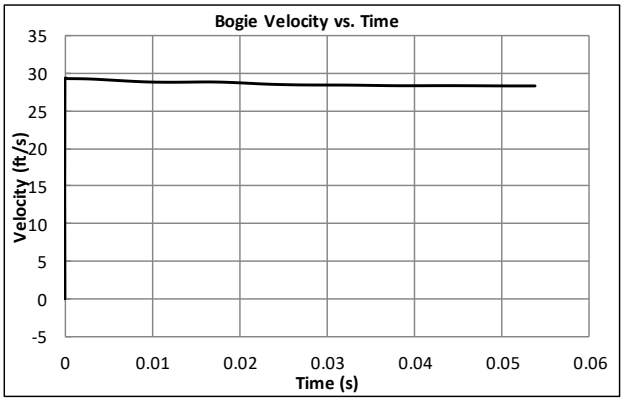

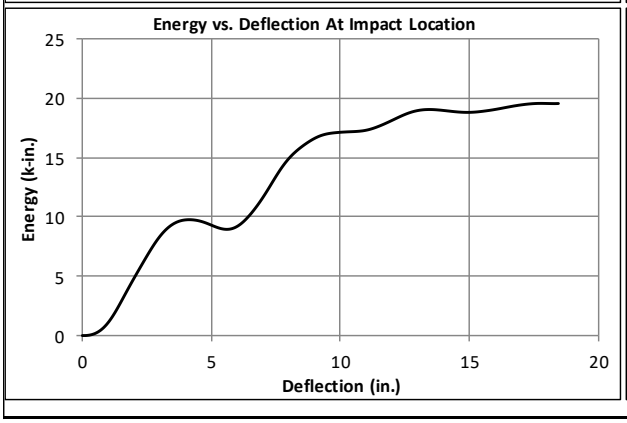

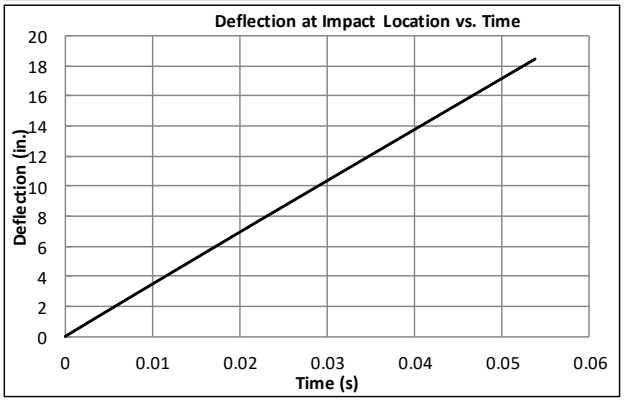

Figure C-20. Test No. 4CMBC-10 Results (EDR-3)

MIDWEST ROADSIDE SAFETY FACILITY

Bogie Test Summary

Test Information	Cable Median Barrier Folded C-Section Post		
Test Number:	4CMBC-11		
Test Date:	8-Nov-2012		
Failure Type:	Post bent and twisted. Data extraction stopped when contact lost with impact head		
Post Properties			
Post Type:	Folded C-Section Post - 7 gauge		
Post Size:	3"x1.625" 7 gauge C-section		
Post Length:	90 in.	228.6 cm	
Embedment Depth:	42 in.	106.7 cm	
Orientation:	Strong		
Soil Properties			
Gradation:	Rigid Sleeve		
Moisture Content:	NA		
Compaction Method:	NA		
Soil Density, γd:	NA		
Bogie Properties			
Impact Velocity:	20.45 mph (30.0 fps)	9.14 m/s	
Impact Height:	27 in.	68.6 cm	
Bogie Mass:	1876 lbs	850.9 kg	
Data Acquired			
Acceleration Data:	DTS		
Camera Data:	AOS-5 Perpendicular		

Test Results Summary		
Max. Deflection:	19.5	in.
Peak Force:	5.5	k
Initial Linear Stiffness:	2.9	k/in.
Total Energy:	32.4	k-in.

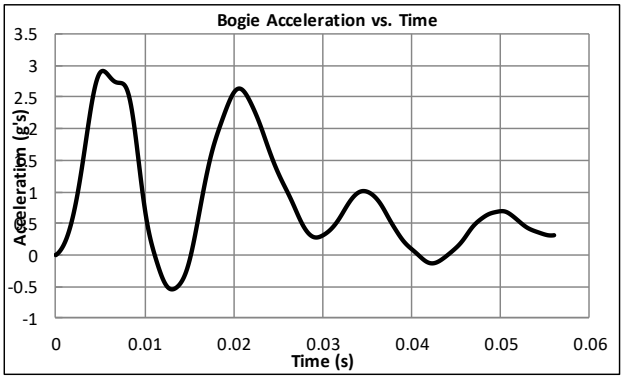

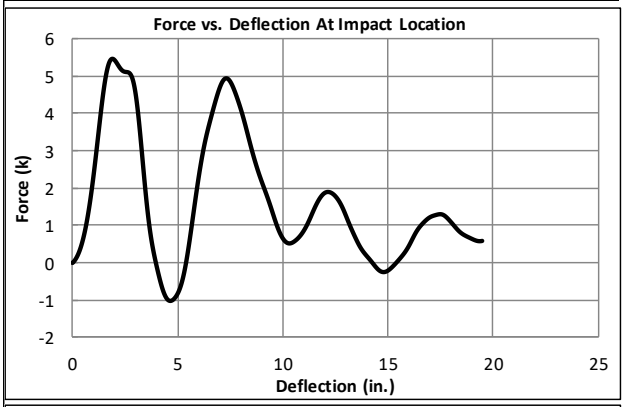

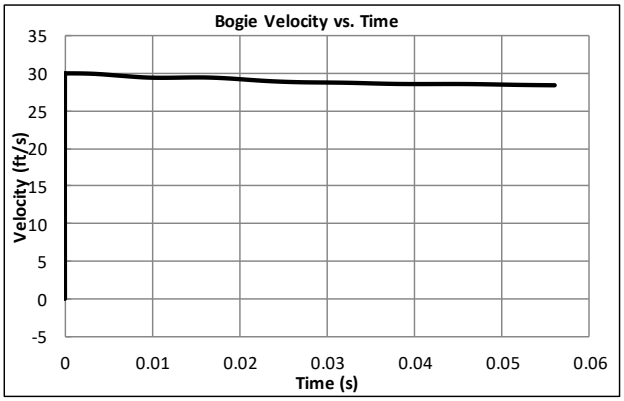

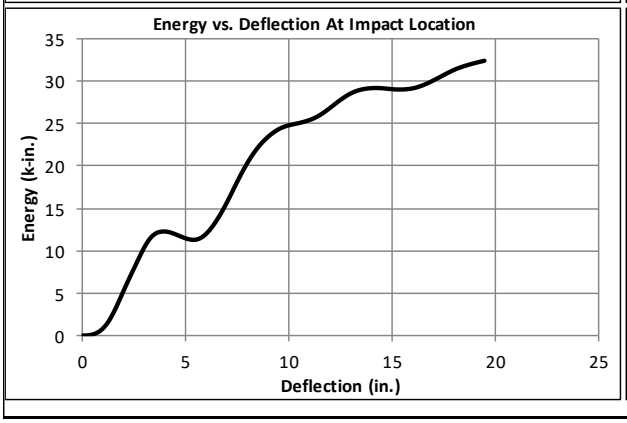

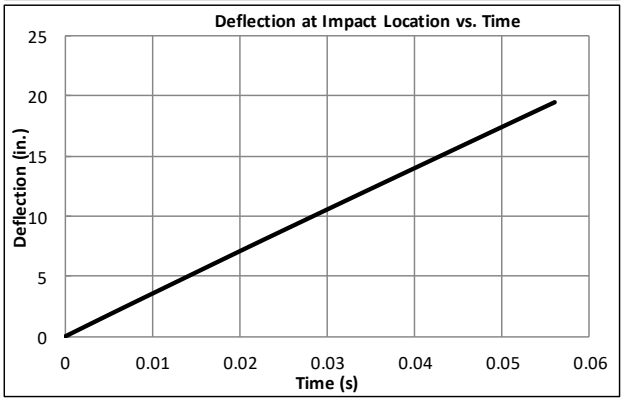

Figure C-21. Test No. 4CMBC-11 Results (DTS)

MIDWEST ROADSIDE SAFETY FACILITY

Bogie Test Summary

Test Information	Cable Median Barrier Folded C-Section Post		
Test Number:	4CMBC-11		
Test Date:	8-Nov-2012		
Failure Type:	Post bent and twisted. Data extraction stopped when contact lost with impact head		
Post Properties			
Post Type:	Folded C-Section Post - 7 gauge		
Post Size:	3"x1.625" 7 gauge C-section		
Post Length:	90 in.	228.6 cm	
Embedment Depth:	42 in.	106.7 cm	
Orientation:	Strong		
Soil Properties			
Gradation:	Rigid Sleeve		
Moisture Content:	NA		
Compaction Method:	NA		
Soil Density, γd:	NA		
Bogie Properties			
Impact Velocity:	20.45 mph (30.0 fps)	9.14 m/s	
Impact Height:	27 in.	68.6 cm	
Bogie Mass:	1876 lbs	850.9 kg	
Data Acquired			
Acceleration Data:	EDR-3		
Camera Data:	AOS-5 Perpendicular		

Test Results Summary		
Max. Deflection:	19.3	in.
Peak Force:	5.7	k
Initial Linear Stiffness:	3.4	k/in.
Total Energy:	37.6	k-in.

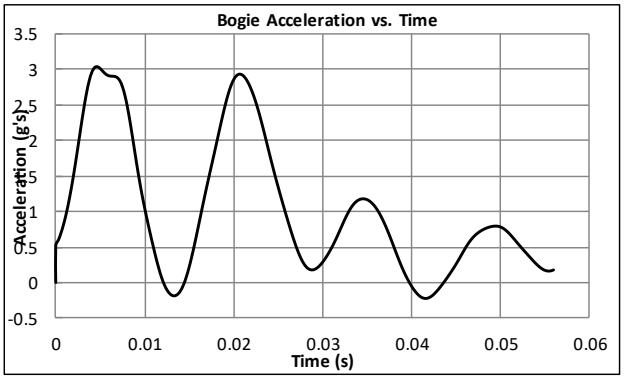

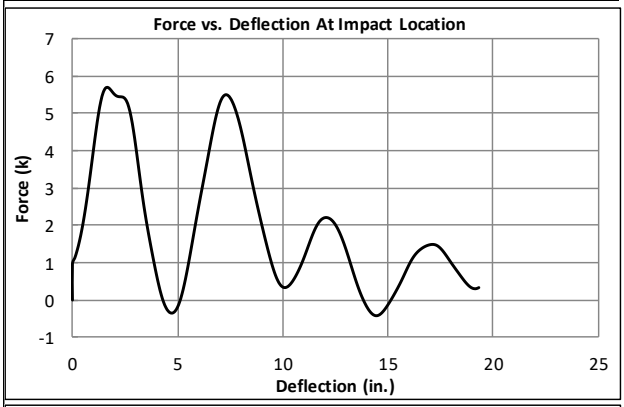

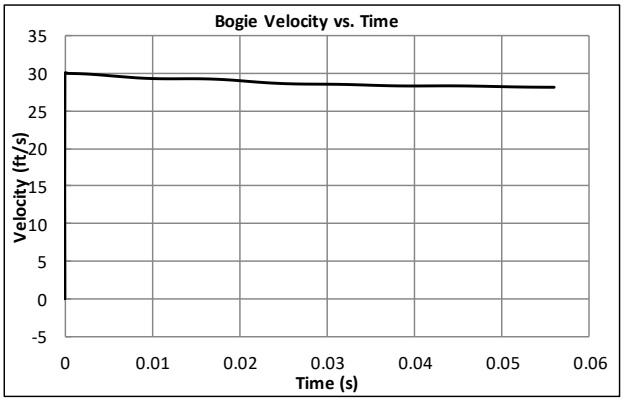

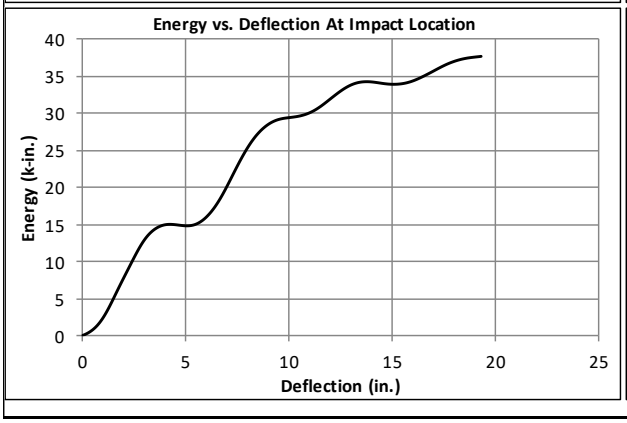

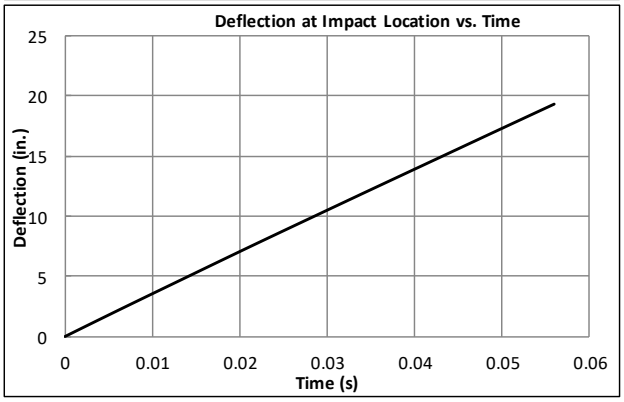

Figure C-22. Test No. 4CMBC-11 Results (EDR-3)

MIDWEST ROADSIDE SAFETY FACILITY

Bogie Test Summary

Test Information	Cable Median Barrier Folded C-Section Post		
Test Number:	4CMBC-12		
Test Date:	8-Nov-2012		
Failure Type:	Post bent and twisted. Data extraction stopped when contact lost with impact head		
Post Properties			
Post Type:	Folded C-Section Post - 7 gauge		
Post Size:	3"x1.625" 7 gauge C-section		
Post Length:	90 in.	228.6 cm	
Embedment Depth:	42 in.	106.7 cm	
Orientation:	Strong		
Soil Properties			
Gradation:	Rigid Sleeve		
Moisture Content:	NA		
Compaction Method:	NA		
Soil Density, γd:	NA		
Bogie Properties			
Impact Velocity:	20.92 mph (30.7 fps)	9.35 m/s	
Impact Height:	27 in.	68.6 cm	
Bogie Mass:	1876 lbs	850.9 kg	
Data Acquired			
Acceleration Data:	DTS		
Camera Data:	AOS-5 Perpendicular		

Test Results Summary		
Max. Deflection:	20.2	in.
Peak Force:	6.2	k
Initial Linear Stiffness:	2.7	k/in.
Total Energy:	35.6	k-in.

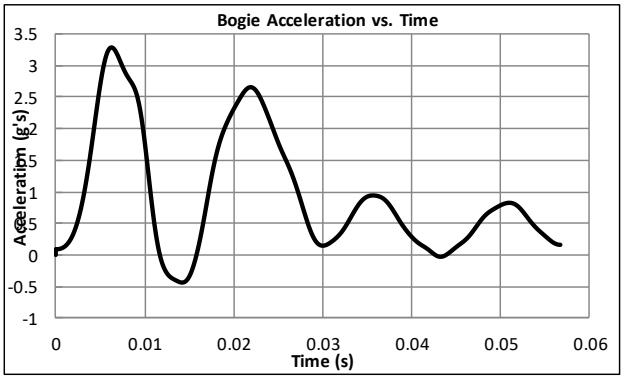

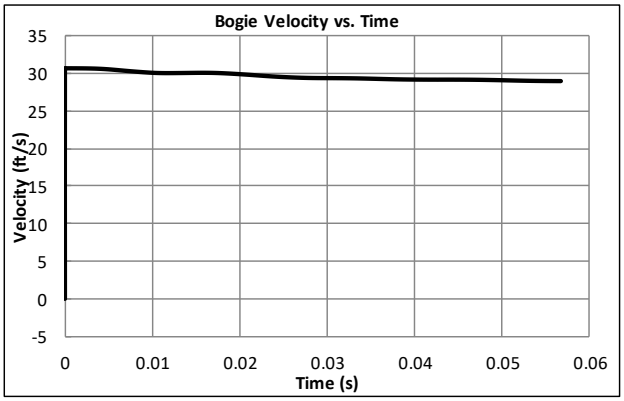

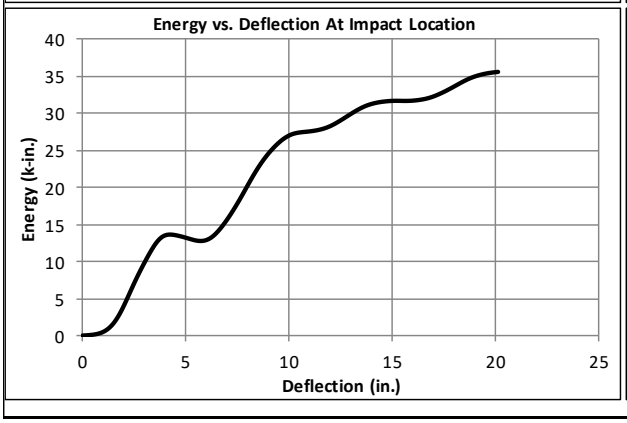

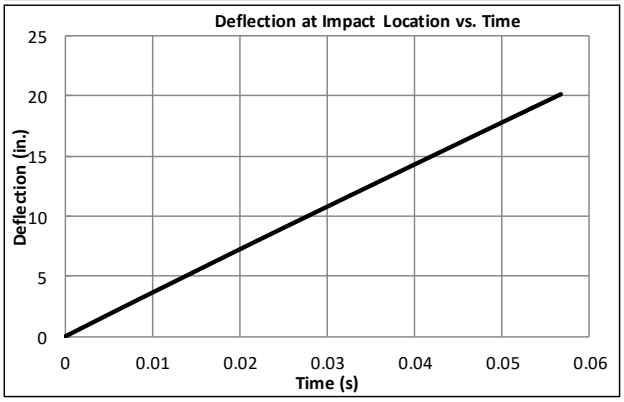

Figure C-23. Test No. 4CMBC-12 Results (DTS)

MIDWEST ROADSIDE SAFETY FACILITY

Bogie Test Summary

Test Information	Cable Median Barrier Folded C-Section Post		**Test Results Summary**	
Test Number:	4CMBC-12		Max. Deflection:	20.0 in.
Test Date:	8-Nov-2012		Peak Force:	5.2 k
Failure Type:	Post bent and twisted. Data extraction stopped when contact lost with impact head		Initial Linear Stiffness:	2.5 k/in.
			Total Energy:	35.0 k-in.
Post Properties				
Post Type:	Folded C-Section Post - 7 gauge			
Post Size:	3"x1.625" 7 gauge C-section			
Post Length:	90 in.	228.6 cm		
Embedment Depth:	42 in.	106.7 cm		
Orientation:	Strong			
Soil Properties				
Gradation:	Rigid Sleeve			
Moisture Content:	NA			
Compaction Method:	NA			
Soil Density, γd:	NA			
Bogie Properties				
Impact Velocity:	20.92 mph (30.7 fps)	9.35 m/s		
Impact Height:	27 in.	68.6 cm		
Bogie Mass:	1876 lbs	850.9 kg		
Data Acquired				
Acceleration Data:	EDR-3			
Camera Data:	AOS-5 Perpendicular			

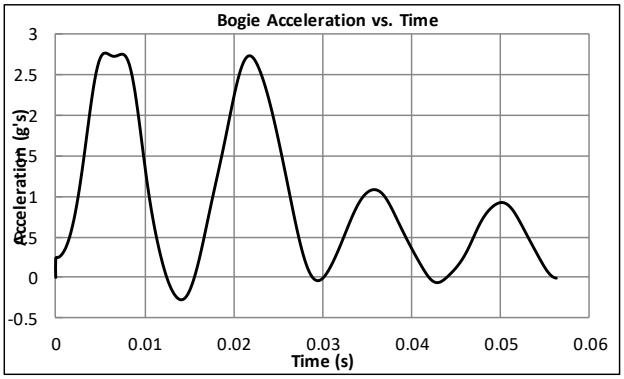

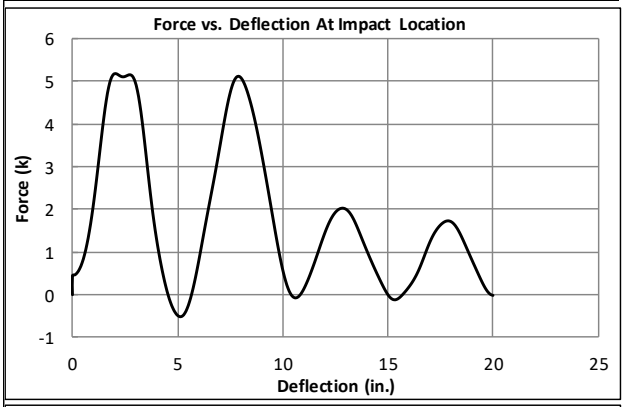

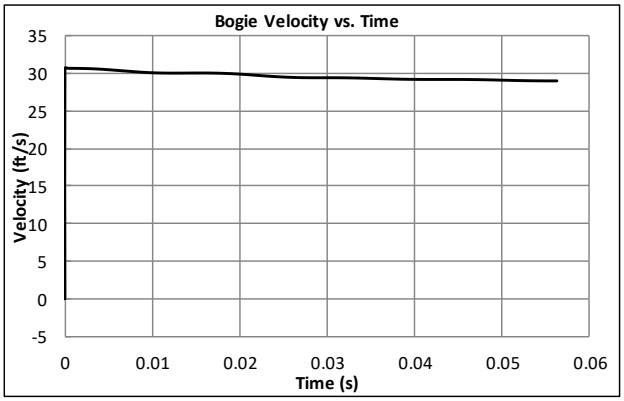

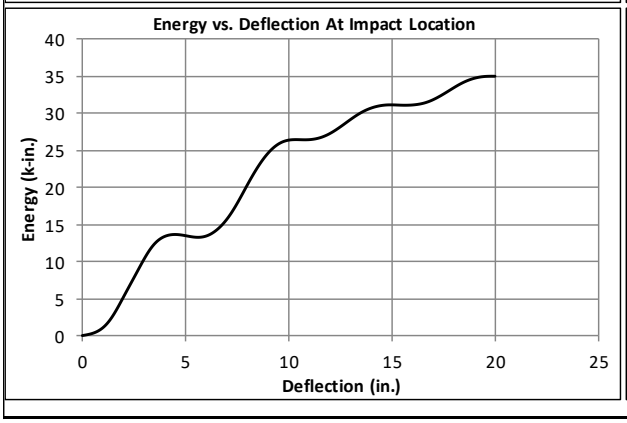

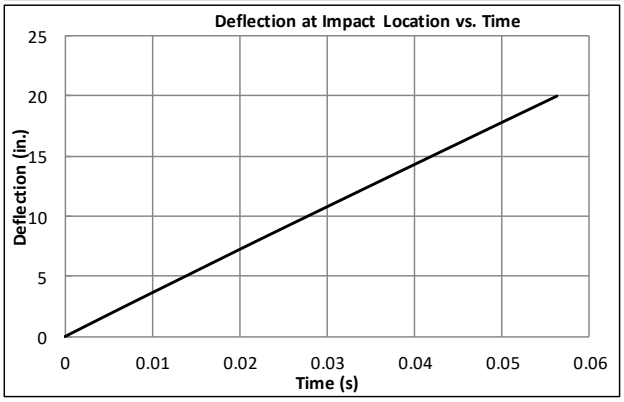

Figure C-24. Test No. 4CMBC-12 Results (EDR-3)

MIDWEST ROADSIDE SAFETY FACILITY

Bogie Test Summary

Test Information	Cable Median Barrier Folded C-Section Post		**Test Results Summary**	
Test Number:	4CMBC-13		Max. Deflection:	20.4 in.
Test Date:	8-Nov-2012		Peak Force:	3.7 k
Failure Type:	Post bent. Data extraction stopped when contact lost with impact head		Initial Linear Stiffness:	1.8 k/in.
			Total Energy:	10.0 k-in.
Post Properties				
Post Type:	Folded C-Section Post - 10 gauge			
Post Size:	3"x1.625" 10 gauge C-section			
Post Length:	90 in.	228.6 cm		
Embedment Depth:	42 in.	106.7 cm		
Orientation:	Weak			
Soil Properties				
Gradation:	Rigid Sleeve			
Moisture Content:	NA			
Compaction Method:	NA			
Soil Density, γd:	NA			
Bogie Properties				
Impact Velocity:	20.31 mph (29.8 fps)	9.08 m/s		
Impact Height:	27 in.	68.6 cm		
Bogie Mass:	1876 lbs	850.9 kg		
Data Acquired				
Acceleration Data:	DTS			
Camera Data:	AOS-5 Perpendicular			

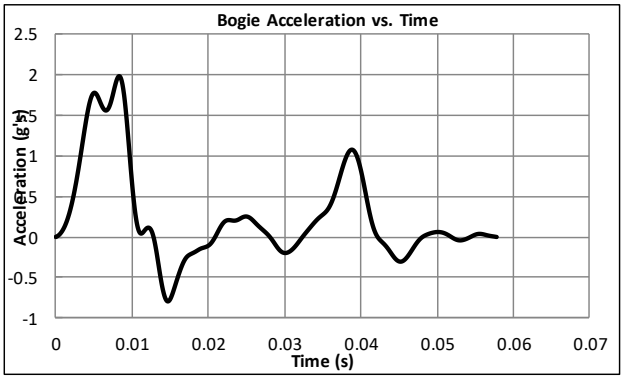

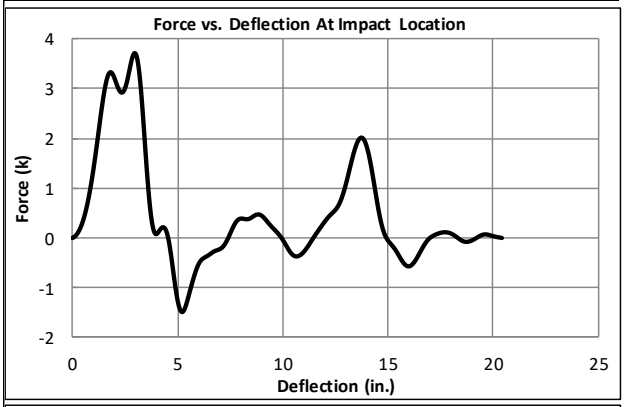

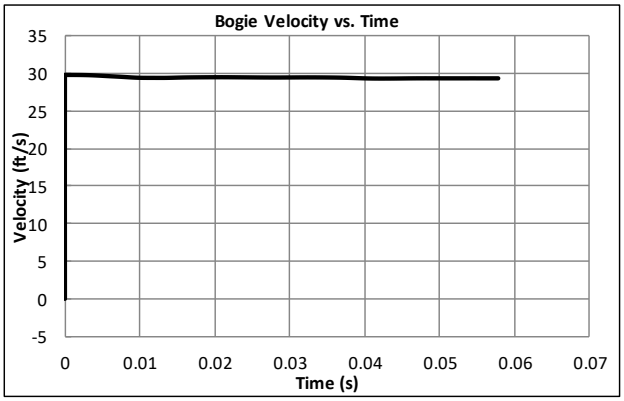

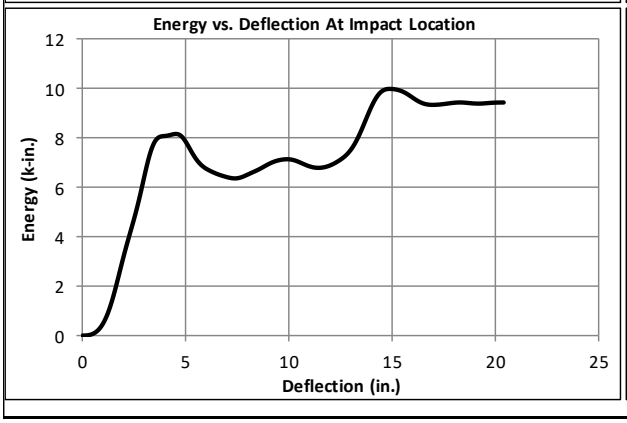

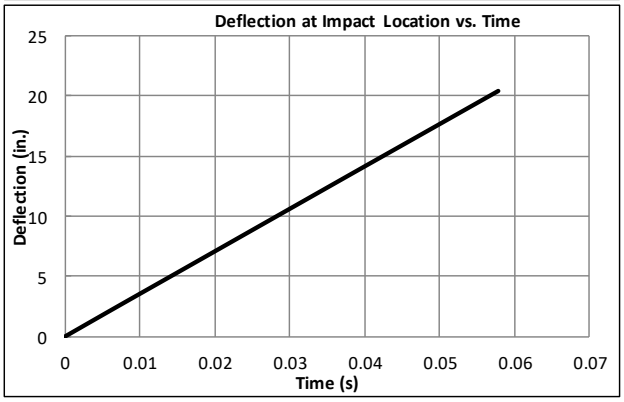

Figure C-25. Test No. 4CMBC-13 Results (DTS)

MIDWEST ROADSIDE SAFETY FACILITY

Bogie Test Summary

Test Information	Cable Median Barrier Folded C-Section Post		**Test Results Summary**	
Test Number:	4CMBC-13		Max. Deflection:	20.4 in.
Test Date:	8-Nov-2012		Peak Force:	4.2 k
Failure Type:	Post bent. Data extraction stopped when contact lost with impact head		Initial Linear Stiffness:	1.9 k/in.
			Total Energy:	17.8 k-in.
Post Properties				
Post Type:	Folded C-Section Post - 10 gauge			
Post Size:	3"x1.625" 10 gauge C-section			
Post Length:	90 in.	228.6 cm		
Embedment Depth:	42 in.	106.7 cm		
Orientation:	Weak			
Soil Properties				
Gradation:	Rigid Sleeve			
Moisture Content:	NA			
Compaction Method:	NA			
Soil Density, γd:	NA			
Bogie Properties				
Impact Velocity:	20.31 mph (29.8 fps)	9.08 m/s		
Impact Height:	27 in.	68.6 cm		
Bogie Mass:	1876 lbs	850.9 kg		
Data Acquired				
Acceleration Data:	EDR-3			
Camera Data:	AOS-5 Perpendicular			

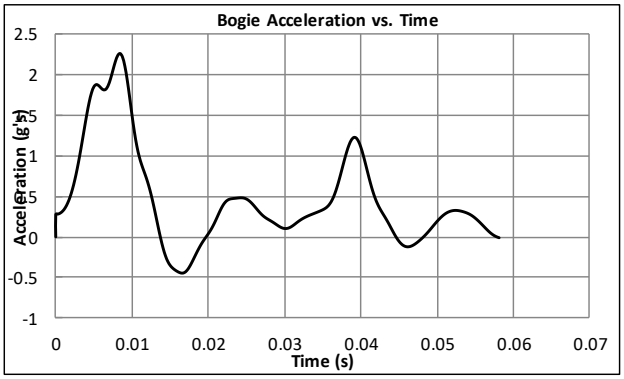

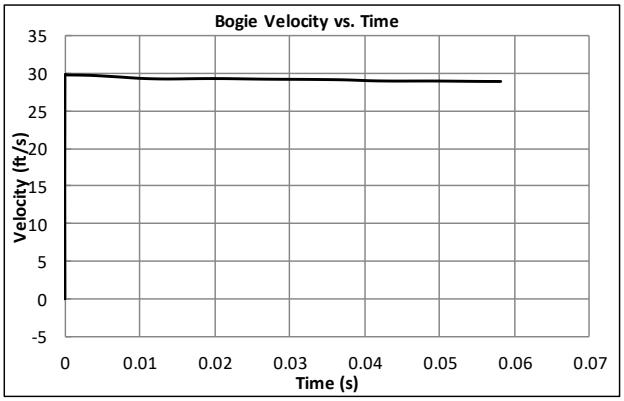

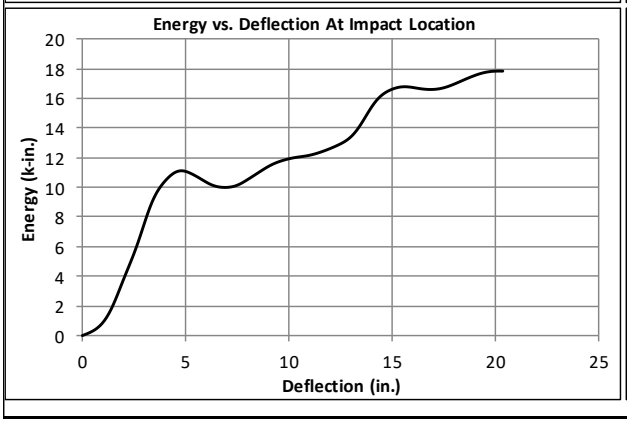

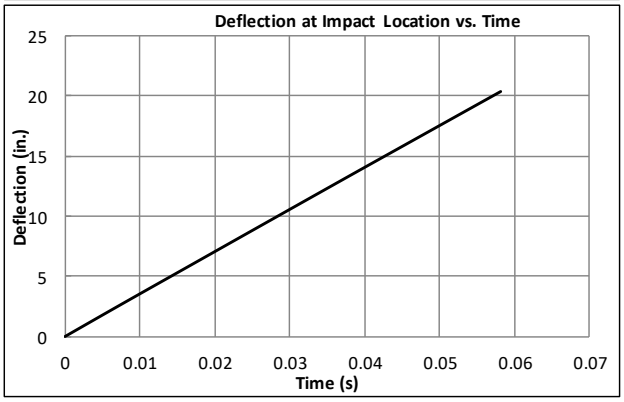

Figure C-26. Test No. 4CMBC-13 Results (EDR-3)

MIDWEST ROADSIDE SAFETY FACILITY

Bogie Test Summary

Test Information	Cable Median Barrier Folded C-Section Post		**Test Results Summary**	
Test Number:	4CMBC-14		Max. Deflection:	21.6 in.
Test Date:	8-Nov-2012		Peak Force:	3.8 k
Failure Type:	Post bent. Data extraction stopped when contact lost with impact head		Initial Linear Stiffness:	1.9 k/in.
			Total Energy:	15.3 k-in.
Post Properties				
Post Type:	Folded C-Section Post - 10 gauge			
Post Size:	3"x1.625" 10 gauge C-section			
Post Length:	90 in.	228.6 cm		
Embedment Depth:	42 in.	106.7 cm		
Orientation:	Weak			
Soil Properties				
Gradation:	Rigid Sleeve			
Moisture Content:	NA			
Compaction Method:	NA			
Soil Density, γd:	NA			
Bogie Properties				
Impact Velocity:	20.96 mph (30.7 fps)	9.37 m/s		
Impact Height:	27 in.	68.6 cm		
Bogie Mass:	1876 lbs	850.9 kg		
Data Acquired				
Acceleration Data:	DTS			
Camera Data:	AOS-5 Perpendicular			

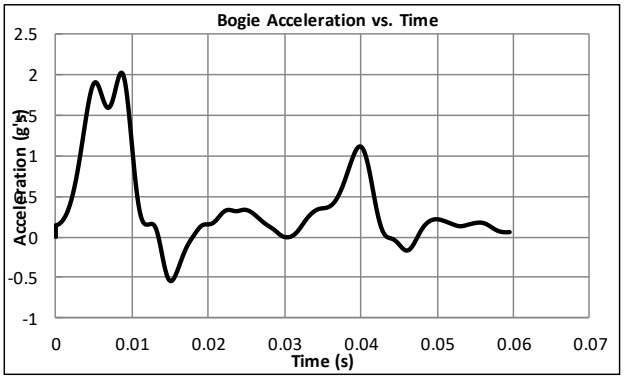

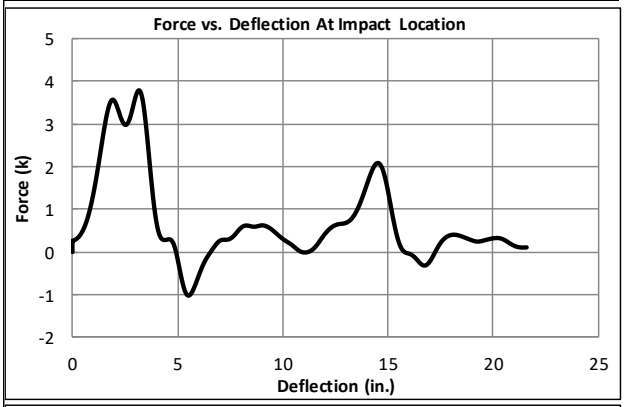

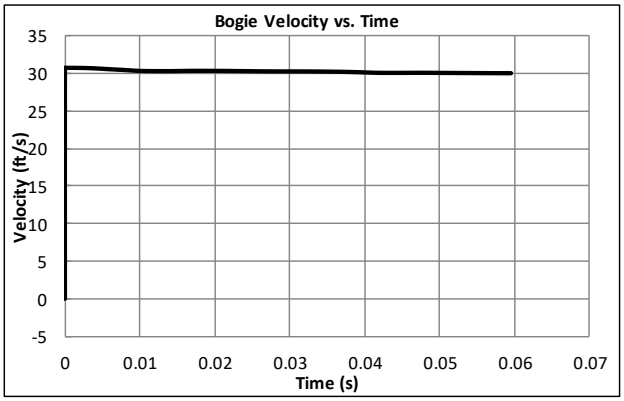

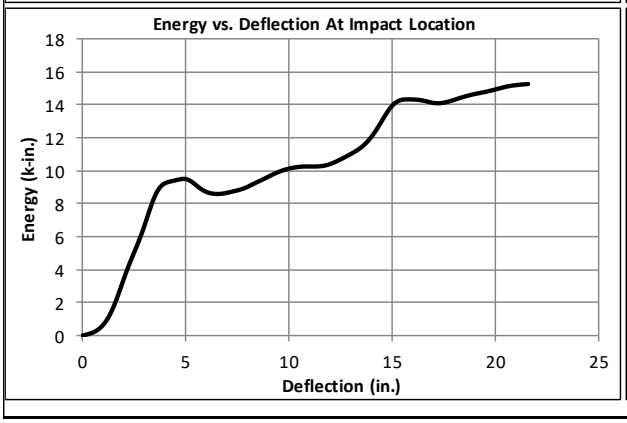

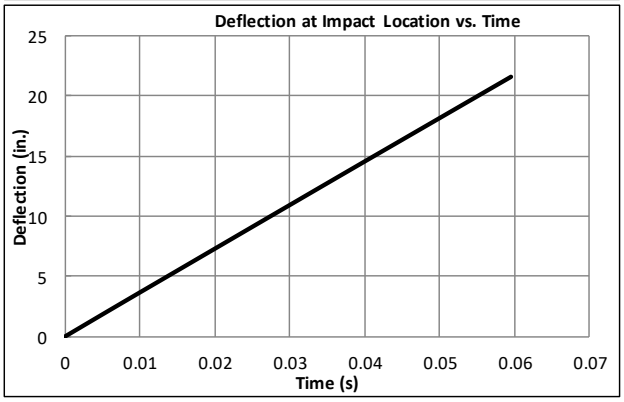

Figure C-27. Test No. 4CMBC-14 Results (DTS)

MIDWEST ROADSIDE SAFETY FACILITY

Bogie Test Summary

Test Information	Cable Median Barrier Folded C-Section Post	
Test Number:	4CMBC-14	
Test Date:	8-Nov-2012	
Failure Type:	Post bent. Data extraction stopped when contact lost with impact head	
Post Properties		
Post Type:	Folded C-Section Post - 10 gauge	
Post Size:	3"x1.625" 10 gauge C-section	
Post Length:	90 in.	228.6 cm
Embedment Depth:	42 in.	106.7 cm
Orientation:	Weak	
Soil Properties		
Gradation:	Rigid Sleeve	
Moisture Content:	NA	
Compaction Method:	NA	
Soil Density, γd:	NA	
Bogie Properties		
Impact Velocity:	20.96 mph (30.7 fps)	9.37 m/s
Impact Height:	27 in.	68.6 cm
Bogie Mass:	1876 lbs	850.9 kg
Data Acquired		
Acceleration Data:	EDR-3	
Camera Data:	AOS-5 Perpendicular	

Test Results Summary		
Max. Deflection:	20.7	in.
Peak Force:	3.8	k
Initial Linear Stiffness:	1.8	k/in.
Total Energy:	21.5	k-in.

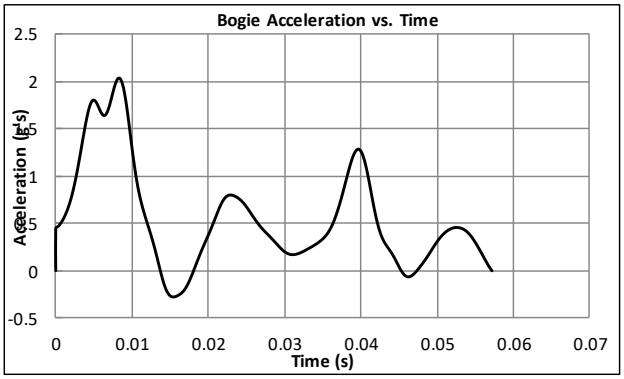

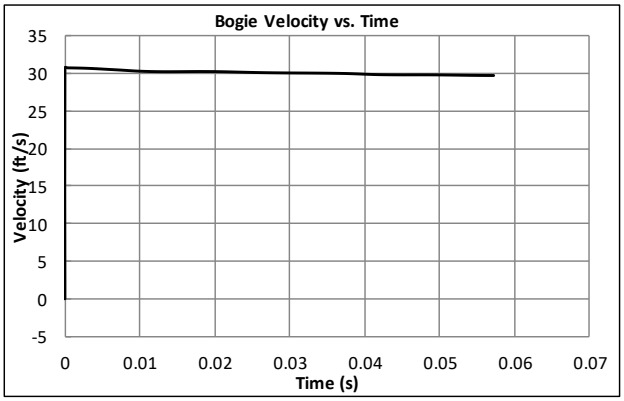

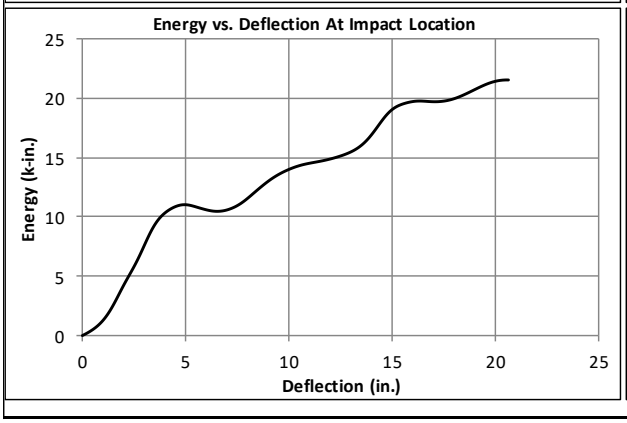

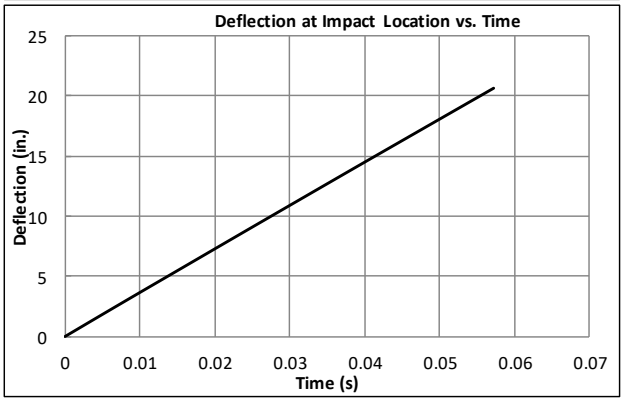

Figure C-28. Test No. 4CMBC-14 Results (EDR-3)

MIDWEST ROADSIDE SAFETY FACILITY

Bogie Test Summary

Test Information	Cable Median Barrier Folded C-Section Post		**Test Results Summary**	
Test Number:	4CMBC-15		Max. Deflection:	19.7 in.
Test Date:	8-Nov-2012		Peak Force:	5.2 k
Failure Type:	Post bent. Data extraction stopped when contact lost with impact head		Initial Linear Stiffness:	2.1 k/in.
			Total Energy:	23.8 k-in.
Post Properties				
Post Type:	Folded C-Section Post - 7 gauge			
Post Size:	3"x1.625" 7 gauge C-section			
Post Length:	90 in.	228.6 cm		
Embedment Depth:	42 in.	106.7 cm		
Orientation:	Weak			
Soil Properties				
Gradation:	Rigid Sleeve			
Moisture Content:	NA			
Compaction Method:	NA			
Soil Density, γd:	NA			
Bogie Properties				
Impact Velocity:	20.65 mph (30.3 fps)	9.23 m/s		
Impact Height:	27 in.	68.6 cm		
Bogie Mass:	1876 lbs	850.9 kg		
Data Acquired				
Acceleration Data:	DTS			
Camera Data:	AOS-5 Perpendicular			

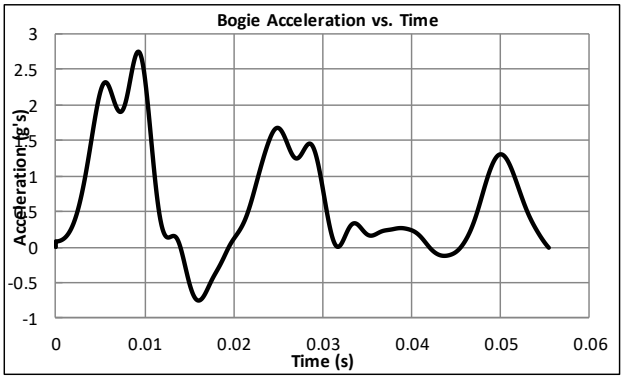

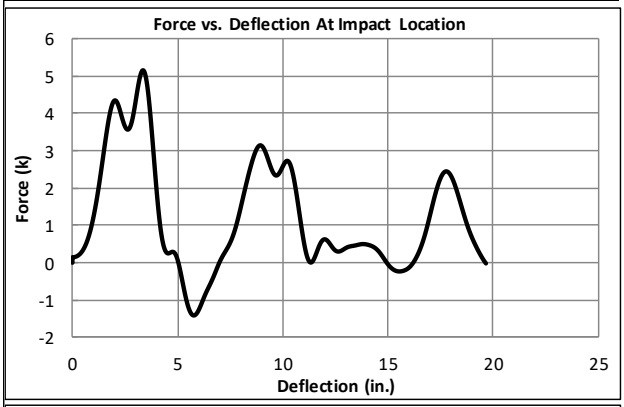

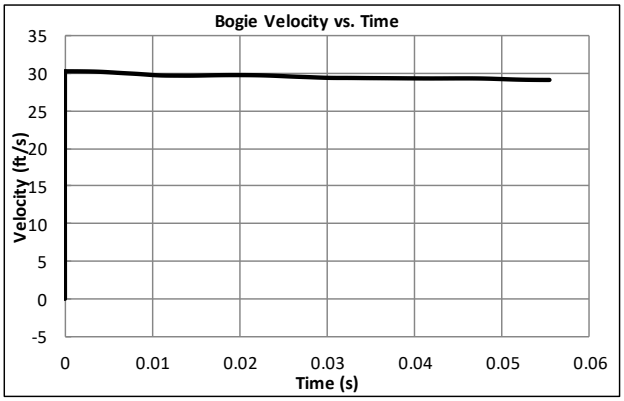

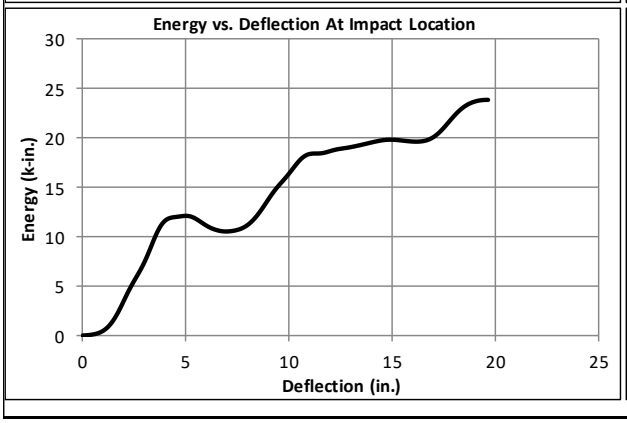

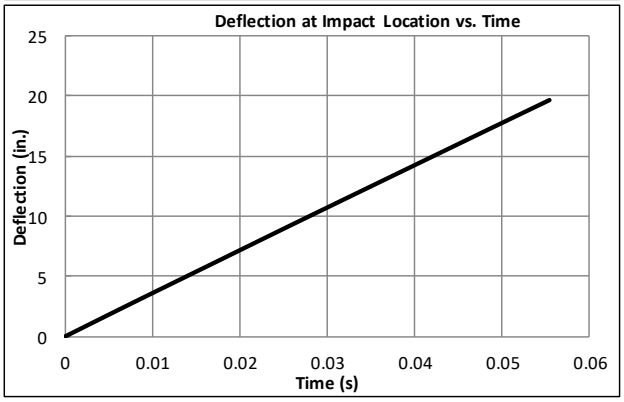

Figure C-29. Test No. 4CMBC-15 Results (DTS)

MIDWEST ROADSIDE SAFETY FACILITY

Bogie Test Summary

Test Information	Cable Median Barrier Folded C-Section Post		
Test Number:	4CMBC-15		
Test Date:	8-Nov-2012		
Failure Type:	Post bent. Data extraction stopped when contact lost with impact head		
Post Properties			
Post Type:	Folded C-Section Post - 7 gauge		
Post Size:	3"x1.625" 7 gauge C-section		
Post Length:	90 in.	228.6 cm	
Embedment Depth:	42 in.	106.7 cm	
Orientation:	Weak		
Soil Properties			
Gradation:	Rigid Sleeve		
Moisture Content:	NA		
Compaction Method:	NA		
Soil Density, γd:	NA		
Bogie Properties			
Impact Velocity:	20.65 mph (30.3 fps)	9.23 m/s	
Impact Height:	27 in.	68.6 cm	
Bogie Mass:	1876 lbs	850.9 kg	
Data Acquired			
Acceleration Data:	EDR-3		
Camera Data:	AOS-5 Perpendicular		

Test Results Summary		
Max. Deflection:	20.3	in.
Peak Force:	4.8	k
Initial Linear Stiffness:	1.9	k/in.
Total Energy:	26.2	k-in.

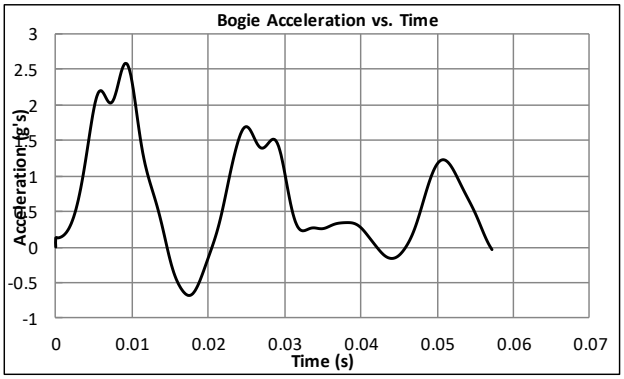

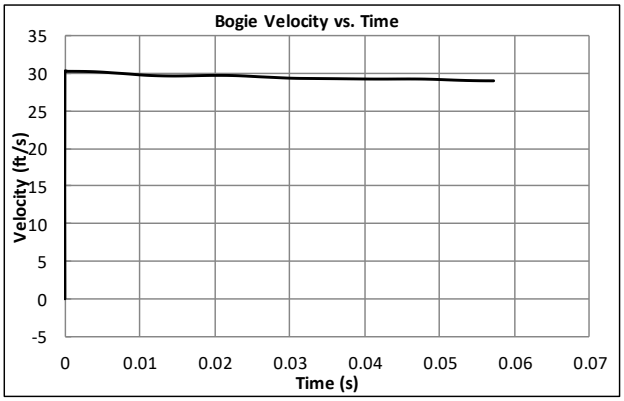

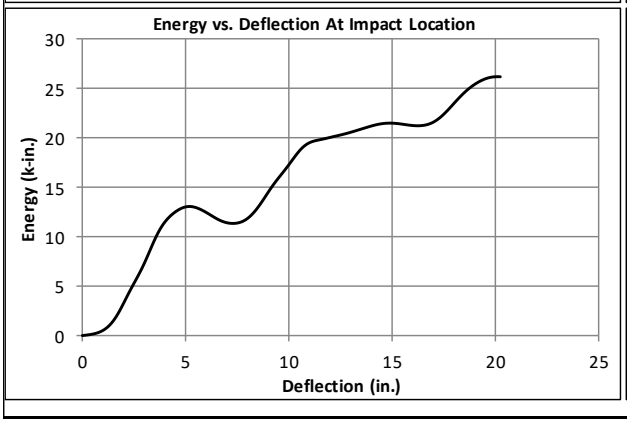

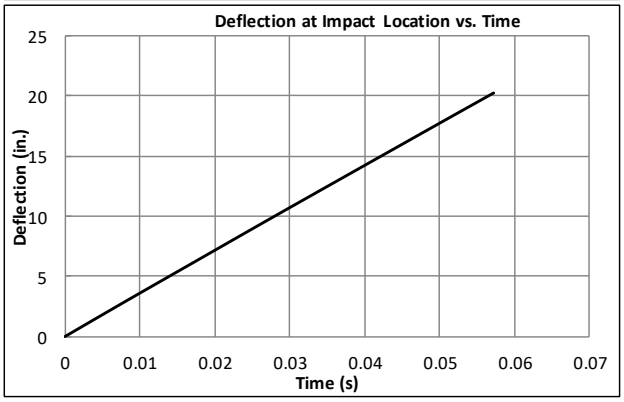

Figure C-30. Test No. 4CMBC-15 Results (EDR-3)

MIDWEST ROADSIDE SAFETY FACILITY

Bogie Test Summary

Test Information	Cable Median Barrier Folded C-Section Post		**Test Results Summary**	
Test Number:	4CMBC-16		Max. Deflection:	23.6 in.
Test Date:	8-Nov-2012		Peak Force:	5.5 k
Failure Type:	Post bent. Data extraction stopped when contact lost with impact head		Initial Linear Stiffness:	2.1 k/in.
			Total Energy:	25.9 k-in.
Post Properties				
Post Type:	Folded C-Section Post - 7 gauge			
Post Size:	3"x1.625" 7 gauge C-section			
Post Length:	90 in.	228.6 cm		
Embedment Depth:	42 in.	106.7 cm		
Orientation:	Weak			
Soil Properties				
Gradation:	Rigid Sleeve			
Moisture Content:	NA			
Compaction Method:	NA			
Soil Density, γd:	NA			
Bogie Properties				
Impact Velocity:	20.71 mph (30.4 fps)	9.26 m/s		
Impact Height:	27 in.	68.6 cm		
Bogie Mass:	1876 lbs	850.9 kg		
Data Acquired				
Acceleration Data:	DTS			
Camera Data:	AOS-5 Perpendicular			

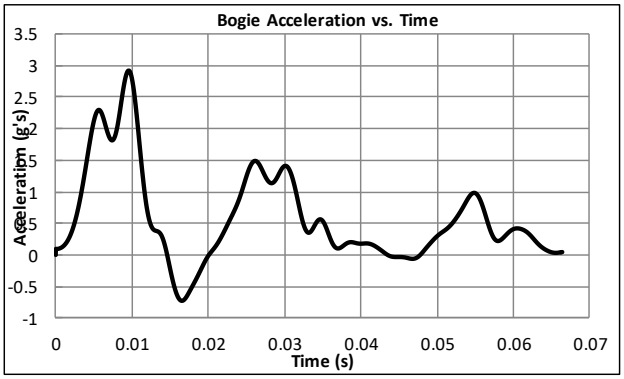

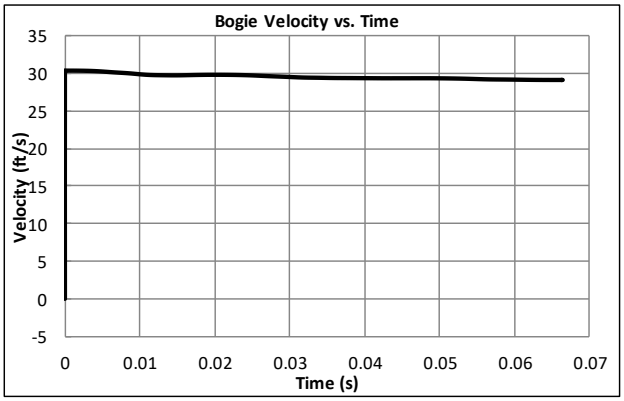

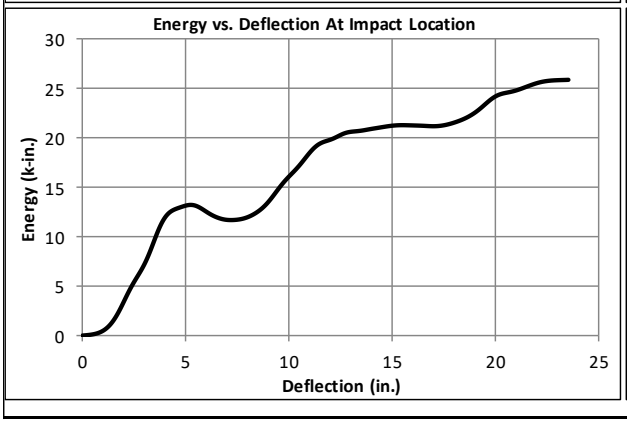

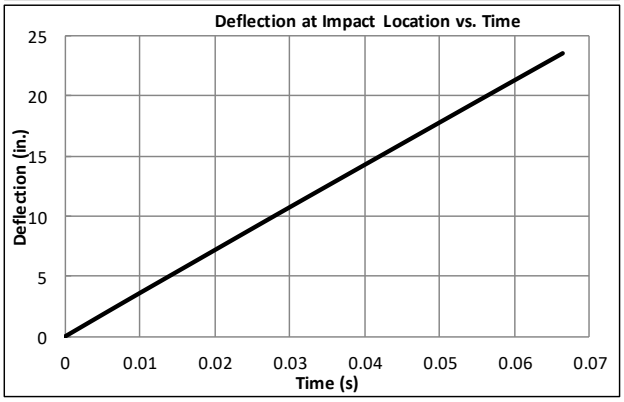

Figure C-31. Test No. 4CMBC-16 Results (DTS)

MIDWEST ROADSIDE SAFETY FACILITY

Bogie Test Summary

Test Information	Cable Median Barrier Folded C-Section Post		**Test Results Summary**	
Test Number:	4CMBC-16		Max. Deflection:	23.1 in.
Test Date:	8-Nov-2012		Peak Force:	4.9 k
Failure Type:	Post bent. Data extraction stopped when contact lost with impact head		Initial Linear Stiffness:	2.0 k/in.
			Total Energy:	29.4 k-in.
Post Properties				
Post Type:	Folded C-Section Post - 7 gauge			
Post Size:	3"x1.625" 7 gauge C-section			
Post Length:	90 in.	228.6 cm		
Embedment Depth:	42 in.	106.7 cm		
Orientation:	Weak			
Soil Properties				
Gradation:	Rigid Sleeve			
Moisture Content:	NA			
Compaction Method:	NA			
Soil Density, γd:	NA			
Bogie Properties				
Impact Velocity:	20.71 mph (30.4 fps)	9.26 m/s		
Impact Height:	27 in.	68.6 cm		
Bogie Mass:	1876 lbs	850.9 kg		
Data Acquired				
Acceleration Data:	EDR-3			
Camera Data:	AOS-5 Perpendicular			

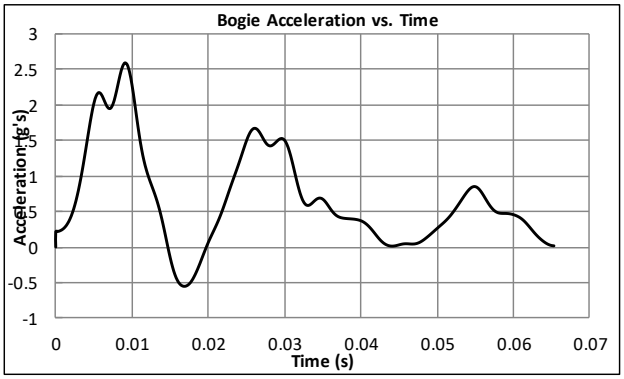

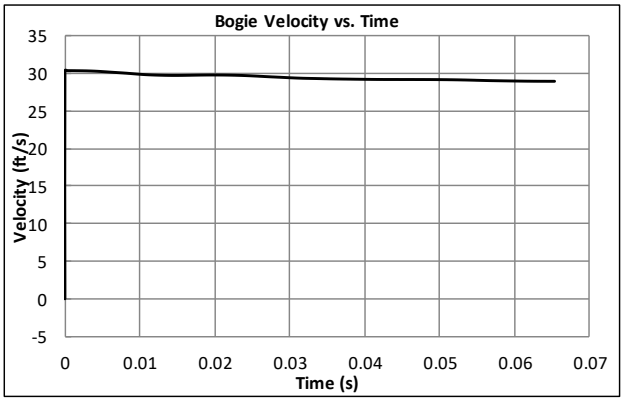

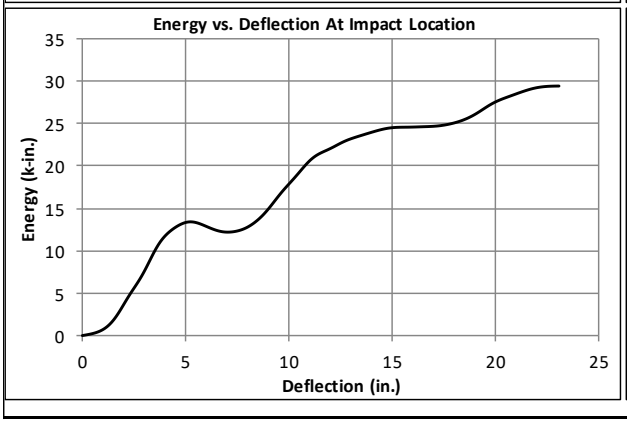

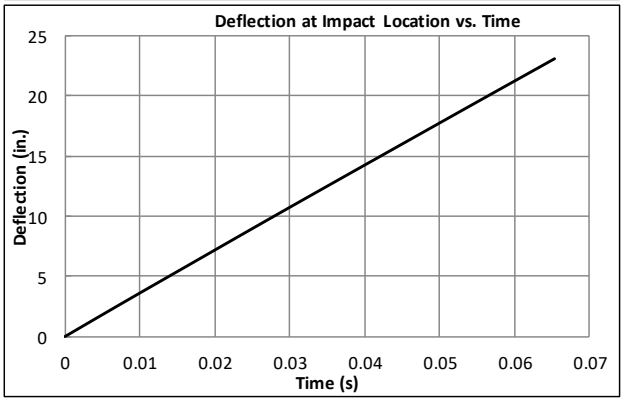

Figure C-32. Test No. 4CMBC-16 Results (EDR-3)

MIDWEST ROADSIDE SAFETY FACILITY

Bogie Test Summary

Test Information	Folded C-section Post Strong Axis	
Test Number:	CPK-1	
Test Date:	11-Feb-2013	
Failure Type:	Post yield and hinge at lower keyway	
Post Properties		
Post Type:	Folded C-section	
Post Size:	3"x1.625"	76.2 mm x 41.3 mm
Post Length:	90 in.	228.6 cm
Embedment Depth:	42 in.	106.7 cm
Orientation:	Strong Axis	
Soil Properties		
Gradation:	NA	
Moisture Content:	NA	
Compaction Method:	NA	
Soil Density, γd:	NA	
Bogie Properties		
Impact Velocity:	20.47 mph (30.0 fps)	9.15 m/s
Impact Height:	27 in.	68.6 cm
Bogie Mass:	1868.6 lbs	847.6 kg
Data Acquired		
Acceleration Data:	SLICE	
Camera Data:	aos7	

Test Results Summary		
Max. Deflection:	12.1	in.
Peak Force:	7.0	k
Initial Linear Stiffness:	#DIV/0!	k/in.
Total Energy:	21.8	k-in.

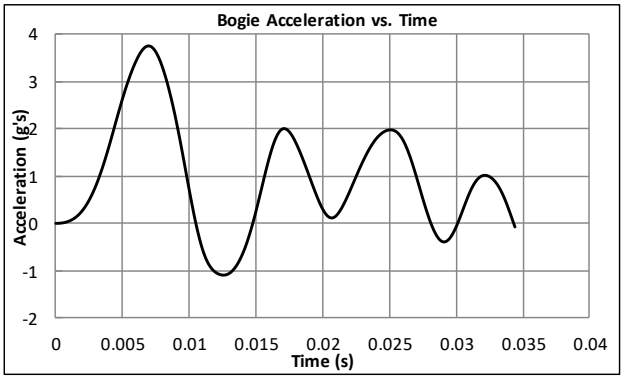

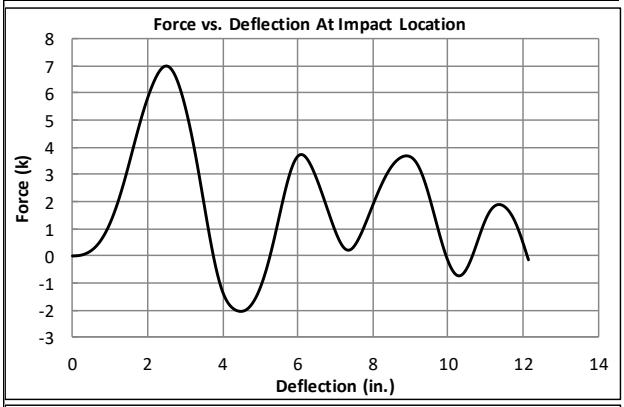

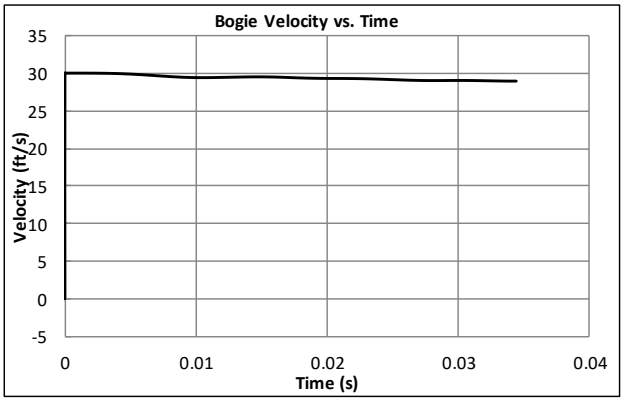

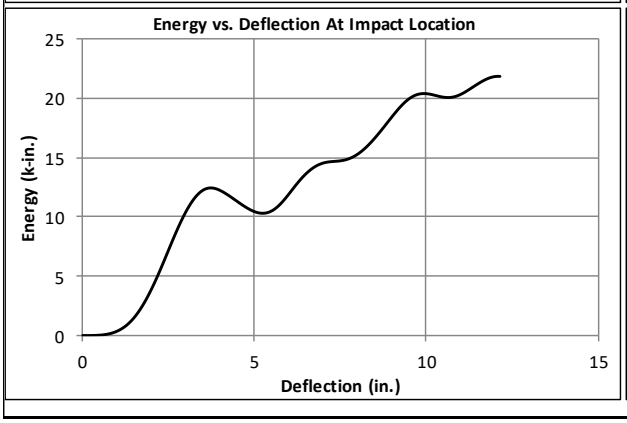

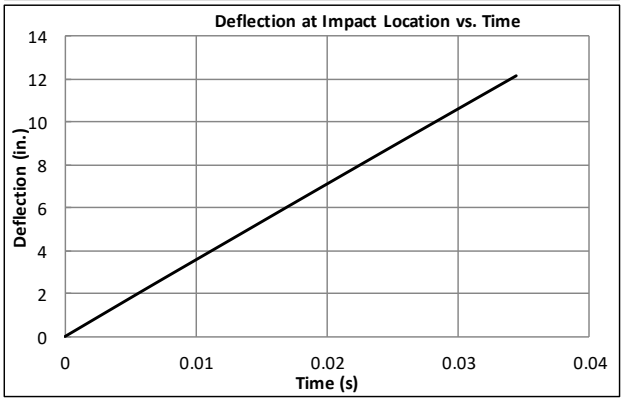

Figure C-33. Test No. CPK-1 Results (DTS-SLICE)

MIDWEST ROADSIDE SAFETY FACILITY

Bogie Test Summary

Test Information	Folded C-section Post Strong Axis	
Test Number:	CPK-1	
Test Date:	11-Feb-2013	
Failure Type:	Post yield and hinge at lower keyway	
Post Properties		
Post Type:	Folded C-section	
Post Size:	3"x1.625"	76.2 mm x 41.3 mm
Post Length:	90 in.	228.6 cm
Embedment Depth:	42 in.	106.7 cm
Orientation:	Strong Axis	
Soil Properties		
Gradation:	NA	
Moisture Content:	NA	
Compaction Method:	NA	
Soil Density, γd:	NA	
Bogie Properties		
Impact Velocity:	20.47 mph (30.0 fps)	9.15 m/s
Impact Height:	27 in.	68.6 cm
Bogie Mass:	1868.6 lbs	847.6 kg
Data Acquired		
Acceleration Data:	EDR-3	
Camera Data:	aos7	

Test Results Summary		
Max. Deflection:	13.1	in.
Peak Force:	4.8	k
Initial Linear Stiffness:	2.4	k/in.
Total Energy:	21.3	k-in.

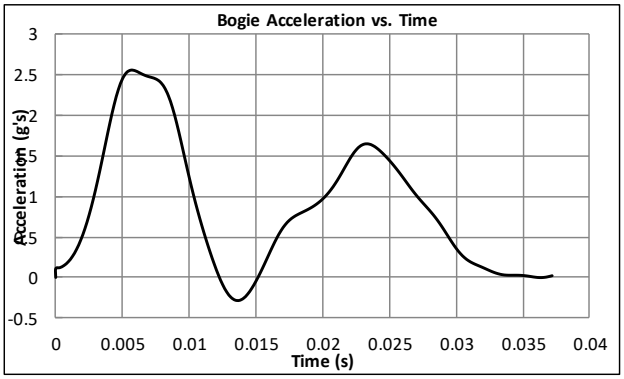

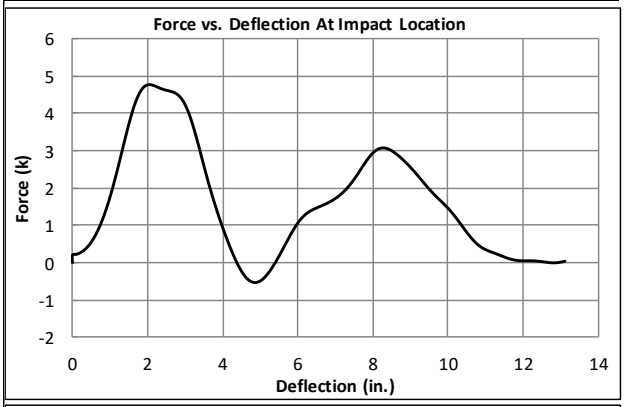

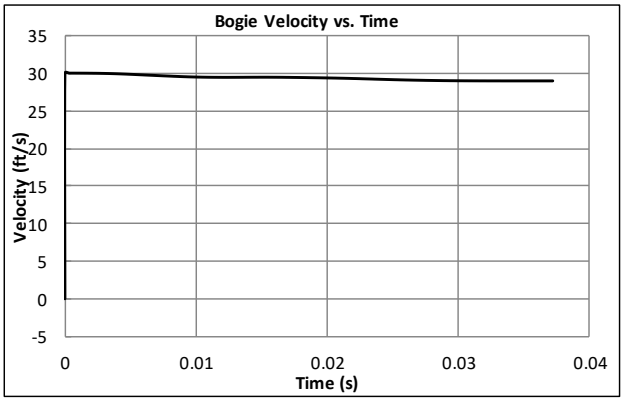

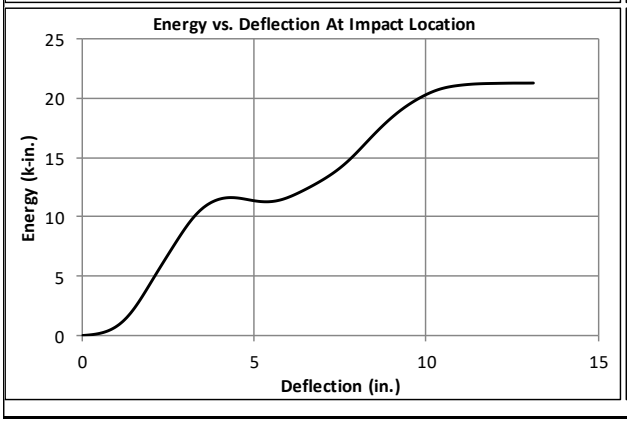

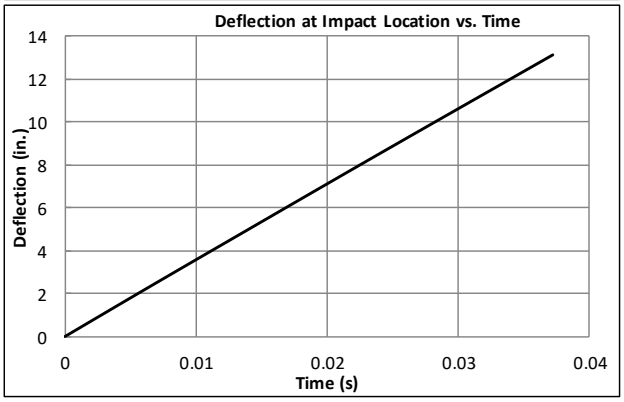

Figure C-34. Test No. CPK-1 Results (EDR-3)

MIDWEST ROADSIDE SAFETY FACILITY

Bogie Test Summary

Test Information	Folded C-section Post Weak Axis	
Test Number:	CPK-2	
Test Date:	11-Feb-2013	
Failure Type:	Post yield and hinge at lower keyway	
Post Properties		
Post Type:	Folded C-section	
Post Size:	3"x1.625"	76.2 mm x 41.3 mm
Post Length:	90 in.	228.6 cm
Embedment Depth:	42 in.	106.7 cm
Orientation:	Weak Axis	
Soil Properties		
Gradation:	NA	
Moisture Content:	NA	
Compaction Method:	NA	
Soil Density, γd:	NA	
Bogie Properties		
Impact Velocity:	20.62 mph (30.2 fps)	9.22 m/s
Impact Height:	27 in.	68.6 cm
Bogie Mass:	1868.6 lbs	847.6 kg
Data Acquired		
Acceleration Data:	SLICE	
Camera Data:	aos7	

Test Results Summary		
Max. Deflection:	10.8	in.
Peak Force:	5.2	k
Initial Linear Stiffness:	#DIV/0!	k/in.
Total Energy:	16.0	k-in.

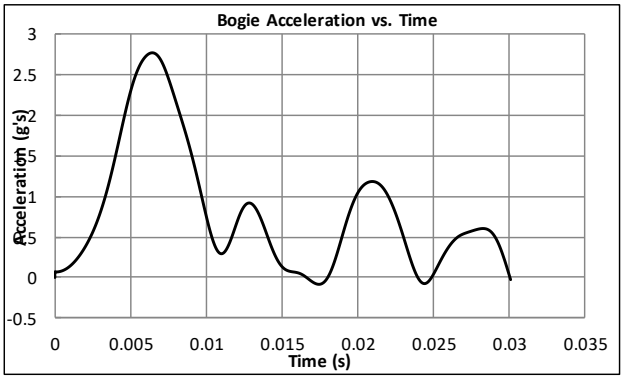

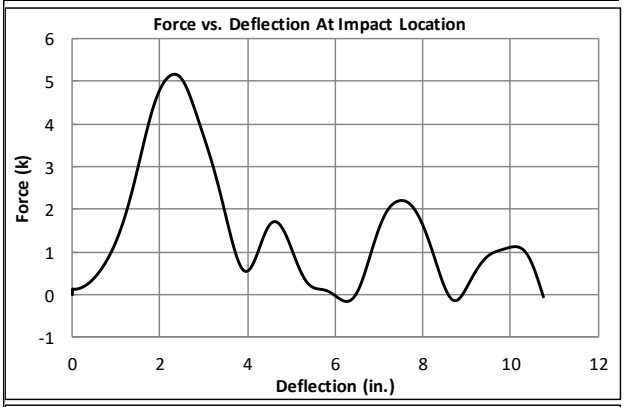

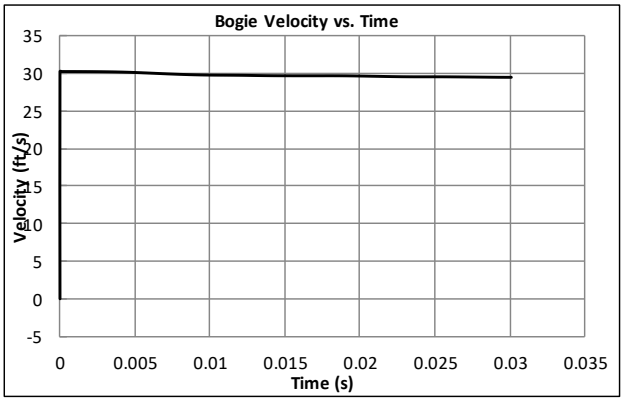

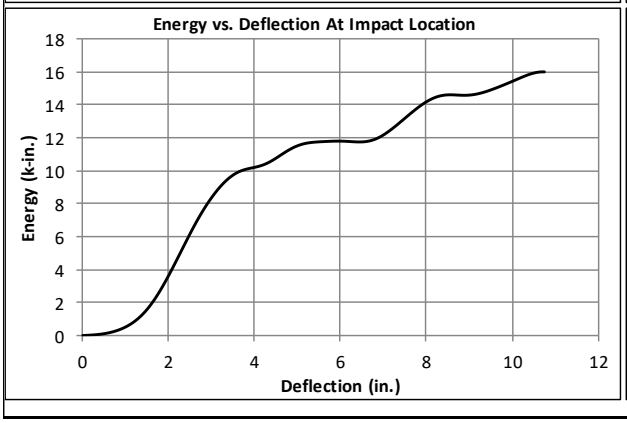

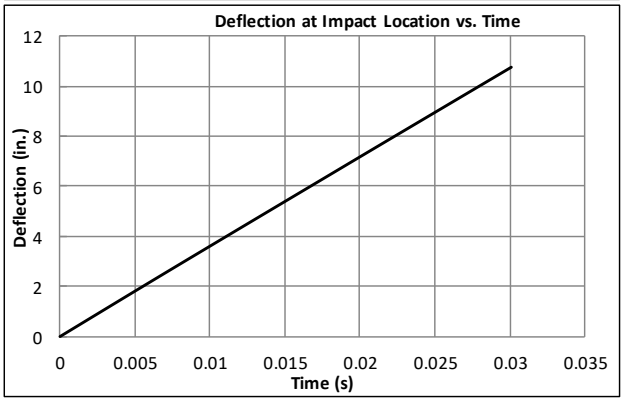

Figure C-35. Test No. CPK-2 Results (DTS-SLICE)

MIDWEST ROADSIDE SAFETY FACILITY

Bogie Test Summary

Test Information	Folded C-section Post Weak Axis	
Test Number:	CPK-2	
Test Date:	11-Feb-2013	
Failure Type:	Post yield and hinge at lower keyway	
Post Properties		
Post Type:	Folded C-section	
Post Size:	3"x1.625"	76.2 mm x 41.3 mm
Post Length:	90 in.	228.6 cm
Embedment Depth:	42 in.	106.7 cm
Orientation:	Weak Axis	
Soil Properties		
Gradation:	NA	
Moisture Content:	NA	
Compaction Method:	NA	
Soil Density, γd:	NA	
Bogie Properties		
Impact Velocity:	20.62 mph (30.2 fps)	9.22 m/s
Impact Height:	27 in.	68.6 cm
Bogie Mass:	1868.6 lbs	847.6 kg
Data Acquired		
Acceleration Data:	EDR-3	
Camera Data:	aos7	

Test Results Summary		
Max. Deflection:	10.6	in.
Peak Force:	3.3	k
Initial Linear Stiffness:	1.9	k/in.
Total Energy:	14.0	k-in.

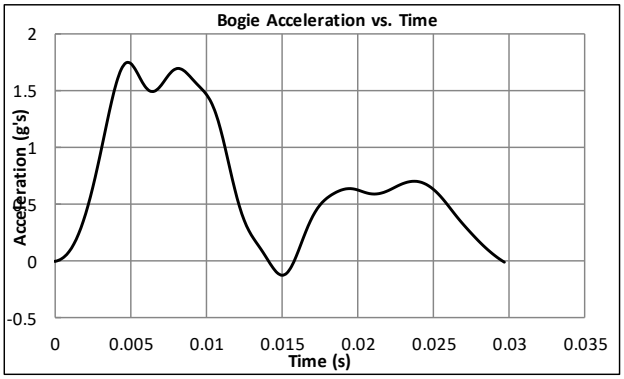

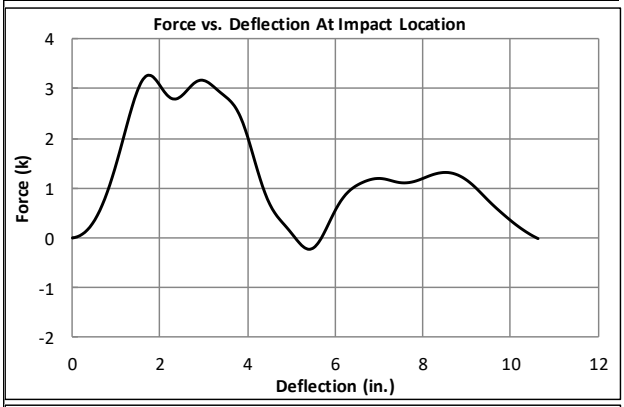

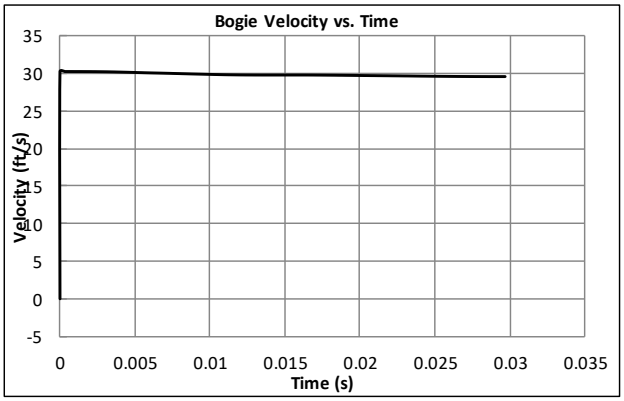

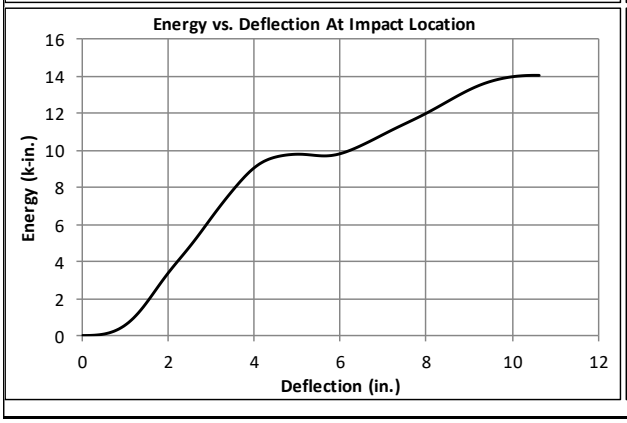

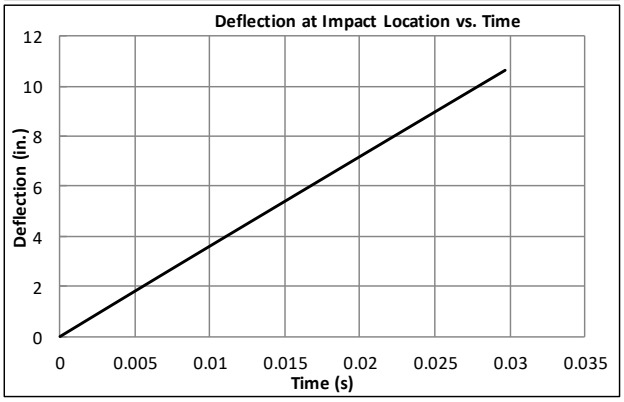

Figure C-36. Test No. CPK-2 Results (EDR-3)

MIDWEST ROADSIDE SAFETY FACILITY

Bogie Test Summary

Test Information	HT Cable Median Barrier Midwest Weak Post Conc		**Test Results Summary**		
Test Number:	CPZ-1		Max. Deflection:	22.8	in.
Test Date:	13-Mar-2013		Peak Force:	4.2	k
Failure Type:	Yielded and bent at groundline		Initial Linear Stiffness:	2.5	k/in.
			Total Energy:	33.5	k-in.
Post Properties					
Post Type:	Folded 7 gauge S-shape post				
Post Size:	3"x1.625"	76.2 mm x 41.3 mm			
Post Length:	80.875 in.	205.4 cm			
Embedment Depth:	42 in.	106.7 cm			
Orientation:	Weak Axis				
Soil Properties					
Gradation:	NA				
Moisture Content:	NA				
Compaction Method:	NA				
Soil Density, γd:	NA				
Bogie Properties					
Impact Velocity:	20.38 mph (29.9 fps)	9.11 m/s			
Impact Height:	27 in.	68.6 cm			
Bogie Mass:	1863 lbs	845 kg			
Data Acquired					
Acceleration Data:	SLICE				
Camera Data:	AOS-7 Perpendicular				

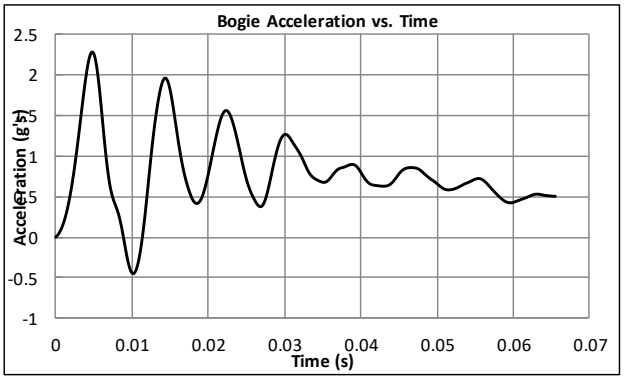

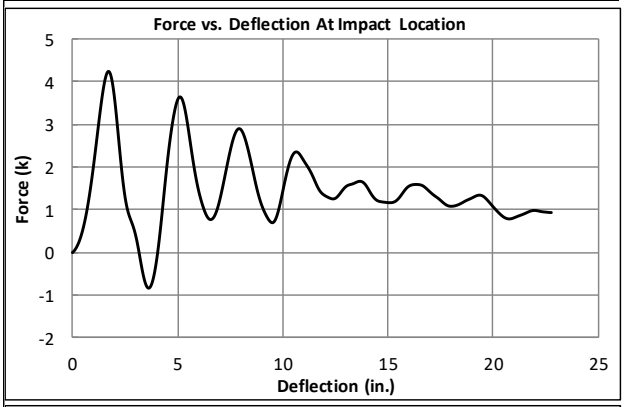

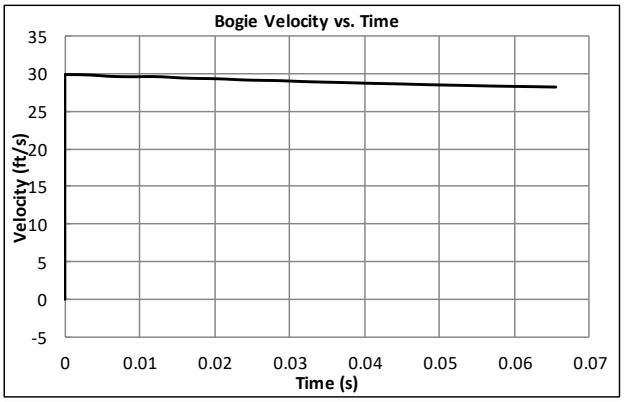

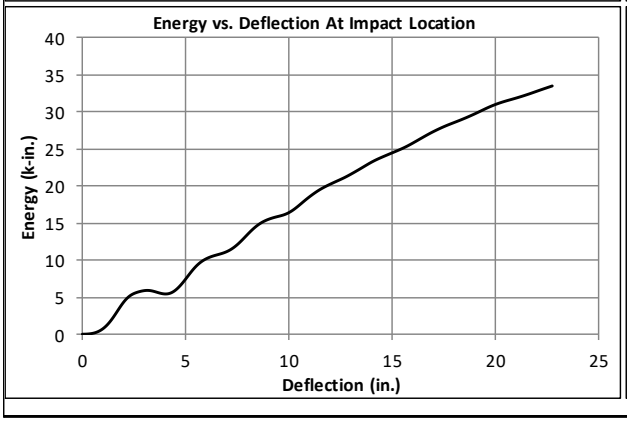

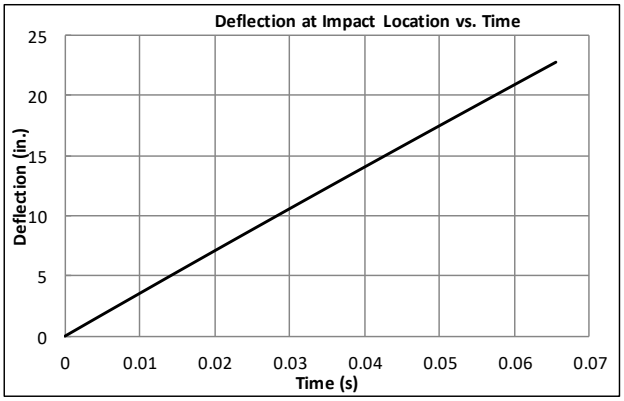

Figure C-37. Test No. CPZ-1 Results (DTS-SLICE)

MIDWEST ROADSIDE SAFETY FACILITY

Bogie Test Summary

Test Information	HT Cable Median Barrier Midwest Weak Post Conc		**Test Results Summary**		
Test Number:	CPZ-1		Max. Deflection:	23.3	in.
Test Date:	13-Mar-2013		Peak Force:	2.5	k
Failure Type:	Yielded and bent at groundline		Initial Linear Stiffness:	1.7	k/in.
			Total Energy:	34.3	k-in.
Post Properties					
Post Type:	Folded 7 gauge S-shape post				
Post Size:	3"x1.625"	76.2 mm x 41.3 mm			
Post Length:	80.875 in.	205.4 cm			
Embedment Depth:	42 in.	106.7 cm			
Orientation:	Weak Axis				
Soil Properties					
Gradation:	NA				
Moisture Content:	NA				
Compaction Method:	NA				
Soil Density, γd:	NA				
Bogie Properties					
Impact Velocity:	20.38 mph (29.9 fps)	9.11 m/s			
Impact Height:	27 in.	68.6 cm			
Bogie Mass:	1863 lbs	845 kg			
Data Acquired					
Acceleration Data:	EDR-3				
Camera Data:	AOS-7 Perpendicular				

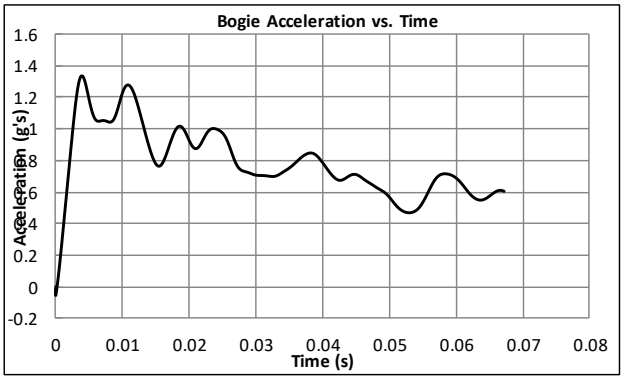

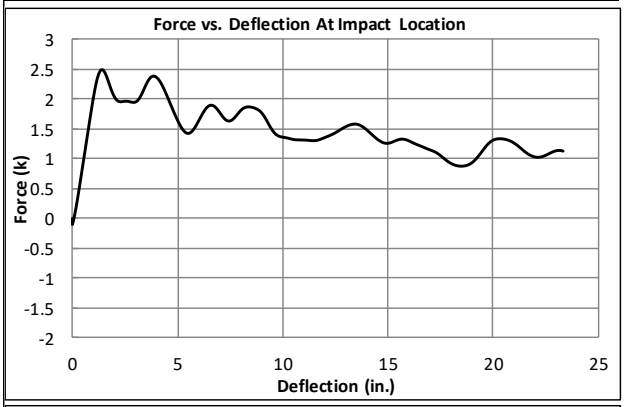

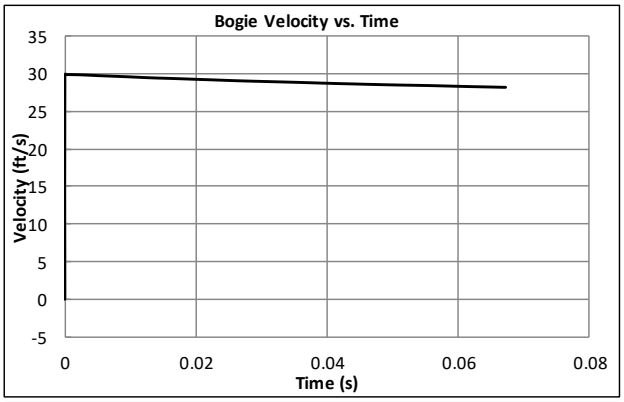

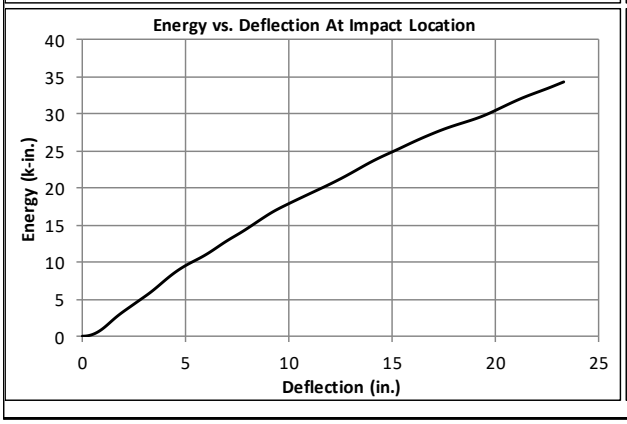

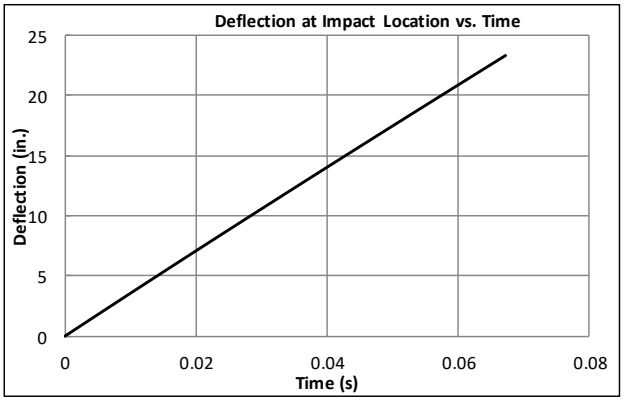

Figure C-38. Test No. CPZ-1 Results (EDR-3)

MIDWEST ROADSIDE SAFETY FACILITY

Bogie Test Summary

Test Information	HT Cable Median Barrier Midwest Weak Post Conc		**Test Results Summary**		
Test Number:	CPZ-2		Max. Deflection:	23.0	in.
Test Date:	13-Mar-2013		Peak Force:	4.4	k
Failure Type:	Yielded and bent at groundline		Initial Linear Stiffness:	2.3	k/in.
			Total Energy:	35.3	k-in.
Post Properties					
Post Type:	Folded 7 gauge S-shape post				
Post Size:	3"x1.625"	76.2 mm x 41.3 mm			
Post Length:	80.875 in.	205.4 cm			
Embedment Depth:	42 in.	106.7 cm			
Orientation:	Strong Axis				
Soil Properties					
Gradation:	NA				
Moisture Content:	NA				
Compaction Method:	NA				
Soil Density, γd:	NA				
Bogie Properties					
Impact Velocity:	19.51 mph (28.6 fps)	8.72 m/s			
Impact Height:	27 in.	68.6 cm			
Bogie Mass:	1863 lbs	845 kg			
Data Acquired					
Acceleration Data:	SLICE				
Camera Data:	AOS-7 Perpendicular				

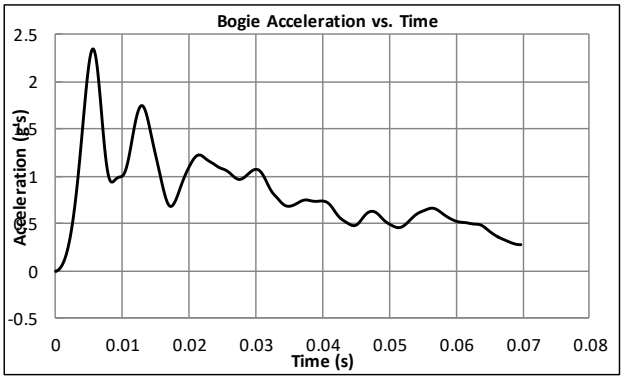

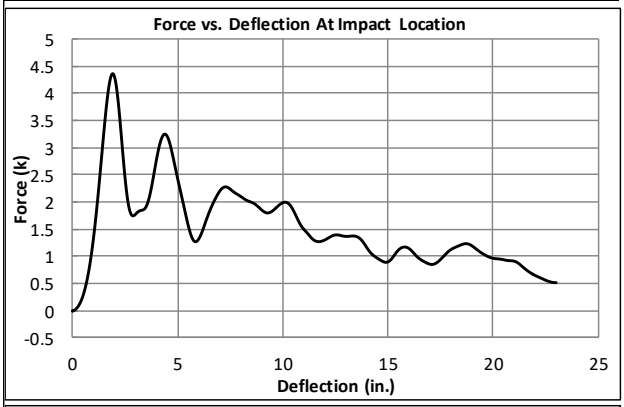

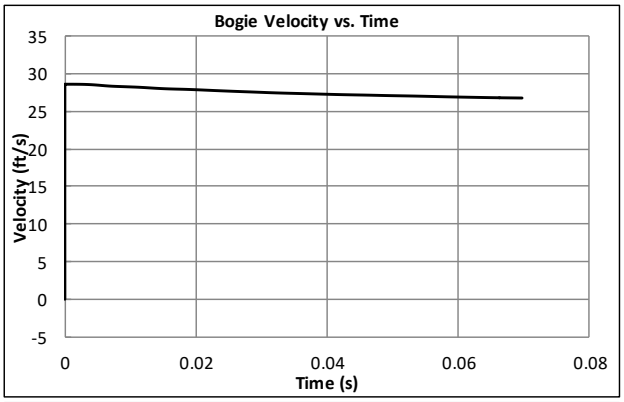

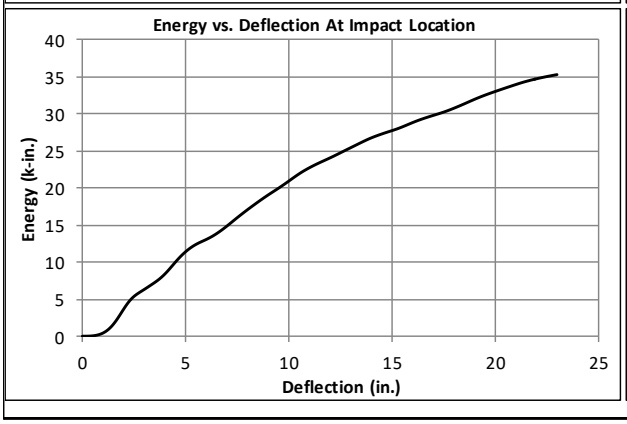

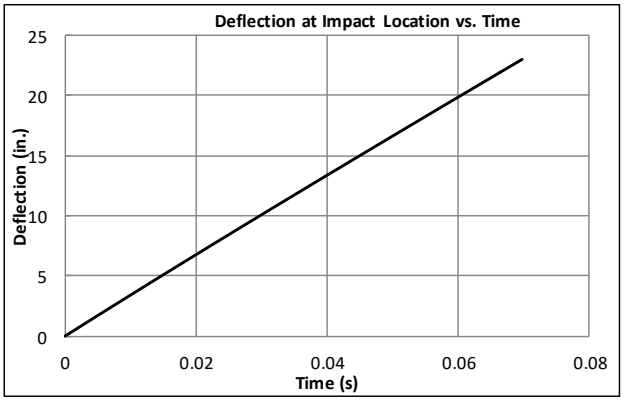

Figure C-39. Test No. CPZ-2 Results (DTS-SLICE)

MIDWEST ROADSIDE SAFETY FACILITY

Bogie Test Summary

Test Information	HT Cable Median Barrier Midwest Weak Post Conc		**Test Results Summary**		
Test Number:	CPZ-2		Max. Deflection:	22.7	in.
Test Date:	13-Mar-2013		Peak Force:	3.8	k
Failure Type:	Yielded and bent at groundline		Initial Linear Stiffness:	2.7	k/in.
			Total Energy:	34.3	k-in.
Post Properties					
Post Type:	Folded 7 gauge S-shape post				
Post Size:	3"x1.625"	76.2 mm x 41.3 mm			
Post Length:	80.875 in.	205.4 cm			
Embedment Depth:	42 in.	106.7 cm			
Orientation:	Strong Axis				
Soil Properties					
Gradation:	NA				
Moisture Content:	NA				
Compaction Method:	NA				
Soil Density, γd:	NA				
Bogie Properties					
Impact Velocity:	19.51 mph (28.6 fps)	8.72 m/s			
Impact Height:	27 in.	68.6 cm			
Bogie Mass:	1863 lbs	845 kg			
Data Acquired					
Acceleration Data:	EDR-3				
Camera Data:	AOS-7 Perpendicular				

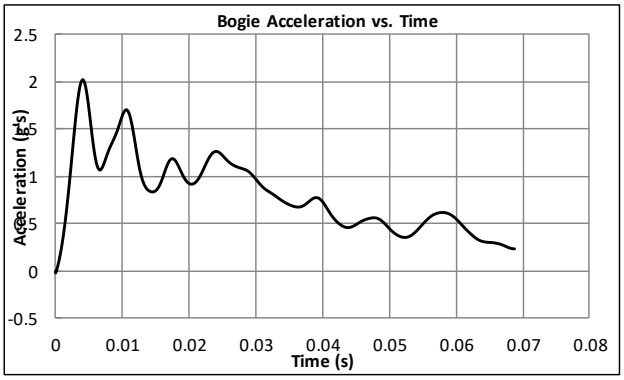

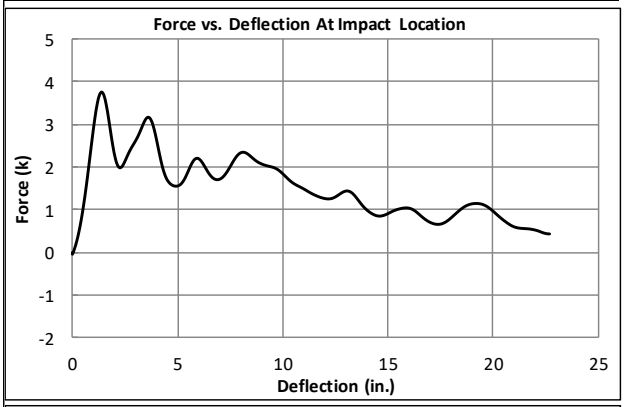

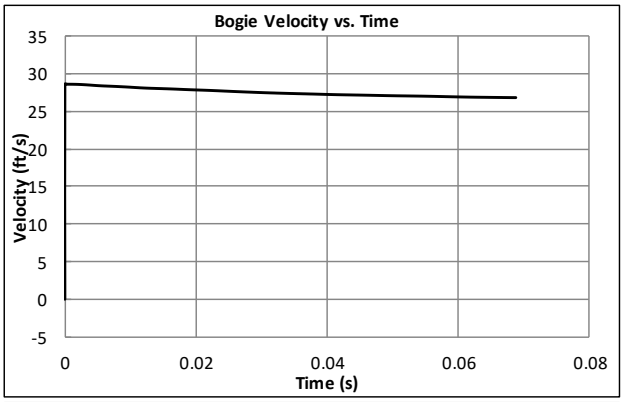

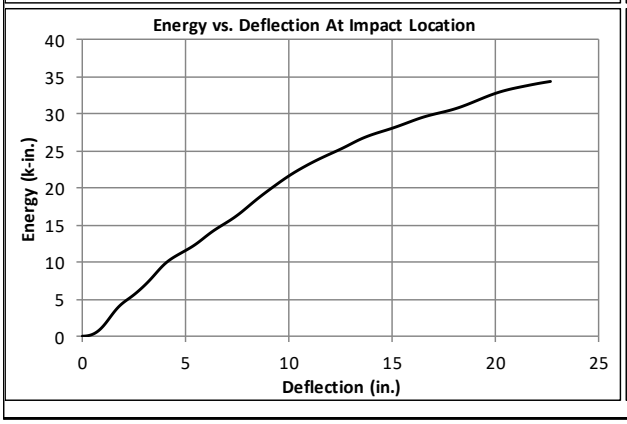

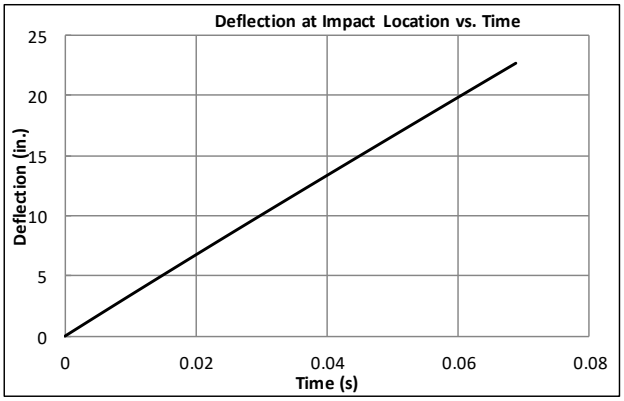

Figure C-40. Test No. CPZ-2 Results (EDR-3)

MIDWEST ROADSIDE SAFETY FACILITY

Bogie Test Summary

Test Information	HT Cable Median Barrier Midwest Weak Post Conc		**Test Results Summary**		
Test Number:	CPZ-3		Max. Deflection:	43.7	in.
Test Date:	13-Mar-2013		Peak Force:	3.5	k
Failure Type:	Yielded and bent at groundline		Initial Linear Stiffness:	0.2	k/in.
			Total Energy:	67.9	k-in.
Post Properties					
Post Type:	Folded 7 gauge S-shape post				
Post Size:	3"x1.625"	76.2 mm x 41.3 mm			
Post Length:	80.875 in.	205.4 cm			
Embedment Depth:	42 in.	106.7 cm			
Orientation:	Strong Axis - Cable Pull				
Soil Properties					
Gradation:	NA				
Moisture Content:	NA				
Compaction Method:	NA				
Soil Density, γd:	NA				
Bogie Properties					
Impact Velocity:	21.09 mph (30.9 fps)	9.43 m/s			
Impact Height:	27 in.	68.6 cm			
Bogie Mass:	1863 lbs	845 kg			
Data Acquired					
Acceleration Data:	SLICE				
Camera Data:	AOS-7 Perpendicular				

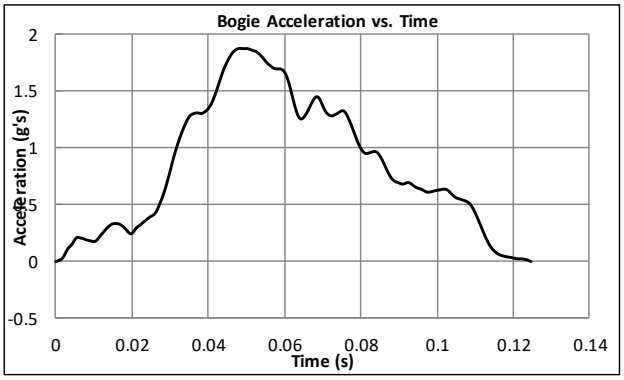

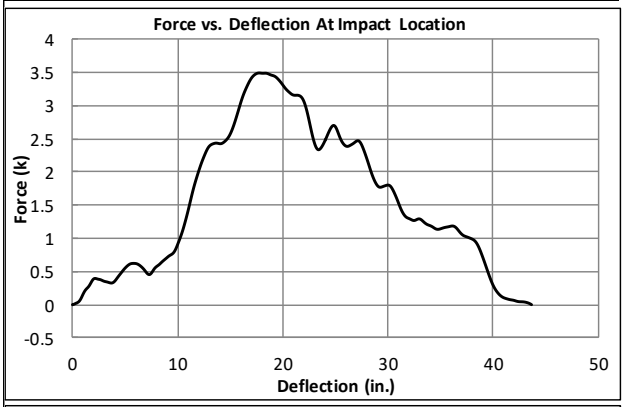

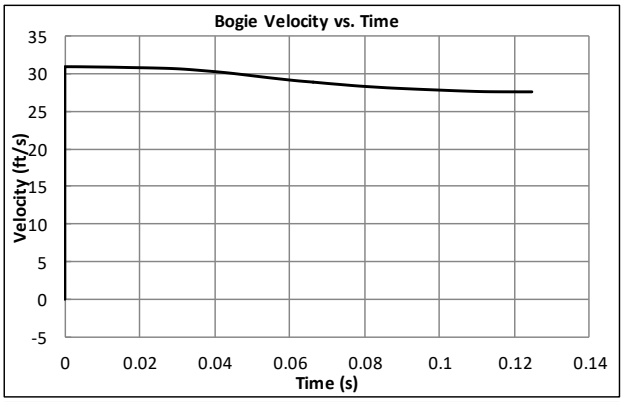

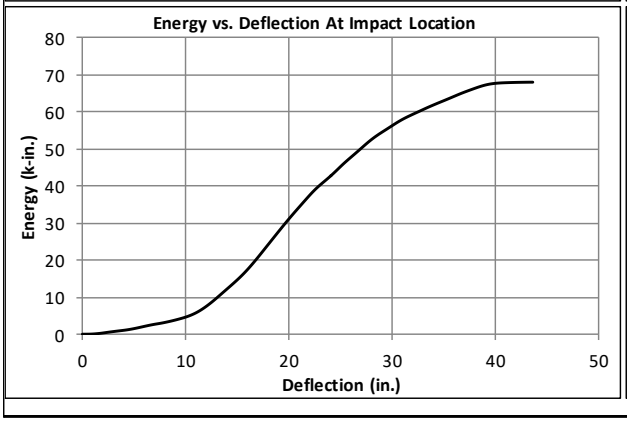

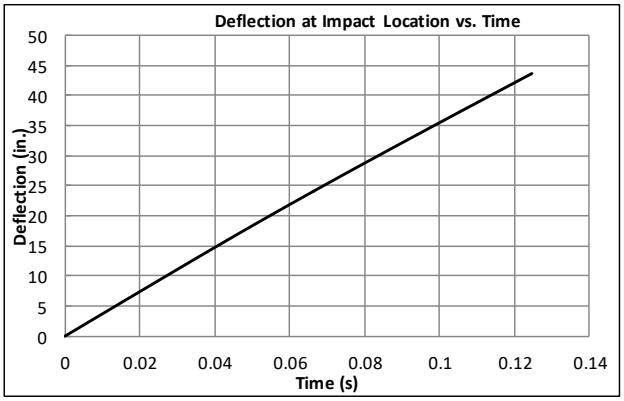

Figure C-41. Test No. CPZ-3 Results (DTS-SLICE)

MIDWEST ROADSIDE SAFETY FACILITY

Bogie Test Summary

Test Information	HT Cable Median Barrier Midwest Weak Post Conc		**Test Results Summary**		
Test Number:	CPZ-3		Max. Deflection:	43.9	in.
Test Date:	13-Mar-2013		Peak Force:	3.0	k
Failure Type:	Yielded and bent at groundline		Initial Linear Stiffness:	0.2	k/in.
			Total Energy:	62.0	k-in.
Post Properties					
Post Type:	Folded 7 gauge S-shape post				
Post Size:	3"x1.625"	76.2 mm x 41.3 mm			
Post Length:	80.875 in.	205.4 cm			
Embedment Depth:	42 in.	106.7 cm			
Orientation:	Strong Axis - Cable Pull				
Soil Properties					
Gradation:	NA				
Moisture Content:	NA				
Compaction Method:	NA				
Soil Density, γd:	NA				
Bogie Properties					
Impact Velocity:	21.09 mph (30.9 fps)	9.43 m/s			
Impact Height:	27 in.	68.6 cm			
Bogie Mass:	1863 lbs	845 kg			
Data Acquired					
Acceleration Data:	EDR-3				
Camera Data:	AOS-7 Perpendicular				

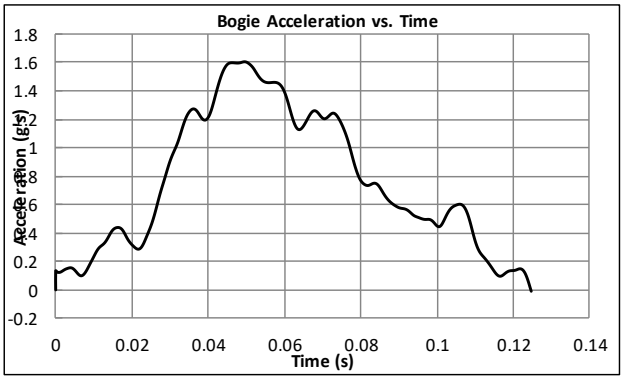

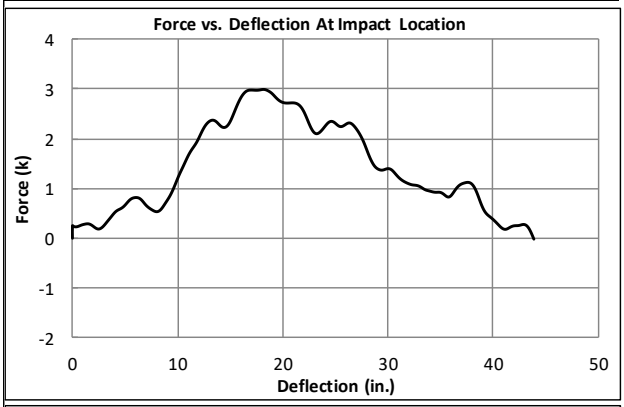

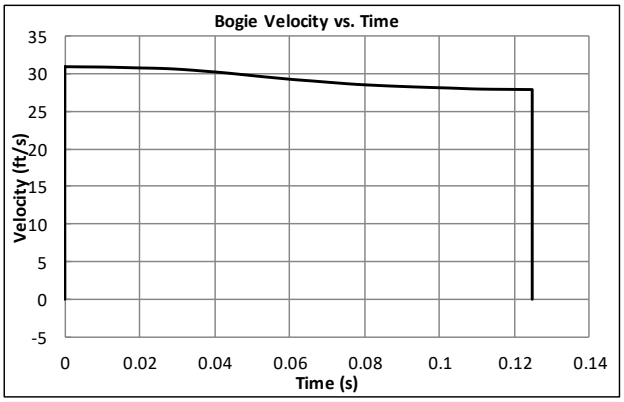

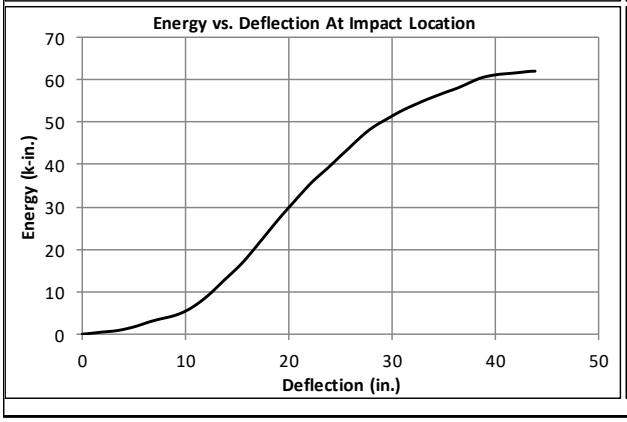

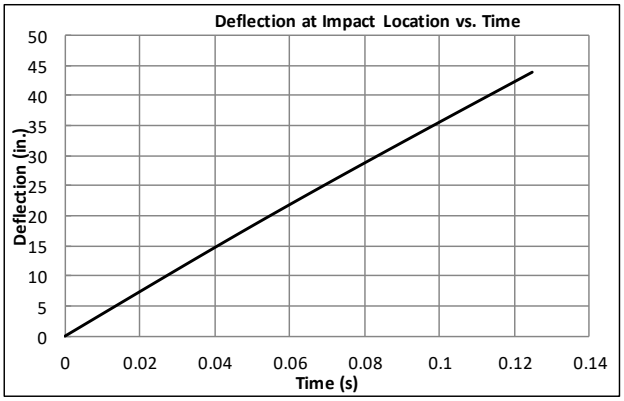

Figure C-42. Test No. CPZ-3 Results (EDR-3)

END OF DOCUMENT